

**IN THE UNITED STATES DISTRICT COURT FOR THE
DISTRICT OF MASSACHUSETTS**

PETER J. MILLER, an individual,
CLIFFORD HOYT, an individual, and
CAMBRIDGE RESEARCH AND
INSTRUMENTATION, INC.,
a Delaware corporation,

Plaintiffs,

v.

PATRICK TREADO, an individual, and
CHEMIMAGE CORP., a Delaware
corporation,

Defendants.

Civil Action No. 05-10367-RWZ

**PLAINTIFF'S MEMORANDUM IN SUPPORT OF
PLAINTIFF'S MOTION TO AMEND COMPLAINT**

Plaintiffs Cambridge Research and Instrumentation, Inc., Peter J. Miller, and Clifford Hoyt pursuant to LR 7.1(b)(1), hereby present a memorandum of reasons, including citations of proper authorities, in support of the accompanying motion for leave to file an amended complaint.

A proposed amended complaint is attached (**Exhibit 1**).

[*NOTE***: PORTIONS OF THIS MEMORANDUM HAVE BEEN REDACTED. A SEPARATE MOTION FOR IMPOUNDMENT IS BEING FILED BY HAND WITH A COMPLETE COPY OF THIS MEMORANDUM. THE REASONS FOR REDACTION ARE EXPLAINED IN THE SEPARATE MOTION. THE [PROPOSED] AMENDED COMPLAINT HAS BEEN SIMILARLY REDACTED.]**

Memorandum in support of
Plaintiffs' Motion for Leave to File
an Amended Complaint

REDACTED VERSION; FILED VIA ECF
(complete version being filed by hand with the Court)

Discovery has barely begun in this case. Documents were first exchanged last Thursday, May 11, 2006. No depositions have been taken; no deposition notices have been served. Defendants' supplemental response to plaintiffs' first set of interrogatories were also served last Thursday, May 11, 2005.

Because no substantive discovery had taken place as of March of this year, plaintiffs and defendants jointly moved this Court to extend the deadlines in the scheduling order, which the Court granted on March 30, 2006. At the time, plaintiffs had asked defendants to agree to extend the deadline for amending the pleadings, inasmuch as all other scheduling deadlines were being extended, but defendants refused. Thus, plaintiffs now move the Court, which has already extended the other scheduling deadlines, to similarly extend the deadline for filing amended pleadings, and to thereby allow plaintiffs to file and serve the attached [Proposed] Amended Complaint (**Exhibit 1**).

When a party asks to amend the pleadings after a deadline set in a scheduling order, Fed. R. Civ. P. 16(b) applies, which states that a scheduling order "shall not be modified except upon a showing of good cause and by leave of the district judge." Fed. R. Civ. P. 16(b); see also *O'Connell v. Hyatt Hotels of P.R.*, 357 F.3d 152, 154-155 (1st Cir. 2004). The decision to extend the deadline set in a scheduling order lies completely within the discretion of the Judge. *Vulcan Tools of P.R. v. Makita U.S.A., Inc.*, 23 F. 3d 564, 565 (1st Cir. 1994) (lower court's decision on a motion to extend a Fed. R. Civ. P. 16(b) scheduling order reviewed under abuse of discretion standard). "Moreover, pretrial orders are to be liberally construed." *Id.* at 566 (quoting James W.M. Moore et al., *MOORE'S FEDERAL PRACTICE* ¶16.19, at 16-90 (2d ed. 1993)).

REDACTED VERSION; FILED VIA ECF
(complete version being filed by hand with the Court)

In *Vulcan Tools*, the district court was affirmed when it held that an amended scheduling order which changed some deadlines (such as the discovery cut-off), but did not change the deadline for filing dispositive motions, “necessarily abolished” the existing deadline for filing dispositive motions, and thus effectively extended that deadline as well. *Id.* at 566 (“..., the court could have concluded that the ‘good cause’ Makita demonstrated for extending the discovery deadline was also good cause for lifting the deadline for filing dispositive motions.”). Likewise here, the “good cause” for extending the other deadlines (end of fact discovery; end of expert discovery; and dispositive motions) is also good cause for extending the deadline for amended pleadings.

Moreover, none of the traditional reasons for not granting leave to amend a pleading are present here. See, e.g., *Vargas v. McNamara*, 608 F.2d 15, 18 (1st Cir. 1979) (amended pleadings typically allowed “in the absence of any apparent or declared reason such as undue delay, bad faith or dilatory motive on the part of movant, repeated failure to cure deficiencies by amendments previously allowed, undue prejudice to the opposing party, [or] futility of the amendment.”). As described above, there was no bad faith or dilatory motive on movants’ part; because discovery has just started, there is no undue delay or undue prejudice to the defendants; and, because this is the first amended pleading, there’s no ‘repeated failure to cure’. The amended pleadings are not futile, as all of the elements of each cause of action has been pled.

When deciding motions for leave to file an amended pleading, the present status of discovery is a primary consideration. See, e.g., *Grant v. News Group*, 55 F.3d 1, 6 (1st Cir. 1979) (affirming the district court’s denial of a motion to amend which had been submitted after the close of discovery); *Stepanischen v. Merchants Despatch Transp. Corp.*, 722 F.2d 922, 933 (1st

Memorandum in support of
Plaintiffs' Motion for Leave to File
an Amended Complaint

REDACTED VERSION; FILED VIA ECF
(complete version being filed by hand with the Court)

Cir. 1983) (filing a motion to amend, filed ten days prior to the close of discovery, showed undue delay); *Acosta-Mestre v. Hilton Int'l of P.R., Inc.*, 156 F. 3d 49 (1st Cir. 1998) (affirming denial of leave to amend where motion had been filed after discovery period had expired). As discussed above, discovery has barely begun in this case.

The same set of facts underlies all of the additional causes of action being asserted in the [Proposed] Amended Complaint.

unbeknownst to plaintiffs, defendants
filed another patent application reciting the same subject matter

See, e.g., ¶32-33, **Ex. 1**, [Proposed] Amended Complaint. That
patent application led to the present patent-in-suit, the '972 patent.

If this motion for leave to file a [Proposed] Amended Complaint is denied, plaintiffs will
be forced to file a separate action seeking the same relief. Because the additional causes of
action in the [Proposed] Amended Complaint concern inventorship of the same subject matter

Memorandum in support of
Plaintiffs' Motion for Leave to File
an Amended Complaint

REDACTED VERSION; FILED VIA ECF
(complete version being filed by hand with the Court)

whose inventorship is presently being contested in this litigation, most of the deponents and witnesses in this action would end up testifying again in the other action, and the separate trials would cover many of the same issues. In terms of judicial efficiency, this would be wastefully duplicative.

have been added to the [Proposed] Amended Complaint. As noted, defendants' fraudulent behavior in regards to the subject matter presently in dispute in this action is the basis for the additional counts in the [Proposed] Amended Complaint. Specifically, the [Proposed] Amended Complaint pleads the following causes of action:

- Count 1: Correction of Inventorship of the '972 patent under 35 U.S.C. §256, i.e., declare plaintiffs Miller and Hoyt inventors (this Count was pled in the original complaint);
- Count 2: Breach of Covenant of Good Faith and Fair Dealing;
- Count 3: Unjust Enrichment;
- Count 4: Intentional and/or Negligent Misrepresentation, Common Law Fraud, and/or Fraudulent Inducement;
- Count 5: Breach of Fiduciary Duty;
- Count 6: Conversion and/or Misappropriation of Patentable Invention;
- Count 7: Unfair and/or Deceptive Acts and/or Practices under ch. 93A, Mass. Gen. L.
- Count 8: Claims under the Racketeer Influenced and Corrupt Organizations (RICO) Act, 18 U.S.C. §§1961-1968
- Count 9: Common Law Civil Conspiracy
- Count 10: Correction of Inventorship of the '476 patent under 35 U.S.C. §256 (alternative relief;

The Court must "examine the totality of the circumstances and exercise sound discretion in light of the pertinent balance of equitable considerations" when deciding a belated motion to amend the pleadings. *Quaker State Oil Ref. Corp. v. Garrity Oil Co.*, 884 F.2d 1510, 1517 (1st Cir. 1979). In light of defendants' fraudulent behavior concerning the subject matter currently in

Memorandum in support of
Plaintiffs' Motion for Leave to File
an Amended Complaint

REDACTED VERSION; FILED VIA ECF
(complete version being filed by hand with the Court)

dispute in this litigation, the equitable considerations and the totality of the circumstances also weigh in favor of allowing plaintiffs to file the attached [Proposed] Amended Complaint.

Accordingly, for all of the foregoing reasons, plaintiffs respectfully request that the Court exercise its discretion to extend the deadline in the original scheduling order for filing amended pleadings, and grant plaintiffs leave to file the attached [Proposed] Amended Complaint.

Respectfully submitted,

**PETER J. MILLER, CLIFFORD HOYT,
and CAMBRIDGE RESEARCH AND
INSTRUMENTATION, INC.,**

By their attorneys:

Dated: May 18, 2006

/s/ Teodor Holmberg
Martin B. Pavane
Teodor J. Holmberg (BBO# 634708)
COHEN, PONTANI, LIEBERMAN AND
PAVANE
551 Fifth Avenue
New York, New York 10176
Tel. (212) 687-2770
Fax (212) 972-5487
E-mail: tidge@cplplaw.com

Brian L. Michaelis (BBO# 555159)
Erin E. McLaughlin (BBO# 647750)
Brown Rudnick Berlack Israels LLP
One Financial Center
Boston, MA 02111
Tel. (617) 856-8200
Fax (617) 856-8201
E-mail: BMichaelis@brownrudnick.com

Memorandum in support of
Plaintiffs' Motion for Leave to File
an Amended Complaint

REDACTED VERSION; FILED VIA ECF
(complete version being filed by hand with the Court)

CERTIFICATE OF SERVICE

I hereby certify that the document identified in the top right-hand portion of this page and filed through the ECF system will be sent electronically to the registered participants as identified on the Notice of Electronic Filing (NEF) on May 18, 2006.

/s/ Teodor Holmberg
Teodor J. Holmberg (BBO# 634708)

I hereby further certify that an unredacted complete copy of this document is being filed by hand with the Court, as an attachment to a Motion to Impound, and that an unredacted complete copy of this document is being served, by first class mail, on May 18, 2006 on.

Anthony J. Fitzpatrick, Esq.
DUANE MORRIS LLP
470 Atlantic Avenue, Suite 500
Boston, MA 02210
617-289-9220 (phone)
617-289-9201 (fax)
ajfitzpatrick@duanemorris.com

Paul D. Weller, Esq.
MORGAN, LEWIS & BOCKIUS LLP
1701 Market Street
Philadelphia, PA 19103

/s/ Teodor Holmberg
Teodor J. Holmberg (BBO# 634708)

**IN THE UNITED STATES DISTRICT COURT FOR THE
DISTRICT OF MASSACHUSETTS**

PETER J. MILLER, an individual,
CLIFFORD HOYT, an individual, and
CAMBRIDGE RESEARCH AND
INSTRUMENTATION, INC.,
a Delaware corporation,

Plaintiffs,

v.

PATRICK TREADO, an individual, and
CHEMIMAGE CORP., a Delaware
corporation,

Defendants.

Civil Action No. 05-10367-RWZ

**[PROPOSED]
AMENDED COMPLAINT**

Plaintiffs Cambridge Research and Instrumentation, Inc. ("CRI"), Peter J. Miller, and Clifford Hoyt, by their attorneys COHEN, PONTANI, LIEBERMAN & PAVANE, submit this [Proposed] Amended Complaint, which will replace plaintiffs' originally filed February 24, 2005 Complaint [D.E. 1].

[**NOTE****: PORTIONS OF THIS [PROPOSED] AMENDED COMPLAINT HAVE BEEN REDACTED. A SEPARATE MOTION TO IMPOUND IS BEING FILED BY HAND WITH A COMPLETE COPY OF THIS DOCUMENT. THE REASONS FOR REDACTION ARE EXPLAINED IN THE MOTION TO IMPOUND.]**

REDACTED VERSION, FILED VIA ECF
(complete version being filed by hand with the Court)

[Proposed] Amended Complaint

PARTIES

1. Plaintiff Cambridge Research and Instrumentation, Inc. ("CRI") is a corporation incorporated under the laws of the State of Delaware and has its principal place of business in the State of Massachusetts. Founded in 1985, CRI develops and sells precision equipment for the measurement and control of light. Such equipment includes, but is not limited to, liquid crystal tunable filters, microscope accessories, and scientific measurement apparatus.

2. CRI has been, and still is, a leading innovator in liquid crystal tunable filter technology. As stated by defendant Patrick Treado during the relevant time of collaboration between CRI and Treado, "CRI's liquid crystal tunable filter (LCTF) technology represents a revolutionary enhancement in imaging spectrometer technology" **Ex. L**, CRI000703, October 28, 1996 letter from Treado to Miller (further stating: "I look forward to CRI's continued success in the development of high-quality LCTF technology for Raman imaging.").

3. Plaintiffs Peter J. Miller and Clifford Hoyt are individuals residing in the State of Massachusetts, are presently employed by CRI, and have been employed by CRI at all times relevant herein.

4. Defendant ChemImage Corporation, formerly known as ChemIcon, Inc. (collectively, "ChemImage"), is a corporation incorporated under the laws of the State of Delaware and has its principal place of business in Pittsburgh, Pennsylvania. ChemImage sells, among other things, Raman imaging microscopy systems.

5. Defendant Patrick Treado is an individual residing in the State of Pennsylvania, and is presently the Chief Technology Officer of ChemImage. Treado was a founder of ChemImage and has been president of ChemImage at times relevant herein.

REDACTED VERSION, FILED VIA ECF
(complete version being filed by hand with the Court)

[Proposed] Amended Complaint

JURISDICTION

6. This is, *inter alia*, an action for inventorship under 35 U.S.C. §256, over which the court has jurisdiction pursuant to 28 U.S.C. §1338(a), and an action for violations of the Racketeer Influenced and Corrupt Organizations (RICO) Act, 18 U.S.C. §§1961-1968, over which the court has jurisdiction pursuant to 18 U.S.C. §1964(c). This is also an action arising under the laws of the State of Massachusetts, over which the court has supplemental jurisdiction pursuant to 28 U.S.C. §1367(a), including, *inter alia*, an action for unfair competition, over which the court has jurisdiction pursuant to 28 U.S.C. §1338(b).

BACKGROUND

7. On January 27, 1993, defendant Patrick Treado contacted plaintiff CRI, and, in particular, plaintiff Clifford Hoyt at CRI, to discuss the use of Liquid Crystal Tunable Filters (LCTFs) in Raman imaging applications. See, e.g., **Exhibit A**, Hoyt's handwritten notes memorializing telephone call (CRI000131-2).

8. This marked the beginning of a collaboration among defendants Treado and ChemImage and plaintiffs CRI, Hoyt, and Miller that lasted at least three years. In the beginning, CRI loaned ChemImage at least one LCTF for use in the collaboration (see, e.g., **Exhibit B**, Treado's letter concerning loan of LCTF, CRI000119), and then became deeply involved in the creation of new devices for Raman imaging using LCTFs, as will be more fully described below.

9. Hoyt and Treado collaborated on writing an article on the use of LCTFs in Raman Imaging in the fall of 1993, which appeared in 1994. See, e.g., **Exhibit C**, Hoyt's edits of the article (CRI000120-126); and **Exhibit D**, H. Morris, C. Hoyt, and P. Treado, "Imaging Spectrometers for Fluorescence and Raman Microscopy: Acousto-Optic and Liquid Crystal Tunable Filters", *Applied Spectroscopy*, vol. 48, no. 7, 1994 (e.g., CRI002409-18).

10. During the time period between January 27, 1993, and December 22, 1993, Hoyt invented the concept of using "infinite space", or infinity-corrected optics, in a Raman

REDACTED VERSION, FILED VIA ECF
(complete version being filed by hand with the Court)

[Proposed] Amended Complaint

imaging device using an LCTF spectrometer, a feature discussed in the *Applied Spectroscopy* article described above (**Ex. C**).

11. After the collaborative article had been accepted for publication, Treado wrote to Hoyt, indicating his intent to continue collaborating, but with focus more on the Near Infrared spectral region ("NIR"). **Exhibit E**, April 27, 1994 note from Treado to Hoyt ("Enclosed is the formal acceptance of the LCTF paper. Let's do it again with NIR filters!") (CRI000118). See also **Exhibit F**, January 10, 1994 handwritten notes of Hoyt ("... Treado ... very excited about Raman prospects ...") (CRI000135-136).

12. The collaboration continued through 1994, while the collaborators discussed and sought funding from different sources. See, e.g., **Exhibit G**, October 21, 1994 letter from Treado to Hoyt, discussing prospective means of funding their further collaboration ("Of course, NIMH is not the only institute that can be targeted for funding.") (CRI000137-139).

13. One of their attempts to obtain funding was via a Small Business Innovation Research (SBIR) Phase I Proposal entitled "High Definition Raman Imaging Microscope" which CRI filed with the National Science Foundation (NSF) in June 1994. **Exhibit H**, 1994 SBIR Proposal (CRI000582-605). Plaintiff Peter J. Miller was listed as the Principal Investigator/Project Director (PI) in the SBIR Phase I Proposal, Hoyt was identified as a "[k]ey CRI researcher", and Treado was listed as a consultant. Treado assisted in the preparation of the SBIR Phase I Proposal.

14. The Phase I Proposal proposed building a chemical imaging system having (a) an illumination source; (b) infinity-corrected optics for collecting and collimating light from an area illuminated by the light source; (c) a Lyot-based LCTF for an imaging spectrometer; and (d) a CCD (charge-coupled device) camera for collecting images from the imaging spectrometer.

15. The Phase I Proposal states that "[t]he first use of LCTF for Raman Microscope was performed at the University of Pittsburgh in a collaborative effort between CRI researchers and Prof. Treado." See **Ex. H**, Sect. E.3 (CRI000589).

16. The June 1994 SBIR Phase I Proposal was rejected on formal grounds, and

REDACTED VERSION, FILED VIA ECF
(complete version being filed by hand with the Court)

[Proposed] Amended Complaint

CRI filed an identical proposal the following year. **Exhibit I**, 1995 SBIR Proposal (CRI000611-635). Once again, Miller was listed as Principal Investigator/Project Director (PI), Hoyt was identified as the "[k]ey CRI researcher", and Treado was listed as a consultant. See, e.g., **Exhibit J**, June 8, 1995 Letter from Treado to Miller, which was an attached exhibit to the 1995 SBIR Phase I Proposal ("... I am providing this letter in support of CRI's Phase I SBIR application ...") (CRI000636).

17. The 1995 Phase I Proposal contemplated using a Lyot-based filter design for the LCTF. See **Ex. I**, CRI000614.

18. However, the Lyot-based LCTF design did not perform well, and Miller began pursuing alternative LCTF designs. During this period, Miller conceived and constructively reduced to practice a new design based on an Evans split-element retarder filter. See, e.g., **Exhibit K**, Final Report for Phase I (CRI000639-664) ("[t]he principal limitation of [the Lyot-based] design is its relatively low transmission, which ranges from 7 to 16 percent. A novel design was devised to overcome this problem, and a model was developed of this new design. Based on the Evans split-element retarder, it should nearly treble the throughput of the LCTF, as described in Section IV, Key Improvements for Phase II." CRI000645).

19. In October 1996, CRI filed a SBIR Phase II Proposal entitled "High Definition Raman Imaging Microscope" with the NSF. **Exhibit L**, 1996 SBIR Phase II Proposal (CRI000665-704). The SBIR Phase II Proposal again listed plaintiff Peter J. Miller as the Principal Investigator/Project Director (PI), and defendant Patrick Treado as a consultant. Defendant Patrick Treado assisted in the preparation of the SBIR Phase II Proposal.

20. As stated therein, the proposed Phase II research would "build on the successful imaging Raman instrument demonstrated in Phase I" and, specifically, that "key improvements will be made: transmission will be doubled (or more) based on a high-efficiency design identified in Phase I, and the long-wavelength limit will be extended from the present 700 nm to 1050 nm. Such an LCTF appears to offer near-revolutionary benefits in certain applications including semiconductor analysis, biomedical imaging, and pharmaceutical research." **Ex. L**, CRI000666.

REDACTED VERSION, FILED VIA ECF
(complete version being filed by hand with the Court)

[Proposed] Amended Complaint

21. One attachment to the SBIR Phase II Proposal was an SBIR Phase III Follow-on Funding Commitment statement signed by Treado, then president of ChemImage (then called "ChemIcon"), on October 24, 1996, and Peter Foukal, president of CRI, on October 25, 1996, in which the first paragraph read:

Whereas ChemIcon Inc. of Pittsburgh, PA desires to obtain access to the LCTF Raman imaging technology being developed by Cambridge Research & Instrumentation, Inc. (CRI) of Cambridge, MA, with application development support from Patrick J. Treado and the University of Pittsburgh, ChemIcon agrees to provide long-term funding to gain access to this technology, in the amount of \$200,000 against which Cambridge Research & Instrumentation will provide LCTF Raman imaging tunable filters.

Ex. L (CRI000702).

22. Thus, the final chemical imaging device produced as a result of the SBIR grants comprised at least the following components: (a) a laser; (b) an infinity-corrected objective (i.e., an objective which produces a collimated beam); (c) an Evans Split-Element LCTF for producing a filtered Raman chemical image; and (d) a detector for collecting the filtered Raman image.

23. Unbeknownst to plaintiffs, on April 22, 1998, Treado filed U.S. Patent App. Ser. No. 09/064,347 with the United States Patent and Trademark Office (PTO). **Exhibit M**, the '347 application (CRI001739-1755). Also submitted with the application is a declaration signed by Treado stating that Treado was the sole inventor of the invention described in the '347 application. The Abstract provides a concise description of what Treado swore he invented:

A Raman chemical imaging system uses a laser illumination source for illuminating an area of a sample. The spectrum of scattered light from the illuminated area of the sample is collected and a collimated beam is produced therefrom. An Evans Split-Element type liquid crystal tunable filter (LCTF) selects a Raman image of the collimated beam. A detector collects the filtered Raman images which are subsequently processed to determine the constituent materials. The Evans Split-Element-type LCTF suitable for high-definition Raman chemical imaging is incorporated into an efficient Raman imaging system that provides significant performance advantages relative to any previous approach to Raman microscopy. The LCTF and associated optical path is physically compact, which accommodates integration of the LCTF within an

REDACTED VERSION, FILED VIA ECF
(complete version being filed by hand with the Court)

[Proposed] Amended Complaint

infinity-corrected optical microscope. The LCTF simultaneously provides diffraction-limited spatial resolution and 9 cm^4 spectral bandpass across the full free spectral range of the imaging spectrometer. The LCTF Raman microscope successfully integrates the utility of optical imaging and the analytical capabilities of Raman spectroscopy which has practical significance in materials analysis, including the diagnosis of cancer.

Exhibit M, CRI001755

24. In the '347 application, Treado emphasizes the use of an Evans Split-Element LCTF as a breakthrough in Raman spectroscopy. See, e.g., **Ex. M**, CRI001742-3 ("The Evans Split-Element LCTF represents a breakthrough technology because it provides spectral resolution comparable to a single stage dispersive monochromator while also providing diffraction-limited spatial resolution."); CRI001746-7 ("An objective of this invention is to provide an LCTF suitable for Raman imaging which can readily and rapidly distinguish between various materials. The LCTF, an Evans Split-Element-type filter, provides ..."); CRI001749-50 ("However, traditional Raman spectroscopy is unable to distinguish between benign and malignant tissue. However, use of a Evans Split-Element LCTF provides the ability to distinguish between normal tissue, malignant tissue, and benign tissue.").

25. Passages in the '347 application are almost-verbatim copies of language in the SBIR proposals. Compare, e.g., the following passage from the '347 application:

The LCTF Split-Element design includes a high-order fixed retarder of thickness D , having retardance R_h , constructed as two elements of thickness $D/2$, with their fast and slow axes crossed. A low-order retarder of retardance R_l is interposed with its fast axis at 45° to that of the $D/2$ elements. Each retarder has an associated liquid crystal tuning element. Such an assembly, placed between suitably oriented crossed polarizers, has a transmission of

$$T(\lambda) = \sin^2(\pi R_l / \lambda) \times \sin^2(\pi R_h / \lambda)$$

The split-element stage is equivalent in its spectral performance to two Lyot stages. By constructing the LCTF as groups of split-element stages, one collapses an N -stage Lyot filter into $N/2$ split-element Lyot stages, and reduces the number of polarizers by $N/2$. The reduction of polarizers is compensated by the increased number of liquid crystal tuning elements which enhance the overall optical throughput.

Ex. M, CRI001749

REDACTED VERSION, FILED VIA ECF
(complete version being filed by hand with the Court)

[Proposed] Amended Complaint

with this passage from the SBIR Phase II Proposal:

The Evans design is illustrated in Figure 6: a high-order fixed retarder of thickness D and retardance R_h is constructed as two elements of thickness $D/2$, with their fast and slow axes crossed, and a low-order retarder of retardance R_l is interposed with its fast axis at 45° to that of the $D/2$ elements. Each retarder has an associated liquid crystal tuning element. Such an assembly, placed between suitably oriented crossed polarizers, has a transmission of

$$T(\lambda) = \sin^2(\pi R_l / \lambda) \times \sin^2(\pi R_h / \lambda)$$

...

so an Evans split-element stage is equivalent in its spectral structure to two Lyot stages. By constructing the LCTF as groups of Evans split stages, one collapses an N -stage Lyot filter into $N/2$ Evans stages, and reduces the number of polarizers by $N/2$.

...

The increase in liquid crystal elements is equal to the decrease in polarizers. However, the loss per polarizer is much higher than that of a liquid crystal cell, so the result is an increase in efficiency.

Ex. L, CRI000672

26. To overcome a prior art rejection during prosecution of the '347 application, Treado submitted a sworn declaration explaining why the Evans Split-Element LCTF is far superior to other LCTFs and/or AOTFs (Acousto-Optical Tunable Filters) for Raman chemical imaging and why no one else would have thought of using an Evans Split-Element LCTF for Raman Chemical Imaging. **Exhibit N**, Treado's Rule 1.132 Declaration, CRI001867-CRI001874. See, e.g., CRI001867 ("Persons having ordinary skill in the art of Raman imaging would not have thought to use an Evans Split Element liquid crystal tunable filter (LCTF) in place of traditional liquid crystal filters."); CRI001868 ("Prior to my invention, Evans Split Element LCTFs were never previously envisioned for Raman imaging," going on to mention the "Treado/Morris article ... in 1989" as an example that "[o]ther researchers in the field of Raman imaging were not active in the tunable filter field"); and CRI001869 ("Prior to my invention, the Evans Split Element filter was thought to not have sufficient spectral resolution for Raman spectroscopy applications. Today, due to my work, it is becoming widely recognized that Evans Split Element LCTFs are a superior technology for Raman imaging when incorporated into a well designed chemical imaging system. However, those practiced in Raman spectroscopy and imaging

REDACTED VERSION, FILED VIA ECF
(complete version being filed by hand with the Court)

[Proposed] Amended Complaint

prior to 1998 would have assessed the performance of Evans Split Element technology based on traditional measures of Raman instrument performance and would likely have rejected the technology.”).

27. The PTO Examiner stated repeatedly that the only difference between the cited prior art and Treado’s invention was the use of an Evans Split Element liquid crystal filter. See, e.g., May 28, 1999 Office Action. When the ‘347 application issued as U.S. Pat. No. 6,002,476 on December 14, 1999 (“the ‘476 patent”), its sole independent claim was directed to a chemical imaging system comprising: (a) a laser; (b) an infinity-corrected objective (i.e., an objective which produces a collimated beam); (c) an Evans Split-Element LCTF for producing a filtered Raman chemical image from the collimated beam; and (d) a detector for collecting the filtered Raman image. **Exhibit O**, the ‘476 patent, CRI001156-1164; see Claim 1 on CRI001164.

28. At no point did Treado or anyone involved with the prosecution of the ‘347 application inform CRI, Miller, or Hoyt of the filing of the ‘347 application. Nor did anyone involved with the prosecution of the ‘347 application disclose to the PTO the collaboration between Treado, ChemImage, CRI, Miller, and Hoyt which resulted in a chemical imaging system having all the elements of Claim 1 of the ‘476 patent.

REDACTED VERSION, FILED VIA ECF
(complete version being filed by hand with the Court)

[Proposed] Amended Complaint

32. On October 13, 2000, Michael Dever, Esq.
filed provisional patent
application serial number 60/239,969 ("the Provisional Application") entitled "Near

REDACTED VERSION, FILED VIA ECF
(complete version being filed by hand with the Court)

[Proposed] Amended Complaint

Infrared Chemical Imaging Microscope" with the United States Patent and Trademark Office (PTO) listing defendant Patrick Treado, Matthew Nelson, Scott Keitzer, and Juliana Riber as inventors. **Exhibit V**, excerpts from the provisional application, CRI001524-CRI001525 (the provisional application cover sheet); CRI001188-CRI001192; CRI001219-CRI001224; CRI001252.

33. The Provisional Application contained over 300 pages of material, including many lab notebooks, though none of the lab notebook pages appears to be dated before 1999. The Provisional Application described an imaging system for Raman chemical imaging in the NIR (**Ex. V**, e.g., CRI001214, CRI001220, CRI001222), comprising (a) a light source, which may be a laser (**Ex. V**, e.g., CRI001252); (b) an infinity-corrected objective (**Ex. V**, e.g., CRI001188, CRI001191); (c) an Evans Split-Element LCTF for producing a Raman chemical image (**Ex. V**, e.g., CRI001190, CRI001220); and (d) a detector for collecting the Raman chemical image (**Ex. V**, e.g., CRI001188, CRI001191, CRI001220).

34. Upon information and belief, the device used by ChemImage, Treado, et al. to generate the reports and data in the Provisional Application was a FALCON Microscope having the CRI-invented and CRI-built Evans Split-Element LCTF. See, e.g., **Ex. V**, CRI001220.

REDACTED VERSION, FILED VIA ECF
(complete version being filed by hand with the Court)

[Proposed] Amended Complaint

37. On October 12, 2001, ChemImage filed with the PTO regular U.S. Patent App. Ser. No. 09/976,391 ("the '391 application") entitled "Near Infrared Chemical Imaging Microscope" which claimed priority from the Provisional Application, listing defendant Patrick Treado, Matthew Nelson, and Scott Keitzer as inventors. **Exhibit Y**, the '391 application (CRI001641-CRI001679).

38. Independent claim 1 of the '391 application as filed recites a chemical imaging system for near infrared radiation comprising (a) a near infrared illumination source, (b) a device for collecting and collimating light from an area illuminated by the illumination source, (c) a near infrared imaging spectrometer for selecting images of said collimated light, and (d) a detector for collecting the images. See **Ex. Y**, CRI001667.

39. Claim 3 of the '391 application recites that the collecting/collimating device (b) in claim 1 may comprise a "refractive type infinity-corrected near infrared optimized microscope objective." See **Ex. Y**, CRI001667.

40. Claim 4 of the '391 application recites that the imaging spectrometer (d) in claim 1 may comprise an "Evans Split-Element liquid crystal tunable" filter. See **Ex. Y**, CRI001667.

41. Thus, the claims of the '391 application covered the subject matter of the '476 patent (and, *a fortiori*, the subject matter of the CRI/ChemImage collaboration), namely, a Raman imaging system with a light source, an infinity-corrected objective, an Evans Split-Element LCTF operating as a spectrometer, and a detector.

43. In an assignment dated January 2004 and recorded at Reel/Frame 014302/0906 at the PTO, defendant Patrick Treado, Matthew Nelson, and Scott Keitzer assigned their rights in the '391 application to defendant ChemImage. **Exhibit Z**, Assignment of '391 application (CRI002027-CRI002033)

REDACTED VERSION, FILED VIA ECF
(complete version being filed by hand with the Court)

[Proposed] Amended Complaint

44. At no point during the prosecution of the '391 application did defendants ChemImage or Patrick Treado inform the PTO of the previous CRI/ChemImage collaboration on Raman imaging microscopes with integrated Evans split-element filters and collected collimated light. Nor did defendants ChemImage and Patrick Treado inform plaintiffs CRI, Peter J. Miller, or Clifford Hoyt of either the Provisional Application or the '391 application.

45. On May 11, 2004, the '391 application issued as U.S. Patent Number 6,734,962 ("the '962 patent"). **Exhibit AA**, the '962 patent (CRI001536-CRI001551).

46. Promptly upon learning of the '962 patent, plaintiff CRI contacted defendant ChemImage about ChemImage's attempt through the claims of the '962 patent to recapture the technology resulting from the CRI/ChemImage collaboration

and demanded that defendants execute a Covenant Not to Sue. Counsel for defendant ChemImage's final response was that defendants found plaintiffs' inventorship contentions "utterly without merit". **Exhibit BB**, January 20, 2005 letter from Daniel H. Golub to Martin B. Pavane (CRI003044-CRI003045).

47. On February 24, 2005, plaintiffs commenced this action by filing the original complaint. [D.E. 1]. Count 1 of the original complaint, which is still pending, sought an order under 35 U.S.C. §256 correcting inventorship of the '962 patent by naming plaintiffs Peter J. Miller and Clifford Hoyt as inventors.

48. More than one month after plaintiffs commenced this action, and unbeknownst to plaintiffs, on April 11, 2005, defendants filed an application with the PTO to "reissue" the '962 patent. **Exhibit CC**, Reissue Declaration of U.S. Reissue App. Ser. No. 11/103,423 ("the Reissue application") (CRI002954-CRI002959). In the sworn Reissue Declaration, defendant Treado, Nelson, and Keitzer assert that they "are **the original and first inventor(s)** of the subject matter which is described and claimed in United States Patent No. 6,734,962 ..." (emphasis added) — the very assertion that plaintiffs are contesting in this litigation. **Ex. CC**, CRI002954.

49. Defendants' Reissue application makes no mention of the inventorship issue

REDACTED VERSION, FILED VIA ECF
(complete version being filed by hand with the Court)

[Proposed] Amended Complaint

raised in plaintiffs' original complaint. Instead, the Reissue application alleges that the named inventors had misunderstood the prior art during the prosecution of the '962 patent. Specifically, Treado, Nelson, and Keitzer declare in the reissue oath that "we may have claimed more than we were entitled to claim ... in view of" two prior art articles, both of which were co-written by Treado. **Ex. CC**, item (6)(e) on page CRI002955. Treado, Nelson, and Keitzer further declare that "we failed to appreciate this error during the prosecution of the patent application." **Ex. CC**, item (6)(f) on page CRI002955. In other words, defendant Treado alleges that he did not understand that the claims of the '962 patent covered subject matter disclosed in the two prior art references he co-wrote.

50. Ostensibly to correct this error, defendant Treado, Nelson, and Keitzer seek in the Reissue application to, *inter alia*, delete the term "scattered" from the claims. **Ex. CC**, item (6)(e) on page CRI002955, item (6)(g) on page CRI002956, and item (6)(i) on pages CRI002957-CRI002958. Upon information and belief, because the deleted term "scattered" connotes Raman scattering (and thus Raman imaging), the true intent of the deletion is to revise the '962 patent claims such that they no longer cover the invention which resulted from the CRI/ChemImage collaboration (which was directed to Raman imaging), i.e., the defendants hope, by excluding Raman imaging from the claims of the '962 patent, to obtain claims for which plaintiffs Miller and Hoyt are not inventors (thereby extinguishing Miller's and Hoyt's rights in the '962 patent).

51. Within two weeks of filing the Reissue application, defendants Treado and ChemImage moved this Court to stay the present litigation in favor of their just-filed Reissue application, claiming that plaintiffs' "inventorship ... claims will be mooted" by the narrowing of the '962 patent claims in the reissue proceedings. See Defendants' April 29, 2005 Motion to, *inter alia*, Stay Count 1 (Inventorship), [D.E. 2], page 10 (emphasis in original). The Court did not stay Count 1. See the Court's June 17, 2005 Order.

52. A reissue oath "must be signed and sworn to or declaration made by the inventor or inventors" and "must be accompanied by the written consent of all assignees." 37 C.F.R. §1.172.

53. Because plaintiffs Miller and Hoyt are inventors of the '962 patent, and they

REDACTED VERSION, FILED VIA ECF
(complete version being filed by hand with the Court)

[Proposed] Amended Complaint

have not assigned their rights to an assignee, defendants' reissue oath required the signatures of Miller and Hoyt. The filing of the reissue oath without all of the inventors' signatures renders defendants' entire Reissue application invalid *ab initio*.

54. Before the '391 application issued as the '962 patent, defendants ChemImage and Patrick Treado filed continuation patent application serial number 10/773,077 ("the '077 application") and continuation-in-part patent application serial number 10/610,481 ("the '481 application"), both of which claim priority from the Provisional Application and the '391 application.

55. The '077 application was abandoned on April 3, 2005. Upon information and belief, this abandonment was deliberate. **Exhibit DD**, August 22, 2005 Notice of Abandonment (CRI002158-CRI002159) (the deliberateness of the abandonment is shown by the fact that it was "[c]onfirmed with Mr. Golub [patent attorney for defendants] on 8/19/2005").

56. On October 5, 2005, defendant ChemImage filed a Petition to Revive the '077 application based on "unintentional" abandonment. **Exhibit EE**, October 5, 2005 Petition to Revive (CRI002851-CRI002852). Despite the fact, upon information and belief, that the '077 application was deliberately abandoned, Golub, defendant ChemImage's patent attorney, swore that the "entire delay in filing the required reply from the due date for the required reply [April 3, 2005] until the filing of a grantable petition under 37 CFR 1.137(b) [October 5, 2005] was unintentional." **Ex. EE**, CRI02852.

57. Upon information and belief, the Petition to Revive the '077 application was fraudulent. See, e.g., Manual of Patent Examining Procedure ("MPEP"), §711.03(c) ("A delay resulting from a deliberately chosen course of action on the part of the applicant is not an 'unintentional' delay within the meaning of 37 1.137(b)."). However, the PTO's policy is to accept the word of the patent attorney signing the Petition, and typically does not review the facts of the abandonment unless prompted to do so. Thus, accepting Golub's word that the abandonment was unintentional, the PTO granted ChemImage's Petition to Revive the '077 application on January 13, 2006. **Exhibit FF**, January 13, 2006 PTO Decision on Petition to Revive (CRI002900).

REDACTED VERSION, FILED VIA ECF
(complete version being filed by hand with the Court)

[Proposed] Amended Complaint

58. Since the beginning of this lawsuit, ChemImage has filed eight continuing applications claiming priority from the '077 application (and thus from the '962 patent being presently litigated); seven of those applications claim priority from the revived '077 application, and three of these applications were filed in the last three months. **Exhibit GG**, PTO Website Continuity Data for the '077 application (CRI004137). The eight applications are: U.S. Pat. App. Ser. Nos. 11/091,126; 11/256,889; 11/257,139; 11/257,219; 11/257,222; 11/366,129; 11/366,762; and 11/366,887. See **Ex. GG**.

59. At least one of the eight applications claims an NIR chemical imaging system capable of Raman imaging comprising an illumination source, an infinity-corrected objective, a spectrometer, and a detector. **Exhibit HH**, Preliminary Amendment in U.S. Pat. Ser. No. 11/091,126 (CRI004138-CRI004142).

60. Because five of the eight patent applications claiming priority from the '077 application have not been published, the subject matter of their claims is unknown, and therefore the plaintiffs do not know whether any of those five applications claim the subject matter invented by plaintiffs Miller and Hoyt.

61. Upon information and belief, (a) the fraudulent revival, after the commencement of the present litigation, of the '077 application, and/or (b) the filing, after commencement of the present litigation, of at least one of the eight continuing applications claiming priority from the '077 application are for the improper purpose of once again claiming subject matter invented by the plaintiffs.

COUNT 1: CORRECTION OF INVENTORSHIP OF '962 PATENT

62. Plaintiffs repeat and reallege the assertions set forth in paragraphs 1 through 61.

63. Plaintiff Peter J. Miller, individually and/or in collaboration with defendant Patrick Treado, contributed to the invention of one or more claims in the '962 patent, including, for example, Miller's conception of the use of an Evans Split-Element liquid crystal tunable filter in a chemical imaging system using near infrared radiation as recited in claim 4 of the '962 patent.

64. Plaintiff Clifford Hoyt, individually and/or in collaboration with defendant Patrick Treado, contributed to the invention of one or more claims in the '962 patent,

REDACTED VERSION, FILED VIA ECF
(complete version being filed by hand with the Court)

[Proposed] Amended Complaint

including, for example, Hoyt's conception of a refractive type infinity-corrected microscope objective as the collecting/collimating device in a chemical imaging system using near infrared radiation as recited in claim 3 of the '962 patent.

65. Wherefore, plaintiffs ask the Court to (a) declare that Peter J. Miller is an inventor of subject matter claimed in one or more of the claims in the '962 patent and (b) order correction of the '962 patent under 35 U.S.C. §256 to reflect Peter J. Miller as an inventor.

66. Wherefore, plaintiffs ask the Court to (a) declare that Clifford Hoyt is an inventor of subject matter claimed in one or more of the claims in the '962 patent and (b) to order correction of the '962 patent under 35 U.S.C. §256 to reflect Clifford Hoyt as an inventor.

67. Wherefore, plaintiffs further ask the Court, if the Court declares plaintiffs Miller and Hoyt inventors of the '962 patent, to declare that U.S. Reissue App. Ser. No. 11/103,423 is null and void because the reissue oath was not signed by all inventors of the original '962 patent.

COUNT 2: BREACH OF COVENANT OF GOOD FAITH AND FAIR DEALING

68. Plaintiffs repeat and reallege the assertions set forth in paragraphs 1 through 67.

70. defendants filed a new patent application (the '391 application) which explicitly claimed the subject matter claimed in the '476 patent. The '391 application issued as the '962 patent on May 11, 2004.

REDACTED VERSION, FILED VIA ECF
(complete version being filed by hand with the Court)

[Proposed] Amended Complaint

75. Wherefore, , plaintiffs ask the Court that plaintiffs Hoyt and Miller be declared inventors of the '476 patent under 35 U.S.C. §256 (see Count 10 below), and that the Court further declare that any patent claiming priority to the '347 application is unenforceable against plaintiffs, plaintiffs' agents, plaintiffs' customers (including end users), and plaintiffs' suppliers because of defendants' unclean hands in the filing of the '391 application.

COUNT 3: UNJUST ENRICHMENT

76. Plaintiffs repeat and reallege the assertions set forth in paragraphs 1 through 75.

77. As detailed above, because of defendants' unjust conduct, defendants have received the '476 and '962 patents

. Benefits of enrichment were conferred on defendants ChemImage and Treado by these and other results of their unjust conduct, and those benefits have been to the detriment of plaintiffs.

78. Upon information and belief, defendants ChemImage and Treado have been conferred benefits, including, but not limited to, two issued patents (and any patent applications claiming priority to those two issued patents), royalties, payments, licensing

REDACTED VERSION, FILED VIA ECF
(complete version being filed by hand with the Court)

[Proposed] Amended Complaint

fees, and/or other compensation from those patents and patent applications, as well as the right to enforce the issued patents, including the right to seek an injunction against others who are manufacturing and/or using plaintiffs' invention.

79. Upon information and belief, defendants ChemImage and Treado have been conferred further benefits, including, but not limited to, publicly presenting ChemImage's employees as sole inventors, and ChemImage as the sole owner, of the two issued patents.

81. Defendants' retention of these and other benefits have been to the detriment of the plaintiffs. Because these benefits resulted, at least partially, from defendants' unjust conduct regarding plaintiffs' invention, the retention of those benefits by the defendants is unjust.

82. Wherefore, plaintiffs ask the court to find defendants ChemImage and Treado jointly, severally, and/or singly liable to plaintiffs for defendants' unjust enrichment.

83. Wherefore, plaintiffs ask the Court to order defendants ChemImage and Treado to make appropriate restitution of any profits, revenues, and benefits to the extent and in the amount deemed appropriate by the court, and such other relief as the Court deems just and proper to remedy defendants' unjust enrichment.

**COUNT 4: INTENTIONAL AND/OR NEGLIGENT MISREPRESENTATION,
COMMON LAW FRAUD, AND/OR FRAUDULENT INDUCEMENT**

84. Plaintiffs repeat and reallege the assertions set forth in paragraphs 1 through 83.

85. During the negotiations for the 2000 Covenant Not to Sue, defendants ChemImage and Treado repeatedly assured plaintiffs that, besides the '476 patent, ChemImage was not seeking patent protection on any of the results from the CRI/ChemImage collaboration.

REDACTED VERSION, FILED VIA ECF
(complete version being filed by hand with the Court)

[Proposed] Amended Complaint

89. Wherefore, plaintiffs ask the court to find defendants ChemImage and Treado jointly, severally, and/or singly liable to plaintiffs for intentional and/or negligent misrepresentation, common law fraud, and/or fraudulent inducement.

92. Wherefore, plaintiffs ask the Court that plaintiffs Hoyt and Miller be declared inventors of the '476 patent under 35 U.S.C. §256 (see Count 10 below), and that the Court further declare that any patent claiming priority to the '347 application is unenforceable against plaintiffs, plaintiffs' agents, plaintiffs' customers (including end users), and plaintiffs' suppliers because of defendants' unclean hands in the filing of the '391 application.

COUNT 5: BREACH OF FIDUCIARY DUTY

93. Plaintiffs repeat and reallege the assertions set forth in paragraphs 1 through 92.

REDACTED VERSION, FILED VIA ECF
(complete version being filed by hand with the Court)

[Proposed] Amended Complaint

94. The joint research conducted during the CRI/ChemImage collaboration resulted in the co-authorship of several scientific articles among plaintiffs Miller and Hoyt and defendant Treado and the development of a commercial product for sale by defendant ChemImage. By its nature, this collaboration gave rise to a relationship of trust and confidence, and thus fiduciary duty, between defendants ChemImage and Treado and plaintiffs CRI, Hoyt, and/or Miller.

96. After giving the appearance of re-establishing their previous relationship of trust and confidence, defendants ChemImage and Treado breached their concomitant fiduciary duty by attempting to, and succeeding at, patenting the invention of plaintiffs Hoyt and Miller (i.e., by filing the '391 application, which resulted in the '962 patent) and by not disclosing said activities to plaintiffs CRI, Hoyt, and Miller.

97. Wherefore, plaintiffs ask the court to find defendants ChemImage and Treado jointly, severally, and/or singly liable for breaching their fiduciary duty to plaintiffs.

REDACTED VERSION, FILED VIA ECF
(complete version being filed by hand with the Court)

[Proposed] Amended Complaint

100. Wherefore, _____, plaintiffs ask the Court
that plaintiffs Hoyt and Miller be declared inventors of the '476 patent under 35 U.S.C. §256 (see Count 10 below), and that the Court further declare that any patent claiming priority to the '391 application is unenforceable against plaintiffs, plaintiffs' agents, plaintiffs' customers (including end users), and plaintiffs' suppliers because of defendants' unclean hands in the filing of the '391 application.

COUNT 6: CONVERSION AND/OR MISAPPROPRIATION OF PATENTABLE INVENTION

101. Plaintiffs repeat and reallege the assertions set forth in paragraphs 1 through 100.

102. Because plaintiffs Hoyt and Miller were inventors of the subject matter of one or more claims of the '391 application when it was filed, plaintiffs Hoyt and Miller are and were entitled to ownership rights in the '391 application as filed, and in the '962 patent which issued from the '391 application.

103. Defendants converted and/or misappropriated plaintiffs' property when they wrongfully exercised acts of control over plaintiffs' property by filing, prosecuting, and/or assigning rights to the '391 application and/or the '962 patent which issued from the '391 application.

104. Defendants converted and/or misappropriated plaintiffs' property when they wrongfully exercised acts of control over plaintiffs' property by filing U.S. Reissue App. Ser. No. 11/103,423, which seeks to make the PTO reissue the '962 patent, and which required the signatures of plaintiffs Hoyt and Miller.

105. Defendants converted and/or misappropriated plaintiffs' property when they wrongfully exercised acts of control over plaintiffs' property by filing an amendment in U.S. Reissue App. Ser. No. 11/103,423, in which defendants sought to remove the subject matter invented by plaintiffs Hoyt and Miller, in an effort to thereby extinguish plaintiffs ownership rights in the '962 patent.

106. Defendants converted and/or misappropriated plaintiffs' property when they wrongfully exercised acts of control over plaintiffs' property by filing (or reviving), prosecuting, and/or assigning one or more patent applications claiming the subject matter invented by plaintiffs Hoyt and Miller, including, at the least, one or more of U.S. Pat. App.

REDACTED VERSION, FILED VIA ECF
(complete version being filed by hand with the Court)

[Proposed] Amended Complaint

Ser. Nos. 10/610,481 (the '481 application); 10/773,077 (the '077 application); 11/091,126; 11/257,139; and 11/257,222.

107. Upon information and belief, defendants converted and/or misappropriated plaintiffs' property when they wrongfully exercised acts of control over plaintiffs' property by filing, prosecuting, and/or assigning one or more (presently unpublished) patent applications which may claim the subject matter invented by plaintiffs Hoyt and Miller, including, at the least, one or more of U.S. Pat. App. Ser. Nos. 11/257,219; 11/366,129; 11/366,762; and 11/366,887.

108. Wherefore, plaintiffs ask the court to find defendants ChemImage and Treado jointly, severally, and/or singly liable for conversion and/or misappropriation of plaintiffs' patentable invention.

109. Wherefore, plaintiffs ask the Court to order defendants ChemImage and Treado to make appropriate restitution, in such an amount as to be determined at trial, to the plaintiffs, and such other relief as the Court deems just and proper to remedy defendants' conversion and/or misappropriation of plaintiffs' patentable invention.

COUNT 7: UNFAIR AND/OR DECEPTIVE ACTS
UNDER MASS. GEN. L., CH. 93A, §§2 AND 11

110. Plaintiffs repeat and reallege the assertions set forth in paragraphs 1 through 109.

111. The acts underlying defendants ChemImage and Treado's breach of the covenant of good faith and fair dealing ; intentional and/or negligent misrepresentation, common law fraud, and/or fraudulent inducement ; unjust enrichment at the expense of plaintiffs, breaches of fiduciary duty owed to plaintiffs CRI, Hoyt, and/or Miller, and/or misappropriation and conversion of the results of the CRI/ChemImage collaboration constitute unfair or deceptive acts or practices under Mass. Gen. L., chap. 93A, §§2 and 11.

112. Insofar as not covered by the preceding paragraphs, defendants' actions in filing, prosecuting, and/or assigning rights to the '391 application and/or the '962 patent which issued from the '391 application were at least in part for claiming ownership of

REDACTED VERSION, FILED VIA ECF
(complete version being filed by hand with the Court)

[Proposed] Amended Complaint

subject matter invented by plaintiffs and claimed in the '391 application (to which plaintiffs have an ownership right)

1. As such, defendants' actions constitute unfair or deceptive acts or practices under Mass. Gen. L., chap. 93A, §§2 and 11 because defendants' actions (1) are within at least the penumbra of some common law, statutory, or other established concept of fairness; (2) are immoral, unethical, oppressive, or unscrupulous; and (3) caused injury to plaintiffs.

113. Insofar as not covered by the preceding paragraphs, defendants' actions in filing and prosecuting U.S. Reissue App. Ser. No. 11/103,423 were at least in part an effort to extinguish plaintiffs ownership rights in the '962 patent. As such, defendants' actions constitute unfair or deceptive acts or practices under Mass. Gen. L., chap. 93A, §§2 and 11 because defendants' actions (1) are within at least the penumbra of some common law, statutory, or other established concept of fairness; (2) are immoral, unethical, oppressive, or unscrupulous; and (3) caused injury to plaintiffs.

114. Insofar as not covered by the preceding paragraphs, defendants' actions in fraudulently reviving the '077 application are believed to be at least in part for the purpose of obtaining ownership rights in the subject matter invented by plaintiffs. As such, defendants' actions constitute unfair or deceptive acts or practices under Mass. Gen. L., chap. 93A, §§2 and 11 because defendants' actions (1) are within at least the penumbra of some common law, statutory, or other established concept of fairness; (2) are immoral, unethical, oppressive, or unscrupulous; and (3) caused injury to plaintiffs.

115. Insofar as not covered by the preceding paragraphs, defendants' actions in filing and prosecuting one or more of U.S. Pat. App. Ser. Nos. 10/610,481 (the '481 application); 11/091,126; 11/257,139; 11/257,219; 11/257,222; 11/366,129; 11/366,762; and 11/366,887 are believed to be at least in part for the purpose of again obtaining ownership rights in the subject matter invented by plaintiffs. As such, defendants' actions constitute unfair or deceptive acts or practices under Mass. Gen. L., chap. 93A, §§2 and 11 because defendants' actions (1) are within at least the penumbra of some common law, statutory, or other established concept of fairness; (2) are immoral, unethical, oppressive, or

REDACTED VERSION, FILED VIA ECF
(complete version being filed by hand with the Court)

[Proposed] Amended Complaint

unscrupulous; and (3) caused injury to plaintiffs.

116. As a result of defendants' unfair or deceptive acts or practices, plaintiffs have suffered a loss of money (e.g., plaintiffs did not share in any monetary benefit accruing to defendants ChemImage and Treado from the filing of any applications and/or the issuance of any patents in the '476 and '962 patent families) and/or property (e.g., ownership of the '476 and '962 patents and/or any other patents which issue from the '962 patent family).

117. Wherefore, plaintiffs ask the court to find defendants ChemImage and Treado jointly, severally, and/or singly liable for committing unfair or deceptive acts or practices under Mass. Gen. L., chap. 93A, §§2 and 11.

121. Wherefore, plaintiffs ask that plaintiffs Hoyt and Miller be declared inventors of the '476 patent under 35 U.S.C. §256 (see Count 10 below), and that the Court further declare that any patent claiming priority to the '391 application is unenforceable against plaintiffs, plaintiffs' agents, plaintiffs' customers (including end users), and plaintiffs' suppliers because of defendants' unclean hands in the filing of the '391 application.

122. Wherefore, plaintiffs ask the Court to award plaintiffs the actual damages

REDACTED VERSION, FILED VIA ECF
(complete version being filed by hand with the Court)

[Proposed] Amended Complaint

caused by defendants' unfair or deceptive acts or practices, in an amount to be determined by the Court, pursuant to ¶5 of §11, chap. 93A, Mass. Gen. L.

123. Wherefore, plaintiffs ask the Court to at least double, but no more than treble, the aforesaid actual damages pursuant to ¶5 of §11, chap. 93A, Mass. Gen. L., because defendants' unfair or deceptive acts or practices have been knowing and willful.

124. Wherefore, plaintiffs ask the Court for reasonable fees and costs incurred in this action, pursuant to ¶6 of §11, chap. 93A, Mass. Gen. L.

COUNT 8: CLAIMS UNDER THE RACKETEER INFLUENCED AND CORRUPT ORGANIZATIONS (RICO) ACT, 18 U.S.C. §§1961-1968

125. Plaintiffs repeat and reallege the assertions set forth in paragraphs 1 through 124.

126. Defendant ChemImage is a corporation capable of owning property (thereby constituting a "person" under 18 U.S.C. §1961(3)) which conducts business in many states (thereby constituting an "enterprise affecting interstate commerce" under 18 U.S.C. §1962).

127. Defendant Treado is a "person" under 18 U.S.C. §1961(3) who is "employed by or associated with" ChemImage, and who "conduct[s] or participate[s] directly or indirectly, in the conduct of" ChemImage's affairs under 18 U.S.C. §1962(c).

128. Defendants have been, and are, executing a scheme or artifice to defraud plaintiffs of their rights to the subject matter invented by plaintiffs and claimed in the '476 patent, the '391 application, and the '962 patent.

130. The acts underlying defendants ChemImage and Treado's breach of the covenant of good faith and fair dealing ; intentional and/or negligent misrepresentation, common law fraud, and/or fraudulent inducement ; unjust enrichment at the expense of plaintiffs; breaches of fiduciary duty owed to plaintiffs CRI, Hoyt, and/or Miller; and/or misappropriation and conversion of the results of the CRI/ChemImage collaboration have been to execute or further that scheme or artifice.

131. Insofar as not covered by the preceding paragraphs, defendants' actions in

REDACTED VERSION, FILED VIA ECF
(complete version being filed by hand with the Court)

[Proposed] Amended Complaint

filing, prosecuting, and/or assigning rights to the '347 application and/or the '476 patent which issued from the '347 application were to execute or further that scheme or artifice.

132. Insofar as not covered by the preceding paragraphs, defendants' actions in filing, prosecuting, and/or assigning rights to the '391 application and/or the '962 patent which issued from the '391 application were to execute or further that scheme or artifice.

133. Insofar as not covered by the preceding paragraphs, defendants' actions in filing and prosecuting U.S. Reissue App. Ser. No. 11/103,423 were to execute or further that scheme or artifice.

134. Insofar as not covered by the preceding paragraphs, defendants' actions in fraudulently reviving the '077 application were to execute or further that scheme or artifice.

135. Insofar as not covered by the preceding paragraphs, defendants' actions in filing and prosecuting one or more of U.S. Pat. App. Ser. Nos. 10/610,481 (the '481 application); 10/773,077 (the '077 application); 11/091,126; 11/256,889; 11/257,139; 11/257,219; 11/257,222; 11/366,129; 11/366,762; and 11/366,887 were to execute or further that scheme or artifice.

136. Upon information and belief, defendants ChemImage and Treado have each committed at least two acts of mail fraud under 18 U.S.C. §1341 and/or wire fraud under 18 U.S.C. §1343 by communicating with defendants' attorneys, with each other, with plaintiffs, and/or by one or more employees, officers, and/or directors of ChemImage communicating with one or more other employees, officers, and/or directors of ChemImage

(b)

during the preparation, filing, prosecution, and issuance of the '347 application, the '476 patent, the '391 application, and/or the '976 patent; (c) during the preparation, filing, and prosecution of U.S. Reissue App. Ser. No. 11/103,423; (d) during the preparation and filing of the petition to revive the '077 application; and (e) during the preparation, filing, and prosecution one or more of U.S. Pat. App. Ser. Nos. 10/610,481 (the '481 application); 10/773,077 (the '077 application); 11/091,126; 11/256,889; 11/257,139; 11/257,219; 11/257,222; 11/366,129; 11/366,762; and 11/366,887; wherein each of defendants ChemImage and Treado have used mail, wire, or radio communications to execute or

REDACTED VERSION, FILED VIA ECF
(complete version being filed by hand with the Court)

[Proposed] Amended Complaint

further a scheme or artifice to defraud plaintiffs.

137. Upon information and belief, defendants ChemImage and Treado have each conspired with the other and/or with one or more agents or attorneys of defendants, and/or one or more employees, officers, and/or directors of ChemImage have conspired with one or more other employees, officers, and/or directors of ChemImage to violate one or more of subsections (a), (b), or (c) of 18 U.S.C. §1962 by agreeing to commit, or in fact committing, at least two acts of racketeering activity (such as, for example, the acts of mail or wire fraud described in the preceding paragraph).

138. By reason of defendants unlawful acts, plaintiffs have suffered ascertainable loss and damages and the injuries suffered by plaintiffs were directly and proximately caused by defendants' racketeering activity as described above.

139. Wherefore, plaintiffs ask the court to find that defendants ChemImage and Treado engaged in a pattern of racketeering activity under 18 U.S.C. §1962(c).

140. Wherefore, plaintiffs ask the court to find that defendants ChemImage and Treado conspired, under 18 U.S.C. §1962(d), to violate 18 U.S.C. §1962(c).

141. Wherefore, plaintiffs ask the Court to issue an appropriate order pursuant to 18 U.S.C. §1964(a), imposing reasonable restrictions on the future activities of defendants ChemImage and Treado, specifically, prohibiting defendants ChemImage and Treado from enforcing any rights to any patent claiming priority to the '391 application against plaintiffs, plaintiffs' agents, plaintiffs' customers (including end users), and plaintiffs' suppliers, because of defendants' racketeering activity.

142. Wherefore, plaintiffs ask the Court for three times the damages sustained by plaintiffs and caused by defendants' racketeering activity, plus the cost of this suit, including reasonable attorneys' fees, pursuant to 18 U.S.C. §1964(c).

COUNT 9: COMMON LAW CIVIL CONSPIRACY

143. Plaintiffs repeat and reallege the assertions set forth in paragraphs 1 through 142.

144. Each of defendants ChemImage and Treado have conspired with each other, and/or with one or more agents or attorneys of defendants, and/or one or more employees, officers, and/or directors of ChemImage have conspired with one or more other employees,

REDACTED VERSION, FILED VIA ECF
(complete version being filed by hand with the Court)

[Proposed] Amended Complaint

officers, and/or directors of ChemImage, to pursue a common plan or agreement (“the conspiracy”) to commit one or more wrongful acts, including, but not limited to, breaching the covenant of good faith and fair dealing ; intentional and/or negligent misrepresentation, common law fraud, and/or fraudulent inducement ; unjust enrichment at the expense of plaintiffs; breaching the fiduciary duty owed to plaintiffs CRI, Hoyt, and/or Miller; and/or misappropriation and conversion of the results of the CRI/ChemImage collaboration

145. Upon information and belief, defendants ChemImage and Treado knew of the common plan or agreement and its purpose, and took affirmative steps to encourage the achievement of the result, including, for example, the wrongful acts of: filing, prosecuting, and/or assigning rights to the ‘391 application and/or the ‘962 patent which issued from the ‘391 application without inventors Miller and Hoyt; filing and prosecuting U.S. Reissue App. Ser. No. 11/103,423 without inventors Miller and Hoyt; fraudulently reviving the ‘077 application; filing and prosecuting patent applications claiming subject matter invented by plaintiffs Miller and Hoyt, including one or more of U.S. Pat. App. Ser. Nos. 10/610,481 (the ‘481 application); 10/773,077 (the ‘077 application); 11/091,126; 11/257,139; 11/257,219; 11/257,222; 11/366,129; 11/366,762; and 11/366,887.

146. Upon information and belief, defendants ChemImage and Treado knew of the common plan or agreement and its purpose, and took affirmative steps to encourage the achievement of the result, including, for example, mail fraud under 18 U.S.C. §1341 and/or wire fraud under 18 U.S.C. §1343; specifically, each of defendants ChemImage and Treado have used mail, wire, or radio communications to execute or further a scheme or artifice to defraud plaintiffs by communicating with defendants’ attorneys, with each other, with plaintiffs, and/or by one or more employees, officers, and/or directors of ChemImage communicating with one or more other employees, officers, and/or directors of ChemImage

(b)

during the preparation, filing, prosecution, and issuance of the ‘347 application, the ‘476 patent, the ‘391 application, and/or the ‘976 patent; (c) during the preparation, filing, and

REDACTED VERSION, FILED VIA ECF
(complete version being filed by hand with the Court)

[Proposed] Amended Complaint

prosecution of U.S. Reissue App. Ser. No. 11/103,423; (d) during the preparation and filing of the petition to revive the '077 application; and (e) during the preparation, filing, and prosecution one or more of U.S. Pat. App. Ser. Nos. 10/610,481 (the '481 application); 10/773,077 (the '077 application); 11/091,126; 11/256,889; 11/257,139; 11/257,219; 11/257,222; 11/366,129; 11/366,762, and 11/366,887.

150. Wherefore, plaintiffs ask the Court that plaintiffs Hoyt and Miller be declared inventors of the '476 patent under 35 U.S.C. §256 (see Count 10 below), and that the Court further declare that any patent claiming priority to the '391 application is unenforceable against plaintiffs, plaintiffs' agents, plaintiffs' customers (including end users), and plaintiffs' suppliers because of defendants' unclean hands in the filing of the '391 application.

151. As a direct, proximate result of this civil conspiracy, plaintiffs have suffered and continue to suffer the loss of their rights to the subject matter invented by plaintiffs and claimed in the '476 patent, the '391 application, and the '962 patent, including the loss of any concomitant benefits, including, but not limited to, two issued patents (and any patent applications claiming priority to those two issued patents), royalties, payments, licensing

REDACTED VERSION, FILED VIA ECF
(complete version being filed by hand with the Court)

[Proposed] Amended Complaint

fees, and/or other compensation from those patents and patent applications, as well as the right to enforce the issued patents, including the right to seek an injunction against others who are manufacturing and/or using plaintiffs' invention.

152. As a direct, proximate result of this civil conspiracy, plaintiffs have suffered and continue to suffer economic losses and general and specific damages, all in an amount to be determined according to proof.

153. Wherefore, plaintiffs ask the court to find defendants ChemImage and Treado have conspired to defraud plaintiffs of their rights to, and concomitant benefits from, the subject matter invented by plaintiffs and claimed in the '476 patent, the '391 application, and the '962 patent.

154. Wherefore, plaintiffs ask the Court for compensatory and punitive damages, such amounts to be determined at trial, including reasonable attorneys' fees.

COUNT 10: CORRECTION OF INVENTORSHIP OF '476 PATENT
(ALTERNATIVE RELIEF)

2

155. Plaintiffs repeat and reallege the assertions set forth in paragraphs 1 through 154.

157. Plaintiff Peter J. Miller, individually and/or in collaboration with defendant Patrick Treado, contributed to the invention of the subject matter of one or more claims in the '476 patent, including, for example, Miller's conception of the use of an Evans Split-Element liquid crystal tunable filter in a chemical imaging system as recited in claim 1 of the '476 patent.

158. Plaintiff Clifford Hoyt, individually and/or in collaboration with defendant Patrick Treado, contributed to the invention of the subject matter of one or more claims in the '476 patent, including, for example, Hoyt's conception of the use of infinity-corrected optics to produce a collimated beam from Raman scattered light in a chemical imaging system as recited in claim 1 of the '476 patent.

159. Wherefore, plaintiffs ask the

REDACTED VERSION, FILED VIA ECF
(complete version being filed by hand with the Court)

[Proposed] Amended Complaint

court to (a) declare that Peter J. Miller is an inventor of the subject matter claimed in the '476 patent and (b) order correction of the '476 patent under 35 U.S.C. §256 to reflect Peter J. Miller as an inventor.

160. Wherefore, plaintiffs ask the court to (a) declare that Clifford Hoyt is an inventor of the subject matter claimed in the '476 patent and (b) order correction of the '476 patent under 35 U.S.C. §256 to reflect Clifford Hoyt as an inventor.

WHEREFORE, plaintiffs respectfully request that this Court:

- on Count 1, declare plaintiffs Peter J. Miller and Clifford Hoyt inventors of the '962 patent and order correction of the '962 patent under 35 U.S.C. § 256 to reflect their status as inventors;

- if the Court declares plaintiffs Miller and Hoyt inventors of the '962 patent, further declare that U.S. Reissue App. Ser. No. 11/103,423 is null and void because the Reissue Oath was not signed by all inventors of the original '962 patent as required by statute;

- on Counts 2, 4, 5, 7, and/or 9,

declare that any patent claiming priority to the '347 application is unenforceable against plaintiffs, plaintiffs' agents, plaintiffs' customers (including end users), and plaintiffs' suppliers because of defendants' unclean hands in the filing of the '391 application;

- on Count 3, order defendants ChemImage and Treado to make appropriate

REDACTED VERSION, FILED VIA ECF
(complete version being filed by hand with the Court)

[Proposed] Amended Complaint

restitution of any profits, revenues, and benefits to the extent and in the amount deemed appropriate by the court, and such other relief as the Court deems just and proper to remedy defendants' unjust enrichment;

- on Count 6, order defendants ChemImage and Treado to make appropriate restitution, in such an amount as to be determined at trial, to the plaintiffs, and such other relief as the Court deems just and proper to remedy defendants' conversion and/or misappropriation of plaintiffs' invention;

- on Count 7, award plaintiffs the actual damages caused by defendants' unfair or deceptive acts or practices, in an amount to be determined by the Court, pursuant to ¶5 of §11, chap. 93A, Mass. Gen. L., to at least double, but no more than treble, the aforesaid actual damages pursuant to ¶5 of §11, chap. 93A, Mass. Gen. L., because defendants' unfair or deceptive acts or practices have been knowing and willful, and reasonable fees and costs incurred in this action, pursuant to ¶6 of §11, chap. 93A, Mass. Gen. L.;

- on Count 8, issue an appropriate order pursuant to 18 U.S.C. §1964(a) prohibiting defendants ChemImage and Treado from enforcing any rights to any patent claiming priority to the '391 application against plaintiffs, plaintiffs' agents, plaintiffs' customers (including end users), and plaintiffs' suppliers, because of defendants' racketeering activity;

- on Count 8, award plaintiffs three times the damages sustained by plaintiffs and caused by defendants' racketeering activity, plus the cost of this suit, including reasonable attorneys' fees, pursuant to 18 U.S.C. §1964(c);

- on Count 9, award plaintiffs compensatory damages, punitive damages, such amounts to be determined at trial, and plaintiffs' costs in this suit, including all reasonable attorneys' fees;

- on Count 10, declare
 plaintiffs Peter J. Miller and Clifford Hoyt inventors of the '476 patent and order correction of the '476 patent under 35 U.S.C. § 256 to reflect their status as inventors;

- on Count 1, and Count 10
 declare this case exceptional under 35 U.S.C. § 285, and award plaintiffs reasonable attorneys' fees

REDACTED VERSION, FILED VIA ECF
(complete version being filed by hand with the Court)

[Proposed] Amended Complaint

- on all Counts,

- (b) award plaintiffs their costs; and
- (c) such other and further relief as this Court shall deem just and proper.

WHEREFORE, pursuant to Fed. R. Civ. P. 38, plaintiffs demand a trial by jury on all issues so triable.

Respectfully submitted,

CAMBRIDGE RESEARCH AND
INSTRUMENTATION, INC.
PETER J. MILLER
CLIFFORD HOYT

by their attorneys

Dated: May 18, 2006

/s/ Martin B. Pavane
Martin B. Pavane
Teodor J. Holmberg (BBO# 634708)
COHEN PONTANI LIEBERMAN & PAVANE
551 Fifth Avenue
New York, New York 10176
Tel. (212) 687-2770
Fax (212) 972-5487
E-mail: tidge@cplplaw.com

Brian L. Michaelis (BBO# 555159)
Erin E. McLaughlin (BBO# 647750)
BROWN RUDNICK BERLACK ISRAELS LLP
One Financial Center
Boston, MA 02111
Tel. (617) 856-8200
Fax (617) 856-8201
E-mail: BMichaelis@brownrudnick.com

REDACTED VERSION, FILED VIA ECF
(complete version being filed by hand with the Court)

[Proposed] Amended Complaint

CERTIFICATE OF SERVICE

I hereby certify that the foregoing redacted document identified in the top right-hand portion of this page and filed through the ECF system will be sent electronically to the registered participants as identified on the Notice of Electronic Filing (NEF) on May 18, 2006.

/s/ Teodor Holmberg
Teodor J. Holmberg (BBO# 634708)

I hereby further certify that an unredacted complete copy of this document is being filed by hand with the Court, as an attachment to a Motion to Impound, and that an unredacted complete copy of this document is being served, by first class mail, postage prepaid, on May 18, 2006 on:

Anthony J. Fitzpatrick, Esq.
DUANE MORRIS LLP
470 Atlantic Avenue, Suite 500
Boston, MA 02210
617-289-9220 (phone)
617-289-9201 (fax)
ajfitzpatrick@duanemorris.com

Paul D. Weller, Esq.
MORGAN, LEWIS & BOCKIUS LLP
1701 Market Street
Philadelphia, PA 19103

/s/ Teodor Holmberg
Teodor J. Holmberg (BBO# 634708)

EXHIBIT A

Treads

1/29/93

Send

Multi Spectral w/ ATOFS,
image-shift

low band to high 1100
At

Kinetic Eluv. imaging
pH monitor

Raman
Imaging
5 min

want video frame rates
every other frame

Low Heterodyne

25 μ s theoretical
1 ms w/ ATOFS

500-700 \rightarrow 2.4 nm

Raman

@ 500 .25 nm sp

400-700

Multispectral Imaging

Princeton Instruments

Windows NT

released Feb

32 bit processing environment

Atlas true multitasking

1) question what range

All Literature

1) Price ranges
Tech note

2) Background lit birefringence & Filters

3) Primary Articles

4) data on

a) operating range for .25 nm @ 500 nm

b) curve on 700 - 1100

752-900 nm 57 nm bp resolution 25-50 wave numbers
constant 50 numbers typical

40mm Dia

AOTF 7 mm Sq Aperture

50 wave numbers
at 700 nm is
.39
Raman Shift

Vibration spectroscopy, 1000 Hz frame/second

Pitcon

Washington Treads for Biophysics

EXHIBIT B



University of Pittsburgh

FACULTY OF ARTS AND SCIENCES
Department of Chemistry

October 15, 1993

Cliff Hoyt
Cambridge Research and Instrumentation, Inc.
21 Erie Street
Cambridge, MA 02139

Dear Cliff:

Enclosed is the liquid crystal tunable filter. We thank you for its use. As a preliminary assessment, I would conclude that given the current state of the technologies, LCTFs are superior to AOTFs for fluorescence emission imaging.

We enclose a MS-DOS 6.0 formatted floppy disk with two image files. They are in TIFF format. An image of 1 micron fluorescent microspheres is included to demonstrate the ability of the LCTF to maintain high image fidelity and provide diffraction-limited imaging performance. We also include a multispectral composite image of rat brainstem tagged for thyrotropin releasing hormone (TRH) and serotonin (5HT). The neurotransmitters are colocalized in reticulo-spinal neurons. These images are representative of the data we collected in the recent study. They are examples of what we will incorporate in the *Applied Spectroscopy* paper. I would request that they be used for your internal use only until we publish.

As soon as I return from FACSS I will work on a draft of the paper. I will be in contact soon.

Sincerely,

A handwritten signature in black ink, appearing to be 'P. Treado'.

Patrick J. Treado
Assistant Professor of Chemistry

EXHIBIT C

preserving image integrity with the advantage of no-moving-mechanical parts. A side-by-side comparison of these two technologies for fluorescence microscopy will be made in this manuscript. The first fluorescence emission images collected through an acousto-optic device will be reported here. In addition, the first use of LCTFs for Raman microscopy will be described to demonstrate LCTF versatility and to demonstrate the applicability of the LCTF to a chemical imaging technique that is complementary to fluorescence microscopy and is of significant analytical importance.

THEORY

Acousto-Optic Tunable Filter

AOTF's are compact, electronically addressable notch filters which can operate from the UV to the IR. The theory and operating principles of the AOTF are established and have been described in detail.¹¹⁻¹⁵ Operation of the AOTF is based on the interaction of light with a traveling acoustic wave in an anisotropic crystal medium. The incident light is diffracted with a narrow spectral bandpass when a rf signal is applied to the device. By changing the applied rf frequency under computer control the spectral passband can be tuned rapidly with the benefit of no-moving-parts. Important features of the AOTF include high optical throughput, moderate spectral resolution, broad free-spectral range, rapid tuning ability, and random accessibility. In addition, the diffracted light intensity can be controlled, or even chopped, by modulating the rf signal level. AOTFs have been incorporated into fluorescence spectrometers¹⁶ and we have previously demonstrated the potential of AOTF's in Raman spectroscopy.¹⁷

An important characteristic of the AOTF is the ability to transmit two-dimensional images at moderately high fidelity. Preliminary considerations of the design principles of AOTF spectrometers for performing fluorescence imaging¹⁸ have been reported, as well as remote sensing imaging spectrometers employing AOTF technology.¹⁹ We have previously described AOTF instruments for visible and near-infrared absorption microscopy^{20,21} and Raman imaging microscopy.²²

Liquid Crystal Tunable Filter

At this time, the liquid crystal tunable filter (LCTF) has not been widely utilized for analytical spectroscopy. This manuscript will summarize LCTF theory described in detail elsewhere.²⁴ (Delete reference 23)

LCTF's are also compact, electronically addressable notch filters which can operate from the near-UV to the IR. However, they achieve tunable bandpass in a fundamentally different way.

The LCTF is comprised of several cascaded stages based on the design of the Lyot birefringent filter which was first developed in 1933²⁵. In traditional Lyot filter design, individual filter stages consist of a birefringent element positioned between parallel linear polarizers. The exit polarizer for a given stage acts as the input polarizer for the following stage. The birefringent elements, usually composed of quartz or calcite, are oriented so that incident light is normal to their optic axes and rotated 45° relative to the linear polarization direction. Incident linearly polarized light is divided into two

equal amplitude paths, the ordinary rays (o-rays) and extraordinary rays (e-rays), that travel at different phase velocities through the birefringent material. In traversing the birefringent element the o-rays and e-rays experience an optical path difference described as the wavelength λ dependent retardance given by Equation 1,

{EMBED Equation |}

(1)

where D_n is the birefringence of the material and d is the material thickness. Upon exiting the birefringent element the o-rays and e-rays pass to a polarization analyzer which is oriented parallel to the input linear polarizer. Only wavelengths of light that are in phase are transmitted by the linear polarizer and presented to the next, cascaded Lyot filter stage. The transmittance of the n th stage is described by Equation 2.

{EMBED Equation |}

(2)

The individual transmittance of 3 cascaded filter stages are described in Figure 1A. The total transmittance of a multiple-stage filter is the product of the individual filter stage transmittance which describes a replicated sinc function²⁶, as shown in Figure 1B. The thickness and the subsequent retardation of the birefringent elements increases in powers of two for each successive stage in the Lyot filter. Each cascaded stage exhibits a transmission spectrum with half the free spectral range and half the bandpass of the previous one. The free spectral range of the entire Lyot filter is determined by stage 1, the stage with the thinnest birefringent element. The bandpass of the device is dictated by the last stage which comprises the thickest element.

The LCTF incorporates nematic liquid crystal wave plates within the Lyot filter geometry that act as electronically controlled phase retarders. An individual LCTF filter stage is diagrammed in Figure 2A. The LC waveplates are oriented with a crystal axis rotated 45° relative to the direction defined by the input linear polarizer. The LC waveplates can be adjusted over a continuous range of retardance levels, enabling continuous tunability of wavelength. With a large applied electrical potential, they add relatively little retardance to the fixed waveplate. With no applied potential, their retardance is at a maximum. In a multi-stage nematic LCTF, there are as many LC wave plates as there are stages. The total retardance of a LCTF stage is expressed by Equation 3.

{EMBED Equation |}

(3)

$G_n F(1)$ is the retardation of the fixed birefringent element given by Eq. (1). $G_n C(1)$ is the additional retardation contributed from the LC waveplate. The retardance of the LC element is selected using the same equation used for the fixed retarders (Equation 1), except that the Δn is no longer fixed and can be varied by changing the electrical potential applied to the LC retarder.

Varying the electrical potential applied to the LC retarders provides accurate and flexible control over the passband wavelength, λ_B . In tuning λ_B , LCTFs take advantage of the fact that the transmission function of the individual tuning elements is periodic. As a result, the optical passband can be tuned over the entire LCTF free-spectral range while no individual tuning element needs to vary in retardance by more than the retardance required to tune over a single period. Individual LC elements are made of two parallel glass substrates, optically polished and coated on their inner faces with indium-tin oxide (ITO) transparent electrodes. The electrode face is treated so that the nematic liquid crystals preferentially align in a selected orientation. The oriented rod-like molecules exhibit electrical and optical anisotropy, and the molecular polarizability is anisotropic, as well. Light polarized along the crystal axis, the e-rays, will experience a larger polarizability than light polarized across the crystal axis, the o-rays, and subsequently the e-rays experience a larger index of refraction than the o-rays.

To vary the retardance of a nematic LC element, an electric field is applied to the ITO electrodes, which induces an electric field that is parallel to the propagation vector of the incident light. The electric field induces a dipole, and the LC molecules experience a torque which tends to align them within the field. Complete molecular reorientation is opposed by the intermolecular spring constant of the LC and the realignment is dependent on the applied field strength. Tuning of the LC element is equivalent to rotating the crystal axis of a uniaxial crystal, which acts to change the birefringence and the resulting retardance, as well.

Nematic LCTFs are attractive technologies for spectral imaging because they have high acceptance angles and can be fabricated with large optical apertures. LCTFs provide acceptable transmittance, moderately narrow bandpass, and rapid switching speeds. The devices are physically compact and mechanically rugged. The most important feature provided by LCTFs is their superior image quality, which does not degrade the diffraction-limited imaging performance provided by the microscope.

EXPERIMENTAL

Figure 3 is a schematic of a tunable fluorescence microscope. Multicolor excitation is provided by ion lasers, specifically an Ar⁺ laser at 514.5 nm (Coherent Innova 330-K), and a Kr⁺ laser at 647.1 nm (Coherent CR-3), or by a Hg lamp (Olympus) employing appropriate notch filters. For multicolor laser excitation the lasers are combined through a dichroic beamsplitter which reflects the green laser and transmits the red. Sample epi-illumination is provided in combination with dielectric interference dichroic beamsplitters (Omega Optical) matched to the appropriate excitation wavelength. Fluorescence image collection is provided by infinity-corrected planachromat 10X (N.A. 0.30), 20X (N.A. 0.46), and 100X (N.A. 0.95) objectives in an upright metallurgical microscope (Olympus BHSM).

The magnified fluorescence emission is projected to the tunable filter which provides electronically controlled wavelength selection. The fluorescence microscope is designed so that the AOTF (Brimrose TEAF2-.60-1.1H) and LCTF (Cambridge Research and Instrumentation, Varispec VIS-38) are interchangeable. While the tunable filters provide significant rejection of the excitation

3

provide comparable sensitivity to fluorescence microscopy, and can lack the specificity of immunolabeling. However, the information content of a Raman spectrum is rich and highly sensitive to the conformation and dynamics of materials. Advancements in microscope, detector, laser rejection filters and spectrometer instrumentation allow Raman microscopy to be performed rapidly and provide high spatial resolution, high fidelity images. Raman microscopy employs similar instrumentation to fluorescence microscopy, and we have previously employed AOTFs as spectral imaging filters to perform Raman spectroscopy and imaging.²²

Figure 10 is a Raman image of 45 nm diameter polystyrene microspheres that have not been tagged with a fluorophore. Fig. 10 demonstrates the first use of LCTF technology to perform Raman imaging microscopy. The LCTF passband is centered at 691.5 nm which corresponds to a filter position of 992 \pm 50 cm^{-1} . Due to the broad bandpass of the LCTF several vibrational bands contribute to the Raman emission image including the relatively intense ring deformation band at 992 cm^{-1} . The image quality demonstrated in Fig. 10 surpasses the imaging performance of the AOTF and is comparable to the highest quality Raman images in the literature.³²⁻³⁴

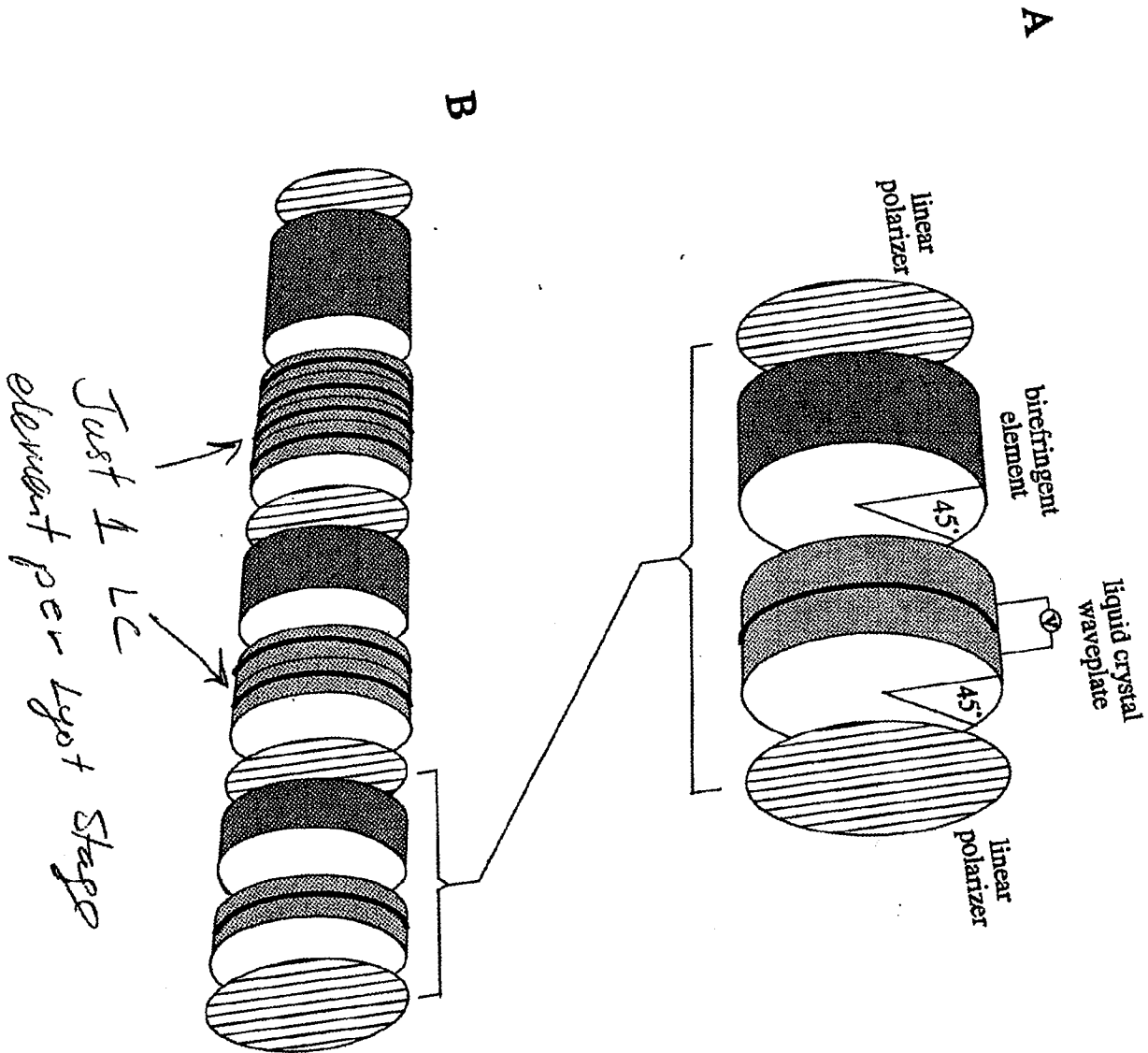
While autofluorescence backgrounds are minimal with the 647 nm Kr⁺ laser excitation employed to generate Fig. 10 it is necessary to ensure that the detected emission is due to Raman scatter and not fluorescence. If present, the fluorescence will generate an image identical to what is shown in Fig. 10. Conventionally, discrimination is made on the basis of the Raman spectrum that is collected with a high resolution spectrometer. Broad emission bands are typically attributed to fluorescence while the distinctively narrow Raman bands that are specific to polystyrene appear at known frequencies. The LCTF provides a broad passband that is not sufficient for resolving individual Raman bands, but is sufficient for discriminating broad fluorescence emission. As a test of fluorescence emission the LCTF was tuned to 720 nm where polystyrene does not exhibit Raman scattering. No significant sample emission was observed. In addition, the AOTF was employed to collect a higher resolution Raman spectrum of the microspheres. The AOTF spectrum substantiated that no autofluorescence was present and Fig. 10 is a Raman emission image.

conclusions

Acousto-optic and liquid crystal no-moving-parts tunable imaging spectrometers have been evaluated with respect to their imaging and spectroscopic performance. AOTFs provide higher peak transmission and spectral resolution but do not provide comparable imaging quality to LCTFs. We have demonstrated that the LCTF does not degrade the imaging performance of the fluorescence microscope to a detectable degree. Also, the relatively broad bandpasses achievable with the LCTFs are a good match for the broad spectral features typical of fluorescence emission, thus providing comparable or more signal at the CCD chip than would be provided by an AOTF.

An optimized fluorescence microscope would combine AOTF and LCTF technologies. AOTFs are solid-state crystals and have high damage thresholds and are well suited to rapid, facile tuning of laser excitation for fluorescence microscopy. In addition, AOTFs provide a unique function in which multiple spectral passbands can be tuned simultaneously. Preliminary demonstration of multiplexed operation

5



spacing of 4.3 mm was 96 ■ 0.5%, 93 ■ 1.6%, and 78 ■ 1.5% for Figs. 5A, 5B and 5C, respectively. The interference filter and LCTF provide significantly improved contrast relative to the AOTF. It is anticipated that the LCTF would not appreciably degrade the 1/2 diffraction-limited spatial resolution performance of a research-grade fluorescence microscope. The achievable spatial resolution of AOTFs are anticipated to reflect the 15% poorer imaging performance observed in Fig. 5C, at a minimum. In practice, the achievable resolution will be significantly worse than a 15% degradation due to the wavelength dependent image shift observed with the AOTF.

The limiting aperture in Fig. 5 is the 512x512 pixel CCD as the projected images exceed the 12.5x12.5 mm² active area of the CCD. In applications where extremely high image fidelity is required, larger CCDs with higher pixel density can be employed. LCTFs would be superior to AOTFs in high fidelity applications because large apertures providing the requisite high optical quality can more readily be manufactured for LCTFs than AOTFs at comparable costs.

The CCD integration times used to collect the images in Fig. 5 are comparable despite the 2.9X higher transmission provided by the AOTF. The LCTF provides a bandpass that is 2.8X broader than the AOTF which approximately offsets the AOTFs higher transmission. Fluorescence emission bands are typically broad and the resolution provided by the LCTF is sufficient for spectral discrimination. In general, the AOTF has the advantage of providing higher throughput at comparable bandpass.

LCTFs can be fabricated to provide high resolution, in fact higher resolution than AOTFs, but not without associated costs in reduced spectral range and peak transmission. Commercial devices can be fabricated to provide 0.025 nm bandpass at 610 nm, but with substantial expense and limited free spectral range. A more realistic filter would provide 0.5 nm bandpass with a free spectral range of 610 +/- 50 nm and a peak transmission approaching 15%.

Results of multispectral fluorescence microscopy performed with the AOTF are illustrated in Figure 6 which includes images of two 15 mm diameter polystyrene microspheres that have been tagged with different fluorescent dyes. Fig. 6A shows the microspheres in brightfield. Fluorescence images are shown in Fig. 6B and 6C employing bandpass filtered Hg lamp excitation at 560 nm. Fig. 6B is collected by tuning the AOTF to select the 602 nm emission of the orange dye labeled sphere that appears at the top left. Fig. 6C is collected at 640 nm and the red dye labeled sphere appears at the bottom right. The orange sphere emission is significant at 640 nm and is visible in Fig. 6C.

The fluorescence emission images of Fig. 6 comprise only two image frames of the spectral image data set that was collected by tuning the AOTF from 560-730 nm at 2 nm intervals. Spectra extracted from x,y coordinates that correspond to the centers of the microspheres are plotted in Figure 7. Fig. 7A corresponds to the orange sphere emission, while Fig. 7B corresponds to the red sphere emission. The multicomponent model system employed here contains only two unique fluorescent constituents which could readily be distinguished using two discrete filters. The model systems chosen for study were selected, in part, because they lack spectroscopic complexity. The samples have simple, well separated emissions that do not vary with time, and the samples have well defined size that can be visualized under brightfield conditions. More complex chemical systems would

CAMBRIDGE RESEARCH & INSTRUMENTATION INC.



Facsimile Transmission Cover Sheet

Total Pages: 7

From: Cliff Hoyt Date: 12/22

Fax: (617) 864-3730

To: Pat Treado
(412) 624-8552

Remarks:

Pat - Most modifications are to the theory
Section. I've taken out any info. specific
to ferroelectric LC's. Additions are in bold.
Happy holidays!

Cliff

21 ERIE STREET, CAMBRIDGE, MASSACHUSETTS 02139

TEL. (617) 491-2627

CRI000126

EXHIBIT D

Imaging Spectrometers for Fluorescence and Raman Microscopy: Acousto-Optic and Liquid Crystal Tunable Filters

HANNAH R. MORRIS, CLIFFORD C. HOYT, and PATRICK J. TREADO*

Department of Chemistry, University of Pittsburgh, Pittsburgh, Pennsylvania 15260 (H.R.M., P.J.T.), and Cambridge Research & Instrumentation Inc., 21 Erie Street, Cambridge, Massachusetts 02139 (C.C.H.)

Acousto-optic tunable filters (AOTF) and liquid crystal tunable filters (LCTF) are evaluated for their suitability as fluorescence microscopy imaging spectrometers. AOTFs are solid-state birefringent crystals that provide an electronically tunable spectral notch passband in response to an applied acoustic field. LCTFs also provide a notch passband that can be controlled by incorporating liquid crystal waveplate retarders within a Lyot birefringent filter. In this paper, spectroscopic performance and imaging quality are contrasted by evaluation of model systems. Studies include transmission imaging of standard resolution targets, multispectral fluorescence emission imaging of tagged polystyrene microspheres, and immunofluorescence imaging of neurotransmitters within rat-brain-stem thin sections. In addition, the first use of LCTFs for Raman microscopy is demonstrated. Raman microscopy is a noninvasive spectral imaging technique that can provide chemically significant image contrast complementary to fluorescence microscopy without the use of stains or tags.

Index Headings: Spectral imaging; Immunofluorescence microscopy; Acousto-optic tunable filter (AOTF); Liquid crystal tunable filter (LCTF); Lyot filter; Polystyrene; Microspheres; Neurotransmitters; Serotonin (5HT); Reticulo-spinal neurons; Raman microscopy.

INTRODUCTION

Fluorescence microscopy is a powerful tool for probing macromolecules, ions, and metabolites within complex biological assemblies. Fluorescence imaging techniques provide the ability to monitor the spatially localized chemical constituents that can dictate cellular function.¹⁻³ In neuroscience, for example, immunofluorescence microscopy provides a means to visualize the distribution of neurotransmitters localized within brain tissue.^{4,5}

Fluorescence microscopes typically employ diffraction-limited refractive optics coupled with sensitive multi-channel detectors for quantitative image detection. Discrete multilayer dielectric interference filters⁶ are often employed for fluorescence emission selection. Dielectric filters are fabricated as large elements with sufficient optical quality to transmit images at high fidelity while maintaining the wide field of view provided by the microscope. Transmittance of 40 to 80% is sufficient to perform imaging of weak fluorophores. The spectral parameters of the discrete filters, including transmittance and bandwidth, are determined at the time of manufacture. In the event the fluorescence spectral emission varies, discrete filters often prove unsatisfactory.

Of increasing importance in fluorescence imaging is the

need to probe dynamic systems or sample multiple spectral parameters simultaneously to understand the interactions of individual components within complex matrices. Multispectral fluorescence microscopy is a means for probing multiple constituents simultaneously with a high degree of sensitivity and specificity. When performed with sufficient time resolution, fluorescence microscopy can be used to visualize the chemical dynamics of living cells.⁷ In order to probe multiple spectral parameters at high speeds, rapid and reproducible filtering technologies are essential.

In current multispectral applications, discrete interference filters are incorporated into filter wheels⁸ employing mechanical rotation for rapid switching. Filter wheels are limited in the number of discrete filters that can practically be housed, and radiation is discriminated when the filters are at rest, which limits their timing resolution. Image misregistration can occur because of movement of the discrete filters, which introduces image blur.

In general, spectral imaging, including fluorescence microscopy, remote sensing employing visible/near-infrared absorption,⁹ and Raman microscopy,¹⁰ would benefit from an imaging spectrometer technology providing high spatial, spectral, and timing resolution. The ideal device would have broad spectral range and a high acceptance angle concomitant with a large physical aperture and would also provide high transmittance and high out-of-band rejection. The imaging spectrometer would be relatively independent of polarization unless, for the systems under investigation, polarization sensitivity is informative. Finally, the ideal technology would be physically compact, mechanically rugged, and electronically controllable.

No single imaging spectrometer currently satisfies all the criteria of an ideal device, although two technologies—acousto-optic tunable filters (AOTF) and liquid crystal tunable filters (LCTF) employing nematic LCs—provide much of the desired functionality. Both technologies simultaneously provide wavelength selection and tunability while preserving image integrity with the advantage of having no moving mechanical parts. A side-by-side comparison of these two technologies for fluorescence microscopy will be made in this paper. The first fluorescence emission images collected through an acousto-optic device will be reported here. In addition, the first use of LCTFs for Raman microscopy will be described to demonstrate the applicability of the LCTF to a chemical imaging technique that is complementary to fluorescence microscopy and is of significant analytical importance.

Received 4 January 1994; accepted 18 April 1994.
* Author to whom correspondence should be sent.

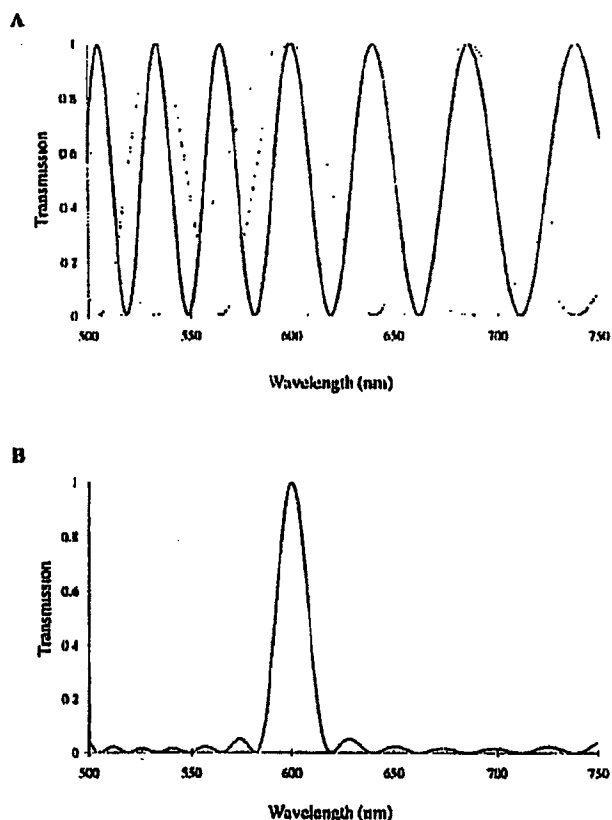


FIG 1. (A) Individual theoretical transmittance of three cascaded filter stages. (B) Total transmittance of the cascaded stages that describes a sinc function.

THEORY

Acousto-Optic Tunable Filter. AOTFs are compact, electronically addressable notch filters which can operate from the UV to the IR. The theory and operating principles of the AOTF are established and have been described in detail.¹¹⁻¹³ Operation of the AOTF is based on the interaction of light with a traveling acoustic wave in an anisotropic crystal medium. The incident light is diffracted with a narrow spectral bandpass when an rf signal is applied to the device. With a change in the applied rf frequency under computer control, the spectral passband can be tuned rapidly with the benefit of no-moving-parts technology. Important features of the AOTF include high optical throughput; moderate spectral resolution; broad, free spectral range; rapid tuning ability; and random accessibility. In addition, the diffracted light intensity can be controlled, or even chopped, by modulating the rf signal level. AOTFs have been incorporated into fluorescence spectrometers,¹⁶ and we have previously demonstrated the potential of AOTFs in Raman spectroscopy.¹⁷

An important characteristic of the AOTF is the ability to transmit two-dimensional images at moderately high fidelity. Preliminary considerations of the design principles of AOTF spectrometers for performing fluorescence imaging¹⁸ have been reported, as well as remote-sensing

imaging spectrometers employing AOTF technology.¹⁹ We have previously described AOTF instruments for visible and near-infrared absorption microscopy^{20,21} and Raman imaging microscopy.²²

Liquid Crystal Tunable Filter. LCTFs are compact, electronically controllable, spectral notch filters which can function from the visible to the near-infrared. However, LCTFs provide the tunable bandpass in a fundamentally different way than AOTFs. LCTFs can employ ferroelectric liquid crystals²³ or nematic liquid crystal waveplates.²⁴ The commercially available device employed in this study uses nematic LC technology, and we focus the discussion on nematic LCTF theory.

The nematic LCTF is comprised of several cascaded stages based on the design of the Lyot birefringent filter, which was first developed in 1933.²⁵ In traditional Lyot filter design, individual filter stages consist of a birefringent element positioned between parallel linear polarizers. The exit polarizer for a given stage acts as the input polarizer for the following stage. The birefringent elements, usually composed of quartz or calcite, are oriented so that incident light is normal to their optic axes and rotated 45° relative to the linear polarization direction. Incident linearly polarized light is divided into two equal amplitude paths, the ordinary rays (*o-rays*) and the extraordinary rays (*e-rays*), that travel at different phase velocities through the birefringent material. In traversing the birefringent element the *o-rays* and *e-rays* experience an optical path difference described as the wavelength (λ)-dependent retardance given by Eq. 1:

$$\Gamma(\lambda) = 2\pi \frac{\Delta n d}{\lambda} \quad (1)$$

where Δn is the birefringence of the material, and d is the material thickness.

Upon exiting the birefringent element, the *o-rays* and *e-rays* pass to a polarization analyzer which is oriented parallel to the input linear polarizer. Only wavelengths of light that are in phase are transmitted by the linear polarizer and presented to the next, cascaded Lyot filter stage. The transmittance of the n th stage is described by Eq. 2:

$$T_n(\lambda) = \cos^2[\Gamma_n(\lambda)/2]. \quad (2)$$

The individual transmittance of three cascaded filter stages is described in Fig. 1A. The total transmittance of a multiple-stage filter is the product of the individual filter stage transmittance that describes a replicated sinc function,²⁶ as shown in Fig. 1B. The thickness and the subsequent retardation of the birefringent elements increase in powers of two for each successive stage in the Lyot filter. Each cascaded stage exhibits a transmission spectrum with half the free spectral range and half the bandpass of the previous one. The free spectral range of the entire Lyot filter is determined by stage 1, the stage with the thinnest birefringent element. The bandpass of the device is dictated by the last stage, which comprises the thickest element.

The LCTF incorporates nematic liquid crystal waveplates within the Lyot filter geometry that act as electronically controlled phase retarders. An individual LCTF filter stage is diagrammed in Fig. 2A. The LC waveplates

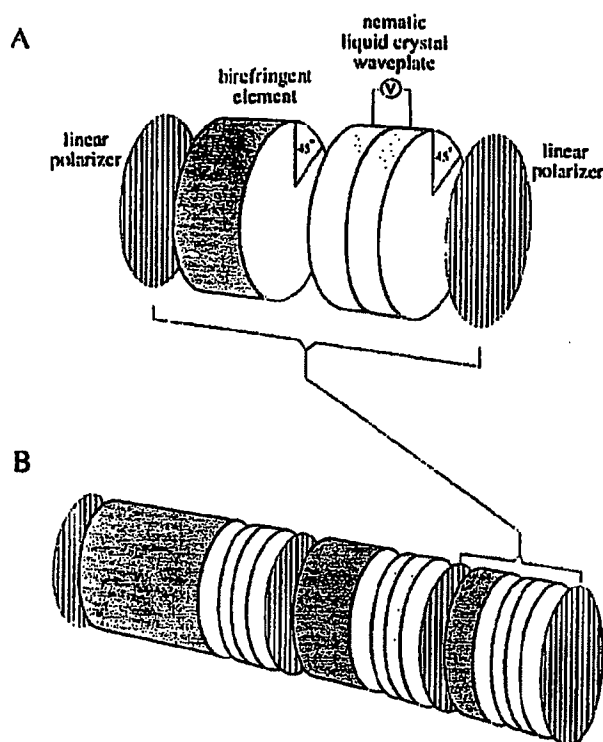


FIG. 2 (A) Diagram of an individual stage of the LCTF. Wavelength tunability controlled by electronically rotating the crystal axes of the liquid crystal waveplate. (B) Diagram of a three-stage Lyot tunable filter. Each consecutive stage employs a single LC waveplate and a fixed retarder with twice the thickness of the previous birefringent element.

are oriented with a crystal axis rotated 45° relative to the direction defined by the input linear polarizer. The LC waveplates can be adjusted over a continuous range of retardance levels, enabling continuous tunability of wavelength. With a large applied electrical potential, the LC adds relatively little retardance to the fixed waveplate. With no applied potential, the LC waveplate retardance is at a maximum. In a multi-stage nematic LCTF as diagrammed in Fig. 2B, there is one LC waveplate per filter stage.

Upon incorporation of LC elements within the Lyot filter, the total retardation is expressed by Eq. 3:

$$\Gamma_n(\lambda) = \Gamma_n^F(\lambda) + \Gamma_n^L(\lambda) \quad (3)$$

$\Gamma_n^F(\lambda)$ is the retardation of the fixed birefringent element given by Eq. 1. $\Gamma_n^L(\lambda)$ is the additional retardation contributed from the LC waveplate, which is also described by Eq. 1, except that Δn can be varied by changing the electrical potential applied to the LC retarder.

Varying the electrical potential applied to the LC retarders provides accurate and flexible control over the passband wavelength, λ_p . In tuning λ_p , LCTFs take advantage of the fact that the transmission function of the individual tuning elements is periodic. As a result, the optical passband can be tuned over the entire LCTF free spectral range, while no individual tuning element needs to vary in retardance by more than the retardance required to tune over a single period.

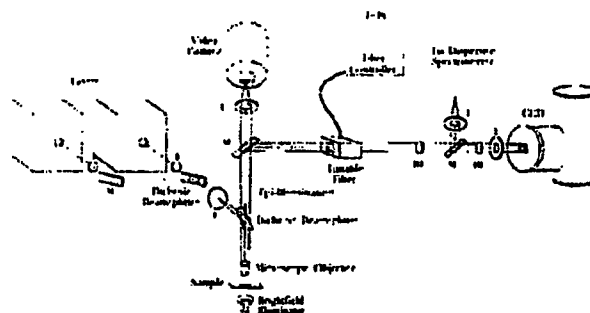


FIG. 3 Schematic diagram of the tunable fluorescence imaging microscope. Multi-color sample epi-illumination provided with a 647.1-nm Kr⁺ laser, a 514.5-nm Ar⁺ laser, or a suitably filtered Hg lamp. Emission images are filtered with the AOTF or LCTF positioned between the microscope and CCD detector. Elements include lenses (L), mirrors (M), a dielectric interference excitation filter (F), and holographic emission filters (HF).

Individual LC elements are made of two parallel glass substrates, optically polished and coated on their inner faces with indium-tin oxide (ITO) transparent electrodes. The electrode face is treated so that the nematic liquid crystals preferentially align in a selected orientation. The oriented rod-like molecules exhibit electrical and optical anisotropy, and the molecular polarizability is anisotropic, as well. Light polarized along the crystal axis, the *e*-rays, will experience a larger polarizability than light polarized across the crystal axis, the *o*-rays, and subsequently the *e*-rays experience a larger index of refraction than the *o*-rays.

To vary the retardance of a nematic LC element, one applies an electric field to the ITO electrodes, which induces an electric field that is parallel to the propagation vector of the incident light. The electric field induces a dipole, and the LC molecules experience a torque which tends to align them within the field. Complete molecular reorientation is opposed by the intermolecular spring constant of the LC, and the realignment is dependent on the applied field strength. Spectral tuning of the LC element is equivalent to rotating the crystal axis of a uniaxial crystal, which acts to change the birefringence and the resulting retardance, as well.

Nematic LCTFs are attractive technologies for spectral imaging because they have high acceptance angles and can be fabricated with large optical apertures. LCTFs provide acceptable transmittance, moderately narrow band-pass, and rapid switching speeds. The devices are physically compact and mechanically rugged. The most important feature provided by LCTFs is their superior image quality, which does not degrade the diffraction-limited imaging performance provided by the microscope.

EXPERIMENTAL

Figure 3 is a schematic of a tunable fluorescence microscope. Multicolor excitation is provided by ion lasers, specifically an Ar⁺ laser at 514.5 nm (Coherent CR-3), and a Kr⁺ laser at 647.1 nm (Coherent Innova 330-K), or by a Hg lamp (Olympus) employing appropriate notch filters. For multicolor laser excitation, the lasers are combined through a dichroic beamsplitter which reflects the

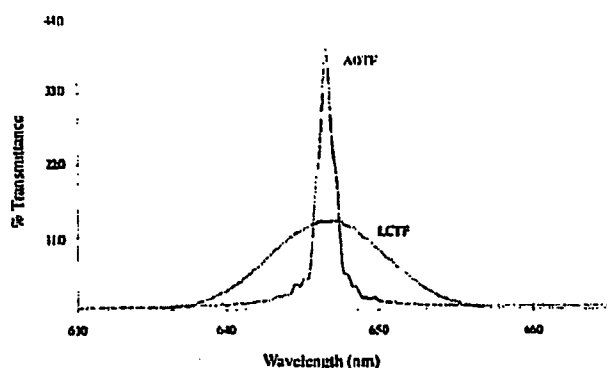


FIG 4 Spectral comparison employing brightfield microscope as broad-band source coupled through the tunable filters to a 0.5-m monochromator with CCD detection. The AOTF provides a bandpass of 2.1 nm (FWHM); the LCTF has a 11.1-nm bandpass

green laser and transmits the red. Sample epi-illumination is provided in combination with dielectric interference dichroic beamsplitters (Omega Optical) matched to the appropriate excitation wavelength. Fluorescence image collection is provided by infinity-corrected planachromat 10× (0.30 NA), 20× (0.46 NA), and 100× (0.95 NA) objectives in an upright metallurgical microscope (Olympus BHSM).

The magnified fluorescence emission is projected to the tunable filter, which provides electronically controlled wavelength selection. The fluorescence microscope is designed so that the AOTF (Brimrose TEAF2-60-1.1H) and the LCTF (Cambridge Research and Instrumentation, Varispec VIS-38) are interchangeable. While the tunable filters provide significant rejection of the excitation wavelength, additional rejection is provided by long-pass colored-glass filters (Omega Optical) when Hg lamp excitation is employed. When laser excitation is used for fluorescence or Raman studies, holographic notch filters (Kaiser Optical HNF-514, HNF-647) provide source attenuation. The filtered image is focused by a multielement optic in combination with a 2.5× projection eyepiece to magnify and present the fluorescence image to a low-noise, 16-bit-dynamic-range, charge-coupled device (CCD) detector (Princeton Instruments 512TKB). The CCD is a back-thinned, back-illuminated device which has 512 × 512 pixels, each 20-μm square. The detector is cooled to cryogenic temperatures (−120°C) with liquid N₂.

For comparison of the calibration and spectroscopic performance of the tunable filters, a quartz tungsten halogen (QTH) lamp is transmitted through the microscope, and transmission spectra are collected with a 0.5-m dispersive monochromator (Chromex 500IS). The monochromator employs CCD detection and is interfaced with the spectral imaging microscope via a 90° turning mirror, as shown in Fig. 3. The instrument parameters employed to collect the AOTF and the LCTF spectra are carefully controlled so that the illumination source intensity, microscope optics, monochromator settings, and CCD integration times are identical.

A 486 PC (Gateway 2000 50/DX2) is used for instrument control, data collection, and spectral image pre-

processing. AOTF control is provided by an AT bus plug-in controller card. LCTF control is provided via RS-232 communication. Acquisition software is written primarily in the C programming language. Spectral image processing and presentation is performed with PC image-processing software operated in *Windows 3.1* (BioScan Optimas 4.01). We also employ a workstation (Silicon Graphics IRIS Indigo R4K) for numerically intensive calculations and for dedicated spectral image processing employing *LinkWinds*, a program developed for remote sensing applications.³⁷ For publication, digital images are printed on a dye sublimation printer.

The spatial resolution provided by the AOTF and the LCTF is evaluated by imaging in brightfield a USAF 1951 resolution target (Rolyn Optics) using high-magnification optics. Fluorescence imaging quality is evaluated for the AOTF by imaging a mixture of 15-μm polystyrene microspheres (Molecular Probes fluorospheres) stained with fluorescence dyes and deposited on glass microscope slides from suspension. Orange and red fluorospheres are excited at 535 nm, and emission maxima are monitored at 602 and 640 nm, respectively. In addition, high-fidelity fluorescence microscopy is performed on 1-μm-diameter carboxylate-modified latex microspheres to demonstrate the ability of the LCTF to provide diffraction-limited spatial resolution.

The suitability of fluorescence emission imaging of intact biological tissues is evaluated by the study of thin sections of rat brainstem tagged for the neurotransmitter serotonin (5HT). Rat-brainstem thin sections (10 μm) are obtained from Sprague-Dawley derived rats weighing 100 to 150 g (BioLab) with the use of standard protocols.⁴ The rats are pretreated with 100 μg colchicine (Sigma) injected into the lateral ventricle. Colchicine disrupts microtubules, leading to decreased transport of neuropeptides and increased neurotransmitter levels in neuronal somata. Immunostaining of the colchicine-treated rats is performed by antibody treatment of the thin section with goat anti-5HT at a ratio of 1 to 100. Secondary antibody immunolabeling is provided by donkey anti-goat immunoglobulin G (IgG) conjugated with Cyanine 3.18 (Biological Detection Systems). The cryostated thin sections are dehydrated, cleared in xylene, mounted on glass microscope slides, and covered with a coverslip using a fade-retarding mounting medium.²⁸

LCTF Raman microscopy is performed on unstained 45-μm-diameter polystyrene microspheres deposited on microscope slides from suspension. Defocused Kr⁺ laser excitation (100 mW) is employed.

RESULTS AND DISCUSSION

The transmission spectra of light directed from the microscope, filtered by the AOTF and LCTF and measured by a dispersive spectrograph, are shown in Fig. 4. At 647 nm the AOTF transmits 40% of the incident, randomly polarized light, while the LCTF peak transmittance is 13.6%. The AOTF and LCTF transmittance values are determined by ratioing the light intensity detected with the appropriate tunable filter in place vs. the light measured without the filter.

The full width at half-maxima (FWHM) of the AOTF and LCTF notch bandpasses when centered at 647 nm

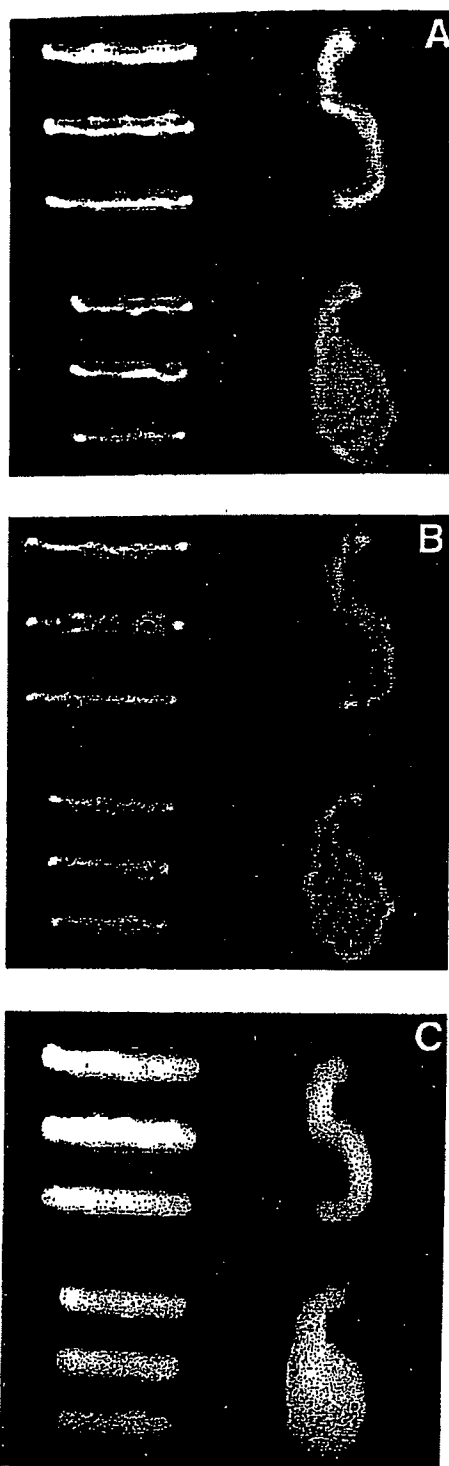


FIG. 5. Resolution target image comparison employing brightfield illumination with 100 \times infinity-corrected objective (0.95 NA). (A) Discrete notch filter in Koehler illumination path; (B) LCTF in emission path; (C) AOTF. Bar target spacing corresponds to (5) 4.9 μ m and (6) 4.3 μ m. No degradation is observed upon insertion of the LCTF, while image blur and loss of contrast is observed with the AOTF.

TABLE I. Comparison of tunable filter performance.

	LCTF	AOTF
Peak transmittance	13.6%	40.0%
Amplitude stability	$\pm 0.46\%$	$\pm 0.80\%$
Tuning reproducibility	$\pm 0.06\%$	$\pm 0.05\%$
Free spectral range	500–741 nm	560–1120 nm
Tunability (minimum increment size)	0.05 nm	0.10 nm
Bandpass (647.1 nm)	11.1 nm	2.1 nm
Aperture	Circular 20-mm diameter	Square 7 \times 7 mm
Acceptance angle	$\pm 7^\circ$	$\pm 5^\circ$
Out-of-band rejection	10^4	10^3
Tuning speed	50 ms	25 μ s

equal 2.1 and 11.1 nm, respectively. The FWHM of the passband determines the filter spectral resolution, assuming that the minimum increment step size is smaller than the filter passband. Both the AOTF and LCTF provide tunability significantly finer than the passband width. Device spectral performance is also evaluated by measuring the free spectral range. The greater the spectral range, the more versatile the device. In addition, the amplitude stability and random tuning reproducibility provide an evaluation of the device precision. The results of these measurements are compiled in Table I.

The tuning speed and out-of-band rejection provided by the competitive technologies are also described in Table I. AOTFs can exhibit relatively strong side lobes, as observed in Fig. 4. The side lobes can be reduced to approximately 3% of the peak transmittance by reducing the rf drive signal amplitude.²⁹ The side lobes corrupt the out-of-band rejection efficiency of the AOTF (10^3), which is an order of magnitude lower than that provided by the LCTF (10^4). Side lobes are not detected with the 10-stage LCTF device employed in this study.

Imaging quality is evaluated by performing transmission imaging of resolution targets and fluorescence imaging of microspheres impregnated with fluorescent dye. Figure 5 illustrates transmission images of USAF 1951 standard resolution targets collected with a 100 \times (0.95 NA) plan achromat objective. The resolution standard contains three bar targets (labeled 5 and 6) which have center-to-center spacings of 4.9 and 4.3 μ m, respectively. Figure 5A is a brightfield image collected with the microscope and projected to the CCD camera in which the illumination source is filtered with a 647-nm dielectric bandpass interference filter having a FWHM of 10.3 nm. The interference filter is placed in the illumination path to minimize the effects of filter nonuniformity on the reference image. The same target is imaged in Fig. 5B without the interference filter, but with the use of an LCTF instead, in which the tunable filter is placed in the emission image path between the microscope and the CCD. Figure 5C was collected with the AOTF, which replaces the LCTF.

It is evident that the LCTF image is virtually identical to the discretely filtered image and that the LCTF does not visibly corrupt the image quality. However, AOTF image quality is degraded with respect to Figs. 5A and 5B. In the vertical dimension of Fig. 5C, which is perpendicular to the dispersion dimension of the AOTF, image blur is visible. The image blur arises from spectral

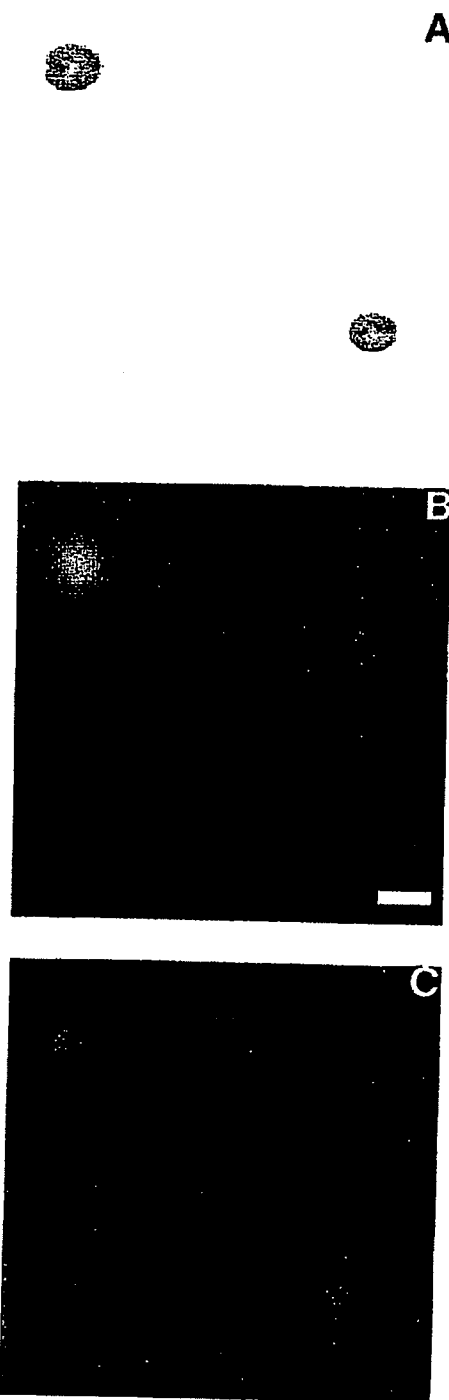


FIG. 6. (A) Brightfield image of two 15- μm -diameter microspheres collected with a 20 \times objective (0.46 NA). The microspheres have been tagged with different fluorophores. (B and C) Fluorescence images collected through the AOTF tuned to the characteristic fluorescence maxima of 602 and 640 nm, respectively. The size bar in panel B corresponds to 15 μm .

dispersion in the TeO_2 crystal.³⁰ The AOTF diffracts a narrow but finite distribution of wavelengths around the center band. As a result, the angle at which the image is diffracted also exhibits a distribution, and the detected spectral image is blurred.

The image blur is compounded by a second image-degrading effect that occurs when the AOTF passband wavelength is changed, resulting in an angular displacement of the image. In the AOTF employed in this study, the image shift as a function of AOTF tuning is 0.01 mrad/nm, which corresponds to a spatial displacement of 0.03 pixels/nm in our optical configuration. In contrast, wavelength-dependent image shift is not observed with the LCTF. The AOTF image shift is reproducible, and image processing can effectively remove the degradation due to image shift. We anticipate that the image-blur component due to dispersion can also be minimized through computational methods similar to those employed for confocal microscopy.³¹ Efforts are underway in our laboratory to implement blur removal numerically.

A quantitative description of image quality involves the measurement of the modulation transfer function (MTF) of the respective spectral imaging systems.³² The MTF describes the ability of the imaging system to generate image contrast as a function of the distance between image bar targets. The percent contrast observed for the smallest target having an edge-to-edge spacing of 4.3 μm was $96 \pm 0.5\%$, $93 \pm 1.6\%$, and $78 \pm 1.5\%$ for Figs. 5A, 5B, and 5C, respectively. The interference filter and LCTF provide significantly improved contrast relative to the AOTF.

It is anticipated that the LCTF will not appreciably degrade the $\lambda/2$ diffraction-limited spatial resolution performance of a research-grade fluorescence microscope. It is also anticipated that the AOTF's achievable spatial resolution will reflect, at a minimum, the 15% degradation observed in Fig. 5C. In practice, the degradation will be significantly worse than 15% due to the wavelength-dependent image shift.

The limiting aperture in Fig. 5 is the 512×512 pixel CCD as the projected images exceed the $12.5 \times 12.5 \text{ mm}^2$ active area of the CCD. In applications where extremely high image fidelity is required, larger CCDs with higher pixel density can be employed. LCTFs would be superior to AOTFs in high-fidelity applications because large, high-optical-quality apertures can more readily be manufactured for LCTFs than for AOTFs.

The CCD integration times used to collect the images in Fig. 5 are comparable despite the $2.9\times$ higher transmission provided by the AOTF. The LCTF provides a bandpass that is $2.8\times$ broader than that of the AOTF, which approximately offsets the AOTF's higher transmission. Fluorescence emission bands are typically broad, and the resolution provided by the LCTF is sufficient for spectral discrimination. In general, the AOTF has the advantage of providing higher throughput at comparable bandpass.

LCTFs can be fabricated to provide high resolution (in fact, higher resolution than that of AOTFs) but not without associated costs in reduced spectral range and peak transmission. Commercial devices can be fabricated to provide 0.025-nm bandpass at 610 nm, but with sub-

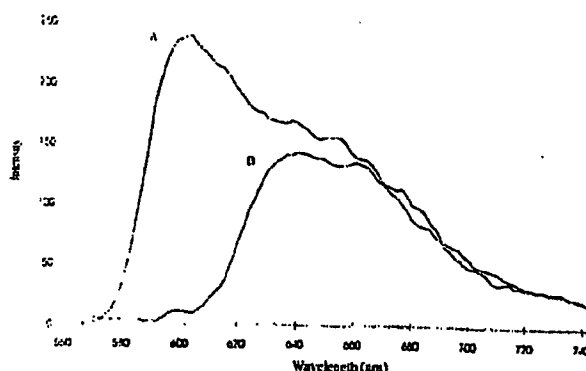


FIG. 7. Fluorescence spectra of tagged polystyrene microspheres collected *in situ* through the AOTF. (A) Orange-tagged microsphere; (B) red-tagged microsphere. The spectra correspond to submicron *x,y* sampling areas and were extracted from the spectral image data set from which the individual images of Fig. 6 were taken.

stantial expense and limited free spectral range. A more realistic filter would provide 0.5-nm bandpass with a free spectral range of 610 ± 50 nm and a peak transmission approaching 15%.

Results of multispectral fluorescence microscopy performed with the AOTF are illustrated in Fig. 6, which includes images of two 15- μ m-diameter polystyrene microspheres that have been tagged with different fluorescent dyes. Figure 6A shows the microspheres in bright-field. Fluorescence images are shown in Fig. 6B and 6C employing bandpass filtered Hg lamp excitation at 560 nm. Figure 6B is collected by tuning the AOTF to select the 602-nm emission of the orange-dye-labeled sphere that appears at the top left. Figure 6C is collected at 640 nm, and the red-dye-labeled sphere appears at the bottom right. The orange-sphere emission is significant at 640 nm and is still visible in Fig. 6C.

The fluorescence emission images of Fig. 6 comprise only two image frames of the spectral image data set that was collected by tuning the AOTF from 560 to 730 nm at 2-nm intervals. Spectra extracted from *x,y* coordinates that correspond to the centers of the microspheres are plotted in Fig. 7. Figure 7A corresponds to the orange-sphere emission, while Fig. 7B corresponds to the red-sphere emission.

The multicomponent model system employed here contains only two unique fluorescent constituents which could readily be distinguished with the use of two discrete filters. The model systems chosen for study were selected because they have simple, well-separated emissions that do not vary with time, and the samples have well-defined size that can be visualized under brightfield conditions. More complex chemical systems would require the flexibility provided by tunable filters. For example, imaging of ion concentration in living cells would benefit from a technology capable of collecting the entire spatial/spectral data set rapidly and noninvasively. A rapidly tunable spectrometer that can be operated in a facile manner is an important development in the methodology of fluorescence microscopy.

Optical microscopy is useful in biological imaging be-



FIG. 8. Tagged microspheres (1- μ m diameter) imaged with a 100 \times objective (0.95 NA) through the LCTF at the emission maximum of 690 nm. The microsphere dimensions are comparable to the size of intracellular material. The figure demonstrates that the LCTF does not degrade image fidelity or resolution and suggests that diffraction-limited spatial resolution is feasible. The size bar corresponds to 500 nm.

cause it can typically provide spatial resolution that corresponds to cellular dimensions. Imaging cellular constituents often requires the highest spatial resolution that can be provided in microscopes limited by far-field diffraction. It is imperative that the spectral imaging technology not corrupt image quality.

Figure 8 is a fluorescence image taken with the LCTF of 1.0- μ m-diameter microspheres tagged with a red-emitting fluorophore that is excited at 647 nm and is imaged at 690 nm. The image quality is superb, and while smaller model systems were not imaged directly, Fig. 8 suggests that it would be feasible to resolve fluorescent features as small as 324 nm—which approaches the Rayleigh diffraction limit for 647-nm radiation. Figure 8 demonstrates that the highest readily achievable image quality provided by optical microscopes is not degraded by the use of LCTF devices.

Final comparisons of the tunable filter technologies were made in a side-by-side fluorescence imaging study of intact biological tissue. Figure 9 shows immunofluorescence microscope images of sectioned caudal rat brainstem that has been secondary-antibody immunolabeled for serotonin (5HT) with Cyanine 3.18 (Cy3). Figure 9A is collected by exciting at 540 nm and tuning the AOTF to the Cy3 emission maximum at 620 nm. Figure 9B is collected with the LCTF tuned to 620 nm, as well. The serotonin is localized within the reticulo-spinal neurons.⁴ Image degradation is visible in Fig. 9A, while no visible image degradation is evident in Fig. 9B.

We employ the Cy3-labeled rat-brainstem sample as a well-characterized model system to compare the fluorescence imaging performance of the competitive spectral

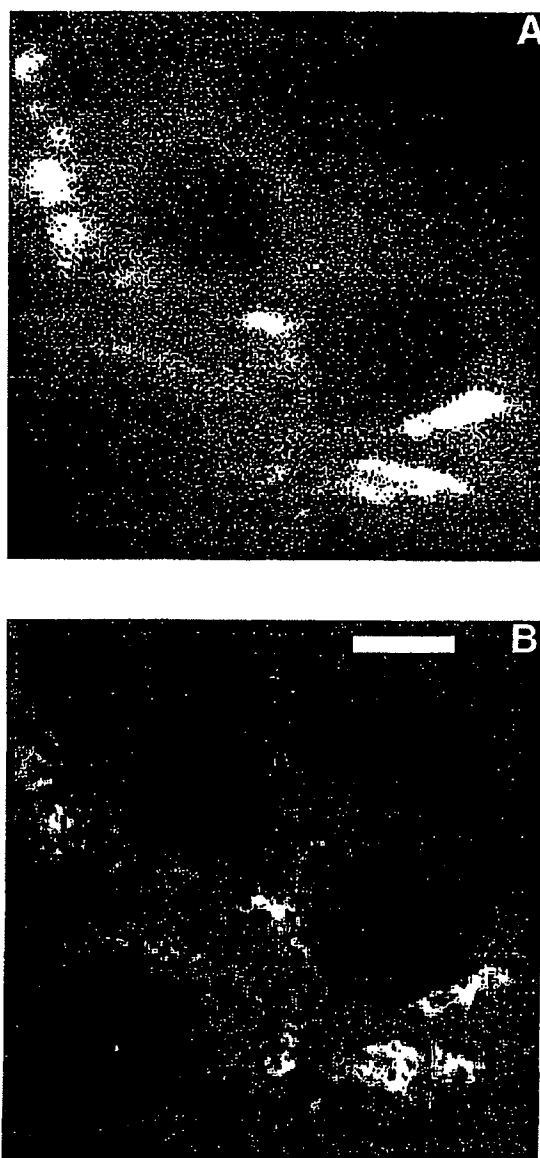


FIG. 9. Images of fluorescence immunolabeled serotonin (5HT) in 10- μ m thin-section rat brainstem. Images collected with Hg lamp excitation filtered at 565 nm and a 20 \times (0.46 NA) objective. (A) AOTF tuned to 620 nm with an integration time of 60 s. Some degradation in image quality is observed upon insertion of the AOTF into the optical train. (B) LCTF tuned to 620 nm with an integration time of 60 s. No image degradation is observed. The size bar in panel B corresponds to 8 μ m.

imaging technologies. The images shown in Fig. 9 are taken from intact brainstem that has been thin-sectioned and fixed prior to immunolabeling, which eliminates the possibility of probing the neurochemical dynamics of the cellular assemblies. In future studies, the use of rapidly tunable spectral filters for multispectral and time-resolved studies of biological systems will be demonstrated.

Raman Microscopy. The utility of fluorescence microscopy in biological analysis is well established. However, potentially invasive fluorescent dyes must be em-

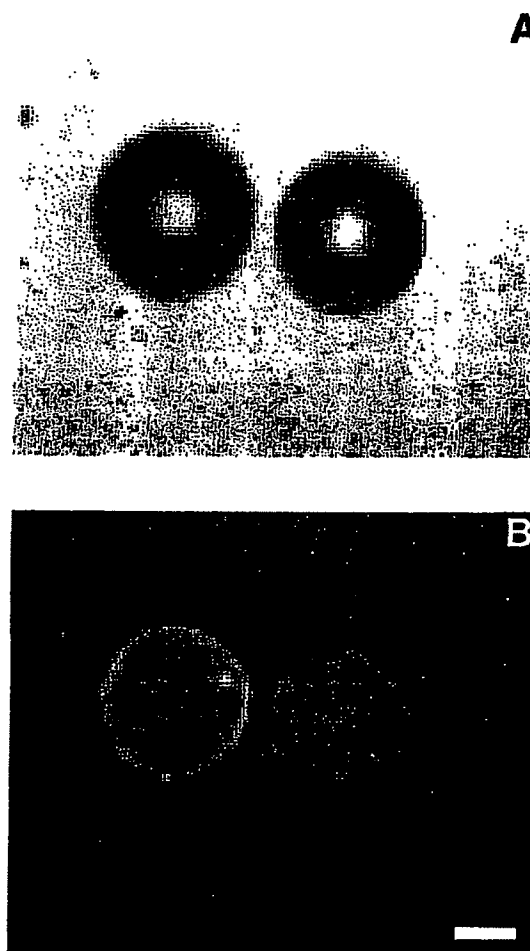


FIG. 10. Raman imaging of 45- μ m-diameter, untagged polystyrene microparticle with a 10 \times objective (0.30 NA). (A) Brightfield image; (B) Raman image with LCTF tuned to 992 cm^{-1} ; 100 mW defocused laser power; 10 s integration time. The size bar in panel B corresponds to 20 μ m.

ployed to generate the specificity and sensitivity that fluorescence imaging techniques enjoy. It would be desirable to obtain analogous spatially resolved chemical information without the use of tags. It would be preferable to employ a spectroscopic signature that is intrinsic to the sample to provide chemically induced image contrast.

Raman imaging microscopy is a spectroscopic technique that can provide image contrast without the use of dyes or stains. Image contrast is based on a material's intrinsic vibrational spectroscopic signature, and Raman microscopy is widely applicable while being noninvasive. Normal Raman microscopy does not provide sensitivity comparable to that for fluorescence microscopy and can lack the specificity of immunolabeling. However, the information content of a Raman spectrum is rich and is highly sensitive to the conformation and dynamics of materials. Advancements in microscope, detector, laser rejection filters, and spectrometer instrumentation allow Raman microscopy to be performed rapidly and provide

high-spatial-resolution, high-fidelity images. Raman microscopy employs instrumentation similar to that for fluorescence microscopy, and we have previously employed AOTFs as spectral imaging filters to perform Raman spectroscopy and imaging.²²

Figure 10 is a brightfield image of ~45- μm -diameter polystyrene microspheres that have not been tagged with a fluorophore. Figure 10B is a Raman image of the microspheres collected in 10 s. Figure 10B demonstrates the first use of LCTF technology to perform Raman imaging microscopy. The LCTF passband is centered at 691.5 nm, which corresponds to a filter position of $992 \pm 130 \text{ cm}^{-1}$. Because of the broad bandpass of the LCTF, several vibrational bands contribute to the Raman emission image, including the relatively intense ring deformation band at 992 cm^{-1} . The image quality demonstrated in Fig. 10B surpasses the imaging performance of the AOTF and is comparable to the highest quality Raman images in the literature.²³⁻²⁵

While autofluorescence backgrounds are minimal with the 647-nm Kr^+ laser excitation employed to generate Fig. 10B, it is necessary to ensure that the detected emission is due to Raman scatter and not fluorescence. If present, the fluorescence will generate an image identical to what is shown in Fig. 10B. Conventionally, discrimination is made on the basis of the Raman spectrum that is collected with a high-resolution spectrometer. Broad emission bands are typically attributed to fluorescence, while the distinctively narrow Raman bands that are specific to polystyrene appear at known frequencies. The LCTF provides a broad passband that is not sufficient for resolving individual Raman bands, but is sufficient for discriminating broad fluorescence emission. As a test of fluorescence emission the LCTF was tuned to 720 nm, where polystyrene does not exhibit Raman scattering. No significant sample emission was observed. In addition, the AOTF was employed to collect a higher-resolution Raman spectrum of the microspheres. The AOTF spectrum substantiated that no autofluorescence was present and that Fig. 10B is a Raman emission image.

CONCLUSIONS AND FUTURE DIRECTIONS

Acousto-optic and liquid crystal no-moving-parts tunable imaging spectrometers have been evaluated with respect to their imaging and spectroscopic performance. AOTFs provide higher transmittance and higher free spectral range than LCTFs at comparable spectral bandpass, but do not provide imaging quality comparable to that for LCTFs. We have demonstrated that the LCTF does not degrade the imaging performance of the fluorescence microscope to a significant degree.

An optimized fluorescence microscope would combine AOTF and LCTF technologies. AOTFs are solid-state crystals and have high damage thresholds, and they are well suited to rapid, facile tuning of laser or broad-band excitation for fluorescence microscopy. In addition, AOTFs provide a unique function in which multiple spectral passbands can be tuned simultaneously. Preliminary demonstration of multiplexed operation of the AOTF has been performed in our laboratory.

The use of LCTF spectral filtering in combination with electronically filtered excitation would provide the ability

to perform time-resolved, fluorescence imaging of multifluorophore-labeled materials. Multispectral investigations of biological tissues are being undertaken in our laboratory. In addition, time-resolved ratio imaging of living cells will be explored.

Raman microscopy is currently being investigated, and we anticipate applying LCTF filters to noninvasive, *in situ* chemical imaging analysis. Raman imaging with LCTFs will provide superb imaging quality and would be capable of providing extremely high fidelity images in combination with CCD detectors having $1\text{K} \times 1\text{K}$ – $4\text{K} \times 4\text{K}$ pixels. The LCTF employed in this study is not optimized for Raman imaging because of the low transmission and the coarse spectral resolution. For optimized Raman imaging performance, a high-resolution (5 cm^{-1}), high-transmission device would be suitable. LCTFs can be manufactured to provide high resolution and moderate transmission, but at a cost to the free spectral range of the device. LCTFs may be best suited for Raman imaging of well-characterized systems where the filter operation can be limited to a specific region of the specimen.

ACKNOWLEDGMENTS

We wish to thank Martin W. Wessendorf, Department of Cell Biology and Neuroanatomy, University of Minnesota for supplying the immunofluorescently labeled rat-brainstem samples employed in this study. We acknowledge partial financial support of this work from the Society of Analytical Chemists of Pittsburgh (SACP) and the Central Research Development Fund, University of Pittsburgh.

1. *Methods in Cell Biology*, D. L. Taylor and Y. L. Wang, Eds. (Academic Press, New York, 1989), Vols. 29.
2. *Methods in Cell Biology*, D. L. Taylor and Y. L. Wang, Eds. (Academic Press, New York, 1989), Vols. 30.
3. K. E. Johnson, *Histology and Cell Biology* (Harwal, Media, Pennsylvania, 1991), p. 271.
4. M. W. Wessendorf, N. M. Appel, T. W. Möllner, and R. P. Eide, *J. Histochem. Cytochem.* 38, 1859 (1990).
5. M. W. Wessendorf, in *Handbook of Chemical Neuroanatomy* (Elsevier Science Publishers, Amsterdam, 1990), p. 1.
6. J. S. Ploem, in *Light Microscopy in Biology*, A. J. Lacey, Ed. (IRL Press, Oxford, 1989), p. 163.
7. D. L. Taylor and Y. L. Wang, *Proc. Nat. Acad. Sci. U.S.A.* 75, 857 (1978).
8. G. R. Bright, G. W. Fisher, J. Ragowska, and D. L. Taylor, *J. Cell Biol.* 104, 1019 (1987).
9. A. F. H. Goetz, G. Vane, J. E. Solomon, and B. N. Rock, *Science* 222, 1147 (1983).
10. P. J. Treado and M. D. Morris, in *Microscopic and Spectroscopic Imaging of the Chemical State*, M. D. Morris, Ed. (Marcel Dekker, New York, 1993), p. 71.
11. S. E. Harris and R. W. Wallace, *J. Opt. Soc. Am.* 59, 744 (1969).
12. I. C. Chang, *Appl. Phys. Lett.* 25, 370 (1974).
13. J. A. Kusters, D. A. Wilson, and D. L. Hammond, *J. Opt. Soc. Am.* 64, 434 (1974).
14. R. W. Dixon, *IEEE J. Quant. Elect.* QE-3, 85 (1967).
15. C. D. Tran, *Anal. Chem.* 64, 971A (1992).
16. C. D. Tran and R. J. Furlan, *Anal. Chem.* 65, 1675 (1993).
17. E. N. Lewis, P. J. Treado, and I. W. Levin, *Appl. Spectrosc.* 47, 539 (1993).
18. I. Kurtz, R. Dwello, and P. Katzka, *Rev. Sci. Instrum.* 58, 1996 (1987).
19. J. Yu, T. H. Chao, and L.-J. Cheng, *Proc. SPIE-Int. Soc. Opt. Eng.* 1347, 644 (1990).
20. P. J. Treado, I. W. Levin, and E. N. Lewis, *Appl. Spectrosc.* 46, 553 (1992).
21. P. J. Treado, I. W. Levin, and E. N. Lewis, *Appl. Spectrosc.* (1994), paper in press.
22. P. J. Treado, I. W. Levin, and E. N. Lewis, *Appl. Spectrosc.* 46, 1211 (1992).

23. H. J. Masterson, G. D. Sharp, and K. M. Johnson, *Opt. Lett.* **14**, 1249 (1989).
24. P. J. Miller, *Metrologia* **28**, 145 (1991).
25. B. Lyot, *C. R. Acad. Sci.* **197**, 1593 (1933).
26. A. Yariv and P. Yeh, *Optical Waves in Crystals* (Wiley, New York, 1984).
27. A. S. Jacobson, Jet Propulsion Laboratory, Pasadena, California.
28. G. D. Johnson and G. M. deC. Nogueira Araujo, *J. Immunol. Methods* **43**, 349 (1981).
29. C. C. Hoyt and D. M. Benson, *Photonics Spectra* **26**, 92 (1992).
30. J. Yu, T. H. Chao, L.-J. Cheng, and J. Lambert, *Proc SPIE-Int Soc. Opt. Eng.* **1347**, 655 (1990).
31. D. A. Agard, *Ann. Rev. Biophys. Bioeng.* **13**, 191 (1984).
32. M. Born and E. Wolf, in *Principles of Optics* (Pergamon, New York, 1965), 3rd ed., p. 483.
33. P. J. Treado, A. Govil, M. D. Morris, K. D. Sternitzke, and R. L. McCreery, *Appl. Spectrosc.* **44**, 1270 (1990).
34. D. N. Batchelder, C. Cheng, and B. J. E. Smith, *Makromol. Chem., Makromol. Symp.* **46**, (1991) 171.
35. G. J. Puppels, M. Grond, and J. Greve, *Appl. Spectrosc.* **47**, 1256 (1993).

EXHIBIT E



University of Pittsburgh

*Faculty of Arts and Sciences
Department of Chemistry*

314 Chevron Science Center
Pittsburgh, Pennsylvania 15260
412-624-8621
Fax: 412-624-8552
E-mail: treado+@pitt.edu

April 27, 1994

Cliff -

Enclosed is the formal acceptance
of the LCTF paper. Let's do
it again with NIR filters!

Pat

P.S. I am decompressing slowly from
our recent phone call.

EXHIBIT F

Pat Treado

1/18/93

① wants quote on "5 nm" 400-720 device
Fax quote

② Very excited about Raman prospects

will send wish list.

uses two lasers sources 514 and 647 nm

ultimate 5 wave numbers

eg 514.5 $514.5 \text{ nm} \Rightarrow 19436.3$ wave
numbers

+ 5 wave numbers
 $\rightarrow 19441.3$ wave numbers
convert back to nm \Rightarrow

514.37 nm

5 wave numbers at 514 is 0.13 nm

at 647 $\Rightarrow 15456$

$15461 \Rightarrow 646.79$

0.21 nm

③ Marketing Data \rightarrow

Big applications \rightarrow 647 - breast Cancer
Alzheimers

514 - corrosion

It they can demonstrate feasibility, say
to devices
they have large industrial support
4 yrs ago 50 Raman spectrometers
w/ microscopes / year

One company selling to this market
Raman microscope
Redistek in England - states
an interference filter.
Sells many to diamond film
industry.

1996 → Pat is organizing Raman Imaging
International in Pittsburgh
- good place to make a splash.

EXHIBIT G

OCT-21-1994 10:47



University of Pittsburgh

*Faculty of Arts and Sciences
Department of Chemistry*

314 Chevron Science Center
Pittsburgh, Pennsylvania 15260
412-624-8621
Fax: 412-624-8552
E-mail: treado+@pitt.edu

October 21, 1994

Mr. Cliff Hoyt
Cambridge Research & Instrumentation Inc.
21 Erie Street
Cambridge, Massachusetts 02139

Dear Cliff:

I talked to Mike Huerta of NIMH about the relevance of LCTF multispectral imaging technology to NIMH SBIR programs. He felt the technology was appropriate and he had several constructive comments which follow:

1. Suggested Title: LCTF Raman Chemical Imaging: New Tools for Mental Health Research
2. For inclusion at the beginning of both the abstract and statement of purpose: This research is closely related to NIMH research topic #92 (Brain Imaging) in the Omnibus Solicitation of the PHS for SBIR grant applications.
3. For inclusion in cover letter: PI (whoever that is; Cliff or Peter) and Mike Huerta, NIMH have discussed the proposal topic and Dr. Huerta has assured us of the relevance of these topics to NIMH's mission.
4. Two weeks prior to the proposal submission date (end of November) fax Mike Huerta (fax # (301) 443-1731) with the following information: (1) name of the PI; (2) business submitting proposal (CRI); (3) title of grant; (4) abstract of proposal. Mike Huerta will contact Division of Research Grants (DRG) to help ensure that the proposal is directed to him.

Of course, NIMH is not the only institute that can be targeted for funding. I went through the SBIR solicitation and several other institute programs are also appropriate:

1. Program 23 (Radiation Research and Medical Imaging Systems, Item 16 in NCI)
2. Program 85 (Biophysics and Physiological Sciences in NIGMS, Items)
3. Program 113 (R&D in Instrumentation ..., Item A in NCRR)

While these other program areas are targetable I would stay with NIMH. Mike Huerta was very enthusiastic about the technology and while he may not be an advocate he is certainly open minded. In the course of my discussions with Mike Huerta it sounded like he was not intimately familiar with Raman imaging. This is only remotely significant in that Meadowlark and Mike Morris submitted an SBIR to NIH. My guess is that the Meadowlark proposal was not submitted

CRI000137

to NIMH. Having the same institute review the two proposals is a double edged sword. The CRI proposal would lose its uniqueness, but in direct comparison with the Meadowlark technology CRI should have a competitive advantage.

The viability of the proposal will depend on the specific problems that we target. We should describe the wide range of mental health areas that LCTFs can impact to indicate the breadth of the technology. Of most importance are the one or two specific application areas we select. The following is a proposed application that is relevant and would display the powers inherent in LCTF based chemically specific imaging technology:

Alzheimer's Disease Tissue Imaging

Rapid chemical image screening of β -amyloid protein deposits in AD brain tissue. Raman chemical imaging would provide the ability to distinguish protein deposits from the brain tissue matrix based on the chemical conformation rather than morphology of the deposits. The LCTF Raman imaging approach would provide an efficient, quantitative method for rapid screening of large brain tissue areas without the need for dyes and stains which would reduce the sample preparation associated with these pathology evaluations. Raman spectroscopic information in concert with morphological information has the potential to provide a more definitive diagnosis of AD than currently can be made. Current optical microscopy evaluations rely on morphology alone.

AD pathology screening is an invasive process performed postmortem. It would be most desirable if Raman imaging could be employed to screen for β -amyloid proteins in living patients. Perhaps the strongest contribution that Raman imaging can make in this area is a more basic biophysical understanding of β -amyloid structure and conformation.

The screening and basic imaging studies are dependent on the ability of Raman spectroscopy to differentiate the structures of amyloid deposits. Preliminary Raman image data that demonstrates the feasibility of the approach would be helpful, but is not essential. Phase I of the project could be focused on establishing the feasibility of the application relying on Raman spectroscopic (non-imaging) studies, in addition to developing the high spectral resolution LCTF technology. In order to perform the feasibility studies it will be necessary to enlist the help of pathology experts who have access to the AD tissue materials. We are currently working with a group at the Armed Forces Institute of Pathology, but their main focus is not AD research. We have an AD Center at Pitt and I have approached them to access the appropriate samples if AFIP is not a better source.

On a separate issue, Peter Miller and I recently discussed the potential of developing LCTFs that would function out to 5 μ m for mid-IR imaging, which would require that LC materials be synthesized that are deuterium labeled. I have discussed the concept with a polymer organic chemist, Toby Chapman, in our department and he feels it would be straightforward to synthesize the appropriate materials, and would be interested in such a development project. I have an initial synthetic approach mapped out by Toby. Issues regarding the economics of such a project are, as

yet, undeveloped. Peter thought this may be suitable as an SBIR project for submission to DOE, for example.

Let me know if you have any questions or comments.

Sincerely,



Patrick J. Treado
Assistant Professor of Chemistry

TOTAL P.04

CRI000139

EXHIBIT H

APPENDIX C

National Science Foundation
Small Business Innovation Research Program

PROJECT SUMMARY

NSF AWARD NO.

NAME OF FIRM Cambridge Research & Instrumentation, Inc.	
ADDRESS 21 Erie Street Cambridge, MA 02139	
PRINCIPAL INVESTIGATOR (NAME AND TITLE) Peter Miller, Staff Scientist	
TITLE OF PROJECT High Definition Raman Imaging Microscope.	
TOPIC TITLE Chemistry	TOPIC NUMBER AND SUBTOPIC LETTER 2.b.
<p align="center">PROJECT SUMMARY</p> <p>Development of the high definition liquid crystal tunable filter (LCTF) described in this proposal will unleash the potential of Raman chemical imaging microscopy for non-invasive chemical characterization of solid-state materials. The LCTF will allow Raman chemical imaging to become a mainstream analytical methodology for the first time, accessible even to non-experts and applicable for routine industrial process monitoring and materials analysis.</p> <p>Raman chemical imaging has the capability to characterize heterogeneous systems without the need for significant sample preparation. Chemical imaging allows one to visualize the composition and spatial distribution of constituents that dictate material function, which is fundamental to characterizing advanced composite materials. An optimized Raman imaging filter based on liquid crystals can readily be used to analyze a wide variety of materials, including polymers, corrosion resistant alloys, and pharmaceuticals.</p> <p>In Phase I, we will demonstrate feasibility by constructing a high resolution LCTF and using it in a microscope to obtain Raman images from test samples. Phase II will involve LCTF optimization and integration into a turnkey high definition Raman microscope consisting of a laser, microscope, LCTF, and CCD detector, together with the appropriate analysis and processing software. C.R.I. has a proven track record commercializing SBIR technology in Phase III.</p> <p>Potential Commercial Applications of the Research</p> <p>A Raman chemical imaging system will have broad applicability in the polymer and coatings industries for chemically specific visualization of domains and defects without the need for sample staining. In-situ monitoring of corrosion in ferrous alloys is another important use, while a third application lies in quantitative studies of polymorphism in pharmaceutical crystalline materials.</p>	
KEY WORDS TO IDENTIFY RESEARCH OR TECHNOLOGY (8 MAXIMUM) Raman, chemistry, spectroscopy, imaging, microscopy	

D. Identification and Significance of the Problem or Opportunity

Development of the high definition liquid crystal tunable filter (LCTF) described in this proposal will unleash the potential of Raman chemical imaging microscopy for non-invasive chemical characterization of solid-state materials. The performance advantages provided by LCTFs will allow Raman chemical imaging to become a mainstream analytical methodology for the first time, accessible even to non-experts and applicable for routine industrial process monitoring and materials analysis.

Raman chemical imaging is an emerging but vital area in chemistry that integrates Raman spectroscopy with imaging technology. Chemical imaging provides the ability to visualize the chemical composition, concentration and dynamics of specific constituents within composite materials, living cells and tissues. Chemical imaging is an interdisciplinary field in its methodology and so it can impact many important areas of science and medicine. Examples of chemical imaging include nuclear magnetic resonance imaging (MRI) employed for clinical diagnosis, and satellite remote sensing for global imaging of ozone depletion.

High-resolution Raman chemical imaging has the potential for characterizing heterogeneous systems rapidly and non-invasively without the need for significant sample preparation. Chemical imaging can visualize *in situ* the composition and spatial distribution of constituents that dictate material function. Understanding the structure/function relationship is fundamental to the characterization of advanced composite materials. The development of an optimized Raman imaging filter based on liquid crystals can readily be applied to the characterization of a wide variety of materials, including polymers, corrosion resistant alloys, and pharmaceuticals.

Raman spectroscopy on the microscopic scale has shown tremendous power as a tool for chemical analysis since the development of the first practical Raman microprobe, a technique which employs a diffraction grating coupled to a CCD detector for rapid collection of Raman microspectra from a single, tiny spot on the sample [1]. Raman spectroscopy is attractive because it provides an almost universally applicable chemically-selective means of contrast generation by relying on the vibrational spectrum intrinsic to a material, without the need for stains or dyes. In addition, high spatial resolution ($\sim 1 \mu\text{m}$) is readily achievable when this technique is combined with optical microscopy.

However, Raman imaging presents significant experimental challenges. The Raman scattering process is inefficient; on average only 1 in 10^8 incident photons scatter inelastically, so Raman microscopy produces signals with low light-levels. This places stringent requirements on the components employed. A number of technological innovations in recent years make it feasible to perform non-imaging Raman spectroscopy routinely. These innovations include high dynamic range charge-coupled device (CCD) detectors and holographic optics for laser light rejection. Despite these innovations, Raman imaging remains cumbersome because of the lack of a high spectral resolution, broad free spectral range, electronically tunable spectrometer technology that simultaneously transmits entire Raman images with high clarity.

The power of Raman spectroscopy is well established for non-imaging characterization of materials, including polymers, semiconductors, biological tissues, catalytic surfaces, corrosion-resistant alloys [2-4]. In polymer studies, for example, Raman spectroscopy is useful for the analysis of chemical composition and structure. The technique can differentiate between internal and external bonds, cis- and trans-isomerism and conjugation. In addition, the helical conformation of polymer chains in the solid-state can be monitored. Raman imaging microscopy provides the ability to visualize polymer chemistry. Internal defects and voids that appear invisible using conventional light microscopy techniques can be characterized with molecular specificity using Raman imaging. Molecular interactions between heterogeneous materials and the homogeneity of mixing processes can also be observed.

The development of broadly tunable, high resolution liquid crystal tunable filter (LCTF) imaging spectrometers as described here will allow Raman microscopy to evolve beyond the scientific curiosity stage, practiced mostly in academic research laboratories, into a powerful technique for materials characterization and industrial process monitoring.

E. Background and Technical Approach

E.1 Background and Technical Approach

Raman imaging provides the ability to visualize samples non-invasively and the methodology requires a tunable filter technology that provides high spatial and spectral resolution. LCTF technology is the only approach that simultaneously provides a broad spectral range, fine spectral resolution, wide acceptance angle, and large optical aperture, while providing high out-of-band rejection. This technology is physically compact, mechanically rugged and electronically controllable without the need for moving mechanical parts.

LCTFs are versatile devices which can function from the visible to the near-infrared, with prospects for operation in the mid-infrared. C.R.I. has pioneered the development of LCTFs, based on nematic liquid crystal technology [5]. These instruments incorporate liquid crystal optical retarders within Lyot birefringent filters, to provide an electronically tunable spectral passband, as shown in Figure 1. LCTFs have large acceptance angles and can be fabricated with large optical apertures. They provide acceptable peak transmittance (15-20%), narrow bandpass (to 0.2 nm), and rapid switching speeds (50 msec). Their out-of-band rejection (10^4) is the highest of any viable tunable filter technology. The throughput, versatility, and spectral purity of the LCTF make it very well-suited for this work.

The most important feature provided by LCTFs is their excellent image quality, which does not degrade the diffraction-limited imaging performance provided by high quality optical systems. LCTFs can be readily combined with imaging optics and high fidelity focal plane array detectors as integral components of high definition chemical imaging systems. Figure 2 is an image of a lupus pathology sample taken with a broadband (35 nm FWHM) LCTF placed between the microscope and a 1024^2 element Kodak Megaplug CCD camera. The image was acquired by taking three monochrome images sequentially, in the blue, green, and red wavelength ranges, which were used to print a 24-bit true-color image. This figure illustrates the unparalleled imaging capability of the LCTF.

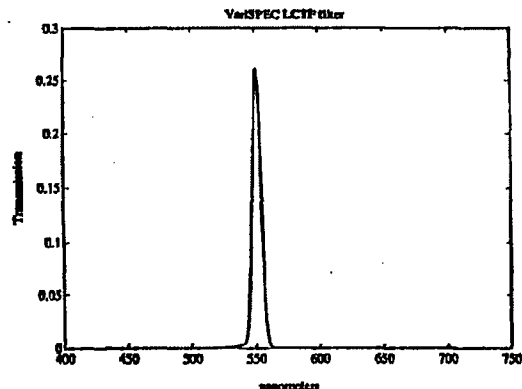


Fig 1. Bandpass of an LCTF with 10 nm FWHM, tuned to 550 nm.

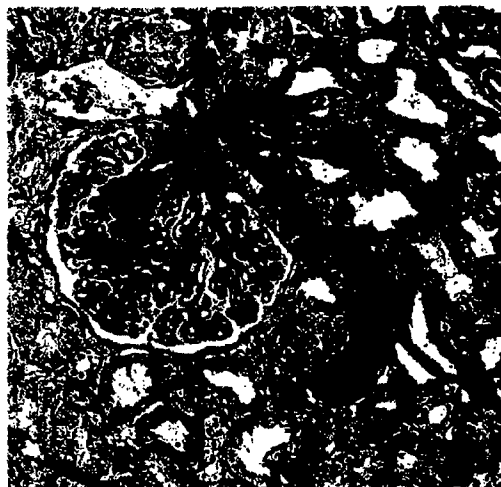


Fig 2. High-resolution image of lupus sample, through LCTF.

A filter with considerably narrower FWHM is contemplated for the present work. Off-the-shelf LCTF's have bandwidths ranging from 5 to 50 nm, and tuning ranges from 400 - 1100 nm. Specialized devices have been made with 0.2 nm passband. The bandwidth of the filter depends only upon the thickness of the fixed crystal retarder elements employed, and manufacture of high-resolution filters does not place more stringent demands on the liquid crystal devices, than when making a spectrally broad filter. A filter with bandwidth of 0.25 nm or less (10 cm^{-1}) would have broad utility for Raman imaging, and construction of such a filter is within the present art. The main technical challenge in making a narrow bandpass device is to maintain high transmission: more elements are required, and the optical loss must be minimized. While light throughput is important, out-of-band rejection is just as important because of the need for discrimination between the Raman band of interest and potential interferences including fluorescence, Rayleigh scattering, and other Raman bands.

E.2 Related Research

Several approaches to Raman microscopy have been developed, including rotating dielectric filter tuning [6], laser scanning [7], spatial multiplexing [8], and tunable excitation with fixed bandpass filtering [9]; however, the last three are not believed to be commercially competitive with the high-resolution imaging discussed in this proposal.

At present there are three viable alternative methods to the LCTF for high-definition Raman imaging, based on rotating dielectric filters, acousto-optic tunable filters (AOTF) [10-11], and liquid crystal etalon (LCE) technologies [12]. The rotating-interference filter approach employs moving mechanical parts to tilt dielectric interference filters, and thus effect wavelength tuning of the Raman emission collected through a microscope. The imaging quality is good at near-normal incidence angles, but upon rotation of the filter the Raman images shift. In practice, the collection of complete Raman

spectral image sets is time-consuming and suffers from spectral artifacts. The technology does not compare favorably with electronically-tunable filters.

In an AOTF, an RF sound wave generated by a piezoelectric transducer passes through a birefringent crystal, establishing a transmission diffraction grating within the crystal. Light meeting a wavelength-dependent momentum condition interacts with the grating and changes its angle or polarization state. The AOTF chief advantages are their tuning speed (25 μ s) and high throughput (40%). Speed is irrelevant in Raman imaging applications: an imaging Raman spectrometer will dwell at each wavelength for a second or more, so microsecond tuning is not needed. Apertures are limited, from 2 to 10 mm square, and the devices accept only highly collimated light. They exhibit relatively strong sidelobes outside the passband, which can be reduced to approximately 3 percent by apodization of the RF signal.

AOTF's have recently been applied to Raman microscopy [10-11]. Because they operate on a diffraction principle, there is an image shift as the AOTF is tuned. This causes problems in multispectral imaging, as precise image-to-image registration cannot readily be achieved without optical redesign of the AOTF, incorporation of compensation optics, or software correction. Further, since passband sidelobes have a different wavelength from the passband center, they are diffracted at different angles, which results in spectral 'smearing' and degraded image resolution. In a side-by-side comparison at 647.1 nm it was observed that use of an AOTF limited the resolution of a microscope image to $\sim 1 \mu$ m, while the LCTF maintained the diffraction-limited resolution of the microscope [13].

Like an LCTF, an AOTF operates on one linear polarization at a time. As a result of this, and internal losses, the maximum throughput is between 40 and 45 percent for highly collimated light. Commercially available imaging AOTF's have bandpasses of 2 nm at 633nm (50 cm^{-1}), several times what is desired. Attaining bandwidth of 10 cm^{-1} may be possible, but only in devices with lower acceptance angle, which effectively reduces the field-of-view seen under the microscope. The wavelength reproducibility of tuning is sufficient for Raman spectroscopy. In summary, AOTFs offer superior speed while sacrificing performance in all other areas: aperture (field-of-view), imaging quality, spectral resolution, and out-of-band rejection.

Another approach to the tunable spectral filter has been taken by Dr. Michael Morris, who has used a liquid crystal etalon (LCE) to collect Raman images [12]. These have liquid crystal material within the cavity of an optical etalon, and the electro-optic action of the liquid crystal material provides an adjustable optical index for tuning. Because only the extra-ordinary optical index n_e is tuned, light incident on the LCE must be linearly polarized. The free-spectral range of an LCE is typically 5 - 25 nm, and finesse ranging from 8 - 25 have been reported [14-15] for near-visible LCE's. Bandwidths as narrow as 0.2 nm should be possible, set by the maximum practical thickness of the liquid crystal layer. However, transmission drops off rapidly with increasing finesse, due to cavity losses. These losses are much higher than in dielectric interference filters or air-spaced etalons, due to scatter in the liquid crystal material and absorption in the alignment and electrode layers [16]. The spectrum of a typical commercial etalon [17] from

Meadowlark Optics is shown in Figure 3A, showing finesse of 8.5 and out-of-band blocking of 36:1 at 570 nm.

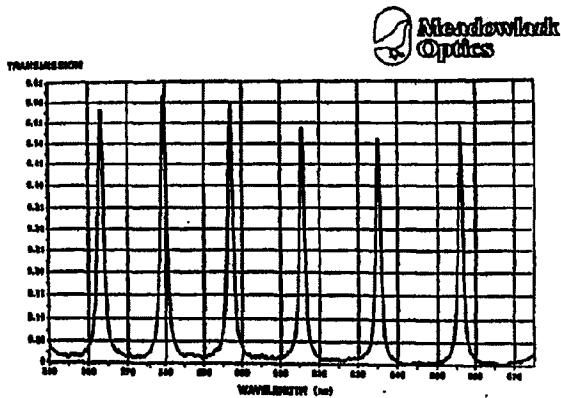


Fig 3A. Bandpass of a commercial LCE device.

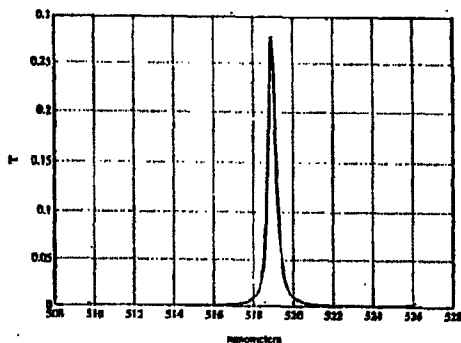


Fig 3B. Bandpass of high-performance LCE made by P.I.

The Principal Investigator has constructed what are believed to be the highest-performance LCE devices to date. A spectrum from one is shown in Figure 3B, exhibiting a finesse of 21, and out-of-band blocking of 204:1. Other devices for infra-red use showed finesse of 53 and blocking of 450:1. But even these high-performance devices have limitations which make them unsuitable for Raman imaging applications. First, while they are mechanically stable, they have great thermal instability. The optical index of liquid crystals has a thermal coefficient 240 times that of quartz [18-19], so there is a large drift, in addition to drift in the electro-optic tuning action. Another source of drift is the thermal coefficient of expansion of liquid crystal fluid, roughly 800 times that of glass. Since liquid crystal material is essentially incompressible, temperature changes cause great pressures within the sealed liquid crystal cavity [20]. This distorts the etalon figure, changing its pass wavelength and degrading its finesse. For these

reasons, their pass wavelength is not stable over time and temperature, and any practical LCE system requires a daily *in situ* wavelength calibration.

Second, LCEs offer limited throughput. While the peak transmission of a low-finesse etalon can be high (up to 60% for polarized light), generally two or more of LCEs are needed in order to obtain sufficient tuning range and high overall finesse. This reduces the transmission and greatly increases the complexity: the two LCE elements must be made to tune together, although each device has substantial tuning drift. Another limit is the field-of-view. The field-of-view is different from that of a simple Fabry-Perot etalon, because the LCE cavity is filled with anisotropic crystalline material that is electro-optically flexed, and exhibits a wide range of orientations at different points throughout the cavity. No analytical expression for the field-of-view has been reported, but measurements suggest that an $f/32$ or slower beam is required for a 15 cm^{-1} device, corresponding to 2° field-of-view [16]. Since the peak transmittance and field-of-view of practical LCE systems are equal to or lower than LCTF figures, throughput will necessarily be lower.

In summary, the imaging quality of LCEs is high, but even the best devices have substantial spectral leakage. A minimum of $10^3:1$ contrast is required to gather high fidelity spectral images, which is beyond the capability of present devices. At least two LCE devices must be ganged together to yield sufficient resolution and free-spectral range, which reduces transmission and adds to system complexity because of tuning difficulties in these parts. There are significant problems with thermal sensitivity and wavelength accuracy, and field-of-view is much less than for LCTF devices.

E.3 Innovativeness and Originality of the Proposed Research

High-performance LCTFs were first demonstrated by the C.R.I. researchers [21-22], and the P.I. holds two patents relating to their construction and tuning [23-24]. C.R.I. has won three industry awards for the VariSPEC filter, based on this technology, and it is presently the only firm supplying scientific-grade LCTF filters.

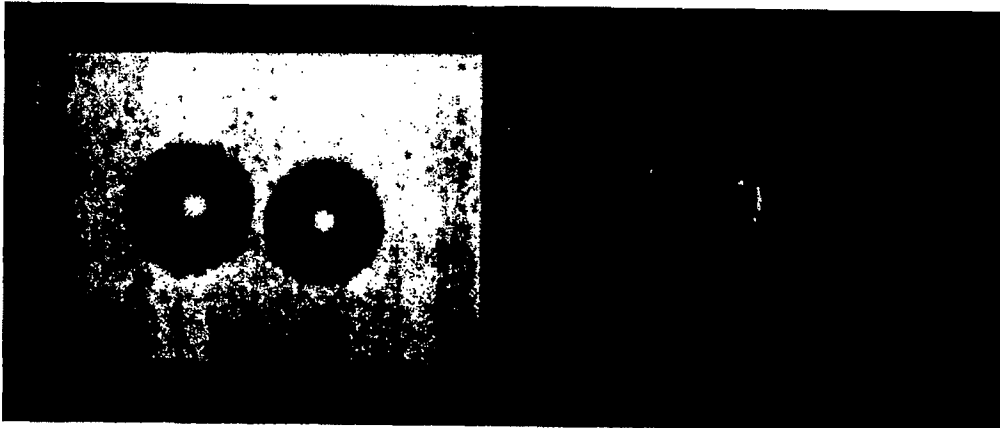


Fig. 4A. Brightfield image of $45\mu\text{m}$ test microspheres.

Fig. 4B. Raman image of the same $45\mu\text{m}$ spheres, taken with LCTF.

The first use of liquid crystal tunable filters for Raman microscopy was performed at the University of Pittsburgh in a collaborative effort between C.R.I. researchers and Prof. Treado [13]. Figure 4A is a brightfield image of a $\sim 45\ \mu\text{m}$ diameter polystyrene microsphere that has not been tagged with a fluorophore. Figure 4B is a Raman image of the microsphere collected in 10 secs. The LCTF passband is centered at 691.5 nm which corresponds to a filter position of $992\ \text{cm}^{-1}$, the relatively intense ring deformation band of polystyrene. The image quality demonstrated in Fig. 4B surpasses the imaging performance of any of the alternative Raman imaging methodologies [6-9].

The diffraction-limited imaging performance of the LCTF combined with its tunability is unparalleled in Raman imaging. The imaging performance combined with the demonstrated reproducible spectral tuning of LCTFs predict that the technology proposed here will revolutionize the practice of Raman imaging.

F. Phase I Research Objectives

F.1 Specific Phase I Objectives

The Phase I Technical Objectives are:

- 1) To use existing computer models to generate a tunable Lyot filter design optimized for Raman spectroscopy;
- 2) To study the integration of such a filter into a microscope imaging system, including optical path, data acquisition, and camera requirements;
- 3) To construct a fully imaging prototype filter according to this design, with resolution of $10\ \text{cm}^{-1}$ or better, tunable over a range of $2500\ \text{cm}^{-1}$;
- 4) To characterize this filter for its spectral properties, including peak transmission, bandwidth, out-of-band rejection, and tuning range;
- 5) To use this filter to obtain true two-dimensional Raman spectroscopy images of test samples; and,
- 6) To prepare a Phase I report describing the results.

F.2 Connection with Phases II and III

Phase I of the anticipated program will demonstrate feasibility by integrating a high resolution LCTF filter into a microscope, and obtaining Raman images of various chemical test samples. Phase II will involve further optimization of the high definition LCTF filter, and development within an integrated, turnkey Raman microscope consisting of a laser, microscope, LCTF, and CCD detector, with processing and analysis software. Microscope integration will be performed in collaboration with ChemIcon, Inc. a start-up company located in Pittsburgh, PA.

In Phase III, ChemIcon will perform the system integration and market these microscopes to existing Raman microspectroscopy customers of ChemIcon, including the six Fortune 500 companies which currently support the

development of Raman microscopy in Prof. Treado's laboratory. Raman microscopy is being applied to analyze a host of materials relevant to the specific industrial sponsors. Size of the mature market is estimated as several hundred microscopy sites, with annual sales of \$5M or more.

G. Phase I Research Plan

G.1 To design a tunable Lyot filter optimized for Raman spectroscopy
Over the past 5 years, the P.I. and co-workers at C.R.I. have developed computer models for the design of Lyot filters, based on the Jones calculus and incorporating spectrally-dependent values for the transmission, absorption, and birefringence of the materials involved. These include routines for calculating response for off-axis rays, and the tuning error of the liquid crystal retarders, based on actual measured statistical variation of these components from ongoing production lots. These models have a proven ability to predict passband width, spectral leakage, and peak transmission.

The principal requirements for a Raman-optimized LCTF are narrow bandwidth, high transmission, low leakage, and wide field-of-view. The tuning range will be 515 - 750 nm, to permit use with various laser sources ranging from 514 nm (Argon) to 647 nm (Krypton). A filter with bandwidth of 0.25 nm at 500 nm (10 cm^{-1}) requires use of calcite or other high-birefringence materials for the fixed retarders. This, coupled with the wide field-of-view requirement, leads to a design based on wide-field elements [25-26]. It is likely that LiNbO_3 will be chosen as the retarder material, rather than calcite, because of its lower δn value. Consequently, its figuring error tolerances are relaxed relative to those of calcite. Also, it is more rugged, and not as prone to chipping and scratching.

High transmission in the filter is given by $T = E^s$, where s is the number of Lyot stages and E is the efficiency per stage. The stage efficiency E is set by losses in the liquid crystal cell, the polarizer, the fixed retarder, and tuning errors. These are input parameters to the design, based on measured values. In the design process, one seeks to minimize the number of stages, s , while meeting the requirements for bandwidth, free-spectral range, and out-of-band blocking. While the classical Lyot design offers little latitude in this regard, such a design is rarely suitable for a tunable filter. This is because the exact value of retardance at each stage will deviate from the idealized binary sequence Lyot described, as it is tuned to various wavelengths. To avoid sidelobes in the resultant filter response, one must add a few additional stages for contrast enhancement. The selection of retardances for these stages plays a crucial role in determining filter performance, and proper choice allows their number to be minimized.

The figure of $s = \log_2(\text{FSR}/\text{FWHM})$ for a classical Lyot design, represents a lower limit for an LCTF design. For a Raman filter, broad pre-filters can be used to define a useful range of 50 nm, so this is an acceptable FSR. This, coupled with the bandwidth FWHM of 0.25 nm, leads to a lower limit of $s=8$. A practical LCTF filter will probably require 3 or more additional stages, or a total of 11.

In addition to the optical components, we will design a suitable mechanical enclosure to provide a stress-free filter mounting. The thermal management approach is to create a nearly isothermal environment, free of gradients across the filter, and to sense the temperature with a medical-grade chip thermistor. This allows monitoring temperature with 0.05 °C precision, which is sufficient to resolve spectral shifts as small as $\delta\lambda \approx .01$ nm in the fixed retarders, corresponding to 1/25 of the filter FWHM. Unlike fixed-wavelength Lyot filters, there is no need to stabilize the filter temperature: the liquid crystal elements will be used to actively compensate for thermal drift in the LiNbO_3 and quartz retarders [24].

G.2 To study integration of an LCTF into a microscope imaging system
Integration of the LCTF into a Raman imaging system will involve both opto-mechanical and software engineering. Key C.R.I. researcher Clifford Hoyt has considerable experience integrating LCTFs in microscopes for fluorescence and pathology applications. Approaches have included placing the LCTF in the infinity-corrected optics path of microscopes such as Zeiss Axioskop and Olympus B-MAX systems, as well as the use of relay optics and telecentric correction systems. The Raman imaging LCTF will have a 20 mm aperture, and an overall length of 40-55 mm, similar to that of LCTF filters previously used for fluorescence work. It is anticipated that Prof. Treado will perform computer-aided optical design, using Zemax XE ray tracing software, to model the integration of the LCTF into microscopes in his laboratory. The location of other strategic components of the Raman system can also be modeled and optimized using this technique.

For the software integration, Prof. Treado will define the necessary features of Windows computer program to control the LCTF and to perform sophisticated multi-spectral image processing. A list of features and functions will be developed for actual software coding in Phase II of the project. Existing software allows Prof. Treado to acquire, display, and store high-resolution Raman images, and to control the filter manually for the Phase I testing.

G.3 To construct a fully imaging prototype filter according to this design
C.R.I. routinely manufactures commercial LCTF's for use in this spectral range, with bandwidths of 5-35 nm. We do not anticipate making any changes to the liquid crystal tuning elements for the present work.

The only special concern we anticipate in assembling this filter relates to reflections at the LiNbO_3 retarders. LCTF filters are normally assembled in an index-matching material which keeps reflections below 0.03% per interface. However, LiNbO_3 has a substantially higher optical index than the other materials used ($n_o=2.30$ vs. $n=1.53$), so it needs to be anti-reflection coated to match its impedance to that of the index-matching material. From the analysis of Staromlynska, inter-reflections limit the extinction of each stage to $1 / [3R^2(1-R)]$, including the effects within the liquid crystal cell [27]. For the coated LiNbO_3 interfaces, a reflection R of 0.5% or less is anticipated, yielding a contrast of 13,400:1 per stage. Since LCTF designs require a contrast of only 100:1 per stage, there should be no problem meeting project goals for the overall filter contrast.

Electronics modules for tuning the liquid crystal cells and sensing the thermistor resistance have been developed in the course of commercial LCTF development, and will be used without modification in the present work.

G.4 To characterize this filter for its spectral properties

The filter will be characterized at C.R.I. using a SPEX 0.5M spectrometer with 0.02 nm resolution. Bandwidth (FWHM) and peak transmission will be measured using a quartz-halogen lamp source, and a Hamamatsu S1336 detector with a Scitec chopper and SRS 810 lock-in amplifier. This provides measurements of peak transmission that are accurate to 2% of the transmission value, and resolves transmission of 10^{-5} or less, for spectral leakage measurements. Tuning range will be checked directly, by observing the filter response as it is tuned across the operating range. Measurements are fully automated using a PC/486 controller, enabling hundreds of spectra to be taken with no operator involvement. Spectral tuning accuracy will be checked at the 543.5 and 632.89 nm laser lines using He-Ne sources.

Off-axis response will be measured by mounting the filter on a two-dimensional rotation stage and observing passband shift as the LCTF orientation is varied. Thermal drift will be measured if time permits, by mounting the filter on a Neslab RTD-110 controlled temperature stage, and measuring passband variations as the LCTF temperature is adjusted over the range 20 - 35 °C.

G.5 To use this filter to obtain two-dimensional Raman spectroscopy images

The LCTF filter will be integrated into microscopes at the University of Pittsburgh for these tests, which will be performed by Prof. Treado. Spectral imaging will be evaluated by measurement of the modulation transfer function (MTF), a quantitative analysis of imaging performance. The MTF will be measured by imaging several standard resolution targets as a function of wavelength, using a Princeton Instruments CCD detector and BioScan OPTIMAS software to acquire the images. Raman imaging performance will be established by evaluation of images of polymer microspheres, routinely used as size and chemical standards by researchers in this field.

Raman imaging evaluation will also be performed on real-world, industrial materials available to Prof. Treado through collaborations with industrial sponsors. Materials will include corrosion-resistant alloys, polymer composites and pharmaceuticals.

G.6 To prepare a Phase I report describing the results.

The P.I., Prof. Treado, and senior C.R.I. personnel will draft a Phase I Final Report for submission to the NSF, including experimental data, images, and technical analysis, in accordance with N.S.F. guidelines.

H. Commercial Potential

H.1 Brief Description of the Company

Cambridge Research and Instrumentation, Inc. was formed in May 1985 with the aims of carrying out research in solar-terrestrial physics and developing

instruments for the accurate measurement and control of light. Dr. Peter Foukal, president of C.R.I., Inc. has published over 100 papers in major refereed journals and conference proceedings. This work on solar astrophysics has also been presented in numerous contributed and invited papers at meetings of the AAS, AGU and IAU. Dr. Foukal has also served on various advisory committees and panels of NASA, NSF, and the National Academy of Sciences, over the past fifteen years. His text book "Solar Astrophysics" was published by Wiley Interscience in May 1990.

C.R.I. maintains active programs at the forefront of solar-terrestrial research, including photometric and radiometric studies of solar irradiance variation, and also remote sensing studies of plasma electric fields in the sun's atmosphere. Much of this work is carried out at the National Solar Observatories stations at Kitt Peak and at Sacramento Peak, and has been supported by the NSF, NASA, and the Air Force.

In electro-optics, C.R.I. has developed the LaseRad and CryoRad cryogenic cavity radiometers as laboratory standards for measurement of radiative flux, with support from the SBIR Programs of the NSF and NASA. These instruments are in use as national standards of light measurement at NIST (ex-NBS), and in Germany, Sweden, Canada, Spain, and at the CNAM in France. C.R.I. also developed and builds commercially the award-winning LS and LFC series laser power stabilizers widely used in electro-optics laboratories, and most recently, the award-winning VariSpec liquid crystal tunable filters. A significant fraction of C.R.I.'s \$1.2M sales volume in the last fiscal year consisted of exports of commercial products to Europe and Japan.

H.2 Commercial Applications

H.2.a Polymer imaging

Raman vibrational spectroscopic imaging of heterogeneous polymer dispersions and polymer thin films will be possible when the LCTF filtering technology is suitably incorporated into a dedicated Raman microscope. Such a device will have broad applicability in the polymer and coatings industries because it will allow for non-invasive, chemically specific visualization of domains and defects in polymer composites without the need for sample staining.

At present, many analytical imaging methodologies are applied to polymer characterization. The optical microscope is employed in combination with a host of optical contrast generation mechanisms including polarization, interference and fluorescence. In general, these methods do not provide chemical specificity and provide limited spatial resolution. For high spatial resolution analysis, polymers are imaged with electron microscopy, usually in combination with osmium tetroxide staining, a difficult and hazardous undertaking. Existing polymer visualization methodologies are problematic. Raman imaging has extraordinary potential in polymer analysis but the power of the technique hinges on the availability of a reliable, high resolution Raman spectral filter.

Prof. Treado is collaborating with a major pharmaceutical firm and Ford Motor Co. to develop Raman imaging instrumentation suitable for characterizing the polymeric materials of importance to these companies. If the suitable

filtering technology can be developed these industrial sponsors will be a ready market for Raman microscopes.

H.2.b Corrosion Imaging

Non-invasive, *in situ* monitoring of temperature-dependent corrosion of steel alloys exposed to phosphate solution is an important application of Raman imaging. This will be performed with long working distance microscope optics to probe samples housed in a programmable high temperature stage, viewing them through protective diamond windows. A rapid and non-invasive method for monitoring corrosion *in situ* provides several capabilities: first, chemical mechanisms of corrosion can be established; second, failure rate predictions that dictate the replacement schedule of strategic materials can be determined, representing a tremendous potential cost saving to industry and government; and, methods to inhibit corrosion can more effectively be evaluated. Methodologies developed here will be generally applicable to any *in situ* Raman imaging application where samples are housed in extreme environments of temperature, pressure, or radiation.

C.R.I. will develop high resolution LCTF technology to be coupled with microscope optics and CCD cameras to provide submicron spatial resolution with sufficient spectral resolution to distinguish the corrosion chemical species. The P.I. and Prof Treado will work with industrial sponsors interested in monitoring *in situ* temperature-dependent corrosion of alloys. At present, Prof. Treado is providing a customized microscope to two Fortune 100 defense contractors who perform these types of measurements under contract to the Department of the Navy. The technologies developed in these programs will be directly applicable for corrosion monitoring aboard Navy ships, and in steam and nuclear power generators. Once Raman corrosion monitoring technology is developed it will be marketed to the commercial power industry.

H.2.c Crystal Polymorphism Imaging

Raman microscopy has the potential for use in quantitative polymorphism characterization of pharmaceutical active-agent crystalline material. Polymorphism occurs in pharmaceuticals in which a chemical constituent may have more than one crystalline structure. This is problematic because an active agent may provide therapeutic benefit only if it is the appropriate crystalline form or polymorph. Raman microscopy can often distinguish spectroscopically between different polymorphs, and Prof. Treado is engaged in a collaboration with a large international pharmaceutical firm to establish the utility of Raman microscopy as a quantitative methodology for discriminating different polymorphs in a quality control application. If feasibility can be established a market for Raman microscopes will be defined. Raman systems relying on LCTFs will then be marketed to pharmaceutical companies for polymorphism quantitation.

H.2.d Biomedical Imaging

Probing biological structures is tractable with Raman spectroscopy. In particular, Raman spectroscopy is effective for analyzing aqueous samples without the interference of the strong OH bands encountered in infrared spectroscopy. In addition, the intrinsic vibrational markers of biological

samples provide chemical selectivity without the need for significant sample preparation or the use of potentially invasive stains or tags. In macroscopic, non-imaging studies of biological materials, the wealth of chemical information provided by Raman spectroscopy is often convoluted due to the complexity of the materials. Raman spectroscopic microscopy focuses the chemical analysis to localized regions of heterogeneous materials, and provides an efficient chemical visualization method. Biological applications of Raman microscopy include resonance Raman studies of carotenoid pigments of bacteria [28], Raman microspectroscopy of gallstones and kidney stones [29], and of DNA in single tumor cells [30].

H.3 Competitive Products

In 1991 SPEX licensed the spatial multiplexing approach co-developed by Prof. Treado at the University of Michigan, but the rapid pace of development in Raman microscopy makes the spatial multiplexing approach obsolete.

In the U.K., Renishaw P.L.C. commercialized a dedicated Raman microscope employing interference filter tuning. The microscope combines Raman imaging optics with a microprobe. In operation, Raman microspectra are collected rapidly at isolated regions of a sample, and then full-frame images are collected with the filters tuned to a few discrete Raman bands. Complete spatial/spectral information cannot readily be collected with this approach. It is well suited to visualization of widely-separated Raman bands, but not to imaging of dense matrices in which complex Raman spectra often overlap and are convoluted. To obtain a definitive evaluation of complex systems, the kind of materials encountered in the real world, the spectral collection and image collection must be integrated, and provide the kind of complete spatial/spectral data available from a tunable imaging spectrometer.

Approaches requiring the use of moving mechanical parts contribute to degraded imaging performance. The imaging performance is especially compromised when widely separate Raman spectral ranges are accessed.

A no-moving-parts approach to Raman microscopy has been successfully demonstrated by Prof. Treado and co-workers at the National Institutes of Health employing AOTFs [7]. Despite the no-moving-parts design, the AOTF imaging quality is handicapped due to the 'spectral smearing' described earlier in Section E.2. Future AOTFs may address these degradations, and may provide the high spectral resolution (10 cm⁻¹), and large optical apertures (~25 mm), anticipated in the proposed technology, but current AOTFs do not. As importantly, the development of optimized AOTFs is much less tractable than the development of LCTF technology. High resolution LCTFs have already been fabricated for other spectroscopic applications and can be optimized readily for Raman microscopy.

AOTF microscopes are currently being commercialized by Brimrose Corp. of America. These devices are not manufactured under license with NIH, which has a patent pending on the technology. If the patent is issued the Brimrose microscopes will infringe on the NIH patent and it is anticipated that the federal government will defend their patent rights.

It is anticipated that the Renishaw Raman microscope is the competitive product for the foreseeable future.

H.4 Advantages of the Proposed Approach Over Existing Technology

The existing competitive technologies are tunable spectral filter designs including rotating dielectric filters, AOTFs and LCEs. The LCTF approach enjoys a competitive advantage over all of these alternatives.

The complete spatial/spectral data generated by LCTF system gives it a clear advantage over rotating dielectric filter systems, because it provides the user with a much more detailed picture of the chemical distribution when characterizing spatially and spectrally complex, real-world samples.

Compared to systems using AOTF filters, an LCTF-based Raman imaging system would offer vastly superior imaging quality. In addition, use of a liquid crystal waveplate at the LCTF entrance enables monitoring the polarization state of the Raman signal. This yields important benefits for studies of oriented anisotropic materials such as crystals, polymers, semiconductors, and fibers. System integration is easier as well, due to the larger aperture and viewing angle the LCTF affords. Turning to LCEs, if these are commercialized in the future, they promise severe limits in terms of spectral calibration, out-of-band blocking, and field-of-view, without offsetting performance benefits in other areas. This suggests that the LCTF will enjoy a competitive advantage over this technology as well.

H.5 Progress in Commercializing Other SBIR Technology

The Principal Investigator has developed several innovative instruments for optical research. He was one of the key members of the team that pioneered the use of cryogenic cavity radiometer for laboratory standards measurements of radiative flux, with support from the Small Business Innovation Research Programs of the NSF and NASA. These instruments are in use as national standards of light measurement at NIST (ex-NBS), the German PTB, CNAM in France, as well as the national laboratories of Sweden, Spain, and Canada. C.R.I. also developed and builds commercially the award-winning LS and LPC series laser power stabilizers used worldwide in electro-optics laboratories, and most recently, the patented VariSpec line of liquid crystal tunable filters. The VariSPEC was supported by NSF and NIH Small Business Innovation Research Programs. These instruments, with over \$2 million in commercial sales, point to a long and successful history both in research and in the development and marketing of scientific research equipment.

I. Principal Investigator and Senior Personnel

PETER J. MILLER

PRINCIPAL INVESTIGATOR

Staff Scientist

Cambridge Research and Instrumentation, Inc.

Education:

1980 B.A. (Astronomy) Williams College
1985 M.S. (Electrical Engineering) Dartmouth College

Memberships:

American Astronomical Society
Optical Society of America

Experience:

1979 Visiting Fellow, JILA/NBS, Boulder, CO
1980-83 Staff Scientist, Atmospheric and Environmental Research, Inc.,
Cambridge, MA
1985 Staff Scientist; Cambridge Research and Instrumentation, Inc.,
Cambridge, MA

Relevant Publications, Reports, and Awards

"Optical Retarder Having Means for Determining the Retardance of the Cell Corresponding to the Sensed Capacitance Thereof", U.S. Patent 5,247,378 (1993).

Laser Focus CTA award, Laser Focus, 29, 115 (1993). Awarded for the VariSpec tunable liquid crystal filter.

R & D 100 Winners Announcement, Research & Development, 34, 12 (1992). Awarded for the VariSpec tunable liquid crystal filter.

"Photonics Circle of Excellence Awards", Photonics Spectra, 26, 5 (1992). Awarded for the VariSpec tunable liquid crystal filter.

"Use of Tunable Liquid Crystal Filters to link Photometric and Radiometric Standards", P. Miller, Metrologia 28, 145, (1991).

"Tunable Narrowband Birefringent Filters for Astronomical Imaging", P. Miller, SPIE Proc. 1235, 466, (1990).

"Liquid Crystal Devices and Systems Using Such Devices." P. Miller, U.S. Patent 4,848,877 (1989).

"Tunable Birefringent Filters Using Liquid Crystals", P. Miller, talk presented at "Optics for Astronomy and Remote Sensing", O.S.A. Topical Meeting, Sept. 26-29, 1988, Falmouth, MA.

CLIFFORD C. HOYT
Staff Scientist
Cambridge Research and Instrumentation, Inc.

Education

1983 B.A. (Physics) Williams College
1987 M.S. (Engineering) M.I.T.

Experience

1983-85 Staff Scientist, Atmospheric and Environmental Research,
Inc., Cambridge, MA
1987- Staff Scientist, Cambridge Research and Instrumentation,
Inc., Cambridge, MA

Relevant Publications

"Imaging Spectrometers for Fluorescence and Raman Microscopy:
Acousto-Optic and Liquid Crystal Tunable Filters", Hannah R. Morris,
Clifford C. Hoyt, and Patrick J. Treado, Appl. Spectrosc. 48, (1994) in
press.

"Merging Spectroscopy and Digital Imaging Enhances Cell Research", C.
Hoyt and D. Benson, Photonics Spectra, 26, 92, (1992).

"Characterization of an absolute cryogenic radiometer as a standard
detector for radiant-power measurements", R.U. Datla, K. Stock, A.C.
Parr, C.C. Hoyt, P.J. Miller, and P.V. Foukal, Appl. Opt., 31:34, 7219-
7225, (1992).

"Cryogenic Radiometers and their Application to Metrology", C.C. Hoyt,
P.V. Foukal, Metrologia, 28:3, 163-168 (1991).

"Liquid Crystal Tunable Filters for Photometry", C. Hoyt, P. Miller,
invited paper, "CORM 90", Rochester Inst. of Tech., May 7-9, (1990).

"Image-Preserving Tunable Filter for Microscopy", C. Hoyt, Phase I SBIR
Final Report to NIH, (1989).

"Comparison Between a Side-Viewing Cryogenic Radiometer and Self-
calibrated Silicon Photodiodes", C. Hoyt, P. Miller, P. Foukal, E.
Zalewski, SPIE Proc 1109, (1989).

"Remote Biomedical Spectroscopic Imaging of Human Artery Wall." Lasers
in Surgery and Medicine, 8:1-9, (1988).

"Spectroscopic Diagnosis for Control of Laser Treatment of
Atherosclerosis." R.R. Richards-Kortum, A. Mahta, T. Kolubayev, C.
Hoyt, J. R. Sacks, M. S. Feld, 1988, Lasers in Surgery and Medicine.

J. Consultants and Subcontracts

Patrick J. Treado
 Assistant Professor of Chemistry
 Department of Chemistry, University of Pittsburgh

Prof. Treado is a recognized expert in the development of Raman chemical imaging, optical microspectroscopic techniques and their application to materials analysis. His letter confirming availability and commitment to this project is included as an Appendix to this Proposal.

Prof. Treado performed his doctoral work under the direction of Prof. Michael D. Morris. His research involved the development of spectroscopic imaging techniques, specifically Raman microscopy and photothermal deflection densitometry, employing Hadamard transform spatial multiplexing. The Raman microscopy technique led to several nationally competitive fellowships and awards being won by Prof. Treado. A patent of the Hadamard Raman microscopy was issued in 1991, and the technology has been licensed by Spex Industries, a spectroscopic instrument manufacturer, for commercial development.

While a postdoctoral fellow at the National Institutes of Health (1990-1992) Prof. Treado performed biophysical studies of model biological membrane assemblies using Raman and infrared spectroscopy. With Dr. Neil Lewis and Dr. Ira Levin, Prof. Treado pioneered the development of chemical imaging methods using acousto-optic tunable filters (AOTFs). Prototype instruments capable of performing visible/near-infrared absorption microscopy and Raman microscopy were developed. A patent covering the use of AOTFs in spectroscopic imaging instruments is pending. His paper describing the first use of AOTF for Raman chemical imaging was awarded the 1993 Meggers Award by the Society for Applied Spectroscopy for the best paper published in Applied Spectroscopy in 1992.

Since joining the University of Pittsburgh, Department of Chemistry as an Assistant Professor in September 1992, Prof. Treado has been engaged in a research program in analytical spectroscopy and chemical imaging, including the first use of an LCTF for Raman imaging, with the P.I. of this proposal.

Selected Publications

1. Hannah R. Morris, Clifford C. Hoyt, and Patrick J. Treado, "Imaging Spectrometers for Fluorescence and Raman Microscopy: Acousto-Optic and Liquid Crystal Tunable Filters", Appl. Spectrosc. 48, (1994) in press.
2. Patrick J. Treado, Ira W. Levin, and E. Neil Lewis, "Indium Antimonide (InSb) Focal Plane Array (FPA) Detection for Near-Infrared Imaging Microscopy", Appl. Spectrosc. 48, (1994) in press.
3. E. Neil Lewis, Patrick J. Treado, and Ira W. Levin, "Near-Infrared and Raman Spectroscopic Imaging", Amer. Lab. in press.
4. Michael D. Schaeberle, John F. Turner, and Patrick J. Treado, "Multiplexed Acousto-Optic Tunable Filter (AOTF) Spectral Imaging Microscopy", Proc. SPIE 2173, (1994) 176.
5. E. Neil Lewis, Patrick J. Treado, and Ira W. Levin, "A Miniaturized, No-Moving-Parts Raman Spectrometer", Appl. Spectrosc. 47, (1993) 539.
6. Patrick J. Treado and Michael D. Morris, "Infrared and Raman Spectroscopic Imaging, Spectroscopic and Microscopic Imaging of the Chemical State", M.D. Morris, Ed. (Marcell Dekker, New York, 1992) pp. 71-108.

7. Patrick J. Treado, Ira W. Levin and E. Neil Lewis, "High-Fidelity Raman Imaging Spectrometry: A Rapid Method Using an Acousto-optic Tunable Filter", *Appl. Spectrosc.* **46**, (1992) 1211.
8. Patrick J. Treado, Ira W. Levin and E. Neil Lewis, "Near-Infrared Acousto-Optic Filtered Spectroscopic Microscopy: A Solid State Approach to Chemical Imaging", *Appl. Spectrosc.* **46**, (1992) 553.
9. Patrick J. Treado, Anurag Govil, Kent D. Sternitzke, Richard L. McCreery and Michael D. Morris, "Hadamard Transform Raman Microscopy of Laser-Modified Graphite Electrodes", *Appl. Spectrosc.* **44**, (1990) 1270.
10. Patrick J. Treado and Michael D. Morris, "Multichannel Hadamard Transform Raman Microscopy", *Appl. Spectrosc.* **44**, (1990) 1.
11. Patrick J. Treado and Michael D. Morris, "Hadamard Transform Spectroscopy and Imaging", *Spectrochimica Acta Rev.* **13**, (1990) 355.
12. Patrick J. Treado and Michael D. Morris, "A Thousand Points of Light: the Hadamard Transform in Chemical Analysis and Instrumentation", *Anal. Chem.* **61**, (1989) 723A.
13. Patrick J. Treado and Michael D. Morris, "A Hadamard Transform Raman Microprobe", *Appl. Spectrosc.* **43**, (1989) 190.
14. Patrick J. Treado and Michael D. Morris, "Hadamard Transform Raman Imaging", *Appl. Spectrosc.* **42**, (1988) 897.
15. Patrick J. Treado and Michael D. Morris, "A Hadamard Transform Raman Microscope", in *Proc. of the International Laser Symposium IV*, R.G. Lerner, Ed. (American Institute of Physics, New York, 1989) 725.
16. Michael D. Morris and Patrick J. Treado, "Hadamard Transform Raman Microscopy", in *Microbeam Analysis-1989*, P.E. Russell, Ed. (San Francisco Press, San Francisco, 1989) 146.

K. Equipment, Instrumentation, Computers, and Facilities

K.1 Facilities available at Cambridge Research & Instrumentation

An equipment item of particular importance to this project is the C.R.I. liquid crystal filter fabrication facility. This facility includes an 8 x 12 foot class-100 clean room, with complete thermal and humidity control; all necessary equipment for fabricating liquid crystal elements of the highest optical quality on glass and quartz substrates; water filtration, substrate handling, and desiccant storage facilities for cleaning and processing to exacting chemical levels; and an 8' Laminar horizontal flow hood for overall assembly in a particle-free, laminar flow environment.

Test equipment at C.R.I. includes a 0.5-meter SPEX spectrometer with 300 and 1200 line/mm gratings for high-resolution spectroscopy (0.025 nm); a quarter-meter visible ISA spectrometer with an EG&G 1024-element reticon detector; an f/4.5 quarter-meter PTI monochromator, equipped with stepper motors under computer control, with visible and IR gratings; a Scitec optical chopper and Stanford Research 810 lock-in amplifier; quartz-halogen, mercury, Kanthal, and Xe arc continuum sources with collimation optics; a mercury line source for wavelength scale calibration; and a variety of silicon, germanium, PbSe, and InGaAs photodiodes, and photodiode preamps with NIST-traceable calibration.

Other relevant equipment includes a Zeiss Axioskop microscope equipped for epi- and kohler illumination; a Dage MTI CCD-72 camera and controller; a

Matrox MVP-AT frame grabber; Optimus image processing software; Sony Trinitron RGB monitor; a Neslab RTD-110 controlled temperature system with heat sink mount for temperature control of optical samples to ± 0.02 °C; He-Ne, Ar⁺⁺, and Nd:YAG lasers with spatial mode filters and beam expanding optics; 6-inch and 1-inch Labsphere integrating spheres; PC/AT and PC/386 computers with 16-bit high-speed data acquisition hardware and software.

In addition to the above equipment, C.R.I. has a PC/486-based CAD center for electronic and mechanical design; an electronics test and production lab equipped to handle analog, digital, and microprocessor assemblies. We have access to complete metal-working facilities for fabricating jigs, special optical fixtures, etc. C.R.I. also maintains a NIST-traceable calibration lab, for detector tests and calibrations at the highest level of accuracy.

K.2 Facilities available to Prof. Treado at the University of Pittsburgh Laboratory Facilities:

Prof. Treado has approximately 1200 ft² of modern laboratory space, equipped for optical spectroscopy (visible/near-infrared absorption, Raman and fluorescence emission), optical spectroscopic imaging microscopy, and wet chemical manipulations.

Computer:

Prof. Treado's laboratory is computer-automated. Data collection is controlled by personal computers running commercial programs and programs written by laboratory personnel. Preliminary spectral image data processing is performed on 486 computers networked to a Silicon Graphics IRIS Indigo R4K workstation. The workstation functions as a file-server and is connected to a magneto-optic disk for mass data storage and retrieval. The workstation also serves as an advanced spectral image processing graphics workstation. It employs a program, LinkWinds, dedicated to processing and visualizing multi-dimensional spectral image data sets, which was developed at the NASA Jet Propulsion Laboratory for remote sensing spectral imaging applications. LinkWinds is an intuitive and interactive package, allowing unparalleled capability for multidimensional graphical analysis.

Major equipment in Prof. Treado's laboratory:

(2) Princeton Instruments CCD detectors interfaced to a Gateway 2000 50 MHz 80486 DX2 computer running BioScan OPTIMAS image processing software; Coherent 330 Krypton ion laser, 400 mW 752 nm, 1 W multiline red; Coherent CR-3 Argon ion laser, 150 mW 514.5 nm; Brimrose TEAF2-.6-1.1 μ acousto-optic tunable filter; Brimrose TEAF2-1.0-2.0 μ acousto-optic tunable filter; Chromex 0.5 m spectrograph for performing dispersive optical spectroscopy, and spectral calibration of the LCTFs; (2) Olympus BH-2 upright microscopes with visible-optimized optics interfaced to a Cohu 4910 b&w video camera for sample positioning and focusing; Kinetic Systems research grade optical table, 4' x

10', Newport research grade optical table, 5' x 10'; EG&G PAR 5110 lock-in amplifier; Electro-Optic Systems InSb photodiode; C.R.I. VariSpec LCTF for fluorescence imaging.

Special materials:

Sophisticated samples suitable for Raman microscopy applications including corrosion test samples, polymeric composites, thin films and coatings on polymer substrates, as well as pharmaceuticals, will be provided by Prof. Treado's external industrial collaborators in the defense, pharmaceutical, and automobile industries.

Other:

The chemistry department maintains the usual array of modern spectroscopic instrumentation available for general access including a scanning electron microscope, Cambridge Instruments S90. A fully equipped electronic and machine shop for instrument fabrication and repair is available. Special purpose equipment can be constructed at J. Baur Machining, Mars, PA, while most instrumentation repair can be handled on-site.

L. Current and Pending Support of P.I. and Senior Personnel

The P.I. has no prior, current, or pending support for development of Raman imaging filters. He is the P.I. of NASA contract NAS7-1246, "Tunable Liquid Crystal Filters for Remote Sensing Applications", which has a duration of two years, from May 18, 1993 - May 17, 1995. This carries a 2 month commitment during the proposed Phase I period of effort.

Clifford Hoyt has been notified of a pending SBIR award from the N.I.H. for a proposal, "High-Efficiency Tunable Fluorescence Emission Filter" (contract number not yet available), which begins September 1, 1994 and ends February 28, 1995. He has a commitment of 3 months, 1 month of which falls within the period of the proposed Phase I effort. In addition, he has been notified of a pending STTR Phase I award, "A Universal Compensator for Polarization Microscopy", from the N.I.H. (contract number not yet available), which begins July 1, 1994 and ends Dec. 31, 1994. Phase II work could begin as early as May 1995, if a follow-on award is made. Finally, he has a commitment of 20 percent to ongoing commercial projects at C.R.I., amounting to 1.2 months during the Phase I period.

M. Equivalent Proposals to Other Federal Agencies

There are no equivalent proposals under consideration by or being submitted to any other Federal Agencies.

N. Budget

The budget is presented on the following page. Funds are budgeted for the purchase of 10 optical retarder of LiNbO_3 @ \$250 each, and \$250 for materials used in making the liquid crystal tuning elements. These supplies will be used to make the prototype LCTF described in the Plan of Work. The computer budget is to allow for maintenance and repair costs for the PC/386 systems.

O. Prior Phase II Awards

Cambridge Research & Instrumentation, Inc., has not received more than 15 Phase II SBIR awards in the past 5 fiscal years.

APPENDIX D

SEE INSTRUCTIONS ON REVERSE

SUMMARY

BEFORE COMPLETING

PROPOSAL BUDGET

ORGANIZATION Cambridge Research & Instrumentation, Inc.		FOR NSF USE ONLY	
		PROPOSAL NO.	DURATION Proposed Granted
PRINCIPAL INVESTIGATOR/PROJECT DIRECTOR Peter Miller		AWARD NO.	
A. SENIOR PERSONNEL: P/PI and Other Senior Associates (List each separately with title, A.S., show number in brackets)		NSF Funded Person-mos.	Funds Requested By Proposer
		CAL	Funds Granted By NSF (If Different)
1. Peter J. Miller, P.I.		1.5	\$ 6560
2. Clifford C. Hoyt, Staff Scientist		2.0	8024
3.			
4.			
5. () OTHERS (LIST INDIVIDUALLY ON BUDGET EXPLANATION PAGE)			
6. (2) TOTAL SENIOR PERSONNEL (1-5)		3.5	14584
B. OTHER PERSONNEL (SHOW NUMBERS IN BRACKETS)			
1. () POST DOCTORAL ASSOCIATES			
2. (1) OTHER PROFESSIONALS (TECHNICIAN, PROGRAMMER, ETC.)		.75	2043
3. () GRADUATE STUDENTS			
4. () UNDERGRADUATE STUDENTS			
5. () SECRETARIAL - CLERICAL			
6. () OTHER			
TOTAL SALARIES AND WAGES (A+B)			16627
C. FRINGE BENEFITS (IF CHARGED AS DIRECT COSTS) .43 X (A+B)			7150
TOTAL SALARIES, WAGES AND FRINGE BENEFITS (A+B+C)			23777
D. PERMANENT EQUIPMENT (LIST ITEM AND DOLLAR AMOUNT FOR EACH ITEM EXCEEDING \$500.) (Do not use for Phase I)			
TOTAL PERMANENT EQUIPMENT			
E. TRAVEL 1. DOMESTIC (INCL. CANADA AND U.S. POSSESSIONS)			
2. FOREIGN (Do not use for Phase I)			
F. PARTICIPANT SUPPORT COSTS			
1. STIPENDS \$			
2. TRAVEL			
3. SUBSISTENCE			
4. OTHER			
() TOTAL PARTICIPANT COSTS			
G. OTHER DIRECT COSTS			
1. MATERIALS AND SUPPLIES See proposal text			2750
2. PUBLICATION COSTS/DOCUMENTATION/DISEMINATION			
3. CONSULTANT SERVICES			
4. COMPUTER (ADPE) SERVICES			200
5. SUBCONTRACTS Prof. Patrick Treado 35 days@420/day			14700
6. OTHER			
TOTAL OTHER DIRECT COSTS			
H. TOTAL DIRECT COSTS (A THROUGH G)			41427
I. INDIRECT COSTS (SPECIFY) Overhead .48 X (A+B+C) = 11413			
TOTAL INDIRECT COSTS G & A .155 X (H + Overhead) = 8190			19603
J. TOTAL DIRECT AND INDIRECT COSTS (H+I)			61030
K. FEE (If requested; maximum equals 7% of J) .065 X J			3970
L. TOTAL COST AND FEE (J + K)			\$65000
PI/PI D TYPED NAME & SIGNATURE Peter Miller <i>PMI. M</i>		DATE 06/10/94	FOR NSF USE ONLY
CO. REP. TYPED NAME & SIGNATURE Peter Foukal <i>Peter Foukal</i>		DATE 06/10/94	INDIRECT COST RATE VERIFICATION
		Date Checked	Date of Rate Sheet
		Initials-DGA	

References

1. T. Hirschfeld, J. Opt. Soc. Am. **63**, (1973) 476.
2. D. I. Bower and W. F. Maddams, The Vibrational Spectroscopy of Polymers, Cambridge University Press, (Cambridge), 1989.
3. P. R. Carey, Biochemical Applications of Raman and Resonance Raman Spectroscopies, Academic Press, (New York), 1982.
4. N. Pessall, A. B. Dunlap, and D. W. Feldman, Corrosion-NACE **33**, 130 (1977).
5. P. J. Miller, Metrologia **28**, (1991) 145.
6. D. N. Batchelder, C. Cheng and B.J.E. Smith, Makromol. Chem., Makromol. Symp. **46**, (1991) 171.
7. M. Bowden, P. Donaldson, D.J. Gardiner, J. Birnie and D.L. Gerrard, Anal. Chem. **63**, (1991) 2915.
8. P. J. Treado and M. D. Morris, Appl. Spectrosc. **44**, (1990) 1.
9. G. Puppels and J. Greve, XIV International Raman Conference, Wurzburg, Germany (1992)
10. P. J. Treado, I. W. Levin and E. N. Lewis, Appl. Spectrosc. **46**, (1992) 1211.
11. E. N. Lewis, P. J. Treado, and I. W. Levin, Appl. Spectrosc. **47**, (1993) 539.
12. M. D. Morris, paper #485, Great Lakes Regional ACS Conference, Ann Arbor, June 2, 1994.
13. H.R. Morris, G.C. Hoyt, and P.J. Treado, Appl. Spectrosc. **48** (1994) in press.
14. F.C. Saunders, G. Parry, Opt. Quantum Electron. **18**, 426 (1986).
15. J.S. Patel, M.A. Saifi, D.W. Berreman, C. Lin, N. Andreadakis, and S.D. Lee, Appl. Phys. Lett. **57** (17), 1718 (1990).
16. P. J. Miller, Final report to under SBIR contract F29601-93-C-0065 (1993).
17. Meadowlark Optics "Tech Flash", Liquid Crystal Filled Fabry-Perot Filter (1994).
18. M. J. Weber, Handbook of Laser Science and Technology, C.R.C. Press, (Boca Raton), 1986.
19. I.-K. Khoo and S.-T. Wu, Optics and Nonlinear Optics of Liquid Crystals, World Scientific, (River Edge, N.J.), 1993.
20. E.B. Priestley, P.J. Wojtowicz, P. Sheng, Introduction to Liquid Crystals, Plenum (New York), 1974.
21. P. J. Miller, SPIE Proc. **1235**, 466 (1990).
22. T. G. Chrien, C. Chovit, P. Miller, SPIE Proc, **1937** 28, (1993).
23. P. J. Miller, U.S. Patent 4,848,877 (1989).
24. P. J. Miller, U.S. Patent 5,247,378 (1993).
25. J. W. Evans, J. Opt. Soc. Am. **39**, 229 (1949).
26. A. M. Title, W. J. Rosenberg, Applied Optics **18** (20), 3443 (1979).
27. J. Staromlynska, IEEE J. Quant. Electr., **28** (2), 501 (1992).
28. R. A. Dalterio, W. H. Nelson, D. Britt, J. Sperry and F. J. Purcell, Appl. Spectrosc. **40**, (1986) 271.
29. H. Ishida, R. Kamoto, S. Uchida, A. Ishitani, K. Iriyama, E. Tsukie, F. Shibata, K. Ishihara and H. Kameda, Appl. Spectrosc. **41**, (1987) 407.
30. F. Sureau, L. Chinsky, C. Amirand, J.P. Ballini, M. Duquesne, A. Laigle, P.Y. Turpin and P. Vigny, Appl. Spectrosc. **44**, (1990) 1047.

EXHIBIT I

APPENDIX B

**NATIONAL SCIENCE FOUNDATION
SBIR PROPOSAL COVER PAGE**
Small Business Innovation Research
Program Solicitation No. 95-59
CLOSING DATE: JUNE 12, 1995

TOPIC NO. 2	SUBTOPIC LETTER (if any) b	TOPIC TITLE Chemistry
PROPOSAL TITLE High Definition Raman Imaging Microscope		
NAME OF PROPOSING SMALL BUSINESS CONCERN Cambridge Research & Instrumentation, Inc.		ADDRESS (including ZIP CODE) 21 Erie Street Cambridge, MA 02139
REQUESTED AMOUNT \$ 65,940	PROPOSED DURATION 6 months	PERIOD OF PERFORMANCE 1/96 - 6/96
THE SMALL BUSINESS CONCERN CERTIFIES THAT:		
1. It is a small business as defined in this solicitation.		Y/N Y
2. It qualifies as a socially and economically disadvantaged business as defined in this solicitation. FOR STATISTICAL PURPOSES ONLY		N
3. It qualifies as a women-owned business as defined in this solicitation. FOR STATISTICAL PURPOSES ONLY		N
4. NSF is the only Federal agency that has received an equivalent or overlapping proposal from the small business concern. If NO, you must disclose equivalent or overlapping proposals and awards as required by this SBIR Solicitation.		Y
5. A minimum of two-thirds of the research will be performed by this firm in Phase I.		Y
6. The primary employment of the principal investigator will be with this firm at the time of award and during the conduct of the research.		Y
7. It will permit the government to disclose the title and technical abstract page, plus the name, address and telephone number of a corporate official if the proposal does not result in an award to parties that may be interested in contacting you further information or possible investment.		Y
8. It will comply with the provisions of the Civil Rights Act of 1964 (P.L. 88-352) and the regulations pursuant thereto.		Y
PRINCIPAL INVESTIGATOR/PROJECT DIRECTOR		
NAME Peter J. Miller		
SOCIAL SECURITY NO. 195-44-3236		TELEPHONE NO. (617) 491-2627
COMPANY OFFICER (FOR BUSINESS AND FINANCIAL MATTERS)		
NAME Dr. Peter V. Foukal		TELEPHONE NO. (617) 491-2627
OTHER INFORMATION		
PRESIDENT'S NAME Peter V. Foukal	YEAR FIRM FOUNDED 1985	NUMBER OF EMPLOYEES AVERAGE PREVIOUS 12 MO.: 13 CURRENTLY: 14

PROPRIETARY NOTICE See Section 5.4 for instructions concerning proprietary information.

Proprietary information is contained on page number(s) _____ of the proposal.

NOTE: The signed Certification Page must be included immediately following this Cover Page with the original copy of the proposal only.

Precedes Proposal Page No. 1

NSF FORM 1207 (SBIR) (3/95)

CRI000611

APPENDIX C

**National Science Foundation
Small Business Innovation Research Program**

PROJECT SUMMARY

NSF PROPOSAL NO.

NAME OF FIRM Cambridge Research & Instrumentation	
ADDRESS 21 Erie Street Cambridge, MA 02139	
PRINCIPAL INVESTIGATOR (NAME AND TITLE) Peter J. Miller, Staff Scientist	
TITLE OF PROJECT High Definition Raman Imaging Microscope	
TOPIC TITLE Chemistry	TOPIC NUMBER AND SUBTOPIC LETTER 2.b
<p align="center">PROJECT SUMMARY</p> <p>This Small Business Innovation Research Phase I project will develop an ultra-narrowband liquid crystal tunable filter (LCTF) as the basis of a Raman chemical imaging microscopy station for non-invasive chemical characterization of solid-state materials. The advantages in performance and practicality provided by this technique will allow Raman chemical imaging to become a mainstream analytical methodology for the first time, accessible even to non-experts and applicable for routine industrial process monitoring and materials analysis.</p> <p>Raman chemical imaging has the capability to characterize heterogeneous systems without the need for significant sample preparation. Chemical imaging allows one to visualize the composition and spatial distribution of constituents that dictate material function, which is fundamental to characterizing advanced composite materials. An optimized Raman imaging system based on an LCTF can readily be used to analyze a wide variety of materials, including polymers, corrosion resistant alloys, and pharmaceuticals.</p> <p>In Phase I, we will demonstrate feasibility by constructing a high resolution filter and using it in a microscope to obtain Raman images from test samples. Phase II will involve filter optimization and integration into a turnkey high definition Raman microscope consisting of a laser, microscope, LCTF, and CCD detector, together with the appropriate analysis and processing software. C.R.I. has a proven track record commercializing SBIR technology in Phase III.</p> <p>Potential Commercial Applications of the Research</p> <p>A Raman chemical imaging system will have broad applicability in the polymer and coatings industries for chemically specific visualization of domains and defects without the need for sample staining. In-situ monitoring of corrosion in ferrous alloys is another important use, while a third application lies in quantitative studies of polymorphism in pharmaceutical crystalline materials.</p>	

D. Identification and Significance of the Problem or Opportunity

The development of broadly tunable, high resolution liquid crystal tunable filter (LCTF) imaging spectrometers as described here will enable Raman chemical imaging to evolve beyond the scientific curiosity stage, practiced mostly in academic research laboratories, into a powerful technique for materials characterization and industrial process monitoring. Raman chemical imaging is an emerging but vital area in chemistry that integrates Raman spectroscopy with imaging technology. Chemical imaging provides the ability to visualize the chemical composition, concentration and dynamics of specific constituents within composite materials, living cells and tissues. Chemical imaging is an interdisciplinary field in its methodology and so it can impact many important areas of science and medicine. Examples of chemical imaging methods include nuclear magnetic resonance imaging (MRI) for clinical diagnosis, and satellite remote sensing for imaging of ozone depletion.

High-resolution Raman chemical imaging has the potential to characterize heterogeneous systems rapidly and non-invasively without the need for significant sample preparation. Chemical imaging can visualize *in situ* the composition and spatial distribution of constituents that dictate material function. Understanding the structure/function relationship is fundamental to the characterization of advanced composite materials. The development of an optimized Raman imaging system based on LCTFs can readily be applied to the characterization of a wide variety of materials, including polymers, corrosion resistant alloys, and pharmaceuticals.

Raman spectroscopy on the microscopic scale has shown tremendous power as a tool for chemical analysis since the development of the first practical Raman microprobe, a technique which employs a diffraction grating coupled to a CCD detector for rapid collection of spectra from a single, tiny spot on the sample [1]. Raman spectroscopy is attractive because it provides an almost universally applicable chemically-selective means of contrast generation by relying on the vibrational spectrum intrinsic to a material, without the need for stains or dyes. In addition, high spatial resolution ($\sim 1 \mu\text{m}$) is readily achievable when this technique is combined with optical microscopy.

However, Raman imaging presents significant experimental challenges. The Raman scattering process is inefficient; on average only 1 in 10^8 incident photons scatter inelastically, so Raman microscopy produces signals with low light-levels. This places stringent requirements on the components employed. A number of technological innovations in recent years make it feasible to perform non-imaging Raman spectroscopy routinely. These innovations include high dynamic range charge-coupled device (CCD) detectors and holographic optics for laser light rejection. Despite these innovations, Raman imaging remains cumbersome because of the lack of a high spectral resolution, broad free spectral range, electronically tunable spectrometer technology that simultaneously transmits entire Raman images with high clarity.

The power of Raman spectroscopy is well established for non-imaging characterization of materials, including polymers, semiconductors, biological tissues, catalytic surfaces, corrosion-resistant alloys [2-4]. In polymer studies, for example, it is useful for the analysis of chemical composition and structure. The technique can differentiate between internal and external bonds, *cis*- and *trans*-isomerism and conjugation. In addition, the helical conformation of polymer chains in the solid-state can be monitored. Raman imaging microscopy provides the ability to visualize polymer chemistry. Internal defects and voids that appear invisible using

conventional light microscopy techniques can be characterized with molecular specificity using Raman imaging. Molecular interactions between heterogeneous materials and the homogeneity of mixing processes can also be observed.

E. Background and Technical Approach

E.1 Background and Technical Approach

Raman imaging provides the ability to visualize samples non-invasively and the methodology requires a tunable filter technology that provides high spatial and spectral resolution. LCTF technology is the only approach that simultaneously provides a broad spectral range, fine spectral resolution, wide acceptance angle, and large optical aperture, while providing high out-of-band rejection. This technology is physically compact, mechanically rugged and electronically controllable without the need for moving mechanical parts.

LCTFs are versatile devices which can function from the visible to the near-infrared, with prospects for operation in the mid-infrared. C.R.I. has pioneered the development of LCTFs, based on nematic liquid crystal technology [5]. These instruments incorporate liquid crystal optical retarders within Lyot birefringent filters, to provide an electronically tunable spectral passband, as shown in Figure 1. LCTFs have large acceptance angles and can be fabricated with large optical apertures. They provide acceptable peak transmittance (15-20%), narrow bandpass (to 0.2 nm), and rapid switching speeds (50 msec). Their out-of-band rejection (10^4) is the highest of any viable tunable filter technology. The throughput, versatility, and spectral purity of the LCTF make it very well-suited for this work.

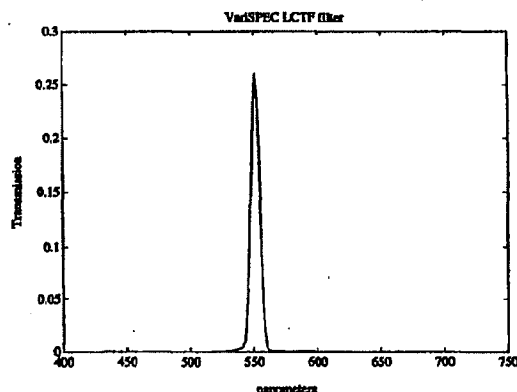


Fig 1. Bandpass of an LCTF with 10 nm FWHM, tuned to 550 nm.

Fig 2. High-resolution image of skin sample, through LCTF.

The most important feature provided by LCTFs is their excellent image quality, which does not degrade the diffraction-limited imaging performance provided by high quality optical systems. LCTFs can be readily combined with imaging optics and high fidelity focal plane array detectors as integral components of high definition chemical imaging systems. Figure 2 shows a trichrome-stained rabbit skin sample,

imaged with a broadband (35 nm FWHM) LCTF placed between the microscope and a 2048² element Kodak Megaplug CCD camera. The image was acquired by taking three monochrome images sequentially, in the blue, green, and red wavelength ranges, which were used to print a 24-bit true-color image. It illustrates the unparalleled imaging capability of the LCTF.

A filter with considerably narrower FWHM is contemplated for the present work. Off-the-shelf LCTF's have bandwidths ranging from 5 to 50 nm, and tuning ranges from 400 - 1100 nm. Specialized devices have been made with 0.2 nm passband. The bandwidth of the filter depends only upon the thickness of the fixed crystal retarder elements employed, and manufacture of high-resolution filters does not place more stringent demands on the liquid crystal devices, than when making a spectrally broad filter. A filter with bandwidth of 0.25 nm or less (10 cm^{-1}) would have broad utility for Raman imaging, and construction of such a filter is within the present art. The main technical challenge in making a narrow bandpass device is to maintain high transmission: more elements are required, and the optical loss must be minimized. While light throughput is important, out-of-band rejection is just as important because of the need for discrimination between the Raman band of interest and potential interferences including fluorescence, Rayleigh scattering, and other Raman bands.

E.2 Related Research

Several approaches to Raman microscopy have been developed, including rotating dielectric filter tuning [6], laser scanning [7], spatial multiplexing [8], and tunable excitation with fixed bandpass filtering [9]; however, the last three are not believed to be commercially competitive with the high-resolution imaging discussed in this proposal.

At present there are three viable alternative methods to the LCTF for high-definition Raman imaging, based on rotating dielectric filters, acousto-optic tunable filters (AOTF) [10-11], and liquid crystal etalon (LCE) technologies [12]. The rotating-interference filter approach employs moving mechanical parts to tilt dielectric interference filters, and thus effect wavelength tuning of the Raman emission collected through a microscope. The imaging quality is good at near-normal incidence angles, but upon rotation of the filter the Raman images shift. In practice, the collection of complete Raman spectral image sets is time-consuming and suffers from spectral artifacts. The technology does not compare favorably with electronically-tunable filters.

In an AOTF, an RF sound wave generated by a piezoelectric transducer passes through a birefringent crystal, establishing a transmission diffraction grating within the crystal. Light meeting a wavelength-dependent momentum condition interacts with the grating and changes its angle or polarization state. The AOTF chief advantages are their tuning speed (25 μs) and high throughput (40%). Speed is irrelevant in Raman imaging applications: an imaging Raman spectrometer will dwell at each wavelength for a second or more, so microsecond tuning is not needed. Apertures are limited, from 2 to 10 mm square, and the devices accept only highly collimated light. They exhibit relatively strong sidelobes outside the passband, which can be reduced to approximately 3 percent by apodization of the RF signal.

AOTF's have recently been applied to Raman microscopy [10-11]. Because they operate on a diffraction principle, there is an image shift as the AOTF is tuned. This

causes problems in multispectral imaging, as precise image-to-image registration cannot readily be achieved without optical redesign of the AOTF, incorporation of compensation optics, or software correction. Further, since passband sidelobes have a different wavelength from the passband center, they are diffracted at different angles, which results in spectral 'smearing' and degraded image resolution. In a side-by-side comparison at 647.1 nm it was observed that use of an AOTF limited the resolution of a microscope image to $\sim 1 \mu\text{m}$, while the LCTF maintained the diffraction-limited resolution of the microscope [13].

Like an LCTF, an AOTF operates on one linear polarization at a time. As a result of this, and internal losses, the maximum throughput is between 40 and 45 percent for highly collimated light. Commercially available imaging AOTF's have bandpasses of 2 nm at 633nm (50 cm^{-1}), several times what is desired. Attaining bandwidth of 10 cm^{-1} may be possible, but only in devices with lower acceptance angle, which effectively reduces the field-of-view seen under the microscope. The wavelength reproducibility of tuning is sufficient for Raman spectroscopy. In summary, AOTFs offer superior speed while sacrificing performance in all other areas: aperture (field-of-view), imaging quality, spectral resolution, and out-of-band rejection.

Another approach to the tunable spectral filter has been taken by Dr. Michael Morris, who has used a liquid crystal etalon (LCE) to collect Raman images [12]. These have liquid crystal material within the cavity of an optical etalon, and the electro-optic action of the liquid crystal material provides an adjustable optical index for tuning. Because only the extraordinary optical index n_e is tuned, light incident on the LCE must be linearly polarized. The free-spectral range of an LCE is typically 5 - 25 nm, and finesse ranging from 8 - 25 have been reported [14-15] for near-visible LCE's. Bandwidths as narrow as 0.2 nm should be possible, set by the maximum practical thickness of the liquid crystal layer. However, transmission drops off rapidly with increasing finesse, due to cavity losses. These losses are much higher than in dielectric interference filters or air-spaced etalons, due to scatter in the liquid crystal material and absorption in the alignment and electrode layers [16]. The spectrum of a typical commercial etalon [17] from Meadowlark Optics is shown in Figure 3A, showing finesse of 8.5 and out-of-band blocking of 36:1 at 570 nm.

The Principal Investigator has constructed what are believed to be the highest-performance LCE devices to date. A spectrum from one is shown in Figure 3B, exhibiting a finesse of 21, and out-of-band blocking of 204:1. Other devices for infra-red use showed finesse of 53 and blocking of 450:1. But even these high-performance devices have limitations which make them unsuitable for Raman imaging applications. First, while they are mechanically rugged, they have great thermal instability. The optical index of liquid crystals has a thermal coefficient 240 times that of quartz [18-19], so there is a large drift, in addition to drift in the electro-optic tuning action. Another source of drift is the thermal coefficient of expansion of liquid crystal fluid, roughly 800 times that of glass. Since liquid crystal material is essentially incompressible, temperature changes cause great pressures within the sealed liquid crystal cavity [20]. This distorts the etalon figure, changing its pass wavelength and degrading its finesse. For these reasons, their pass wavelength is not stable over time and temperature, and any practical LCE system requires a daily *in situ* wavelength calibration.

Second, LCEs offer limited throughput. While the peak transmission of a low-finesse etalon can be high (up to 60% for polarized light), generally two or more of LCEs

are needed in order to obtain sufficient tuning range and high overall finesse. This reduces the transmission and greatly increases the complexity: the two LCE elements must be made to tune together, although each device has substantial tuning drift. Another limit is the field-of-view. The LCE field-of-view is different from that of a simple Fabry-Perot etalon, because the LCE cavity is filled with anisotropic crystalline material that is electro-optically flexed, and exhibits a wide range of orientations at different points throughout the cavity. No analytical expression for the field-of-view has been reported, but measurements suggest that an $f/32$ or slower beam is required for a 15 cm^{-1} device, corresponding to 2° field-of-view [16]. In comparison, an LCTF affords a 15° field. Since both the peak transmittance and the field-of-view of practical LCE systems are equal to or lower than LCTF figures, throughput will necessarily be lower.

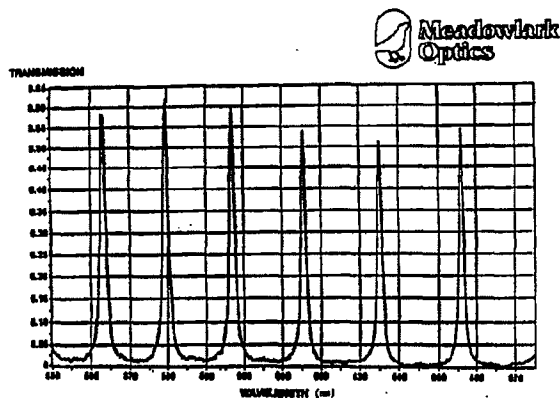


Fig 3A. Bandpass of a commercial LCE device.

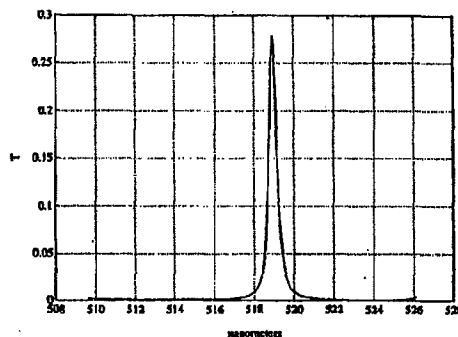


Fig 3B. Bandpass of high-performance LCE made by the P.I.

In summary, the imaging quality of LCEs is high, but even the best devices have substantial spectral leakage. A minimum of $10^3:1$ contrast is required to gather high fidelity spectral images, which is beyond the capability of present devices. At least two LCE devices must be ganged together to yield sufficient resolution and

free-spectral range, which reduces transmission and adds to system complexity because of tuning difficulties in these parts. There are significant problems with thermal sensitivity and wavelength accuracy, and throughput is much less than for LCTF devices.

E.3 Innovativeness and Originality of the Proposed Research

High-performance LCTFs were first demonstrated by the C.R.I. researchers [21-22], and the P.I. holds two patents relating to their construction and tuning [23-24]. C.R.I. has won three industry awards for the VariSPEC filter, based on this technology, and it is presently the only firm supplying scientific-grade LCTF filters.

The first use of liquid crystal tunable filters for Raman microscopy was performed at the University of Pittsburgh in a collaborative effort between C.R.I. researchers and Prof. Treado [13]. Figure 4A is a brightfield image of a $\sim 45\ \mu\text{m}$ diameter polystyrene microsphere that has not been tagged with a fluorophore. Figure 4B is a Raman image of the microsphere collected in 10 secs. The LCTF passband is centered at 691.5 nm which corresponds to a filter position of $992\ \text{cm}^{-1}$, the relatively intense ring deformation band of polystyrene. The image quality demonstrated in Fig. 4B surpasses the imaging performance of any of the alternative Raman imaging methodologies [6-9].

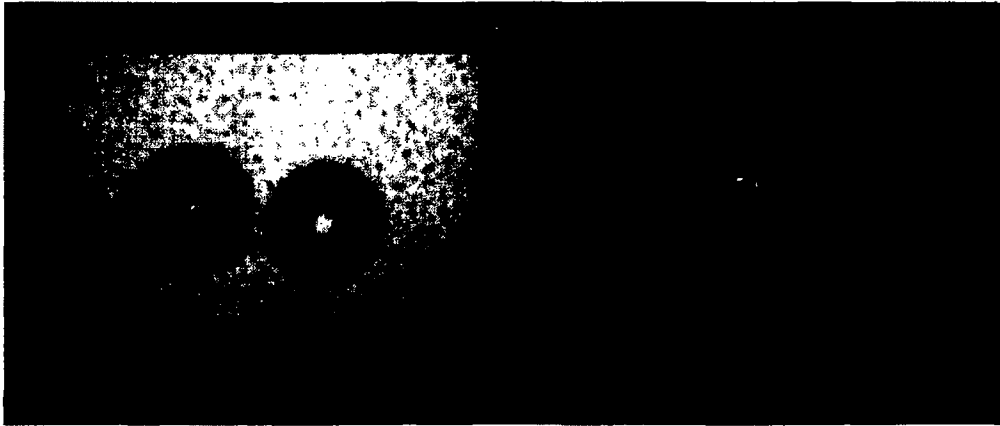


Fig. 4A. Brightfield image of fluorescence-tagged $45\ \mu\text{m}$ spheres.

Fig. 4B. Raman image of untagged $45\ \mu\text{m}$ spheres, taken with LCTF.

The diffraction-limited imaging performance of the LCTF combined with its tunability is unparalleled in Raman imaging. The imaging performance combined with the demonstrated reproducible spectral tuning of LCTFs predict that the technology proposed here will revolutionize the practice of Raman imaging.

F. Phase I Research Objectives

F.1 Specific Phase I Objectives

The Phase I Technical Objectives are:

- 1) To use existing computer models to generate a tunable Lyot filter design optimized for Raman spectroscopy;
- 2) To study the integration of such a filter into a microscope imaging system, including optical path, data acquisition, and camera requirements;
- 3) To construct a fully imaging prototype filter according to this design, with resolution of 10 cm^{-1} or better, tunable over a range of 2500 cm^{-1} ;
- 4) To characterize this filter for its spectral properties, including peak transmission, bandwidth, out-of-band rejection, and tuning range;
- 5) To use this filter to obtain true two-dimensional Raman spectroscopy images of test samples; and,
- 6) To prepare a Phase I report describing the results.

F.2 Connection with Phases II and III

Phase I of the anticipated program will demonstrate feasibility by integrating a high resolution LCTF filter into a microscope, and obtaining Raman images of various chemical test samples. Phase II will involve further optimization of the high definition LCTF filter, and development within an integrated, turnkey Raman microscope consisting of a laser, microscope, LCTF, and CCD detector, with processing and analysis software. Microscope integration will be performed in collaboration with ChemIcon, Inc. a start-up company located in Pittsburgh, PA., with expertise in this area.

In Phase III, ChemIcon will perform the system integration and market these microscopes to existing Raman microspectroscopy customers of ChemIcon, including the six Fortune 500 companies which currently support the development of Raman microscopy in Prof. Treado's laboratory. Raman microscopy is being applied to analyze a host of materials relevant to the specific industrial sponsors. Size of the mature market is estimated as several hundred microscopy sites, with annual sales of \$5M or more.

G. Phase I Research Plan

G.1 To design a tunable Lyot filter optimized for Raman spectroscopy

Over the past 5 years, the P.I. and co-workers at G.R.I. have developed computer models for the design of Lyot filters, based on the Jones calculus and incorporating spectrally-dependent values for the transmission, absorption, and birefringence of the materials involved. These include routines for calculating response for off-axis rays, and the tuning error of the liquid crystal retarders, based on actual measured statistical variation of these components from ongoing production lots. These models have a proven ability to predict passband width, spectral leakage, and peak transmission.

The principal requirements for a Raman-optimized LCTF are narrow bandwidth, high transmission, low leakage, and wide field-of-view. The tuning range will be 515 - 750 nm, to permit use with various laser sources ranging from 514 nm (Argon) to 647 nm (Krypton). A filter with bandwidth of 0.25 nm at 500 nm (10 cm^{-1}) requires use

of calcite or other high-birefringence materials for the fixed retarders. This, coupled with the wide field-of-view requirement, leads to a design based on wide-field elements [25-26]. It is likely that LiNbO_3 will be chosen as the retarder material, rather than calcite, because of its lower δn value. Consequently, its figuring error tolerances are relaxed relative to those of calcite. Also, it is more rugged, and not as prone to chipping and scratching.

High transmission in the filter is given by $T = E^s$, where s is the number of Lyot stages and E is the efficiency per stage. The stage efficiency E is set by losses in the liquid crystal cell, the polarizer, the fixed retarder, and tuning errors. These are input parameters to the design, based on measured values. In the design process, one seeks to minimize the number of stages, s , while meeting the requirements for bandwidth, free-spectral range, and out-of-band blocking. While the classical Lyot design offers little latitude in this regard, such a design is rarely suitable for a tunable filter. This is because the exact value of retardance at each stage will deviate from the idealized binary sequence Lyot described, as it is tuned to various wavelengths. To avoid sidelobes in the resultant filter response, one must add a few additional stages for contrast enhancement. The selection of retardances for these stages plays a crucial role in determining filter performance, and proper choice allows their number to be minimized.

The figure of $s = \log_2(\text{FSR}/\text{FWHM})$ for a classical Lyot design, represents a lower limit for an LCTF design. For a Raman filter, broad pre-filters can be used to define a useful range of 50 nm, so this is an acceptable FSR. This, coupled with the bandwidth FWHM of 0.25 nm, leads to a lower limit of $s=8$. A practical LCTF filter will probably require 3 or more additional stages, or a total of 11.

In addition to the optical components, we will design a suitable mechanical enclosure to provide a stress-free filter mounting. The thermal management approach is to create a nearly isothermal environment, free of gradients across the filter, and to sense the temperature with a medical-grade chip thermistor. This allows monitoring temperature with 0.05 °C precision, which is sufficient to resolve spectral shifts as small as $\delta\lambda \approx .01$ nm in the fixed retarders, corresponding to 1/25 of the filter FWHM. Unlike fixed-wavelength Lyot filters, there is no need to stabilize the filter temperature: the liquid crystal elements will be used to actively compensate for thermal drift in the LiNbO_3 and quartz retarders [24].

G.2 To study integration of an LCTF into a microscope imaging system

Integration of the LCTF into a Raman imaging system will involve both opto-mechanical and software engineering. Key C.R.I. researcher Clifford Hoyt has considerable experience integrating LCTFs in microscopes for fluorescence and pathology applications. Approaches have included placing the LCTF in the infinity-corrected optics path of microscopes such as Zeiss Axioskop and Olympus B-MAX systems, as well as the use of relay optics and telecentric correction systems. The Raman imaging LCTF will have a 20 mm aperture, and an overall length of 40-55 mm, similar to that of LCTF filters previously used for fluorescence work. It is anticipated that Prof. Treado will perform computer-aided optical design, using Zemax XE ray tracing software, to model the integration of the LCTF into microscopes in his laboratory. The location of other strategic components of the Raman system can also be modeled and optimized using this technique.

For the software integration, Prof. Treado will define the necessary features of Windows computer program to control the LCTF and to perform sophisticated multi-spectral image processing. A list of features and functions will be developed for actual software coding in Phase II of the project. Existing software allows Prof. Treado to acquire, display, and store high-resolution Raman images, and to control the filter manually for the Phase I testing.

G.3 To construct a fully imaging prototype filter according to this design
C.R.I. routinely manufactures commercial LCTF's for use in this spectral range, with bandwidths of 5-35 nm. We do not anticipate making any changes to the liquid crystal tuning elements for the present work.

The only special concern we anticipate in assembling this filter relates to reflections at the LiNbO_3 retarders. LCTF filters are normally assembled in an index-matching material which keeps reflections below 0.03% per interface. However, LiNbO_3 has a substantially higher optical index than the other materials used ($n_o=2.30$ vs. $n=1.53$), so it needs to be anti-reflection coated to match its impedance to that of the index-matching material. From the analysis of Staromlynska, inter-reflections limit the extinction of each stage to $1 / [3R^2(1-R)]$, including the effects within the liquid crystal cell [27]. For the coated LiNbO_3 interfaces, a reflection R of 0.5% or less is anticipated, yielding a contrast of 13,400:1 per stage. Since LCTF designs require a contrast of only 100:1 per stage, there should be no problem meeting project goals for the overall filter contrast.

Electronics modules for tuning the liquid crystal cells and sensing the thermistor resistance have been developed in the course of commercial LCTF development, and will be used without modification in the present work.

G.4 To characterize this filter for its spectral properties

The filter will be characterized at C.R.I. using a SPEX 0.5M spectrometer with 0.02 nm resolution. Bandwidth (FWHM) will be checked with He-Ne laser and H_α lamp sources, while peak transmission will be measured using a quartz-halogen source, and a Hamamatsu S1336 detector with a Scitec chopper and SRS 810 lock-in amplifier. This provides measurements of peak transmission that are accurate to 2% of the transmission value, and resolves transmission of 10^{-5} or less, for spectral leakage measurements. Tuning range will be checked directly, by observing the filter response as it is tuned across the operating range. Measurements are fully automated using a PC/486 controller, enabling hundreds of spectra to be taken with no operator involvement. The wavelength scale calibration will be checked at the 543.5 and 632.89 nm laser lines using He-Ne sources.

Off-axis response will be measured by mounting the filter on a two-dimensional rotation stage and observing passband shift as the LCTF orientation is varied. Thermal drift will be measured if time permits, by mounting the filter on a Neslab RTD-110 controlled temperature stage, and measuring passband variations as the LCTF temperature is adjusted over the range 20 - 35 °C.

G.5 To use this filter to obtain two-dimensional Raman spectroscopy images

The LCTF filter will be integrated into microscopes at the University of Pittsburgh for these tests, which will be performed by Prof. Treado. Spectral imaging will be

evaluated by measurement of the modulation transfer function (MTF), a quantitative analysis of imaging performance. The MTF will be measured by imaging several standard resolution targets as a function of wavelength, using a Princeton Instruments CCD detector and BioScan OPTIMAS software to acquire the images. Raman imaging performance will be established by evaluation of images of polymer microspheres, routinely used as size and chemical standards by researchers in this field.

Raman imaging evaluation will also be performed on real-world, industrial materials available to Prof. Treado through collaborations with industrial sponsors. Materials will include corrosion-resistant alloys, polymer composites and pharmaceuticals.

G.6 To prepare a Phase I report describing the results.

The P.I., Prof. Treado, and senior C.R.I. personnel will draft a Phase I Final Report for submission to the NSF, including experimental data, images, and technical analysis, in accordance with N.S.F. guidelines.

H. Commercial Potential

H.1 Brief Description of the Company

Cambridge Research and Instrumentation, Inc. was formed in May 1985 with the aims of carrying out research in solar-terrestrial physics and developing instruments for the accurate measurement and control of light. Dr. Peter Foukal, president of C.R.I., Inc. has published over 100 papers in major refereed journals and conference proceedings. This work on solar astrophysics has also been presented in numerous contributed and invited papers at meetings of the AAS, AGU and IAU. Dr. Foukal has also served on various advisory committees and panels of NASA, NSF, and the National Academy of Sciences, over the past fifteen years. C.R.I. maintains active programs at the forefront of solar-terrestrial research, including photometric and radiometric studies of solar irradiance variation, and also remote sensing studies of plasma electric fields in the sun's atmosphere.

In electro-optics, C.R.I. has developed the LaseRad and CryoRad cryogenic cavity radiometers as laboratory standards for measurement of radiative flux, with support from the SBIR Programs of the NSF and NASA. These instruments are in use as national standards of light measurement at NIST (ex-NBS), and in Germany, Sweden, Canada, Spain, and at the CNAM in France. C.R.I. also developed and builds commercially the award-winning LS and LPC series laser power stabilizers widely used in electro-optics laboratories, and most recently, the award-winning VariSpec liquid crystal tunable filters. A significant fraction of C.R.I.'s \$1.8M sales volume in the last fiscal year consisted of exports of commercial products to Europe and Japan.

H.2 Commercial Applications

H.2.a Polymer imaging

Raman vibrational spectroscopic imaging of heterogeneous polymer dispersions and polymer thin films will be possible when the LCTF filtering technology is suitably incorporated into a dedicated Raman microscope. Such a device will have broad applicability in the polymer and coatings industries because it will allow for

non-invasive, chemically specific visualization of domains and defects in polymer composites without the need for sample staining.

At present, many analytical imaging methodologies are applied to polymer characterization. The optical microscope is employed in combination with a host of optical contrast generation mechanisms including polarization, interference and fluorescence. In general, these methods do not provide chemical specificity and provide limited spatial resolution. For high spatial resolution analysis, polymers are imaged with electron microscopy, usually in combination with osmium tetroxide staining, a difficult and hazardous undertaking. Existing polymer visualization methodologies are problematic. Raman imaging has extraordinary potential in polymer analysis but the power of the technique hinges on the availability of a reliable, high resolution Raman spectral filter.

Prof. Treado is collaborating with a major pharmaceutical firm and Ford Motor Co. to develop Raman imaging instrumentation suitable for characterizing the polymeric materials of importance to these companies. If the suitable filtering technology can be developed, these industrial sponsors will form a ready market for Raman microscopes.

H.2.b Corrosion Imaging

Non-invasive, *in situ* monitoring of temperature-dependent corrosion of steel alloys exposed to phosphate solution is an important application of Raman imaging. This will be performed with long working distance microscope optics to probe samples housed in a programmable high temperature stage, viewing them through protective diamond windows. A rapid and non-invasive method for monitoring corrosion *in situ* provides several capabilities: first, chemical mechanisms of corrosion can be established; second, failure rate predictions that dictate the replacement schedule of strategic materials can be determined, representing a tremendous potential cost saving to industry and government; and, methods to inhibit corrosion can more effectively be evaluated. Methodologies developed here will be generally applicable to any *in situ* Raman imaging application where samples are housed in extreme environments of temperature, pressure, or radiation.

C.R.I. will develop high resolution LCTF technology to be coupled with microscope optics and CCD cameras to provide submicron spatial resolution with sufficient spectral resolution to distinguish the corrosion chemical species. The P.I. and Prof. Treado will work with industrial sponsors interested in monitoring *in situ* temperature-dependent corrosion of alloys. At present, Prof. Treado is providing a customized microscope to two Fortune 100 defense contractors who perform these types of measurements under contract to the Department of the Navy. The technologies developed in these programs will be directly applicable for corrosion monitoring aboard Navy ships, and in steam and nuclear power generators. Once Raman corrosion monitoring technology is developed it will be marketed to the commercial power industry.

H.2.c Crystal Polymorphism Imaging

Raman microscopy has the potential for use in quantitative polymorphism characterization of pharmaceutical active-agent crystalline material. Polymorphism occurs in pharmaceuticals in which a chemical constituent may have more than one crystalline structure. This is problematic because an active agent may provide

therapeutic benefit only if it is the appropriate crystalline form or polymorph. Raman microscopy can often distinguish spectroscopically between different polymorphs, and Prof. Treado is engaged in a collaboration with a large international pharmaceutical firm to establish the utility of Raman microscopy as a quantitative methodology for discriminating different polymorphs in a quality control application. If feasibility can be established a market for Raman microscopes will be defined. Raman systems relying on LCTFs will then be marketed to pharmaceutical companies for polymorphism quantitation.

H.2.d Biomedical Imaging

Probing biological structures is tractable with Raman spectroscopy. In particular, Raman spectroscopy is effective for analyzing aqueous samples without the interference of the strong OH bands encountered in infrared spectroscopy. In addition, the intrinsic vibrational markers of biological samples provide chemical selectivity without the need for significant sample preparation or the use of potentially invasive stains or tags. In macroscopic, non-imaging studies of biological materials, the wealth of chemical information provided by Raman spectroscopy is often convoluted due to the complexity of the materials. Raman spectroscopic microscopy focuses the chemical analysis to localized regions of heterogeneous materials, and provides an efficient chemical visualization method. Biological applications of Raman microscopy include resonance Raman studies of carotenoid pigments of bacteria [28], Raman microspectroscopy of gallstones and kidney stones [29], and of DNA in single tumor cells [30].

H.3 Competitive Products

In 1991 SPEX licensed the spatial multiplexing approach co-developed by Prof. Treado at the University of Michigan, but the rapid pace of development in Raman microscopy makes the spatial multiplexing approach obsolete.

In the U.K., Renishaw P.L.C. commercialized a dedicated Raman microscope employing interference filter tuning. The microscope combines Raman imaging optics with a microprobe. In operation, Raman microspectra are collected rapidly at isolated regions of a sample, and then full-frame images are collected with the filters tuned to a few discrete Raman bands. Complete spatial/spectral information cannot readily be collected with this approach. It is well suited to visualization of widely-separated Raman bands, but not to imaging of dense matrices in which complex Raman spectra often overlap and are convoluted. To obtain a definitive evaluation of complex systems, the kind of materials encountered in the real world, the spectral collection and image collection must be integrated, and provide the kind of complete spatial/spectral data available from a tunable imaging spectrometer.

Approaches requiring the use of moving mechanical parts contribute to degraded imaging performance. The imaging performance is especially compromised when widely separate Raman spectral ranges are accessed.

A no-moving-parts approach to Raman microscopy has been successfully demonstrated by Prof. Treado and co-workers at the National Institutes of Health employing AOTFs [7]. Despite the no-moving-parts design, the AOTF imaging quality is handicapped due to the 'spectral smearing' described earlier in Section E.2. Future AOTFs may address these degradations, and may provide the high spectral resolution (10 cm⁻¹), and large optical apertures (~ 25 mm), anticipated in the proposed technology, but

current AOTFs do not. As importantly, the development of optimized AOTFs is much less tractable than the development of LCTF technology. High resolution LCTFs have already been fabricated for other spectroscopic applications and can be optimized readily for Raman microscopy.

AOTF microscopes are currently being commercialized by Brimrose Corp. of America. These devices are not manufactured under license with NIH, which has a patent pending on the technology. If the patent is issued the Brimrose microscopes will infringe on the NIH patent and it is anticipated that the federal government will defend their patent rights.

It is anticipated that the Renishaw Raman microscope is the competitive product for the foreseeable future.

H.4 Advantages of the Proposed Approach Over Existing Technology

The existing competitive technologies are tunable spectral filter designs including rotating dielectric filters, AOTFs and LCEs. The LCTF approach enjoys a competitive advantage over all of these alternatives.

The complete spatial/spectral data generated by LCTF system gives it a clear advantage over rotating dielectric filter systems, because it provides the user with a much more detailed picture of the chemical distribution when characterizing spatially and spectrally complex, real-world samples.

Compared to systems using AOTF filters, an LCTF-based Raman imaging system would offer vastly superior imaging quality. In addition, use of a liquid crystal waveplate at the LCTF entrance enables monitoring the polarization state of the Raman signal. This yields important benefits for studies of oriented anisotropic materials such as crystals, polymers, semiconductors, and fibers. System integration is easier as well, due to the larger aperture and viewing angle the LCTF affords. Turning to LCEs, if these are commercialized in the future, they promise severe limits in terms of spectral calibration, out-of-band blocking, and field-of-view, without offsetting performance benefits in other areas. This suggests that the LCTF will enjoy a competitive advantage over this technology as well.

H.5 Progress in Commercializing Other SBIR Technology

The Principal Investigator has developed several innovative instruments for optical research. He was one of the key members of the team that pioneered the use of cryogenic cavity radiometer for laboratory standards measurements of radiative flux, with support from the Small Business Innovation Research Programs of the NSF and NASA. These instruments are in use as national standards of light measurement at NIST (ex-NBS), the German PTB, CNAM in France, as well as the national laboratories of Sweden, Spain, and Canada. C.R.I. also developed and builds commercially the award-winning LS and LPC series laser power stabilizers used worldwide in electro-optics laboratories, and most recently, the patented VariSpec line of liquid crystal tunable filters. The VariSPEC was supported by NSF and NIH Small Business Innovation Research Programs. These instruments, with over \$2 million in commercial sales, point to a long and successful history both in research and in the development and marketing of scientific research equipment.

I. Principal Investigator and Senior Personnel

PETER J. MILLER
Staff Scientist

PRINCIPAL INVESTIGATOR

Cambridge Research and Instrumentation, Inc.

Education:

1980 B.A. (Astronomy) Williams College
1985 M.S. (Electrical Engineering) Dartmouth College

Memberships:

American Astronomical Society
Optical Society of America

Experience:

1979 Visiting Fellow, JILA/NBS, Boulder, CO
1980-83 Staff Scientist, Atmospheric and Environmental Research, Inc.,
Cambridge, MA
1985 Staff Scientist; Cambridge Research and Instrumentation, Inc., Cam-
bridge, MA

Relevant Publications, Reports, and Awards

"Multispectral imaging with a liquid crystal tunable filter", P. Miller, SPIE
Proc. 2345, (in press).

"Optical Retarder Having Means for Determining the Retardance of the Cell
Corresponding to the Sensed Capacitance Thereof", U.S. Patent 5,247,378
(1993).

Laser Focus CTA award, Laser Focus, 29, 115 (1993). Awarded for the VariSpec
tunable liquid crystal filter.

T. Chrien, C. Chovit, P. Miller, "Imaging spectrometry using a liquid crystal
tunable filter", Proc. SPIE 1937, 257 (1993).

R & D 100 Winners Announcement, Research & Development, 34, 12 (1992).
Awarded for the VariSpec tunable liquid crystal filter.

"Photonics Circle of Excellence Awards", Photonics Spectra, 26, 5 (1992).
Awarded for the VariSpec tunable liquid crystal filter.

"Use of Tunable Liquid Crystal Filters to link Photometric and Radiometric
Standards", P. Miller, Metrologia 28, 145, (1991).

"Tunable Narrowband Birefringent Filters for Astronomical Imaging", P.
Miller, SPIE Proc. 1235, 466, (1990).

"Liquid Crystal Devices and Systems Using Such Devices." P. Miller, U.S.
Patent 4,848,877 (1989).

CLIFFORD C. HOYT
Staff Scientist
Cambridge Research and Instrumentation, Inc.

Education

1983 B.A. (Physics) Williams College
1987 M.S. (Engineering) M.I.T.

Experience

1983-85 Staff Scientist, Atmospheric and Environmental Research, Inc.,
Cambridge, MA
1987- Staff Scientist, Cambridge Research and Instrumentation, Inc.,
Cambridge, MA

Relevant Publications

"Towards Higher Res, Lower Cost Quality Color and Multispectral Imaging",
Advanced Imaging 10, 53 (1995).

"Imaging Spectrometers for Fluorescence and Raman Microscopy: Acousto-Optic
and Liquid Crystal Tunable Filters", Hannah R. Morris, Clifford C. Hoyt, and
Patrick J. Treado, Appl. Spectrosc. 48, 857 (1994).

P. Foukal, P. Miller, C. Hoyt, "Liquid Crystal Tunable Light Filters for
Surveillance and Remote Sensing Applications", Proc. SPIE 1952, 168 (1993).

"Merging Spectroscopy and Digital Imaging Enhances Cell Research", C. Hoyt
and D. Benson, Photonics Spectra, 26, 92, (1992).

"Liquid Crystal Tunable Filters for Photometry", C. Hoyt, P. Miller, Invited
paper, "CORM 90", Rochester Inst. of Tech., May 7-9, (1990).

"Image-Preserving Tunable Filter for Microscopy", C. Hoyt, Phase I SBIR Final
Report to NIH, (1989).

"Remote Biomedical Spectroscopic Imaging of Human Artery Wall", C.C. Hoyt,
R.R. Richards-Kortum, J.R. Sacks, M.S. Feld, Lasers in Surgery and Medicine,
8:1-9, (1988).

"Spectroscopic Diagnosis for Control of Laser Treatment of Atherosclerosis."
R.R. Richards-Kortum, A. Mahta, T. Kolubayev, C. Hoyt, J. R. Sacks, M. S.
Feld, 1988, Lasers in Surgery and Medicine.

J. Consultants and Subcontracts

Patrick J. Treado
 Assistant Professor of Chemistry
 Department of Chemistry, University of Pittsburgh

Prof. Treado is a recognized expert in the development of Raman chemical imaging, optical microspectroscopic techniques and their application to materials analysis. His letter confirming availability and commitment to this project is included as an Appendix to this Proposal.

Prof. Treado performed his doctoral work under the direction of Prof. Michael D. Morris. His research involved the development of spectroscopic imaging techniques, specifically Raman microscopy and photothermal deflection densitometry, employing Hadamard transform spatial multiplexing. The Raman microscopy technique led to several nationally competitive fellowships and awards being won by Prof. Treado. A patent of the Hadamard Raman microscopy was issued in 1991, and the technology has been licensed by Spex Industries, a spectroscopic instrument manufacturer, for commercial development.

While a postdoctoral fellow at the National Institutes of Health (1990-1992) Prof. Treado performed biophysical studies of model biological membrane assemblies using Raman and infrared spectroscopy. With Dr. Neil Lewis and Dr. Ira Levin, Prof. Treado pioneered the development of chemical imaging methods using acousto-optic tunable filters (AOTFs). Prototype instruments capable of performing visible/near-infrared absorption microscopy and Raman microscopy were developed. A patent covering the use of AOTFs in spectroscopic imaging instruments is pending. His paper describing the first use of AOTF for Raman chemical imaging was awarded the 1993 Meggers Award by the Society for Applied Spectroscopy for the best paper published in Applied Spectroscopy in 1992.

Since joining the University of Pittsburgh, Department of Chemistry as an Assistant Professor in September 1992, Prof. Treado has been engaged in a research program in analytical spectroscopy and chemical imaging, including the first use of an LCTF for Raman imaging, with the P.I. of this proposal.

Selected Publications

1. E. Neil Lewis, Patrick J. Treado, Robert C. Reeder, Gloria M. Story, Anthony e. Dowrey, Curtis Marcott, and Ira W. Levin, "Fourier Transform Step-Scan Imaging Interferometry: High Definition Chemical Imaging in the Infrared Spectral Region", J. Amer. Chem. Soc. in press.
2. Hannah R. Morris, Michael D. Schaeberle, and Patrick J. Treado, "Chemical Imaging with Tunable Filters: Methods and Applications", Proc. SPIE 2385, (1995) 89.
3. Hannah R. Morris, Clifford C. Hoyt, and Patrick J. Treado, "Imaging Spectrometers for Fluorescence and Raman Microscopy: Acousto-Optic and Liquid Crystal Tunable Filters", Appl. Spectrosc. 48, (1994) 857.
4. Patrick J. Treado, Ira W. Levin, and E. Neil Lewis, "Indium Antimonide (InSb) Focal Plane Array (FPA) Detection for Near-Infrared Imaging Microscopy", Appl. Spectrosc. 48, (1994) 607.
5. E. Neil Lewis, Patrick J. Treado, and Ira W. Levin, "Near-Infrared and Raman Spectroscopic Imaging", Amer. Lab. 26, (1994) 16.

6. Michael D. Schaeberle, John F. Turner, and Patrick J. Treado, "Multiplexed Acousto-Optic Tunable Filter (AOTF) Spectral Imaging Microscopy", *Proc. SPIE* **2173**, (1994) 176.
7. E. Neil Lewis, Patrick J. Treado, and Ira W. Levin, "A Miniaturized, No-Moving-Parts Raman Spectrometer", *Appl. Spectrosc.* **47**, (1993) 539.
8. Patrick J. Treado and Michael D. Morris, "Infrared and Raman Spectroscopic Imaging, Spectroscopic and Microscopic Imaging of the Chemical State", M.D. Morris, Ed. (Marcell Dekker, New York, 1992) pp. 71-108.
9. Patrick J. Treado, Ira W. Levin and E. Neil Lewis, "High-Fidelity Raman Imaging Spectrometry: A Rapid Method Using an Acousto-optic Tunable Filter", *Appl. Spectrosc.* **46**, (1992) 1211.
10. Patrick J. Treado, Ira W. Levin and E. Neil Lewis, "Near-Infrared Acousto-Optic Filtered Spectroscopic Microscopy: A Solid State Approach to Chemical Imaging", *Appl. Spectrosc.* **46**, (1992) 553.
11. Patrick J. Treado, Anurag Govil, Kent D. Sternitzke, Richard L. McCreery and Michael D. Morris, "Hadamard Transform Raman Microscopy of Laser-Modified Graphite Electrodes", *Appl. Spectrosc.* **44**, (1990) 1270.
11. Patrick J. Treado and Michael D. Morris, "Multichannel Hadamard Transform Raman Microscopy", *Appl. Spectrosc.* **44**, (1990) 1.
12. Patrick J. Treado and Michael D. Morris, "Hadamard Transform Spectroscopy and Imaging", *Spectrochimica Acta Rev.* **13**, (1990) 355.
13. Patrick J. Treado and Michael D. Morris, "A Thousand Points of Light: the Hadamard Transform in Chemical Analysis and Instrumentation", *Anal. Chem.* **61**, (1989) 723A.

K. Equipment, Instrumentation, Computers, and Facilities

K.1 Facilities available at Cambridge Research & Instrumentation

An equipment item of particular importance to this project is the C.R.I. liquid crystal filter fabrication facility. This facility includes an 8 x 12 foot class-100 clean room, with complete thermal and humidity control; all necessary equipment for fabricating liquid crystal elements of the highest optical quality on glass and quartz substrates; water filtration, substrate handling, and desiccant storage facilities for cleaning and processing to exacting chemical levels; and an 8' Laminaire horizontal flow hood for overall assembly in a particle-free, laminar flow environment.

Test equipment at C.R.I. includes a 0.5-meter SPEX spectrometer with 300 and 1200 line/mm gratings for high-resolution spectroscopy (0.025 nm); a quarter-meter visible ISA spectrometer with an EG&G 1024-element reticon detector; a Scitec optical chopper and Stanford Research 810 lock-in amplifier; quartz-halogen, mercury, Kanthal, and Xe arc continuum sources with collimation optics; a mercury line source for wavelength scale calibration; and a variety of silicon, germanium, PbSe, and InGaAs photodiodes, and photodiode preamps with NIST-traceable calibration.

Other relevant equipment includes a Zeiss Axioskop microscope equipped for epi- and kohler illumination; a Dage MTI CCD-72 camera with TEC-1 cooler, single-line gate, and controller; a Matrox MVP-AT frame grabber; Optimus image processing software; Sony Trinitron RGB monitor; a Neslab RTD-110 controlled temperature system with heat sink mount for temperature control of optical samples to +/- 0.02 °C; He-Ne, Ar⁺⁺, and Nd:YAG lasers with spatial mode filters and beam expanding optics; 6-inch

6. Michael D. Schaeberle, John F. Turner, and Patrick J. Treado, "Multiplexed Acousto-Optic Tunable Filter (AOTF) Spectral Imaging Microscopy", *Proc. SPIE* **2173**, (1994) 176.
7. E. Neil Lewis, Patrick J. Treado, and Ira W. Levin, "A Miniaturized, No-Moving-Parts Raman Spectrometer", *Appl. Spectrosc.* **47**, (1993) 539.
8. Patrick J. Treado and Michael D. Morris, "Infrared and Raman Spectroscopic Imaging, Spectroscopic and Microscopic Imaging of the Chemical State", M.D. Morris, Ed. (Marcell Dekker, New York, 1992) pp. 71-108.
9. Patrick J. Treado, Ira W. Levin and E. Neil Lewis, "High-Fidelity Raman Imaging Spectrometry: A Rapid Method Using an Acousto-optic Tunable Filter", *Appl. Spectrosc.* **46**, (1992) 1211.
10. Patrick J. Treado, Ira W. Levin and E. Neil Lewis, "Near-Infrared Acousto-Optic Filtered Spectroscopic Microscopy: A Solid State Approach to Chemical Imaging", *Appl. Spectrosc.* **46**, (1992) 553.
11. Patrick J. Treado, Anurag Govil, Kent D. Sternitzke, Richard L. McCreery and Michael D. Morris, "Hadamard Transform Raman Microscopy of Laser-Modified Graphite Electrodes", *Appl. Spectrosc.* **44**, (1990) 1270.
12. Patrick J. Treado and Michael D. Morris, "Multichannel Hadamard Transform Raman Microscopy", *Appl. Spectrosc.* **44**, (1990) 1.
13. Patrick J. Treado and Michael D. Morris, "Hadamard Transform Spectroscopy and Imaging", *Spectrochimica Acta Rev.* **13**, (1990) 355.
14. Patrick J. Treado and Michael D. Morris, "A Thousand Points of Light: the Hadamard Transform in Chemical Analysis and Instrumentation", *Anal. Chem.* **61**, (1989) 723A.

K. Equipment, Instrumentation, Computers, and Facilities

K.1 Facilities available at Cambridge Research & Instrumentation

An equipment item of particular importance to this project is the C.R.I. liquid crystal filter fabrication facility. This facility includes an 8 x 12 foot class-100 clean room, with complete thermal and humidity control; all necessary equipment for fabricating liquid crystal elements of the highest optical quality on glass and quartz substrates; water filtration, substrate handling, and desiccant storage facilities for cleaning and processing to exacting chemical levels; and an 8' Laminare horizontal flow hood for overall assembly in a particle-free, laminar flow environment.

Test equipment at C.R.I. includes a 0.5-meter SPEX spectrometer with 300 and 1200 line/mm gratings for high-resolution spectroscopy (0.025 nm); a quarter-meter visible ISA spectrometer with an EG&G 1024-element reticon detector; a Scitec optical chopper and Stanford Research 810 lock-in amplifier; quartz-halogen, mercury, Kanthal, and Xe arc continuum sources with collimation optics; a mercury line source for wavelength scale calibration; and a variety of silicon, germanium, PbSe, and InGaAs photodiodes, and photodiode preamps with NIST-traceable calibration.

Other relevant equipment includes a Zeiss Axioskop microscope equipped for epi- and kohler illumination; a Dage MTI CCD-72 camera with TEC-1 cooler, single-line gate, and controller; a Matrox MVP-AT frame grabber; Optimus image processing software; Sony Trinitron RGB monitor; a Neslab RTD-110 controlled temperature system with heat sink mount for temperature control of optical samples to +/- 0.02 °C; He-Ne, Ar⁺⁺, and Nd:YAG lasers with spatial mode filters and beam expanding optics; 6-inch

and 1-inch Labsphere integrating spheres; PC/AT and PC/386 computers with 16-bit high-speed data acquisition hardware and software.

In addition to the above equipment, C.R.I. has a PC/486-based CAD center for electronic and mechanical design; an electronics test and production lab equipped to handle analog, digital, and microprocessor assemblies. We have access to complete metal-working facilities for fabricating jigs, special optical fixtures, etc. C.R.I. also maintains a NIST-traceable calibration lab, for detector tests and calibrations at the highest level of accuracy.

K.2 Facilities available to Prof. Treado at the University of Pittsburgh Laboratory Facilities:

Prof. Treado has approximately 1200 ft² of modern laboratory space, equipped for optical spectroscopy (visible/near-infrared absorption, Raman and fluorescence emission), optical spectroscopic imaging microscopy, and wet chemical manipulations.

Computer:

Data collection is controlled by PC/486 stations running commercial programs and programs written by laboratory personnel. The PCs are networked to a Silicon Graphics IRIS Indigo R4K workstation, which functions as a file-server and is connected to a magneto-optic disk for mass data storage and retrieval. The Silicon Graphics machine also serves as an advanced spectral image processing workstation using the program Link Winds. This program was developed at the NASA Jet Propulsion Laboratory for remote sensing spectral imaging applications, and provides unmatched capability for multidimensional graphical analysis.

Major equipment in Prof. Treado's laboratory:

(2) Princeton Instruments CCD detectors interfaced to a Gateway 2000 50 MHz 80486 DX2 computer running BioScan OPTIMAS image processing software; Coherent 330 Krypton ion laser, 400 mW 752 nm, 1 W multiline red; Coherent CR-3 Argon ion laser, 150 mW 514.5 nm; Chromex 0.5 m spectrograph for performing dispersive optical spectroscopy, and spectral calibration of the LCTFs; (2) Olympus BH-2 upright microscopes with visible-optimized optics interfaced to a Cohu 4910 b&w video camera for sample positioning and focusing; Kinetic Systems research grade optical table, 4' x 10'; Newport research grade optical table, 5' x 10'; EG&G PAR 5110 lock-in amplifier; E-Tec scanning electron microscope; Electro-Optic Systems InSb photodiode; C.R.I. Varispec LCTF for fluorescence imaging.

Special materials:

Sophisticated samples suitable for Raman microscopy applications including corrosion test samples, polymeric composites, thin films and coatings on polymer substrates, as well as pharmaceuticals, will be provided by Prof. Treado's external industrial collaborators in the defense, pharmaceutical, and automobile industries.

Other:

The chemistry department maintains the usual array of modern spectroscopic instrumentation available for general access. Fully equipped electronics and machine shops for instrument and prototype fabrication are available.

L. Current and Pending Support of P.I. and Senior Personnel

The P.I. has no prior, current, or pending support for development of Raman imaging filters. He has a commitment of 12% to the N.I.H. SBIR Phase II proposal, "High-Efficiency Tunable Fluorescence Emission Filter", #R43-MH53690-01, currently under review. If awarded, it involves a 3 week effort during the Phase I period. He also anticipates a 10% commitment to the N.I.H. STTR project, "A Universal Compensator for Polarization Microscopy", number R41 GM51644-01. This project is currently in Phase I and a Phase II proposal will be submitted in December '95. If an award is made, work would begin in May '96 or later, requiring 1 week of effort during the proposed Phase I period.

Clifford Hoyt is P.I. on both of the proposals listed above, with commitments of 50% to R43-MH53690-01 and an anticipated 30% commitment to R41-GM51644-01. The former proposal, if awarded, includes a 3 month commitment during the Phase I period. The latter project would not result in a contract award until May 1996 or later, and would involve 2-3 weeks' effort during the Phase I period.

M. Equivalent Proposals to Other Federal Agencies

There are no equivalent proposals under consideration by or being submitted to any other Federal Agencies.

N. Budget

The budget is presented on the following page. Funds are budgeted for the purchase of 10 optical retarder of LiNbO_3 @ \$250 each, and \$250 for materials used in making the liquid crystal tuning elements. These supplies will be used to make the prototype LCTF described in the Plan of Work. The computer budget is to allow for maintenance and repair costs for the PC/386 systems.

APPENDIX D

(SEE INSTRUCTIONS ON REVERSE

SUMMARY

BEFORE COMPLETING)

PROPOSAL BUDGET

FOR NSF USE ONLY

ORGANIZATION Cambridge Research & Instrumentation, Inc.		PROPOSAL NO.		DURATION (MONTHS) Proposed _____ Granted _____	
PRINCIPAL INVESTIGATOR/PROJECT DIRECTOR Peter Miller		AWARD NO.			
A. SENIOR PERSONNEL: PI/PI and Other Senior Associates (List each separately with title, A.6, show number in brackets)		NSF Funded Person-mos.	Funds Requested By Proposer	Funds Granted By NSF (If Different)	
		CAL			
1. Peter J. Miller, P.I.		2.5	\$ 11,480	\$	
2. Clifford C. Hoyt, Staff Scientist		1.0	4,213		
3.					
4.					
5. () OTHERS (LIST INDIVIDUALLY ON BUDGET EXPLANATION PAGE)					
6. (2) TOTAL SENIOR PERSONNEL (1-5)		3.5	15,693		
B. OTHER PERSONNEL (SHOW NUMBERS IN BRACKETS)					
1. () POST DOCTORAL ASSOCIATES					
2. (1) OTHER PROFESSIONALS (TECHNICIAN, PROGRAMMER, ETC.)		.75	2,145		
3. () GRADUATE STUDENTS					
4. () UNDERGRADUATE STUDENTS					
5. () SECRETARIAL - CLERICAL					
6. () OTHER					
TOTAL SALARIES AND WAGES (A+B)			17,838		
C. FRINGE BENEFITS (IF CHARGED AS DIRECT COSTS) .38 x (A+B)			6,778		
TOTAL SALARIES, WAGES AND FRINGE BENEFITS (A+B+C)			24,616		
D. PERMANENT EQUIPMENT (LIST ITEM AND DOLLAR AMOUNT FOR EACH ITEM EXCEEDING \$5,000.) (Do not use for Phase I)					
TOTAL PERMANENT EQUIPMENT					
E. TRAVEL 1. DOMESTIC (INCL. CANADA AND U.S. POSSESSIONS)					
2. FOREIGN (Do not use for Phase I)					
F. PARTICIPANT SUPPORT COSTS					
1. STIPENDS \$ _____					
2. TRAVEL _____					
3. SUBSISTENCE _____					
4. OTHER _____					
() TOTAL PARTICIPANT COSTS					
G. OTHER DIRECT COSTS					
1. MATERIALS AND SUPPLIES see proposal text		2,750			
2. PUBLICATION COSTS/DOCUMENTATION/DISSEMINATION					
3. CONSULTANT SERVICES					
4. COMPUTER (ADPE) SERVICES		200			
5. SUBCONTRACTS Prof. Patrick Treado 35 days @ 420/day		14,700			
6. OTHER					
TOTAL OTHER DIRECT COSTS					
H. TOTAL DIRECT COSTS (A THROUGH G)		42,266			
I. INDIRECT COSTS (SPECIFY) Overhead .46 x (A+B+C) = 11,323					
TOTAL INDIRECT COSTS G & A .15 x (H + Overhead) = 8,038		19,361			
J. TOTAL DIRECT AND INDIRECT COSTS (H+I)		61,627			
K. FEE (If requested; maximum equals 7% of J) .07 x J		4,313			
L. TOTAL COST AND FEE (J + K)		\$ 65,940		\$	
PI/PI TYPED NAME & SIGNATURE Peter Miller		DATE 6/7/95	FOR NSF USE ONLY		
CO. REP. TYPED NAME & SIGNATURE Peter Foukal		DATE 6/7/95	INDIRECT COST RATE VERIFICATION		
		Date Checked	Date of Rate Sheet	Initials-DGA	

References

1. T. Hirschfeld, J. Opt. Soc. Am. 63, (1973) 476.
2. D. I. Bower and W. F. Maddams, The Vibrational Spectroscopy of Polymers, Cambridge University Press, (Cambridge), 1989.
3. P. R. Carey, Biochemical Applications of Raman and Resonance Raman Spectroscopies, Academic Press, (New York), 1982.
4. N. Pessall, A. B. Dunlap, and D. W. Feldman, Corrosion-NACE 33, 130 (1977).
5. P. J. Miller, Metrologia 28, (1991) 145.
6. D. N. Batchelder, C. Cheng and B.J.E. Smith, Makromol. Chem., Makromol. Symp. 46, (1991) 171.
7. M. Bowden, P. Donaldson, D.J. Gardiner, J. Birnie and D.L. Gerrard, Anal. Chem. 63, (1991) 2915.
8. P. J. Treado and M. D. Morris, Appl. Spectrosc. 44, (1990) 1.
9. G. Puppels and J. Greve, XIV International Raman Conference, Wurzburg, Germany (1992)
10. P. J. Treado, I. W. Levin and E. N. Lewis, Appl. Spectrosc. 46, (1992) 1211.
11. E. N. Lewis, P. J. Treado, and I. W. Levin, Appl. Spectrosc. 47, (1993) 539.
12. M. D. Morris, paper #485, Great Lakes Regional ACS Conference, Ann Arbor, June 2, 1994.
13. H.R. Morris, C.C. Hoyt, and P.J. Treado, Appl. Spectrosc. 48 (1994) in press.
14. F.C. Saunders, G. Parry, Opt. Quantum Electron. 18, 426 (1986).
15. J.S. Patel, M.A. Saifi, D.W. Berreman, C. Lin, N. Andreadakis, and S.D. Lee, Appl. Phys. Lett. 57 (17), 1718 (1990).
16. P. J. Miller, Final report to under SBIR contract F29601-93-C-0065 (1993).
17. Meadowlark Optics "Tech Flash", Liquid Crystal Filled Fabry-Perot Filter (1994).
18. M. J. Weber, Handbook of Laser Science and Technology, C.R.C. Press, (Boca Raton), 1986.
19. I.-K. Khoo and S.-T. Wu, Optics and Nonlinear Optics of Liquid Crystals, World Scientific, (River Edge, N.J.), 1993.
20. E.B. Priestley, P.J. Wojtowicz, P. Sheng, Introduction to Liquid Crystals, Plenum (New York), 1974.
21. P. J. Miller, SPIE Proc. 1235, 466 (1990).
22. T. G. Chrien, C. Chovit, P. Miller, SPIE Proc. 1937 28, (1993).
23. P. J. Miller, U.S. Patent 4,848,877 (1989).
24. P. J. Miller, U.S. Patent 5,247,378 (1993).
25. J. W. Evans, J. Opt. Soc. Am. 39, 229 (1949).
26. A. M. Title, W. J. Rosenberg, Applied Optics 18 (20), 3443 (1979).
27. J. Staromlynska, IEEE J. Quant. Electr., 28 (2), 501 (1992).
28. R. A. Dalterio, W. H. Nelson, D. Britt, J. Sperry and F. J. Purcell, Appl. Spectrosc. 40, (1986) 271.
29. H. Ishida, R. Kamoto, S. Uchida, A. Ishitani, K. Iriyama, E. Tsukie, F. Shibata, K. Ishihara and H. Kameda, Appl. Spectrosc. 41, (1987) 407.
30. F. Sureau, L. Chinsky, C. Amirand, J.P. Ballini, M. Duquesne, A. Laigle, P.Y. Turpin and P. Vigny, Appl. Spectrosc. 44, (1990) 1047.

current AOTFs do not. As importantly, the development of optimized AOTFs is much less tractable than the development of LCTF technology. High resolution LCTFs have already been fabricated for other spectroscopic applications and can be optimized readily for Raman microscopy.

AOTF microscopes are currently being commercialized by Brimrose Corp. of America. These devices are not manufactured under license with NIH, which holds a patent on the technology. Unless a license is arranged between these parties, Brimrose microscopes will infringe on the NIH patent, adding legal problems to the technical limitations described above.

For these reasons, it is anticipated that the Renishaw Raman microscope will be the only viable competitor for the foreseeable future.

H.4 Advantages of the Proposed Approach Over Existing Technology

The existing competitive technologies are tunable spectral filter designs based on rotating dielectric filters, and emerging designs based on AOTFs and LCEs. The LCTF approach enjoys a competitive advantage over all of these alternatives.

The complete spatial/spectral data generated by LCTF system gives it a clear advantage over rotating dielectric filter systems, because it provides the user with a much more detailed picture of the chemical distribution when characterizing spatially and spectrally complex, real-world samples.

Compared to systems using AOTF filters, an LCTF-based Raman imaging system would offer vastly superior imaging quality. In addition, use of a liquid crystal waveplate at the LCTF entrance enables monitoring the polarization state of the Raman signal. This yields important benefits for studies of oriented anisotropic materials such as crystals, polymers, semiconductors, and fibers. System integration is easier as well, due to the larger aperture and viewing angle the LCTF affords. Turning to LCEs, if these are commercialized in the future, they promise severe limits in terms of spectral calibration, out-of-band blocking, and field-of-view, without offsetting performance benefits in other areas. This suggests that the LCTF will enjoy a competitive advantage over this technology as well.

H.5 Progress in Commercializing Other SBIR Technology

The Principal Investigator has developed several innovative instruments for optical research. He was one of the key members of the team that pioneered the use of cryogenic cavity radiometer for laboratory standards measurements of radiative flux, with support from the Small Business Innovation Research Programs of the NSF and NASA. These instruments are in use as national standards of light measurement at NIST (ex-NBS), the German PTB, CNAM in France, as well as the national laboratories of Sweden, Spain, and Canada. C.R.I. also developed and builds commercially the award-winning LS and LPC series laser power stabilizers used worldwide in electro-optics laboratories, and most recently, the patented VariSpec line of liquid crystal tunable filters. The VariSPEC was supported by NSF and NIH Small Business Innovation Research Programs. These instruments, with over \$2 million in commercial sales, point to a long and successful history both in research and in the development and marketing of scientific research equipment.

EXHIBIT J



University of Pittsburgh

Faculty of Arts and Sciences
Department of Chemistry

314 Chevron Science Center
Pittsburgh, Pennsylvania 15260
412-624-8821
Fax: 412-624-8552
E-mail: treado+@pitt.edu

June 8, 1995

Mr. Peter Miller
Cambridge Research & Instrumentation Inc.
21 Erie Street
Cambridge, Massachusetts 02139

Dear Mr. Miller:

In my work at the University of Pittsburgh, I am pursuing the development of Raman chemical imaging microscopy and its application to materials science, biomedicine and industrial process monitoring. Much of the research has been funded under industrial sponsorship because of its near-term economic significance. Industrial funding has been provided by the defense, pharmaceutical and automotive industries.

The most significant current limitation in Raman imaging methodology is the lack of a high resolution tunable filter technology. CRI's track record in liquid crystal tunable filter (LCTF) development and commercialization suggests that the last remaining technological limitation in Raman imaging may soon be resolved. I am committed to aiding the Raman LCTF development process and I am providing this letter in support of CRI's Phase I SBIR application to the National Science Foundation entitled "High Definition Raman Imaging Microscope".

My role in the project will be as a consultant. I will assist in the development of LCTFs, and I will perform the application studies that will establish the utility of LCTF Raman chemical imaging. My consultant rate is \$420/day. After Phase I is successfully demonstrated, I anticipate working with CRI in Phase II by developing Raman imaging microscope systems employing high definition LCTFs.

Through my involvement with industrial, and biomedical end users of Raman chemical imaging microscopy, I will assist in the transfer of the technology to the marketplace.

I look forward to CRI's success in LCTF development for Raman imaging.

Sincerely,

A handwritten signature in black ink, appearing to read "Pat Treado".

Patrick J. Treado
Assistant Professor of Chemistry

EXHIBIT K

Final Report on SBIR Phase I Contract DMI-9560600
"High Definition Raman Imaging Microscope"

submitted to the
National Science Foundation
Arlington, VA 22230

by
Cambridge Research & Instrumentation, Inc.
Cambridge, MA 02139

Paul J. Ne
Principal Investigator

John F. Foley
President

9/13/96
Date

9/13/96
Date

This material is based upon work supported by the National Science Foundation under award number DMI-9560600. Any opinions, findings, and conclusions or recommendations are those of the author(s) and do not necessarily reflect the views of the National Science Foundation.

Abstract

Technical Summary.

During Phase I, a liquid crystal tunable filter (LCTF) was designed, built, and characterized for use in Raman chemical imaging. The filter has a design bandwidth of 8 cm^{-1} and a tuning range of 500 - 650 nm, or 4600 cm^{-1} . Unlike other tunable elements for Raman imaging, the LCTF is free of optical distortions, spectral leakage, or image shift with tuning.

The actual filter performance met all model predictions, and was successfully integrated into an optical microscope employing a 514.5 nm Ar^+ laser source coupled via fiber-optics to provide uniform illumination through infinity-corrected microscope optics. Raman images were collected using a cooled CCD camera. Sample spectra obtained through the LCTF are identical with spectra of the same samples acquired with a conventional (non-imaging) dispersive spectrometer employing CCD multichannel detection. Images collected with the LCTF Raman chemical imaging system provide essentially diffraction-limited resolution, as verified with USAF test targets and quantitative CTF analysis. Raman images of model systems clearly surpass all previous Raman imaging data.

The LCTF Raman system is robust, not prone to thermal drift, and defines the state-of-the art in Raman imaging technology. It promises to usher in a new era of practical Raman imaging, and has the potential to revolutionize Raman microscopy. However, the devices produced to date represent only the first generation of LCTF Raman development. Outstanding LCTF Raman issues are to improve throughput, to develop improved filters for the red/near-IR range appropriate for use with He-Ne, Kr^+ or laser diode sources, and to exploit confocal volume Raman imaging; these issues will be addressed in Phase II.

Commercial Potential

Compared to existing, non-imaging systems, the LCTF Raman system adds the powerful ability to image chemical species in heterogeneous samples, and to map out spatial distributions and features. This is a key benefit in working with real-world samples, which tend to be heterogeneous on the spatial scales of interest.

In many cases, the spectral bands of interest are known, and the measurement consists of identifying the presence and/or location of various species in a sample. Present practice is to use non-imaging systems such as a scanned microspot, which provide rich spectral data but limited (or inefficient) collection of spatial data. Use of a LCTF Raman system is the ideal way to produce the desired data set, which was not previously practical to obtain. One expects that a LCTF Raman system would also include a conventional fiber feed to a dispersive spectrometer, to provide standard spectral data along with the new spectral imaging capability.

We anticipate that a turnkey Raman chemical imaging system would be a new and powerful tool, used broadly by industrial and academic researchers. Beyond the research market, the emergence of industrial markets depends on the utility of this approach in specific applications, which must be determined through evaluations and case-by-case comparison against present methods.

I. Statement of Phase I Objectives

- i) To use existing computer models to generate a tunable Lyot filter design optimized for Raman spectroscopy;
- ii) To study the integration of such a filter into a microscope imaging system, including optical path, data acquisition, and camera requirements;
- iii) To construct a fully imaging prototype filter according to this design, with resolution of 10 cm^{-1} or better, tunable over a range of 2500 cm^{-1} ;
- iv) To characterize this filter for its spectral properties, including peak transmission, bandwidth, out-of-band rejection, and tuning range;
- v) To test this filter to obtain true two-dimensional Raman spectroscopy images of test samples;
- vi) To prepare a Phase I report describing the results.

II. Summary Description of Research, Results, and Commercial PotentialII.a Research and Results

i) Computer model of Lyot filter for Raman spectroscopy

The filter was designed with a computer model based on the Jones calculus of polarization state. Measured values of retardance and dispersion are used for liquid crystal and mineral crystal elements. We chose x-cut LiNbO_3 retarders for the high-order Lyot stages, and quartz for the lower-order stages. A total of 18 elements were employed, each of which is continuously tunable by means of liquid crystal variable retarder elements. Modeled passband and out-of-band rejection are shown in Figure 1.

ii) Integration with microscope

The system was constructed around an Olympus BHSM-2 microscope, as shown in Figure 2. Epi-illumination is provided by an Ar^+ laser (Coherent CR-3) coupled through a fiber before impinging on a high-performance dielectric notch bandpass filter (OCA Microplasma) to reject the silica Raman bands developed within the fiber. The conditioned laser light fills the back aperture of the microscope objective and excites the sample. Raman scatter is collected by the same infinity-corrected objective and presented to two holographic notch filters which remove laser back-scatter. The Raman signal then passes through the LCTF and is imaged onto a cooled CCD camera (Princeton Instruments TE-CCD-768-k/2). Raman light is also coupled efficiently via a swing-away mirror to a fiber-optic bundle, prior to passing through the LCTF. The Raman

fiber-optic is coupled to a dispersive Raman spectrograph employing multichannel CCD detection and allows the system to perform as an efficient confocal Raman microprobe when this is desired.

iii) Filter construction

The LCTF was built using similar techniques to those developed for previous filters with broader passband (a few nm). The only significant issue was a difficulty in obtaining the LiNbO_3 retarders needed to achieve a narrow passband. These parts have a large aspect ratio (up to 100:1), and the surfaces must be parallel to 5" of arc. We worked with a vendor to identify a polishing process which produced these parts with high yield. Subsequent filter construction proceeded smoothly.

iv) Filter characterization

We tested the LCTF for bandpass, transmission, out-of-band rejection, free spectral range, and tuning accuracy using a 0.5m spectrometer. All were in good agreement with model predictions. The bandpass is 7.6 cm^{-1} and is free of sidebands; transmission ranges from 6.7 to 16.3 percent; rejection is $>10^4:1$ for out-of-band light; the filter is tunable over a range of 4600 cm^{-1} , in milliseconds, with no moving parts. Repeatability is 0.38 cm^{-1} over this range.

v) Raman imaging of test samples

Figure 3a shows the spectrum of a polystyrene microsphere, taken with the LCTF by tuning it sequentially to various wavelengths and recording the image intensity; Figure 3b shows a spectrum of the same samples taken with a non-imaging Raman microprobe and a dispersive spectrometer. Note the agreement of spectral features and relative intensities in the two Figures, indicating excellent spectral performance by the LCTF.

Figure 4 shows a brightfield image of the 2μ microspheres, taken with a 100x microscope objective, which demonstrates diffraction-limited spatial resolution. Airy rings are visible in this image, taken through the LCTF. A Raman image at 992 cm^{-1} is shown as Figure 5, with a 500 nm size bar shown for reference. The quality of this image is unmatched in Raman imaging to date.

II.b Commercial potential

Compared to existing, non-imaging systems, the Raman LCTF system adds the novel ability to visualize the distribution (morphology and architecture) of chemical species in heterogeneous samples with molecular compositional specificity. Raman images can be collected rapidly, non-invasively, with limited or no sample preparation, at high spatial resolution ($< 250 \text{ nm}$) and with high fidelity where the number of image pixels is limited by the number of pixels on the CCD detector. Most important, every image pixel has a Raman spectrum associated with it whose quality is identical to that obtained with conventional non-imaging spectrometers. These key benefits make Raman imaging practical for the first time in the analysis of real-world samples, which are chemically heterogeneous on the spatial scales of interest.

With the development of the LCTF Raman system, it is now practical to collect simultaneously high spatial/spectral resolution data sets of complex unknown materials having millions of pixels. The LCTF Raman imaging system is the ideal way to produce the desired data set, which was not previously practical to obtain. At the same time, the capability to perform conventional Raman microspectroscopy is intrinsically valuable, and one expects that a commercial Raman LCTF system would also include a fiber-optic feed to a dispersive spectrometer, to provide standard Raman spectral data along with the new spectral imaging capability.

We anticipate that such a turnkey Raman chemical be a new and powerful tool, used broadly by industrial and academic researchers for material analysis. In addition, we anticipate that process chemists would take full advantage of the Raman chemical imaging approach to perform at-line failure analysis and ultimately to perform non-invasive in-line Raman imaging of materials during the production process. The emergence of industrial markets, in particular the process monitoring markets, awaits beta-site research with industry partners to quantify benefits of the LCTF approach in specific applications.

III. Detailed Description of Research and Results

i) Design LCTF optimized for Raman imaging

The first step was to model a Lyot filter with the desired bandwidth and free spectral range. A Lyot stage consists of a retarder, liquid crystal tuning element, and a linear polarizer, while a Lyot filter¹ consists of several stages placed optically in series. The filter has a spectral resolution which is determined by the FWHM of the thickest retarder element, while unwanted adjacent orders are blocked by subsequent thinner stages. Thus the overall free spectral range (FSR) is set by the thinnest retarder element. Excepting for dispersion, the bandwidth of a retarder is constant in wavenumbers, or quadratic in λ , and a Lyot filter behaves in like manner.

In designing the Raman LCTF, existing models and techniques were used, which have been repeatedly verified in work with filters having broader bandpass. These use the Jones calculus², which tracks the polarization state for forward-propagating light. The model ignores reflections at interfaces, which has not been observed to introduce errors, as all components are index-matched in the final assembly. Dispersion values for the liquid crystals and fixed retarders are based on measured values, as are the wavelength-dependent polarizer transmission and extinction $k_1(\lambda)$ and $k_2(\lambda)$.

One new concern was the need for high-value retarders, to provide the high spectral resolution sought. Use of such components brings with it possible problems of field-of-view and thermal stability. A second concern was that, because the ratio of FSR : FWHM is high, a large number of stages would be required, leading to low transmission and overall complexity. These concerns are now discussed in detail.

LiNbO₃ was chosen for the high-value retarders, for the following reasons:

- a) it is readily available in apertures of 30 mm or more;

- b) it has a high index of refraction $n_o \approx 2.30$;
- c) it exhibits moderate birefringence $\delta n \approx 0.09$; and,
- d) LiNbO_3 can be fabricated using conventional methods.

The first and last insure that one can obtain the material and have waveplates built. The high index yields a wider field-of-view, since off-axis spectral shifts scale as $1/n_o^2$. The third factor is important, because if the birefringence is too low, overly thick elements are required and the filter becomes unwieldy. For example, if the highest order stage were quartz, it would have to be 3.5 cm thick, which is not practical. On the other hand, high- δn materials bring other fabrication problems: to achieve uniformity across the aperture with a high- δn material, the parallelism requirement becomes extreme. In all these regards, LiNbO_3 appears to be a superior choice to calcite except when constructing very narrowband (sub-Angstrom) filters.

Models of off-axis performance indicated that, while superior to other materials, LiNbO_3 would still exhibit unacceptable off-axis spectral shifts. For this reason, wide-field elements were used for the thickest five retarder elements. These consist of a pair of elements, each with half the required thickness, separated by a half-wave plate. The two elements are oriented with their crystal axes crossed, and the half-wave plate is oriented at 45° . This arrangement, often used in narrowband solar H_α filters, greatly increases the field of view compared to a simple retarder element. Models indicated that this would yield a $\pm 7^\circ$ field-of-view, well in excess of the requirement.

The problem of thermal drift is not so easily solved by design. Thermal drift in wavelength, per $^\circ\text{C}$, is a significant fraction of the FWHM of the filter. Rather than devise a thermally stabilized enclosure, the design used a thermistor in the filter housing to monitor the actual temperature of the filter elements; this is sensed by the control electronics module, which then adjusts the drive voltage to the liquid crystal elements, and actively compensates for any drift in the retarders.

To address the need for a large number of stages, two approaches were used. First, the filter was constructed in two detachable modules, one containing the highest-order elements, and one with the lower-order elements. This simplified the construction, and avoided problems in handling a single unwieldy component. The two modules may be joined to form a single, light-tight assembly. Second, to minimize the losses inherent in a many-stage filter, a high-transmission polarizer was used. Optical losses are below 2% per liquid crystal element at these wavelengths, and the retarders are nearly lossless, so polarizer absorption is the dominant term in determining overall filter transmission. Since the Raman system was to be used over the range 500 - 650 nm, where polarizer materials exhibit high dichroism, a lightly dyed material could be used, to provide higher transmission while still insuring adequate extinction. Most common polarizer material, like Polaroid HN38, is more heavily dyed to avoid leakage in the violet spectral range; this cuts transmission unnecessarily.

Based on this choice of materials, a design was developed for an 18 stage Lyot filter. It meets the bandwidth, tuning range, stability, field-of-view and

image quality requirements for Raman imaging. The filter constructed in Phase I was built to this design, and performed as predicted.

The principal limitation of this design is its relatively low transmission, which ranges from 7 to 16 percent. A novel design was devised to overcome this problem, and a model was developed of this new design. Based on the Evans split-element retarder, it should nearly treble the throughput of the LCTF, as described in Section IV, Key Improvements for Phase II.

ii) Integration into microscope

The first task in integrating the LCTF into a Raman imaging system was the selection of a laser excitation source. Normally, each application brings with it factors that determine the optimal excitation wavelength; however, given the budget limitations of the Phase I effort, a single Ar⁺ laser wavelength of 514.5 nm was chosen due to its availability in Dr. Treado's laboratory. Integration of the laser source into an existing upright optical microscope was achieved by coupling the laser source via a 200 μ m core quartz fiber optic as the illumination source transfer line. Fiber-optic coupling enables uniform illumination of the sample. The output of the fiber-optic is collimated and then filtered using a high performance dielectric bandpass filter to remove silica Raman bands that develop in the fiber-optic. The filtered light is presented to the rear aperture of the infinity-corrected microscope objective, which produces uniform Koehler epi-illumination (180° backscattering) of the sample. In the epi-illumination configuration, the sample is illuminated and the Raman signal is collected through the same infinity-corrected objective. Two holographic filters are used to reject the Rayleigh scatter from the sample and to transmit the Stokes (red-shifted) Raman image through the LCTF and to optics that project a magnified image of the sample onto the CCD detector. A swing-away mirror provides access to the Raman light prior to the LCTF and redirects it to a relay lens which couples it into a fiber bundle. The fiber bundle feeds it into a dispersive 0.5m spectrograph with multichannel CCD detection, and allows the system to perform as an efficient confocal Raman microprobe.

A principal requirement in Raman imaging is to detect the weak Raman signal levels efficiently, in the presence of much brighter laser excitation and interfering background (usually fluorescence) signals. The holographic notch rejection filters provide rejection efficiency of at least 10¹²:1 for the Raman vs. the Rayleigh scattering. In addition, the four orders of rejection provided by the LCTF allows discrimination of weak Raman features in the same image field of view as intensely fluorescent species. Discrimination is feasible with a Lyot filter due to its high rejection efficiency, in contrast with tunable etalons that exhibit lower efficiency (100:1) and evidence fluorescence artifacts in the putative Raman images. If fluorescence background exists at the same wavelength as the Raman bands of interest, the LCTF will not distinguish between the two signals. Rather, the microscopist must rely on the use of high dynamic range detectors (16 or 14 bits) to simultaneously record both signals. Using spectral subtraction, ratioing, or multivariate techniques the fluorescence can be further discriminated from the Raman information. In certain cases, fluorescence is too strong to be

differentiated from weak Raman features. The best strategy in this case is to employ a different laser wavelength to excite the sample outside the fluorescence excitation band.

The fiber optic feed to the spectrometer is provided because the capability to perform conventional Raman microspectroscopy is intrinsically valuable. One expects that a commercially viable Raman LCTF system would also include a fiber-optic feed to a dispersive spectrometer, to provide standard Raman spectral data along with the new spectral imaging capability.

iii) Filter construction

A diagram of the filter is provided in Figure 6. The liquid crystal optics, polarizers, and quartz retarders were built using techniques developed for other, broad-passband LCTFs. New techniques were developed to permit use of LiNbO_3 retarders, as follows.

First, while obtaining suitable LiNbO_3 was straightforward, there were difficulties having it polished with suitable flatness and parallelism. Single-sided polishing methods gave good finish and flatness, but poor parallelism, while double-sided polishing tended to chip the parts or to round the edges. These problems were most serious when fabricating the thinnest retarders (0.013" thick), due to the high diameter:thickness ratio of 96:1. Tests were made of different polishing compounds and machine settings, and a process was identified which produced good parts, thus solving the problem.

Second, the high index of LiNbO_3 had to be accommodated. Normal LCTF filters are assembled using index-matching epoxy, to join the many elements, and to eliminate reflections at boundaries. This reduces the mechanical complexity of the resulting system, and improves the optical performance. This approach is quite effective when all materials have similar indices; however, $n_o = 2.30$ for LiNbO_3 , so parts made from this material had to be antireflection coated to match their impedance to that of the epoxy ($n \approx 1.51$). While not a common coating, it was available with a reflection $< 0.5\%$ over the range 500 - 750 nm. To ensure there would be no adhesion problems or chemical interactions, a test blank of LiNbO_3 was made, coated, and epoxied to precision BK-7 windows. No problems were observed in this test piece, or in the prototype filter work.

Next, the wide-field retarder design required $\lambda/2$ waveplates. These were constructed using polyvinyl alcohol (PVA) sheet retarder, stripped of its plastic lamination using the method of Title, and glued between borosilicate windows. The nominal retardance was 280 nm, so optimum performance was at 560 nm. In this design, the effect of $\lambda/2$ waveplate retardance error is to reduce the peak transmission, rather than to add leakage. An improved method might be to use achromatic $\lambda/2$ plates, using the design of Pancharatnam, which would improve the peak transmission. However, there is an even better method based on the Evans split element approach, as discussed below.

Finally, all retarders (quartz and LiNbO_3) were characterized to identify the spectral locations λ_m of their maxima, for which $R = m\lambda_m$. These are used to

define the wavelength scale of the filter. For the high-order retarders, this was performed on a 0.5M spectrometer, to provide sufficient resolution (0.02 nm). Assembly proceeded normally, and the filter was completed without incident.

iv) Filter characterization

Figure 7 shows the filter bandpass when tuned to 532 nm. The bandwidth, defined as the full-width at half-maximum (FWHM) is 0.20 nm, or 7.6 cm^{-1} . Peak transmission is 11 percent, and average out-of-band leakage is 0.01% over the range 500 - 650 nm. All are in agreement with model predictions. Repeatability was assessed by cycling the LCTF from one wavelength setting to another, then back. Spectra were taken of the LCTF transmission, with a fixed-grating CCD spectrometer, to measure any variation in passband after cycling. Shift was 0.38 cm^{-1} , or 0.01 nm, which is within the measurement error of the test.

Image quality was assessed in three ways. First, a USAF 1951 resolution test target was imaged in bright-field illumination, with and without the LCTF present. These are presented as Figure 8a) and 8b). No image degradation is visible. The center-to-center spacing of the finest grid is 4.3μ . Second, 2μ polystyrene microspheres were imaged in bright-field illumination, as was shown earlier in Figure 4. Diffraction-limited performance was obtained, and Airy rings are plainly visible.

A more quantitative measure was obtained by determining the contrast transfer function $\text{CTF}(\omega)$, which assesses the contrast reduction when a square-wave intensity pattern of a certain spatial frequency ω is imaged through an optical element. To date, it has not been the practice when developing Raman microscopes to employ CTF analysis to assess imaging performance. This is due in large part to the ability of CTFs to reveal very subtle deficiencies in imaging systems, whereas previous Raman imaging approaches have exhibited resolution which is considerably worse than the diffraction-limit. It is anticipated that CTF analysis will, in time, become a standard method for assessing Raman imaging performance, just as it (and the related MTF) are in other imaging disciplines.

In general, the CTF for a series of elements is the product of the CTF of each optical element. The CTF was measured for the imaging system with no filter, with the LCTF, with an IR cutoff filter that blocks light with $\lambda > 700 \text{ nm}$, and with a 532 nm narrowband dielectric filter. These were compared against the theoretical CTF for a diffraction-limited image. Data was taken using a 5x, 0.1NA objective and a 1951 USAF resolution target. The results were:

Table 1.	CTF for various filters
filter type	contrast reduction (relative to diffraction limit)
no filter	-28.2% +/- 13.6%
IR cutoff only	-12.2% +/- 10.6%
LCTF	- 6.7% +/- 6.3%
532 nm filter	- 2.3% +/- 3.5%

The greatest contrast reduction occurred when no filter was present, and is due to residual chromatic aberrations in the microscope optics. Better performance was obtained with the infrared rejection filter engaged, and better still when a narrowband filter was used, because the resulting image was taken in monochromatic light. The LCTF introduced slightly more contrast reduction than the dielectric filter, but both performed quite well. In conclusion, the image contrast degradation introduced by the LCTF, while measurable with digital CTF methods, is minimal.

v) Raman imaging of test samples

Raman images were taken of several samples including model systems comprised of microspheres, and real-world samples including polymer thin films, polymer blends, semiconductors, and corrosion thin films. Figure 9 shows a multi-component corrosion sample, which includes KNO_3 , TiO_2 , and WO_3 films. A bright-field image (A) reveals little information that would allow discrimination of the components. By tuning the LCTF to the wavelengths corresponding to the characteristic Raman bands of each individual species, however, very specific information is obtained. Image (B) was obtained with the LCTF tuned to the 1057 cm^{-1} stretch band of NO_3^- , and indicates regions of KNO_3 , while image (C) was taken at the 604 cm^{-1} band of TiO_2 , and image (D) shows the 797 cm^{-1} band of WO_3 . Chemical specificity is obtained, and a high-definition view revealing specific molecular components and their associated morphology is produced. Each image is collected in 60 seconds.

Indeed, a complete spectral data cube was obtained, by taking successive images of the corrosion sample, as the LCTF was tuned by 3 cm^{-1} wavelength steps. The result is a near diffraction-limited image for which a complete Raman spectrum is available at every point in the image. The molecular composition of the individual components is evident more clearly in spectra extracted from individual pixels in the data cube, plotted in Figure 10. The availability of such detailed data is unprecedented in Raman chemical imaging.

Note that there is no smearing or image degradation evident in the corrosion images. Further, the image registration is perfect despite tuning the LCTF. This is a clear advantage of the LCTF over competing technologies such as AOTFs, rotating dielectric filters, or tunable etalons. This implies that the LCTF Raman microscope is suited to the use of numerical deconvolution confocal Raman imaging employing widefield illumination, as discussed below in Section IV. This numerical approach to volumetric imaging has been developed for

fluorescence microscopy at discrete wavelengths, and requires a mechanically stable, high image-quality microscope.

One can quantify the amount of image shift which results from LCTF tuning. The only significant source of image shift is prism action; that is, wedge in the LCTF, coupled with dispersion in the materials employed, to produce a wavelength-dependent angular shift. Wedge in the retarder elements is of order 20 micro-radians, and dispersion in index is 0.015 over the spectral range involved. Thus, prism action in these components is utterly negligible: 0.32 microradians, or 0.06 " of arc. More important is wedge in the liquid crystal cells, polarizers, and other elements, as they are less tightly toleranced in manufacture. In all, the image shift in tuning is approximately 2" of arc, still well below the diffraction limit of any microscope objective.

IV. Identification of Key Improvements

a) filter transmission

In Phase I, we have constructed an LCTF designed for Raman use, and have demonstrated performance that is unmatched by competitive Raman technologies, which include AOTFs, tunable LC etalon, rotating dielectric filters, and confocal point-scanning Raman microprobes.

AOTFs were first studied for Raman microscopy by Dr. Treado several years ago and provide substantially degraded spatial and spectral performance relative to the LCTF. Tunable etalons provide low free spectral range, low transmission, and poor out-of-band rejection performance. Rotating dielectric filters exhibit low spectral resolution and introduce significant image shift during operation. At present, the only imaging technology that can arguably compete with the LCTF is the point scanning Raman microprobe, due primarily to the high spectral resolution obtainable with the point scan technique. The Raman microprobe employs a dispersive spectrograph in combination with a multichannel detector to rapidly collect Raman spectra from point-localized regions in the sample.

In a Raman microprobe, light from a point in the sample is dispersed across a CCD detector, and light of a large range of wavelengths is captured at once. Flux from spatial regions outside the point being imaged, is ignored. To acquire a complete spectrum takes only a single exposure of a CCD located at the exit focal plane of a spectrograph. The integration time to produce a given signal in counts per CCD element is determined by a number of parameters, including the laser power density at the sample, the concentration of the analyte, the scattering cross-section of the sample at the laser wavelength, the sample scattering volume, the collection efficiency of the microscope, the quantum efficiency of the detector, and the peak transmission of the spectrometer and its dispersion. The greater the dispersion, in nm/pixel, the longer an exposure is required. If an $m \times n$ image were desired, it requires stepping across the image, and taking mn total exposures. Roughly, the acquisition time scales linearly with dispersion (resolution), and quadratically with the spatial resolution sought (m or n).

On the other hand, an LCTF-based imaging Raman system employs widefield illumination, and views all regions of the sample simultaneously at a spatial resolution limited by diffraction (~ 250 nm). During operation, the LCTF transmits a single wavelength at a time, and absorbs the rest. To acquire a complete $m \times n$ image takes only a single exposure, and the integration time to produce a given signal level in counts per CCD element is determined by the same sample, laser power density, and microscope parameters that were considered above, except that the peak transmission of the LCTF and its bandwidth replace the spectrograph transmission and its dispersion as governing parameters. If the LCTF bandwidth is greater, a greater total flux lands on the CCD, assuming the Raman bandwidth exceeds the LCTF bandwidth. If a spectrum of k points were desired, a total of k exposures would be required. For high spectral resolution, k is large and the LCTF bandwidth must be reduced as well, so the acquisition time scales quadratically with resolution.

It appears that a non-imaging system is favored when:

- a complete (dense) spectrum is required rapidly; and,
- an image is not desired,

while an imaging LCTF system might be favored when:

- the species are known a priori, so only a reduced number of spectral points are sampled, to uniquely differentiate the analyte species; or,
- an image is desired.

Numerical considerations favor the LCTF by 50,000 : 1 when an image is required and only a handful of spectral planes need be sampled. However, if a dense spectrum is needed and imaging is not required, a microprobe will be several hundred times faster at gathering purely spectral data. These considerations are inherent to comparing dispersive vs. imaging filter architectures, and the viability of the imaging approach as a tool for Raman use will depend on the relative amount and type of information that a given application requires.

Despite the inherent benefits of the LCTF for imaging, the peak transmittance of the present device is less than optimal. Indeed, throughput is the primary limitation of the present LCTF. While cooled CCD detectors have more than adequate sensitivity to accommodate the reduced throughput of the LCTF for many applications, long integration times (minutes) are required to collect the Raman spectral image information. However, the peak transmittance can be improved significantly in a second-generation device, and this will be a major focus of the Phase II research effort.

There are two reasons for the low transmission of the Phase I prototype LCTF. First, a Lyot filter operates in polarized light, and loses half of the input signal at the first polarizer. Second, absorptive losses in the many optical elements leads to low efficiency. These can both be addressed, as follows.

It is possible to use a polarizing beam-splitter (PBS) to separate the two polarization components of incident light; to convert the unwanted component by means of a $\lambda/2$ plate, so that it also passes through the LCTF; and, to recombine the components with a second $\lambda/2$ plate and a second PBS, after they exit the LCTF. This arrangement has been built successfully for LCTFs used in

fluorescence microscopy. Losses in the PBS and other elements limit the efficiency to 90% of the theoretical maximum. Still, this is nearly twice the 50% efficiency which is achieved when only one component is utilized. Image quality suffers if the two beams are not well-registered upon re-combination, but resolution of 1024 x 1024 pixels can be achieved readily without degradation. Also, the use of PBS elements adds approximately 3 cm. of glass to the optical path, but this can generally be accommodated in an infinity-corrected microscope beam without trouble. This approach could provide a factor of 1.8 in throughput over the present system.

Second, it is possible to use a design described by Evans³ for use in solar H_α and Ca_K filters to gain a further improvement of approximately 2:1. Recall that the high-order stages are constructed using a so-called wide-field construction, where two high-order retarders of equal thickness are placed with their crystal axes orthogonal, on either side of a $\lambda/2$ plate, which is oriented at 45°. This produces a wider field of view than a simple retarder. However, it is possible to construct such a stage where the $\lambda/2$ plate is replaced by one of the lower-order retarder elements, which is actively tuned by a liquid crystal element so it exhibits $n+1/2$ waves of retardance at the passband. This has several beneficial effects. First, it eliminates the need for the $\lambda/2$ plate. Also, if the two high-order retarders R_{H1} and R_{H2} are well-matched, the transmission of the stage is given by:

$$T(\lambda) = \sin^2(\pi(R_{H1} + R_{H2})/\lambda) \cdot \sin^2(\pi R_L/\lambda)$$

so it has the same effect as two simple Lyot stages, one with retardance $R_{H1} + R_{H2}$, and one with retardance R_L . Such a stage, termed an Evans split element stage, has the same spectral filtration as two simple Lyot stages. A single stage was assembled to test this concept, and its actual transmission is shown along with model data in Figure 11. The high-frequency period is developed by the high-order retardance $R_{H1} + R_{H2}$ (two 0.072" $LiNbO_3$ elements), while the low-frequency period is due to R_L (0.060" quartz). Excellent agreement was achieved, and this approach looks very promising.

Using this design, the number of stages is cut in half, with a corresponding drop in the number of polarizers and in the filter's absorptive loss. However, more retarder elements and liquid crystal elements are needed. While these are optically efficient, the complexity is increased, as is the stringency of optical tolerancing. These improvements, along with further optimization of the materials used throughout the LCTF, are natural avenues for improving the filter throughput. In the best case, it should be possible to produce an LCTF with transmission of 30% or more, for unpolarized incident light.

b) longer wavelength range

Another area for improvement is the LCTF free spectral range, which is presently limited to use with Ar^+ or doubled Nd:YAG laser sources. To operate with 647 nm Kr^+ sources, or laser diodes, an LCTF would have to tune over the range 650 - 1050 nm. These sources are used to reduce sample fluorescence, especially in biomaterials, or when working with certain types of samples such

as semiconductors, to obtain greater source penetration depth. In addition, red laser sources take advantage of the higher quantum efficiency of CCDs to red radiation. Since the spectral resolution of an LCTF is constant in wavenumber as it is tuned, the present retarder design will give adequately high spectral resolution. The retarders and liquid crystal cells all exhibit high transmission in the near-IR, somewhat above their visible-range values.

The spectral restrictions in the present filter are due to the dichroic polarizer materials, the LiNbO_3 coatings, and the limited operating range of the $\lambda/2$ plates. The latter would be removed by use of the Evans split element design just described, and would then cover the necessary range. Dielectric coatings can be obtained to couple the LiNbO_3 to an $n \approx 1.51$ index with $R < 0.5\%$ over this range. Thus, only the polarizer presents a significant problem to construction of LCTFs for use with these longer wavelength sources.

Conventional sheet polarizer material is unacceptably lossy for use in a multi-stage Lyot filter. We have worked with an outside vendor to develop a novel polarizer for the near-IR, with 1000:1 contrast and markedly improved transmission. This material is used in a commercial line of LCTF filters, and has proven to be reliable. Transmission of the IR materials is shown in Figure 12, alongside the very high-efficiency dichroic polarizer used in visible range LCTFs. Preliminary models indicate that a high-performance Raman filter built could be built using this material, with specifications for bandwidth, out-of-band blocking, and peak transmission that would be comparable to a visible-range device.

c) confocal LCTF Raman imaging

Based on the high demonstrated image quality of the LCTF Raman system, we intend to explore its suitability for Raman confocal volumetric imaging, using a series of height-stepped exposures and numerical deconvolution techniques to develop a three-dimensional map of the sample. If successful, this would provide nondestructive depth profiling of chemical concentrations in samples, at a spatial resolution of ~ 250 nm, with minimal or no preparation. Such an instrument would be a powerful diagnostic tool for a great many industrial processes. It would be especially valuable in depth profiling of semiconductor impurities and dopants, thin-film corrosion systems, adhesive bonding systems, and similar applications. This is a potential high-payoff area which could have a technical and commercial return vastly exceeding that of the normal (non-volumetric) imaging LCTF Raman.

V. Assessment of Commercial Potential

There appears to be an emerging research market among spectroscopists, materials scientists, biomedical researchers, and process chemists for a commercial version of the Raman LCTF, and/or complete turnkey imaging Raman systems. Newly-available image information which the Raman LCTF makes available, has excited some 'visionary' users, who perceive great potential in this approach. Already, several such people have contacted us to arrange for sample tests or possible purchase of such equipment, citing specific research

programs which would benefit from imaging Raman data. This encourages us to believe that the Raman LCTF has a solid future as a research instrument.

It remains to be seen whether the power of imaging Raman techniques will become significant in broader analytical chemical practice, or not. This depends as much on the nature of the applications involved, and what is gained by visualizing the structure and morphology of species, as it does on the performance of the LCTF *per se*. An imaging Raman system is a new tool, complementary to and different from a spectrometer, and its utility is not yet proven. To compete in the long-term, the imaging Raman approach must offer unique data which is perceived as critical to an application, or it must produce data similar to that of other instruments, but do so in a more efficient or convenient way.

Several applications have emerged where the imaging Raman approach appears to offer a compelling benefit of this type. One area is in silicon processing, to assess strain and lattice deformation, and others are in pharmaceuticals, paper products, steam power generation, and waste water treatment. A partial list of industrial partners, whose researchers have already contacted Dr. Treado to assess the LCTF Raman approach for use in their application, includes Kodak, Westinghouse, Lockheed Martin, Bayer Polymers, Bayer Consumer Products, ICI Materials, Unilever, Proctor & Gamble, Ford, PPG, Johnson & Johnson, Union Carbide, Medtronic, Alza, Eli Lilly, and Glaxo-Wellcome. If LCTF Raman were to establish itself in any of these areas, there would be significant markets (a few dozen instruments/yr) in industrial research and materials analysis as well as in pure research.

References

1. Lyot, B., *Compt. Rend.*, 197, 1593 (1933).
2. Jones, R. C., *J. Opt. Soc. Am.* 31, 488 (1941).
3. Evans, J. W., *J. Opt. Soc. Am.* 48, 142 (1958).

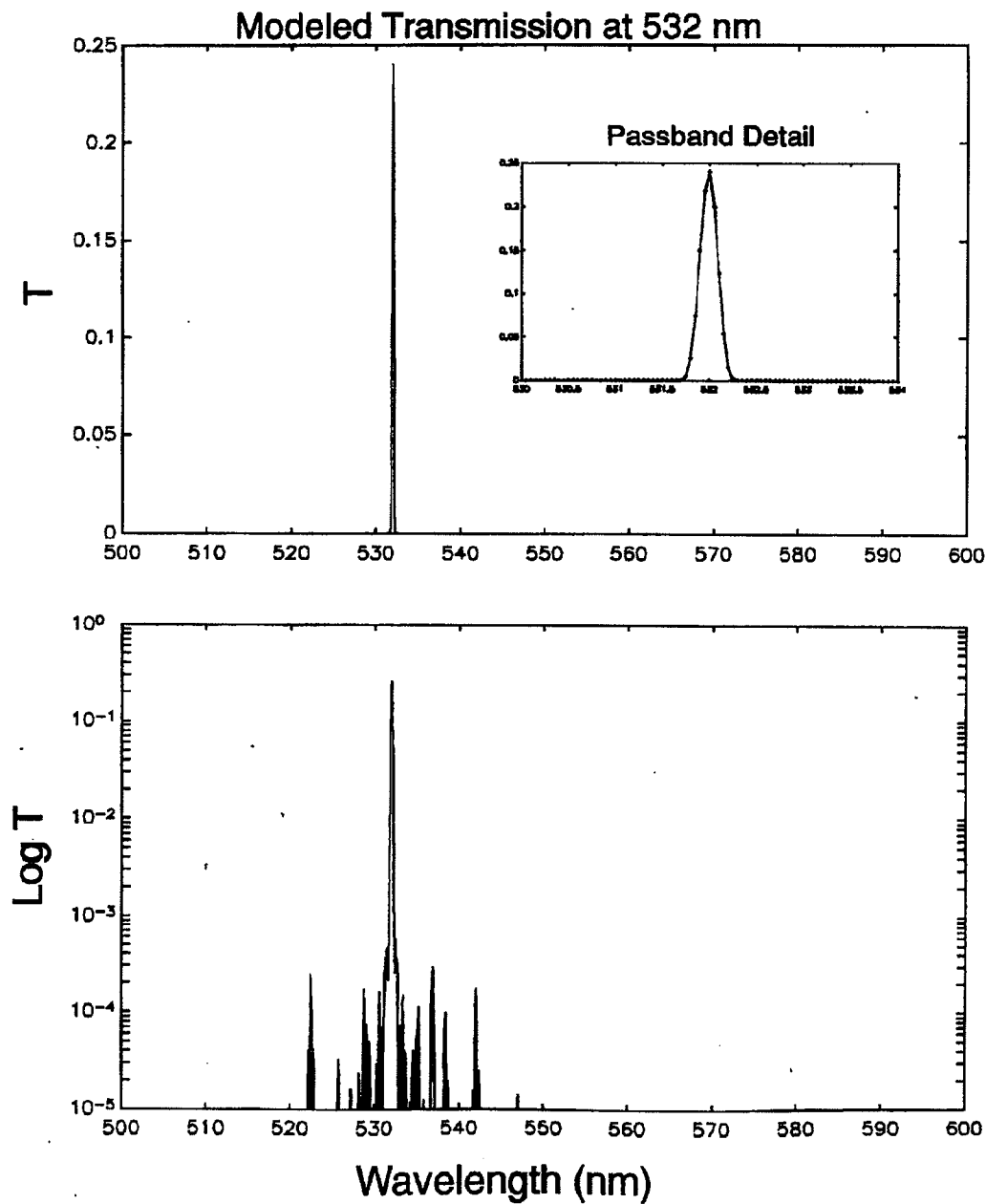


Figure 1. Model LCTF performance when tuned to 532 nm, shown on linear and logarithmic scales. Passband detail is shown in the inset.

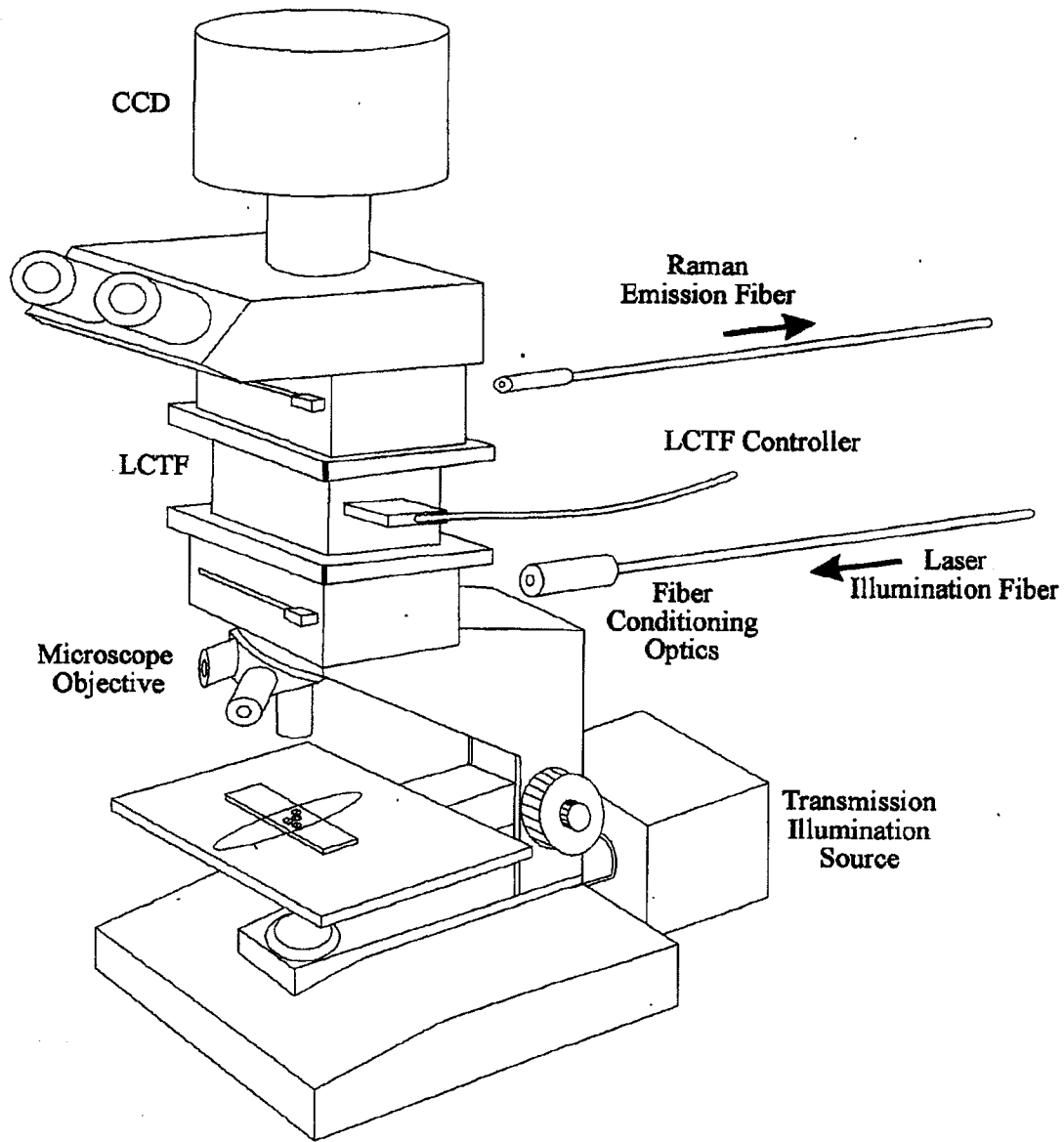


Figure 2. Diagram of the LCTF Raman filter integrated onto the optical microscope.

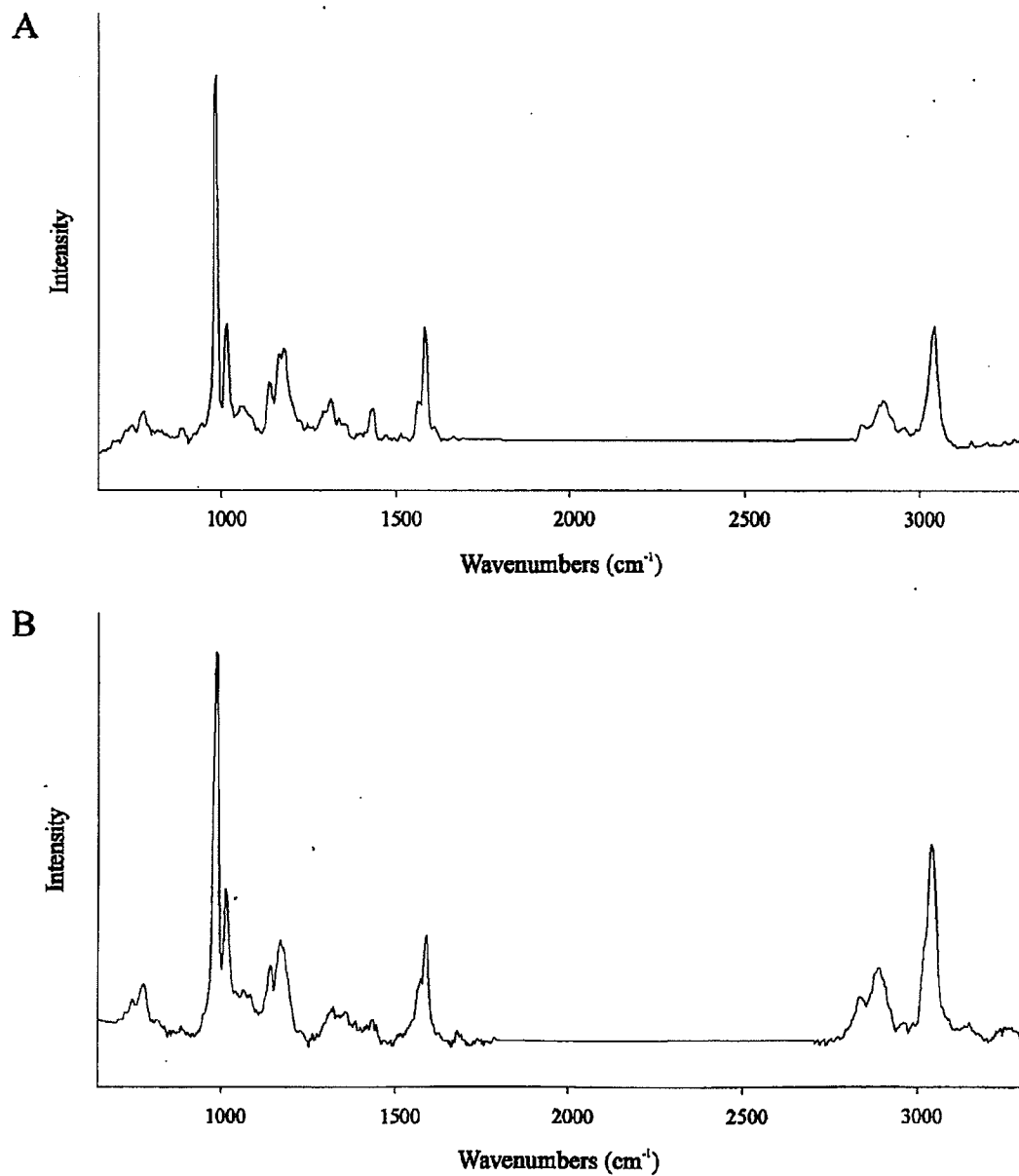


Figure 3. The top figure shows a Raman spectrum of polystyrene microsphere, obtained with the LCTF, while the lower figure shows the Raman spectrum of the same sample taken through a conventional (non-imaging) dispersive spectrometer system.

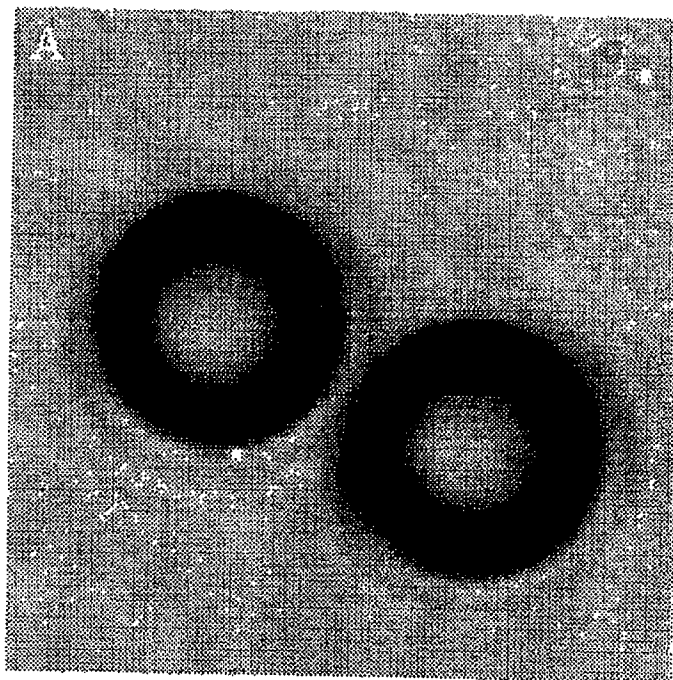


Figure 4. Diffraction-limited image of 2 μm polystyrene spheres (brightfield).

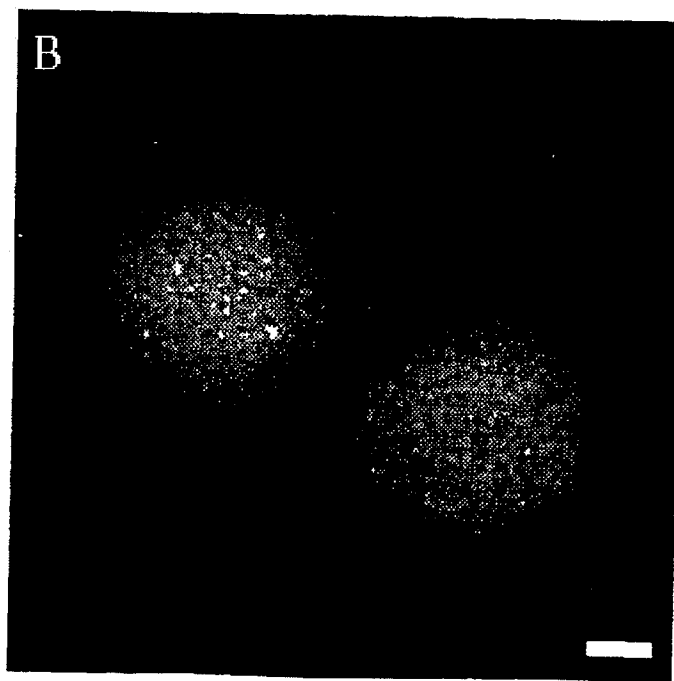


Figure 5. Raman image at 992 cm^{-1} of the same sample. Note 500 nm size bar shown for reference.

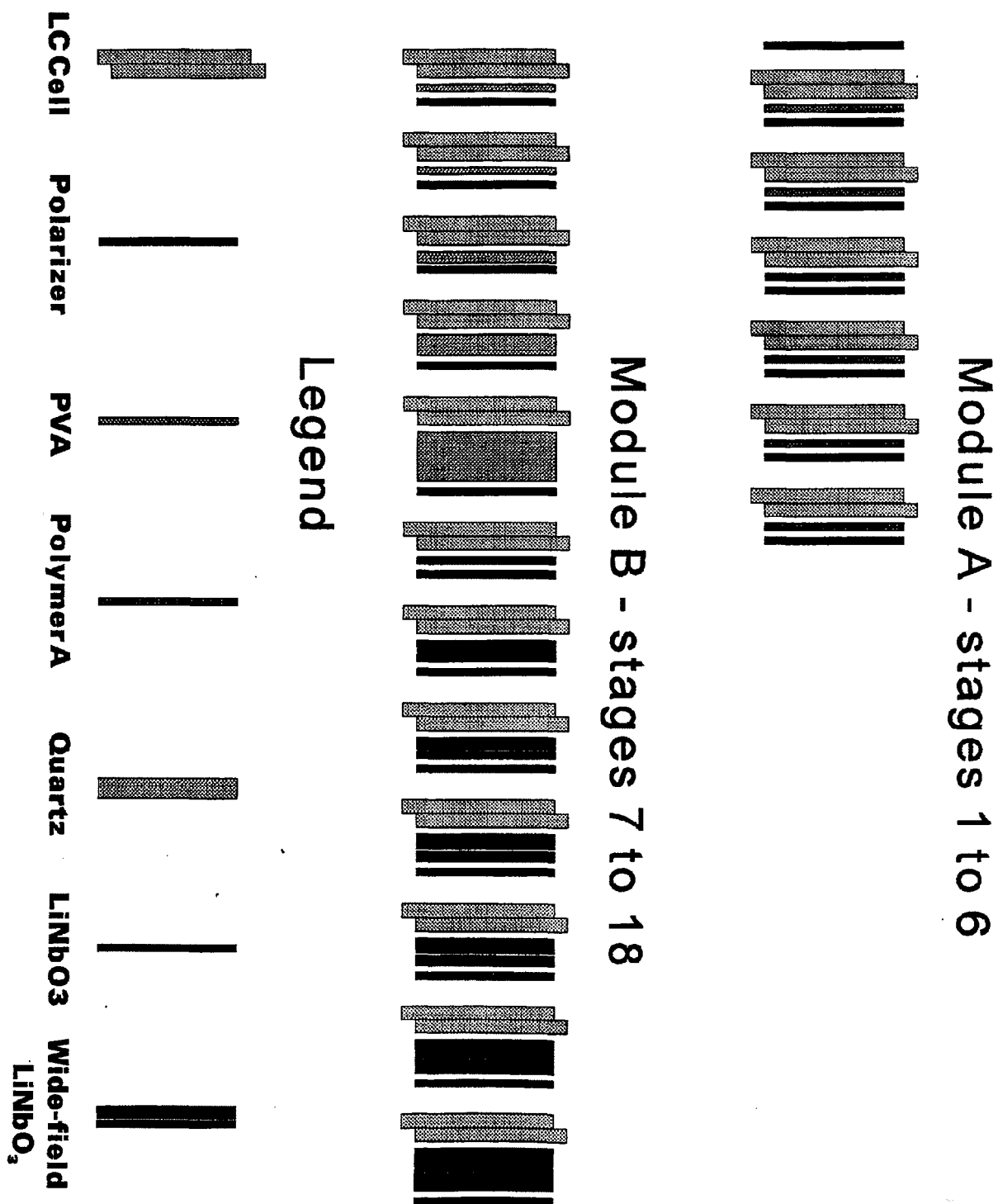


Figure 6. Diagram of the optical components of the Raman LCTF filter. Thicknesses of components have been increased for clarity (not to scale).

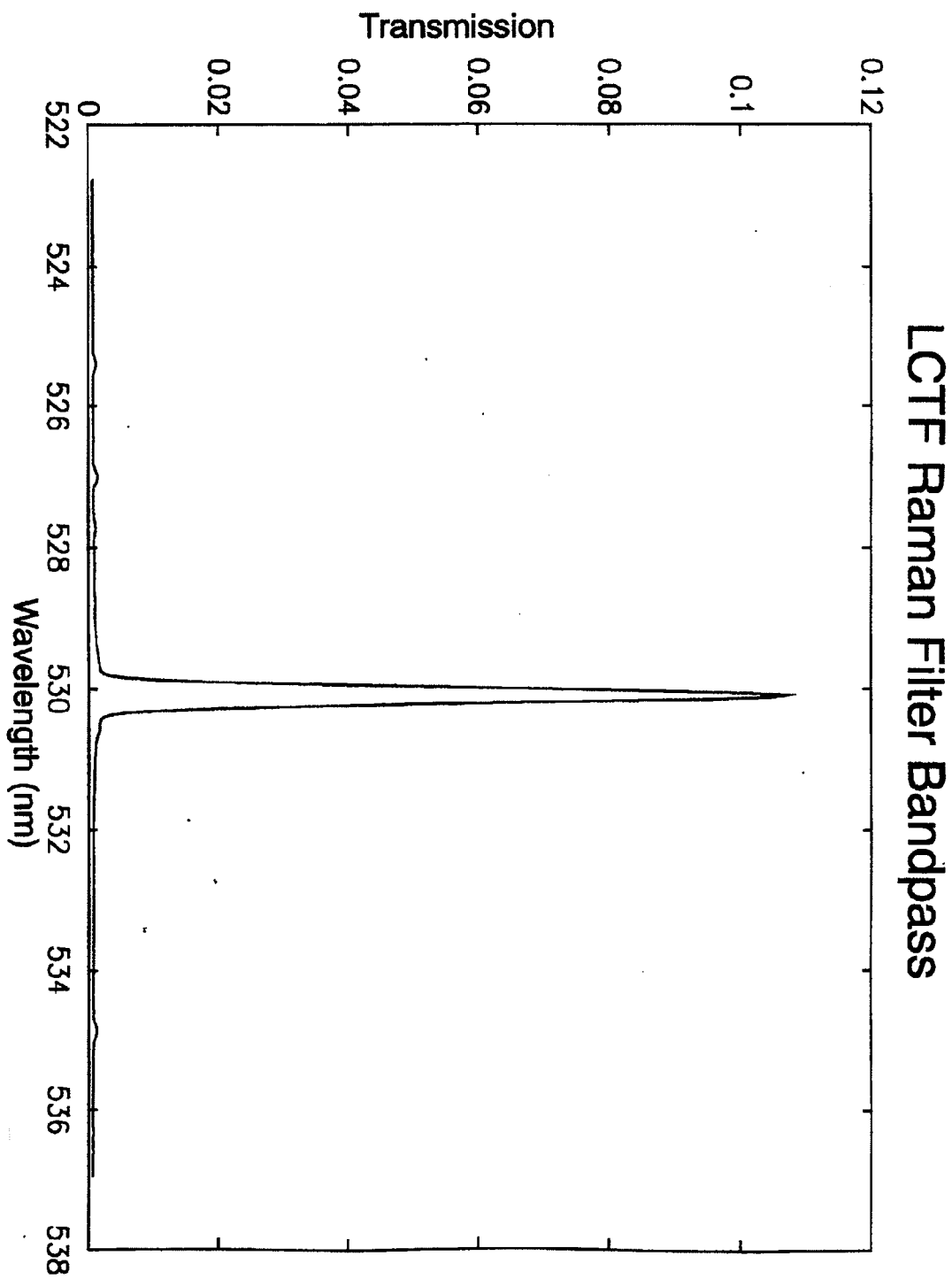


Figure 7. Passband of the prototype LCTF Raman filter, tuned to 532 nm. FWHM of the filter (corrected for the resolution of the test spectrometer) is 0.20 nm.

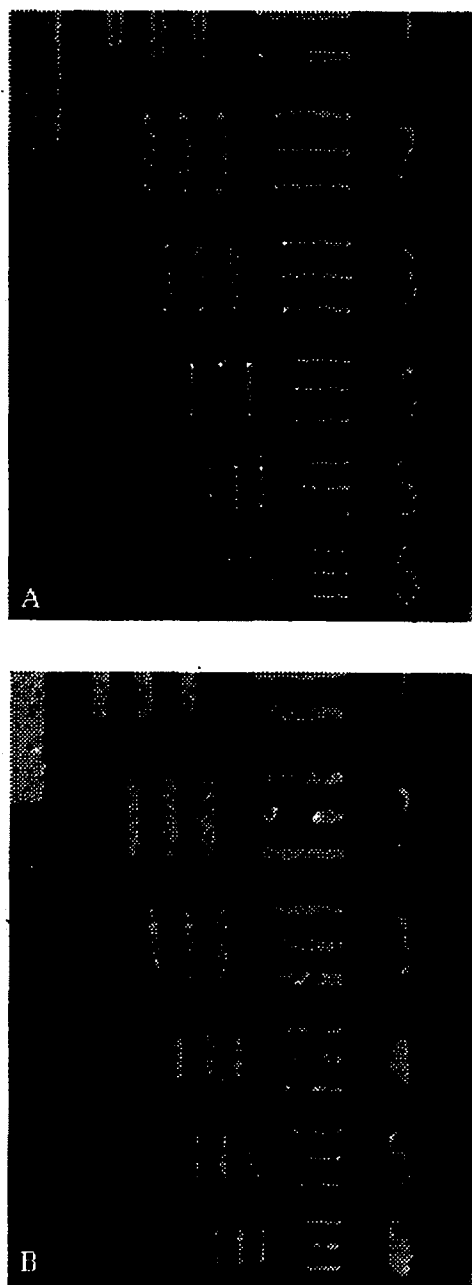


Figure 8. Images of a 1951 USAF resolution target without (top) and with (bottom) the LCTF Raman filter. Center spacing of finest grid is 4.3 μm . No degradation is apparent in the digital images.

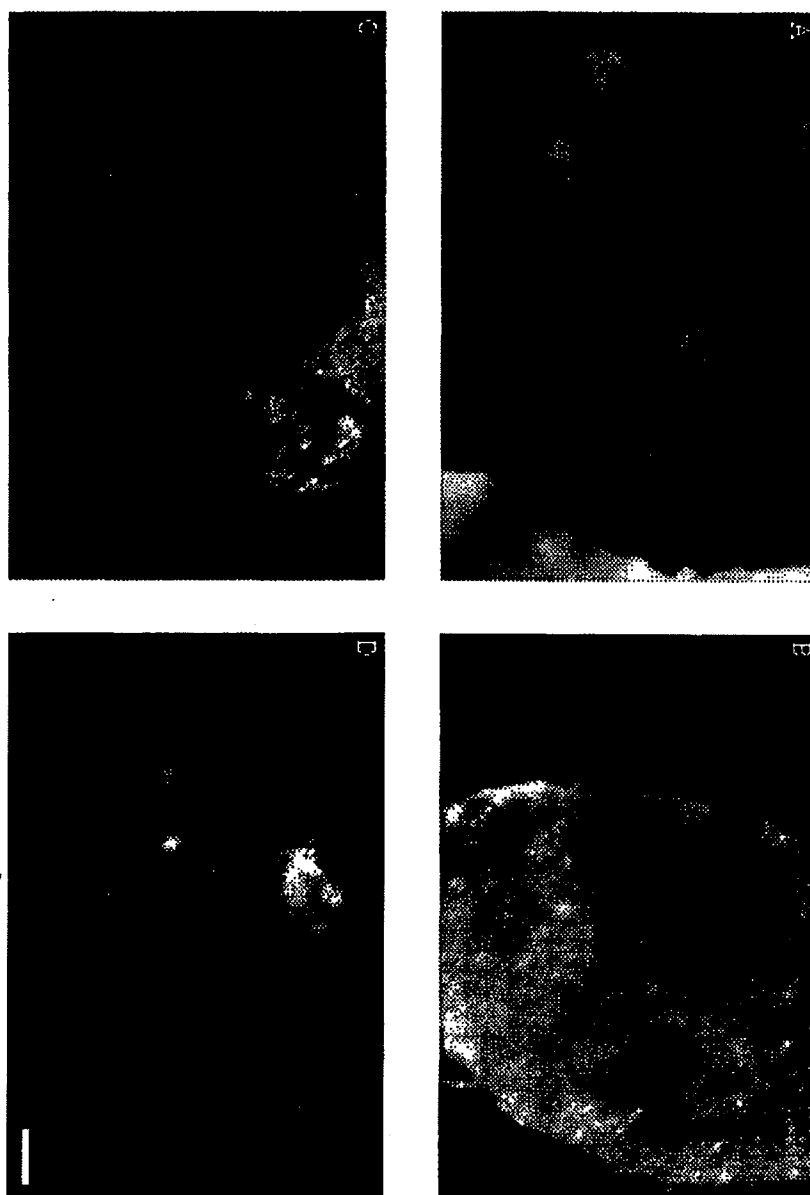


Figure 9. Images of corrosion sample in (A) brightfield; (B) the 1057 cm^{-1} stretch band of NO_3^- ; (C) the 604 cm^{-1} band of TiO_2 ; and, (D) the 797 cm^{-1} band of WO_3 , showing chemical specificity as the filter selects each analyte in turn.

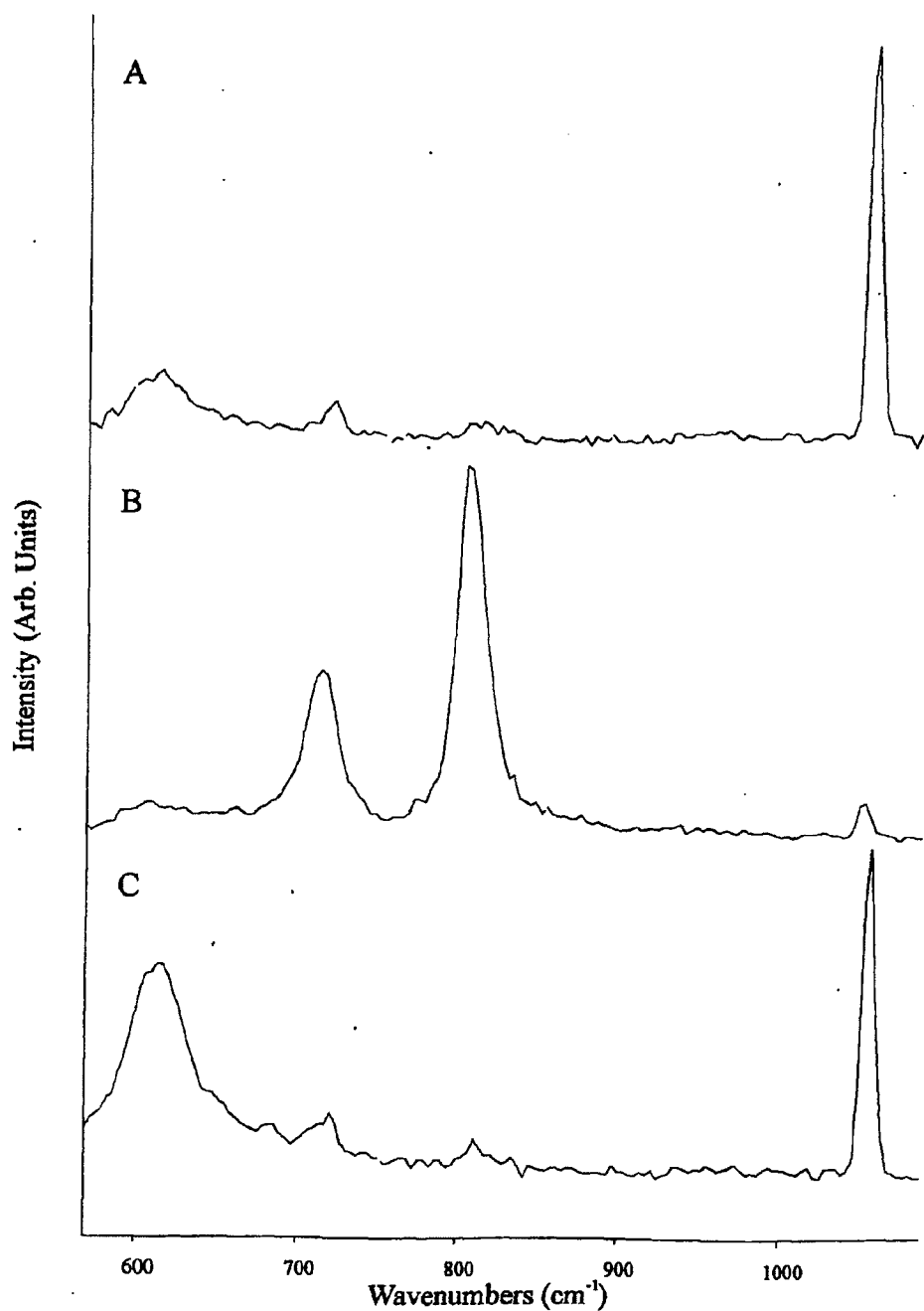


Figure 10. Spectra from individual pixels of Figure 9, showing (A) KNO₃; (B) WO₃; (C) TiO₂. Full spectra exist for each point in the sample.

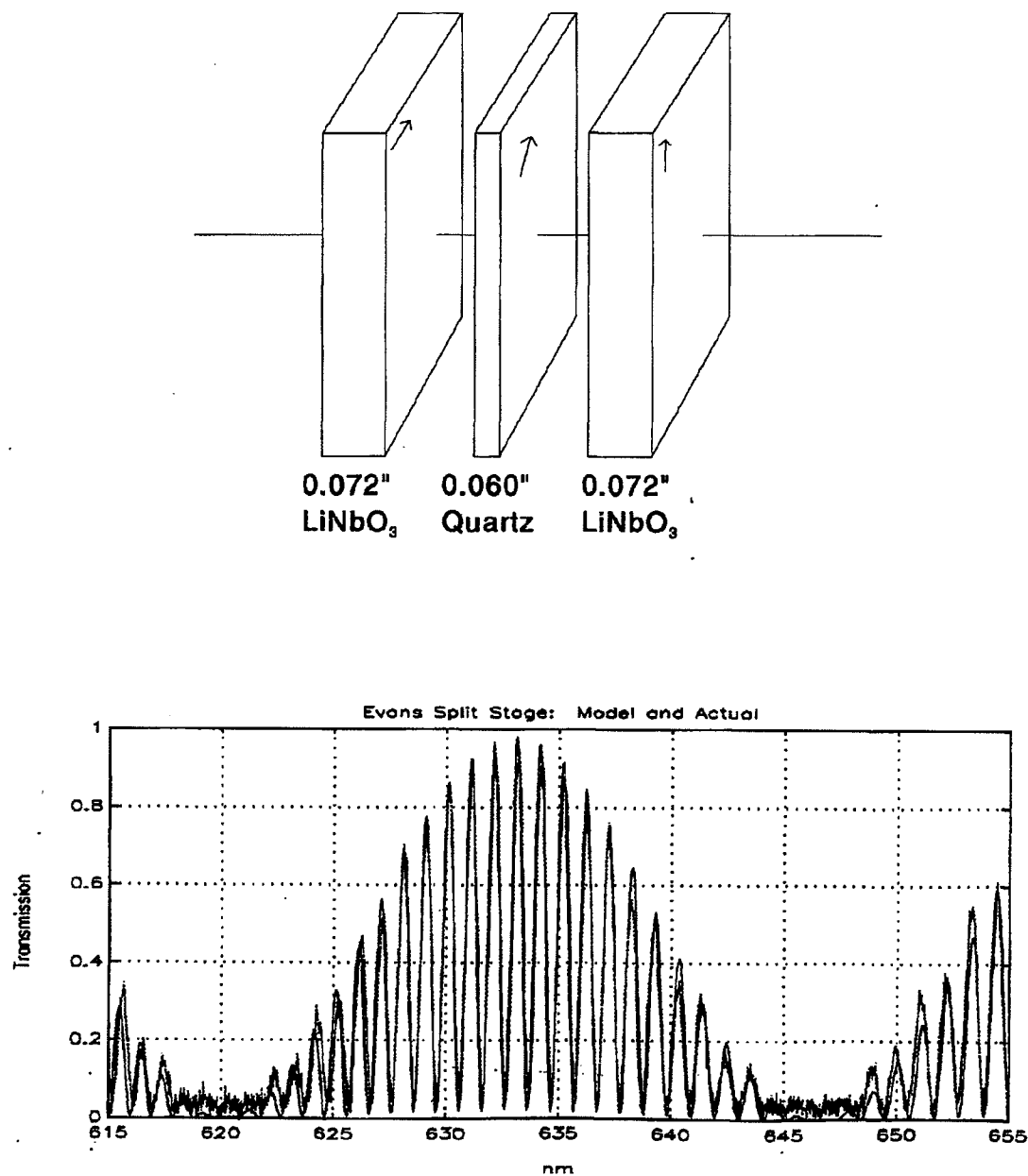


Figure 11. Above is pictured a diagram of an Evans stage, along with model and actual data from a test piece. The high frequency spectral resolution is due to the LiNbO₃, while the low-frequency envelope is due to the quartz. It can replace two simple stages in a Lyot filter.

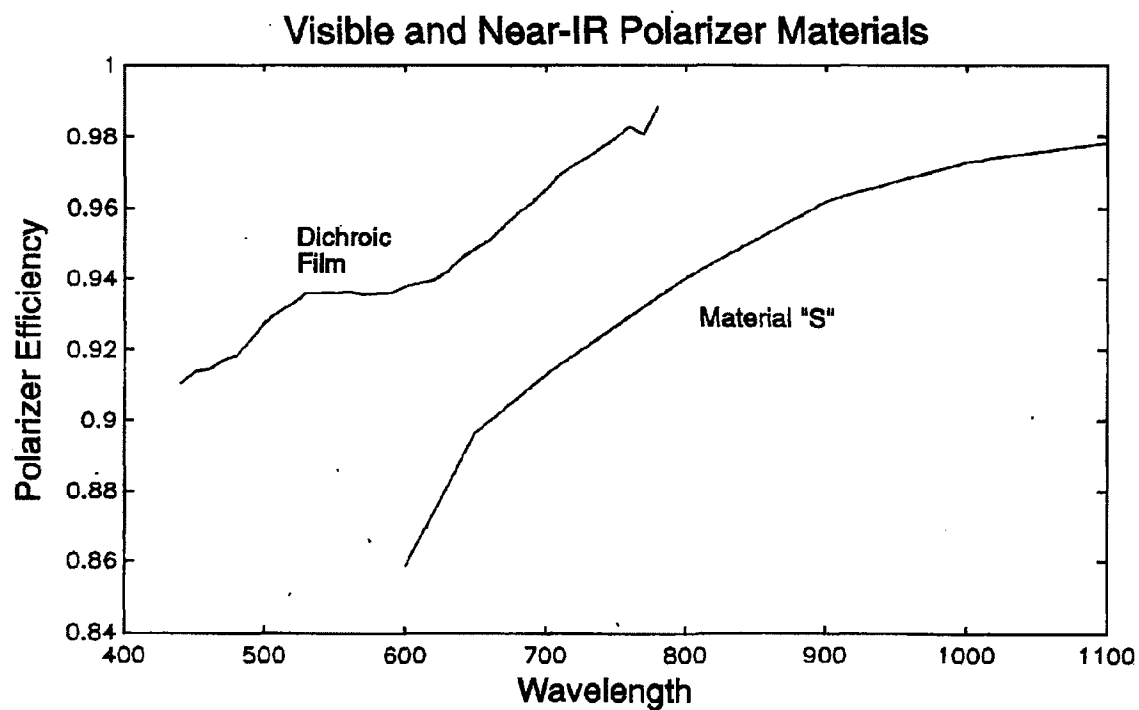


Figure 12. Transmission of single layers of visible and near-IR polarizer material proposed for use in second-generation LCTF red/IR devices. All transmission data are net of Fresnel losses.

EXHIBIT L

**NATIONAL SCIENCE FOUNDATION
SBIR PHASE II PROPOSAL COVER PAGE
Small Business Innovation Research**

TOPIC NO. 2	SUBTOPIC LETTER (If any) B	TOPIC TITLE Chemistry	
PROPOSAL TITLE High-Definition Raman Imaging Microscope			
NAME OF PROPOSING SMALL BUSINESS CONCERN Cambridge Research & Instrumentation Inc.		ADDRESS (Including ZIP CODE) 21 Erie Street Cambridge, MA 02139	
EMPLOYER IDENTIFICATION NUMBER (EIN) OR TAXPAYER IDENTIFICATION NUMBER (TIN) 04-2868535			
REQUESTED AMOUNT \$ 300,000	PROPOSED DURATION 24 months	PERIOD OF PERFORMANCE 8/1/97 - 7/31/99	
THE SMALL BUSINESS CONCERN CERTIFIES THAT:			Y/N
1. It is a small business as defined in the SBIR Phase I - Phase II Instruction Guide.			Y
2. It qualifies as a socially and economically disadvantaged business as defined in SBIR Phase I - Phase II Instruction Guide. FOR STATISTICAL PURPOSES ONLY			N
3. It qualifies as a women-owned business as defined in SBIR Phase I - Phase II Instruction Guide. FOR STATISTICAL PURPOSES ONLY			N
4. NSF is the only Federal agency that has received this proposal (or an overlapping or equivalent proposal) from the small business concern. If No, you must disclose overlapping or equivalent proposals and awards as required by SBIR Phase I - Phase II Instruction Guide. (See Section Part III, Subsection D.1(II))			Y
5. A minimum of one-half of the research will be performed by this firm in Phase II.			Y
6. The primary employment of the principal investigator will be with this firm at the time of award and during the conduct of the research.			Y
7. It will permit the government to disclose the title and technical abstract page, plus the name, address and telephone number of a corporate official if the proposal does not result in an award to parties who may be interested in contacting you further information or possible investment.			Y
8. It will comply with the provisions of the Civil Rights Act of 1964 (P.L. 88-352) and the regulations pursuant thereto.			Y
PRINCIPAL INVESTIGATOR/PROJECT DIRECTOR			
NAME Peter J. Miller		TITLE Staff Scientist	
SOCIAL SECURITY NO. 195-44-3236		TELEPHONE NO. (617) 491-2627	
E-MAIL ADDRESS pjmiller@world.std.com		FAX NO. (617) 864-3730	
NAME Peter V. Foukal		TITLE President	TELEPHONE NO. (617) 491-2627
COMPANY OFFICER (FOR BUSINESS AND FINANCIAL MATTERS)			
OTHER INFORMATION			
PRESIDENT'S NAME Peter V. Foukal	YEAR FIRM FOUNDED 1985	NUMBER OF EMPLOYEES AVERAGE PREVIOUS 12 MO.: 16 CURRENTLY: 18	

PROPRIETARY NOTICE See Part III, Subsection D.1 for instructions concerning proprietary information.
(Check here ☐ if proposal contains proprietary information.)

NOTE: The signed Certification Page must be included immediately following this Cover Page with the original copy of the proposal only.

Proposal Page No. 1

NSF FORM 1207 (SBIR) (5/96)

B-1

CRI000665

**National Science Foundation
Small Business Innovation Research Program**

PROJECT SUMMARY

NSF PROPOSAL NO.
DMI-9560600

NAME OF FIRM		Cambridge Research & Instrumentation, Inc.	
ADDRESS		21 Erie Street Cambridge, MA 02139	
PRINCIPAL INVESTIGATOR (NAME AND TITLE)			
Peter J. Miller, Staff Scientist			
TITLE OF PROJECT			
High-Definition Raman Imaging Microscope			
TOPIC TITLE		TOPIC NUMBER AND SUBTOPIC LETTER	
Chemistry		2.B	
<p align="center">PROJECT SUMMARY</p> <p>Project Summary</p> <p>This Small Business Innovation Research Phase II project will build on the successful imaging Raman instrument demonstrated in Phase I, and produce second-generation instruments and software which fully exploit the potential of this new technique. In Phase I, chemical species were imaged using a narrowband liquid crystal tunable filter (LCTF) and CCD camera integrated into a Raman microscope. Diffraction-limited spatial images were obtained with complete (and spatially independent) Raman spectra at each pixel in the image, yielding an image cube with two spatial axes and one spectral axis. The novel LCTF approach renders high-definition Raman imaging feasible for the first time, and brings the power and specificity inherent in Raman spectral analysis to the imaging of chemical species.</p> <p>In Phase II, key improvements will be made: transmission will be doubled (or more) based on a high-efficiency design identified in Phase I, and the long-wavelength limit will be extended from the present 700 nm to 1050 nm. Such an LCTF appears to offer near-revolutionary benefits in certain applications including semiconductor analysis, biomedical imaging, and pharmaceutical research. Performance in these areas will be assessed experimentally in Phase II. Finally, data analysis methods will be developed to extract chemical species information from the large, spatially resolved datasets involved.</p> <p>Commercial sales of LCTF Raman imaging systems are estimated at \$21M over the next 5 years, for research, semiconductor, diamond, pharmaceutical, and power generation industries.</p>			
Key Words to Identify Research or Technology (8 maximum)			
Raman, imaging, liquid crystal tunable filter			

D. Synopsis of Phase I Research Results

D.1 Overview

During Phase I, a liquid crystal tunable filter (LCTF) was designed, built, and characterized for use in Raman chemical imaging. The filter has a design bandwidth of 8 cm^{-1} and a tuning range of 500 - 650 nm, or 4600 cm^{-1} . Unlike other tunable elements for Raman imaging, the LCTF is free of optical distortions, spectral leakage, or image shift with tuning.

The actual filter performance met all model predictions, and was successfully integrated into an optical microscope employing a 514.5 nm Ar^{++} laser source coupled via fiber-optics to provide uniform illumination through infinity-corrected microscope optics. Raman images were collected using a cooled CCD camera. Sample spectra obtained through the LCTF are identical with spectra of the same samples acquired with a conventional (non-imaging) dispersive spectrometer employing CCD multichannel detection. Images collected with the LCTF Raman chemical imaging system provide essentially diffraction-limited resolution, as verified with USAF test targets and quantitative CTF analysis. Raman images of model systems clearly surpass all previous Raman imaging data.

The LCTF Raman system is robust, not prone to thermal drift, and promises to usher in a new era of practical Raman imaging. It is fair to state that LCTFs define the state-of-the-art in Raman imaging technology and have the potential to revolutionize Raman microscopy. However, the devices produced to date represent only the first generation of LCTF Raman development. Outstanding LCTF Raman issues are to improve throughput, and to develop improved filters for the red/near-IR range appropriate for use with He-Ne, Kr^{++} or laser diode sources; these issues will be addressed in Phase II.

Compared to existing, non-imaging systems, the LCTF Raman system adds the powerful ability to image chemical species in heterogeneous samples, and to map out spatial distributions and features. This is a key benefit in working with real-world samples, which tend to be heterogeneous on the spatial scales of interest.

D.2 Phase I objectives

The Objectives listed in the Phase I proposal were:

- i) To use existing computer models to generate a tunable Lyot filter design optimized for Raman spectroscopy;
- ii) To study the integration of such a filter into a microscope imaging system, including optical path, data acquisition, and camera requirements;
- iii) To construct a fully imaging prototype filter according to this design, with resolution of 10 cm^{-1} or better, tunable over a range of 2500 cm^{-1} ;

- iv) To characterize this filter for its spectral properties, including peak transmission, bandwidth, out-of-band rejection, and tuning range;
- v) To test this filter to obtain true two-dimensional Raman spectroscopy images of test samples;
- vi) To prepare a Phase I report describing the results.

D.3 Phase I results

The Phase I results are now presented for each of these objectives in turn.

i) Computer model of Lyot filter for Raman spectroscopy

The filter was designed with a computer model based on the Jones calculus of polarization state. Measured values of retardance and dispersion are used for liquid crystal and mineral crystal elements. We chose x-cut LiNbO₃ retarders for the high-order Lyot stages, and quartz for the lower-order stages. A total of 18 elements were employed, each of which is continuously tunable by means of liquid crystal variable retarder elements. Modeled passband and out-of-band rejection are shown in Figure 1.

ii) Integration with microscope

The system was constructed around an Olympus BHS-2 microscope, as shown in Figure 2. Epi-illumination is provided by an Ar⁺⁺ laser (Coherent CR-3) coupled through a fiber before impinging on a high-performance dielectric notch bandpass filter (OCA Microplasma) to reject the silica Raman bands developed within the fiber. The conditioned laser light fills the back aperture of the microscope objective and excites the sample. Raman scatter is collected by the same infinity-corrected objective and presented to two holographic notch filters which remove laser back-scatter. The Raman signal then passes through the LCTF and is imaged onto a cooled CCD camera (Princeton Instruments TE-CCD-768-k/2). Raman light is also coupled efficiently via a swing-away mirror to a fiber-optic bundle, prior to passing through the LCTF. The Raman fiber-optic is coupled to a dispersive Raman spectrograph employing multichannel CCD detection and allows the system to perform as an efficient confocal Raman microprobe.

iii) Filter construction

The LCTF was built using similar techniques to those developed for narrowband fluorescence filters. The only significant issue was a difficulty in obtaining the LiNbO₃ retarders needed to achieve a narrow passband. These parts have a large aspect ratio (up to 100:1), and the surfaces must be parallel to 5" of arc. We worked with a vendor to identify a double-sided polishing process which produced these parts with high yield. Subsequent filter construction proceeded smoothly.

iv) Filter characterization

We tested the LCTF for bandpass, transmission, out-of-band rejection, free spectral range, and tuning accuracy using a 0.5m spectrometer. All

were in good agreement with model predictions. The bandpass is 7.6 cm^{-1} and is free of sidebands; transmission ranges from 6.7 to 16.3 percent; rejection is $>10^4:1$ for out-of-band light; the filter is tunable over a range of 4600 cm^{-1} , in milliseconds, with no moving parts. Repeatability is 0.38 cm^{-1} over this range.

v) Raman imaging of test samples

Figure 3a shows the spectrum of a polystyrene microsphere, taken with the LCTF by tuning it sequentially to various wavelengths and recording the image intensity; Figure 3b shows a spectrum of the same samples taken with a Raman microprobe and a dispersive spectrometer. Note the agreement of spectral features and relative intensities in the two Figures, indicating excellent spectral performance by the LCTF.

Figure 4 shows a brightfield image of the 2μ microspheres, taken with a 100x microscope objective, which demonstrates diffraction-limited spatial resolution. Airy rings are visible in this image, taken through the LCTF. A Raman image at 992 cm^{-1} is shown as Figure 5, with a 500 nm size bar shown for reference. The quality of this image is unmatched in Raman imaging.

D.4 Identification and Significance of the Problem or Opportunity

Compared to existing, non-imaging systems, the Raman LCTF system adds the powerful ability to visualize the distribution (morphology and architecture) of chemical species in heterogeneous samples with molecular compositional specificity. Raman images can be collected rapidly, non-invasively, with limited or no sample preparation, at high spatial resolution ($< 250 \text{ nm}$) and with high fidelity where the number of image pixels is limited by the number of pixels on the CCD detector. Most importantly, every image pixel has associated with it a Raman spectrum whose quality is identical to that obtained with conventional non-imaging spectrometers. These key benefits make Raman imaging practical for the analysis of real-world samples, which are chemically heterogeneous on the spatial scales of interest.

For many samples, unique, well-resolved Raman spectral bands of interest are often known, or are readily identified by Raman microspectroscopy. The LCTF Raman chemical imaging measurement then consists of identifying the presence and/or location of analyte species in a sample by imaging at the characteristic analyte Raman spectral bands. In general, it is not necessary to have a complete Raman spectrum at each image pixel in order to characterize sample chemistry and morphology. This is due in part to the intrinsic redundancy of a typical Raman spectrum. Several regions of the spectrum can be used to generate analyte-specific image contrast. For well-characterized samples that require a limited number of spectral channels for analysis of chemical content, but exhibit complex sample morphology, the LCTF approach is clearly superior to competitive techniques because of the inherent efficiency of analyzing all spatial channels simultaneously in a massively parallel fashion.

Present practice is to use non-imaging systems such as a scanned microspot, which yield complete spectral data but limited (or inefficient) collection of

spatial data. Use of a Raman LCTF system is ideal for these cases, and yields the desired data set, which was not previously practical to obtain. Since the hardware required is similar to that used in standard microspot work, one expects that a Raman LCTF system would also include a conventional fiber feed to a dispersive spectrometer, to provide standard spectral data along with the new spectral imaging capability.

For complex samples that are not well-characterized, past practice was to collect high resolution Raman spectra at a limited number of sampling points (pixels) using laser point scanning or line scanning Raman microprobes. Again, these microprobes provided rich spectral data but inefficient collection of spatial data. For example, point scanning would involve focusing the laser to a small spot ($\sim 1 \mu\text{m}$ diameter) on a sample and rastering it in the X and Y dimensions to construct a Raman image. If it required 1 second to acquire each point spectrum, it would take over 3 days to map a 512×512 pixel image. Of course, each image pixel would contain a complete Raman spectrum.

Because the requisite sample acquisition time is impractical, point scanning Raman imaging has not flourished despite having been commercially available from a variety of instrument manufacturers since the mid 1970's. With the development of the LCTF Raman system, it is now practical to collect simultaneously high spatial/spectral resolution data sets of complex unknown materials having millions of pixels. The LCTF Raman imaging system is the only way to produce such a data set at present.

E. Phase II Research Objectives

The Phase II Objectives are the following:

- i) to utilize improved designs to improve the transmission of Raman LCTF filters, resulting in a value at least twice that of the Phase I prototype;
- ii) to develop a near-IR (NIR) version of the Raman LCTF which extends the long-wavelength operating limit from the present value of 700 nm to a minimum of 1050 nm;
- iii) to construct and characterize a minimum of one visible-range and one NIR-range Raman LCTF which incorporate these improvements;
- iv) to assess experimentally the benefits of Raman LCTF imaging in key areas including semiconductor, biomedical, and pharmaceutical measurements;
- v) to make at least one of these LCTF instruments available to beta-site researchers for high-definition Raman imaging, on a revolving basis;

- vi) to develop data analysis methods which exploit the newly-available imaging spectroscopic information, and which render the large data sets tractable;

F. Phase II Research Plan

The Research plan follows directly from the Objectives above, and is discussed for each objective in turn.

- i) to utilize improved designs to improve the transmission of Raman LCTF filters, resulting in a value at least twice that of the Phase I prototype;

The two main sources of optical loss in the Phase I prototype are absorption in the polarizers and imperfect waveplate action arising from the use of simple $\lambda/2$ plates to construct the wide-field retarder stages. The former term may be nearly halved, and the latter eliminated completely, by revising the filter high-order filter stages from Lyot's first-type wide-field design to the Evans split-element design¹ as described below. This will yield an improved filter transmission ranging from 1.55 - 3.1 times that of the Phase I prototype, depending on wavelength. It is believed that such a filter, when built, will be the first tunable filter ever constructed using the Evans design.

The prototype is a tunable Lyot design, consisting of an 18-stage filter where each stage comprises a fixed quartz or LiNbO_3 fixed retarder; a tunable liquid crystal waveplate; and a linear polarizer. In all, the light passes through 19 polarizer elements, each of which has a transmission of ≈ 0.94 , and 18 liquid crystal cells, each with a transmission of 0.98. So, cell and polarizer losses set an upper limit to the filter transmission of

$$T_{\text{upper limit}} = (0.94^{19}) \times (0.98^{18}) \approx 0.20, \quad [\text{Eq. 1}]$$

or 20 percent. Actual peak transmission was observed to be 16 percent at 600 nm, indicating some additional loss due to factors such as tuning error in the liquid crystal elements and absorption in the retarders and epoxies.

Transmission at other wavelengths was lower, even after allowing for the wavelength-dependent nature of the polarizer and cell losses. This is because simple (non-achromatic) $\lambda/2$ waveplates were used in the wide-field LiNbO_3 stages. There were five such waveplates, made of polycarbonate film and tuned for best operation at 610 nm. Over the LCTF tuning range 500 - 700 nm, the efficiency of polarization conversion for these five elements in series ranges from 0.4 - 1.0. Combined with the polarizer and cell losses, this results in an overall transmission ranging from 8 - 20 percent, while actual values for the Phase I prototype ranged from approximately 7 to 16 percent, mirroring the range anticipated for this mechanism.

The 'split-element' design of Evans cuts the number of polarizers in half, plus one, reducing this loss term significantly. Evans stages are used

instead of the Lyot wide-field retarder stages, eliminating the $\lambda/2$ waveplates and their associated losses as well. The Evans design is illustrated in Figure 6: a high-order fixed retarder of thickness D and retardance R_h is constructed as two elements of thickness $D/2$, with their fast and slow axes crossed, and a low-order retarder of retardance R_l is interposed with its fast axis at 45° to that of the $D/2$ elements. Each retarder has an associated liquid crystal tuning element. Such an assembly, placed between suitably oriented crossed polarizers, has a transmission of

$$T(\lambda) = \sin^2(\pi R_l / \lambda) \cdot \sin^2(\pi R_h / \lambda), \quad [\text{Eq. 2}]$$

for ideal polarizers with neither loss or leakage.

Again for ideal polarizers, the transmission of a single Lyot stage with retardance R between crossed polarizers is:

$$T(\lambda) = \sin^2(\pi R / \lambda), \quad [\text{Eq. 3}]$$

so an Evans split-element stage is equivalent in its spectral structure to two Lyot stages. By constructing the LCTF as groups of Evans split stages, one collapses an N -stage Lyot filter into $N/2$ Evans stages, and reduces the number of polarizers by $N/2$.

Note that the number of liquid crystal tuning elements increases, since both of the $D/2$ half-elements in an Evans stage must be actively tuned, as well as the R_l element, for a total of three tuning elements per Evans stage. The increase in liquid crystal elements is equal to the decrease in polarizers. However, the loss per polarizer is much higher than that of a liquid crystal cell, so the result is an increase in efficiency.

The Evans design offers a 55% improvement in throughput relative to the Phase I prototype, based purely on absorptive losses, and an additional improvement of 100% or more by eliminating the wide-field retarders and the attendant $\lambda/2$ waveplate chromatic error. In all, a transmission of 24.8% is anticipated, compared with the 6.7% - 16% of the Phase I prototype.

A single Evans stage was built during Phase I to confirm feasibility of construction, and it performed to predictions as shown in Figure 7. Such a design requires tighter tolerancing of the liquid crystal elements, compared to a Lyot design: the permissible error in the liquid crystal elements which tune the $D/2$ retarders are halved, as errors in either element contribute to wavelength error for the stage. Also, the extinction of the stage is limited to a level given by the expression

$$T_{\min} = \sin^2(\pi(\delta R)/\lambda) \quad [\text{Eq. 4}]$$

for the minima corresponding to the term $\sin^2(\pi R_l/\lambda)$ in Equation [2]. This is true even for ideal polarizers: the R_l minimum occurs because the retardance of the two $D/2$ elements subtracts and cancels to produce a minimum; if they differ in retardance by δR , the cancellation is imperfect and the depth of the minimum is reduced.

The liquid crystal retarders constructed for this work are readily tuned with an accuracy of ± 6 nm anywhere within their operating range. This results in a worst-case δR of 12 nm, for an acceptably low T_{\min} of 0.7% for the stage. Recall that the filter achieves a high rejection of out-of-band light not through extreme contrast in any single stage, but through the concerted action of several stages with low-to-moderate contrast. Models which use the Jones calculus rather than the simplified equations [2] and [3] confirm that overall filter leakage will not be unacceptably degraded through use of the Evans design.

Similarly, while better uniformity across the aperture on the fixed D/2 retarders is desirable, present materials appear adequate for use in an Evans design. The Phase I parts have ± 9 nm variation across their aperture; the majority of this is radial due to spherical figure error in the pieces. This has only a slight impact on passband accuracy, and causes a center-to-edge shift in passband center of 0.24 cm^{-1} . Considering leakage, one can see that figure errors which are common to both D/2 parts, such as matched spherical power, will cancel when the retardance of the two D/2 elements subtracts (as occurs at the R_1 minima). So, improving the figure of these components will increase passband uniformity across the aperture somewhat, but will not have a significant effect on leakage. To the extent it is achieved, this improvement will occur through using the expanded schedule of the Phase II effort. During Phase I, there was insufficient time to iterate with the vendor and reduce the figure error in what were already quite acceptable pieces.

- ii) to develop a near-IR (NIR) version of the Raman LCTF which extends the long-wavelength operating limit from the present value of 700 nm to a minimum of 1050 nm;

The P.I. has developed a high-efficiency NIR polarizer during a previous NASA project directed towards remote sensing projects. It is a special version of a commercially-available polarizer, optimized for the NIR range extending to the end of silicon CCD response at 1050 nm. While conventional sheet-polarizer is heavily dyed and has relatively low transmission as a result, the transmission of this material is greater than 90% at all NIR wavelengths, and above 94% over the range 800 - 1050 nm. It is thus ideal for use with laser diode sources at 780 nm and longer. Data for this material and for a standard material are given in Figure 7.

Design of a high-performance NIR Raman LCTF will be based on the Evans design described above, to minimize the number of polarizers and their absorptive loss. In this spectral range, the liquid crystal tuning elements exhibit extremely high transmission (99% at 850), so the requirement of an Evans design for a larger number of these parts does not reduce LCTF performance greatly. Acceptable tuning error, retarder error, and optical figure error all scale directly with the wavelength, and so are more easily met in the NIR than the visible; at the same time, the bandwidth of an LCTF is constant (in cm^{-1}) with wavelength. That is, except for dispersion, the bandwidth of an NIR filter will be the same as an identical filter constructed for use in the visible. Accordingly, a design with resolution of approximately 8 wavenumbers

is contemplated, using the same LiNbO_3 retarder components and dimensions as in the Phase I prototype.

- iii) to construct and characterize a minimum of one visible-range and one NIR-range Raman LCTF which incorporate these improvements;

Techniques have been developed at CRI over the past eight years for the manufacture of the liquid crystal cells required for this work. Similarly, the assembly of these components together with polarizers, retarders, and precision windows into completed LCTFs has become highly advanced through the commercial sale of these instruments. With the introduction of a 'ruggedized' construction last year, these filters can survive temperatures from -200C to +60C, and humidity of up to 80%. The electronics and techniques for tuning the liquid crystal retarder elements, based on an active capacitive sensing method, are also well-established. Software to calculate the required amount of liquid crystal tuning action in each stage, accounting for dispersion and thermal drift in the retarder elements, has been run successfully for four years. These areas are not seen as involving risk or needing further development during the Phase II effort, either for the visible or the NIR filter.

The two unusual requirements of Raman LCTF construction are to obtain high-order LiNbO_3 retarders, and to make a large number of spectral measurements at extremely high resolution. Based on the Phase I work, obtaining the retarders is practical although we will work to improve the figure slightly. Turning to the need for spectrometry, this is felt first during construction, when the quartz and LiNbO_3 retarders are scanned to provide a spectral calibration scale, but it also occurs when a filter has been completed, in order to measure its performance. At present, this is done using a Spex 0.5M scanning spectrometer with a chopper, lock-in amplifier and computerized data acquisition. This takes a great deal of time: a single spectral scan contains 1000 - 1500 points and requires a 1s integration time per point to get sufficient signal:noise ratio. Aside from the inconvenience, it is difficult to maintain retarders at a steady temperature in air for the required duration (20 minutes). Characterizing the leakage of an LCTF as it is scanned across its range requires one hundred such scans, or 33 hours of continuous scanning. Many important measurements are simply impractical as a result.

In Phase II, the scanning spectrometer will be replaced with a high resolution transmissive holographic instrument that covers the entire spectral range (500 - 750 nm for the visible filter, or 650 - 1050 nm for the NIR filter) across the active area of a 1" CCD detector. A resolution of 10 cm^{-1} per pixel is quite sufficient for the characterization of the LiNbO_3 retarders and other components, as these items have periodic, sinusoidal spectra; determination of the peaks can be fitted to considerably less than one pixel. Only one measurement, that of detailed bandpass shape, requires higher resolution. Note, however, that it requires only a small spectral range to be scanned, so it is quite practical to perform this on the scanning, rather than CCD-based, instrument.

A CCD-based instrument will provide a spectrum in approximately 2-3 seconds, making it possible to characterize the LCTF much more completely. Also, debugging any problem in the filters will be enormously easier with such an instrument. Characterization will include measurements of peak transmission, bandpass shape, leakage of out-of-band light, free spectral range, and tuning accuracy, as in Phase I. Additional work in Phase II will focus on the response for off-axis rays and thermal drift measurements. Improved values for the thermal drift of $\delta n(\lambda)$ for LiNbO_3 and quartz will be sought and incorporated into the LCTF thermal drift compensation routines.

- iv) to assess experimentally the benefits of Raman LCTF imaging in key areas including semiconductor, biomedical, and pharmaceutical measurements;

Applications for a Raman imaging microscope are diverse because almost every manufactured or natural material has a unique, intrinsic Raman spectral fingerprint which can be harnessed to generate molecule-specific image contrast without performing invasive sample staining procedures. The broad applicability of Raman imaging is one of its many attractive features.

During the Phase II investigation, we will focus on a limited number of materials and applications. The top candidates will be selected, in part, based on the suitability of the candidate material for Raman analysis, as well as the economic significance of the application. A material is defined as being suitable if it evidences molecular compositional heterogeneity on a spatial scale that can be sampled with an optical microscope. In addition, the sample must not exhibit fluorescence that exceeds the dynamic range of the detector during the Raman imaging experiment. We have further selected target applications that represent sizable markets, in the likely event that benefits of LCTF Raman imaging are identified and demonstrated. Finally, the selection process is guided by the access to technical personnel within target organizations that recognize already the potential of LCTF Raman imaging. Dr. Treado has identified an extensive user base that have expressed considerable interest in the technology; these users have made real world samples available to the University of Pittsburgh so that a feasibility assessment can take place.

One very important application is in the non-invasive characterization of silicon semiconductors. Here, one would use LCTF Raman imaging to visualize the effect of ion implantation and thermal annealing on stress and polycrystalline distribution in the silicon lattice. The benefits of LCTF Raman imaging for this purpose can be assessed by comparing the quality and cost effectiveness of information collected by Raman imaging analysis with the information collected by competitive techniques. For example, lattice disorder and defects are currently monitored in silicon semiconductors using laser-scanning photoluminescence techniques. While this technique is sensitive to localized defects in semiconductors, photoluminescence is relatively nonspecific and does not provide sufficient information on the molecular composition of defect structures, whereas Raman would provide this compositional information. In addition, the impact of a localized defect or other heterostructure implanted in the Si lattice, can be monitored by

visualizing the perturbation (stress or disorder) of the Si lattice conformation.

This has value in the semiconductor and photonics device marketplace because LCTF Raman imaging can be used for failure analysis and quality control. In fact, there is significant potential that LCTF Raman imaging can evolve into an in-line process monitoring tool to inspect potential failure sites in highly integrated Si devices. The benefit would be a non-invasive approach to monitor and reject devices at an intermediate stage of processing before many thousands of dollars are invested in manufacturing high performance integrated circuits or photonics devices (for example, CCD detectors) from these Si wafers.

Additional applications include the following:

- Raman characterization of corrosion (bio-initiated or environment-initiated) occurring at microfractures in surfaces;
- thin film and coatings characterization, including the analysis of molecular compositional and conformational heterogeneity in polymer films;
- polymer blend domain structure analysis;
- content uniformity characterization of intact pharmaceutical tablets;
- oriented polymer fiber characterization;
- non-invasive analysis of combinatorial generated systems for pharmaceutical drug development; and,
- quantitative histopathology.

An important Government application is in exobiology, specifically the search for life on Mars. NASA has expressed interest in an implementation of LCTF Raman imaging technology for a Mars lander to monitor surface mineralogy, and to screen for organic content that might suggest the past presence of life. LCTF devices have already undergone successful environmental testing for thermal/vacuum, flammability, and radiation load for such a mission². Samples provided by collaborators of Dr. Treado currently reside at the University of Pittsburgh and are available for analysis.

- v) to make at least one of these LCTF instruments available to beta-site researchers for high-definition Raman imaging, on a revolving basis;

In Phase I and to date, essentially all the imaging Raman LCTF measurements of real-world samples have been made by Dr. Patrick Treado at U/Pitt. During Phase II, at least one Raman LCTF will be made available to other beta-site researchers on a revolving basis. There are three reasons for this:

- it will provide valuable feedback from other leading Raman spectroscopists, who are perhaps more neutral in their assessment of this approach than the P.I., by virtue being disinterested in its success. Whether such feedback confirms or challenges our high expectations about the potential of the imaging LCTF Raman approach, a more complete picture of its utility will be obtained.

- it will help to identify new applications, through testing of the filter in areas related to their individual research interests. As a new tool, the Raman LCTF will prove well-suited to some tasks and ill-suited to others. To find the matches requires insight into both the applications and the technology; putting these together requires collaboration with top researchers in a variety of areas.
- it will provide a scientifically valuable validation of the Phase I work, by other members of the community.

The Raman LCTF will be made available for a period of approximately 90 days, as progress and schedules warrant. As indicated in the Project Milestones, the filters will be completed well before the end of the first year, leaving considerable time for beta-site groups to use the filter. One such beta-site is already arranged with Dr. Desari of MIT's Harrison Spectroscopy Laboratory. He has agreed to work in this capacity in the Phase II effort, and has suitable laser, microscope, imaging, and computer equipment to make use the Raman LCTF. Additional beta-site users are being solicited, and we will seek to accommodate as many as is practical during the Phase II period.

- vi) to develop data analysis methods which exploit the newly-available imaging spectroscopic information, and which render the large data sets tractable;

There is a well-developed practice of Raman spectral analysis for point or spatially non-resolved data, including feature identification, principal component analysis, and quantitation of analyte species. These provide means to answer particular questions about the sample, such as what species are present, amounts, oxidation states, and so on. Such analyses can already be conducted on a pixel-by-pixel basis for the data sets collected using the LCTF Raman approach, using existing software packages.

However, our experience during the Phase I effort indicates that, while this type of analysis remains vital with Raman imaging data, it does not tell the whole story. To harvest the newly available spatial-spectral information, one wishes to answer new questions such as: what is the spatial distribution of each species, how do locations of two species correspond, are the structures co-incident or distinct, and similar queries. The answers often need to be displayed as high-resolution images rather than numerically. So there is a need, at a minimum, to integrate the analysis with improved display; that is, to permit various spectral-derived parameters to be calculated for each pixel, and then to display the derived parameters in image form.

This requirement defines a first level of data analysis which will be implemented in Phase II as a 'toolbox' of functions in a high-level interactive programming environment such as MatLab or ENVI, which is widely used in the remote sensing community for analysis of multi-spectral image cubes with two spatial dimensions and one spectral dimension. During the Phase II effort, we will discover what data specific tools are useful, and also which are compute-efficient to apply to a large data set. For this exploratory work, the desire for rapid feedback and interactive analysis is

paramount, and exploration speed, rather than computational speed, is to be maximized. This goal would be met with a 'toolbox' approach in either of the proposed programming environments.

Based on the experience of the remote sensing community, there may also be a need for algorithms to sort through the large data sets and assess which spectral bands and features are informative, and which are not. If this is possible, it may lead to significant reduction in the size of the dataset and the processing time. Methods for this are presently used in the remote sensing community; their aptness for use in imaging Raman analysis will be assessed during Phase II. If promising, these algorithms or variants of them will form the basis of a second-level 'toolbox', to help extract the most meaning from the information which the Raman image cube provides.

G. Commercial Potential

The clearest indicators of commercial potential are: C.R.I.'s demonstrated history of successes in commercializing SBIR developments; the presence of a Phase III partner who has committed to a follow-on funding agreement to gain access to the instruments being developed; and, a commercialization plan which seeks to exploit commercially the inherent potential of the LCTF Raman technology being developed.

G.1 C.R.I.'s demonstrated success in commercializing SBIR technology
Cambridge Research and Instrumentation, Inc., (CRI, Inc.) is a small (17 permanent employees) high-tech firm founded in 1985, with strengths in electro-optics and in space physics. Projected revenues in the current year are \$3.2 M, of which about 70% is derived from commercial sales and the remainder from federal agency research contracts and grants. About 40% of the commercial sales consist of exports, primarily to Japan and W. Europe.

CRI's first (NSF SBIR-supported) product was a cryogenic absolute radiometer, for highest accuracy radiative flux measurements. The LaserRad and CryoRad-series radiometers, which sell for \$75K - 150K, are now in use at national and aerospace metrology laboratories world-wide, as primary irradiance standards. A second successful product whose development was also supported in part by NASA and NSF SBIR awards, is an electro-optic servo system, priced between \$4K - 8K, for control of laser power and removal of laser flux variations. The LPC-series stabilizers won two industrial awards in 1989, and CRI is the major world wide supplier of such systems into applications ranging from biomedical research to semi-conductor manufacturing. Cumulative sales in these two CRI products already exceed \$5M, and annual sales continue to rise.

G.2 Phase III partnership and follow-on funding

A Phase III Follow-on Funding Commitment (FOFC) has been negotiated between C.R.I. and ChemIcon in the amount of \$200,000, in return for first access to the technology being developed in Phase I and Phase II work. ChemIcon has already introduced a line of Raman microscopes based on the Phase I prototype, and have quotations pending with several customers totaling over \$300K. They anticipate significantly larger markets as the improved Phase II devices become available, and as the utility of this new approach is assessed in key industrial applications.

G.3 Commercialization Plan

The Phase III commercialization plan is attached in Appendix 2, and discusses the size of specific markets, competitive factors, patents, and other factors related to the commercial introduction of an LCTF Raman filter product.

H. Principal Investigator and Senior Personnel

PETER J. MILLER
Staff Scientist

PRINCIPAL INVESTIGATOR

Cambridge Research and Instrumentation, Inc.

Education:

1980	B.A. (Astronomy)	Williams College
1985	M.S. (Electrical Engineering)	Dartmouth College

Memberships:

American Astronomical Society
Optical Society of America

Experience:

1979	Visiting Fellow, JILA/NBS, Boulder, CO
1980-83	Staff Scientist, A.E.R., Inc., Cambridge, MA
1985	Staff Scientist; Cambridge Research and Instrumentation, Inc., Cambridge, MA

Relevant Publications, Reports, and Awards

"Liquid crystal tunable filter Raman chemical imaging", H. R. Morris, C. C. Hoyt, P. Miller, P. J. Treado, Appl. Spectroscopy 50 6, 805 (1996).

"Liquid crystal tunable filters: theory and application to spectroscopy", P. J. Miller, FACSS Annual Meeting, (1996).

"The development of a compact imaging spectrometer using liquid crystal tunable filter technology", J.A. Faust, A. Biswas, G. H. Bearman, T. Chrien, P. J. Miller, O.S.A. Annual Meeting (1996).

"Multispectral imaging with a liquid crystal tunable filter", P. Miller, SPIE Proc. 2345, in press (1994).

"Optical Retarder Having Means for Determining the Retardance of the Cell Corresponding to the Sensed Capacitance Thereof", U.S. Patent 5,247,378 (1993).

T. Chrien, C. Chovit, P. Miller, "Imaging spectrometry using a liquid crystal tunable filter", Proc. SPIE 1937, 257 (1993).

R & D 100 Winners Announcement, Research & Development, 34, 12 (1992). Awarded for the VariSpec tunable liquid crystal filter.

"Photonics Circle of Excellence Awards", Photonics Spectra, 26, 5 (1992). Awarded for the VariSpec tunable liquid crystal filter.

"Use of Tunable Liquid Crystal Filters to link Photometric and Radiometric Standards", P. Miller, Metrologia 28, 145, (1991).

"Liquid Crystal Devices and Systems Using Such Devices." P. Miller, U.S. Patent 4,848,877 (1989).

I. Consultants and Subawards

PATRICK J. TREADO

Assistant Professor	University of Pittsburgh	(1992 - present)
President	ChemIcon Inc.	(1994 - present)

EDUCATION:

1985	B.S. (Chemistry)	Georgetown University
1990	PH.D. (Analytical Chemistry)	University of Michigan
1990-1992	POSTDOC (Biophysics)	National Institutes of Health

CONSULTING EXPERIENCE:

Cambridge Research & Instrumentation; Unilever; Westinghouse Electric Corporation; Ford Motor Co.; Eli Lilly; Lockheed Martin; Proctor & Gamble; Eastman Kodak; Medtronic; Johnson & Johnson; Bayer; PPG Industries

Prof. Treado is a recognized expert in the development of Raman microscopy and its application to materials analysis. His letter confirming availability and commitment to this project is included as an Appendix to this Proposal.

Prof. Treado's doctoral research involved the development of widefield Raman microscopy techniques which led to a patent and several nationally competitive fellowships and awards being won by Prof. Treado. As a postdoctoral fellow at NIH, Prof. Treado pioneered the application of imaging spectrometers (acousto-optic tunable filters and step-scan interferometers) to Raman, NIR and IR imaging microscopy with Neil Lewis and Ira Levin. This work resulted in a broad patent. In addition, papers describing the research received the 1993 and 1995 Spectroscopy for Applied Spectroscopy Meggers Awards.

Since joining the University of Pittsburgh, Department of Chemistry, Prof. Treado has been engaged in the application of fluorescence, IR and Raman chemical imaging to chemical analysis. In 1994, Prof. Treado founded ChemIcon Inc., a company dedicated to commercializing chemical imaging technologies, including Raman microprobes for continuous process monitoring, fluorescence imaging systems to support drug discovery and Raman imaging microscopes.

Selected Publications

1. Nicole K. Kline and Patrick J. Treado, Raman Chemical Imaging of Breast Tissue, *J. Ram. Spectrosc.* (1996) submitted.
2. Michael D. Schaeberle, Costas G. Karakatsanis, Clifford J. Lau, and Patrick J. Treado, Raman Chemical Imaging: Histopathology of Inclusions in Human Breast Tissue, *Anal. Chem.* 68, (1996) 1829.
3. Hannah R. Morris, Clifford C Hoyt, Peter Miller, and Patrick J. Treado, Liquid Crystal Tunable Filter (LCTF) Raman Chemical Imaging, *Appl. Spectrosc.* 50, (1996) 805.
4. John F. Turner II and Patrick J. Treado, Near-Infrared Acousto-Optic Tunable Filter Hadamard Transform Spectroscopy, *Appl. Spectrosc.* 50, (1996) 277.

5. Nicole J. Kline and Patrick J. Treado, Raman Chemical Imaging of Disease States, *Proc. XVth ICORS*, S. A. Asher, Ed., (Wiley, Chichester, 1996) 1190.
6. Hannah R. Morris and Patrick J. Treado, LCTF Raman Chemical Imaging of Thermoplastic Olefin (TPO) Architecture, *Proc. XVth ICORS*, S. A. Asher, Ed., (Wiley, Chichester, 1996) 1186.
7. Michael D. Schaeberle and Patrick J. Treado, LCTF Raman Chemical Imaging of Semiconductors, *Proc. XVth ICORS*, S. A. Asher, Ed., (Wiley, Chichester, 1996) 1188.
8. John F. Turner II and Patrick J. Treado, The Application of Chemometrics to Raman Chemical Imaging, *Proc. XVth ICORS*, S. A. Asher, Ed., (Wiley, Chichester, 1996) 1202.
9. Michael D. Schaeberle, Costas G. Karakatsanis, Clifford J. Lau, and Patrick J. Treado, Raman Chemical Imaging: Noninvasive Visualization of Polymer Blend Architecture, *Anal. Chem.* 67, (1995) 4316.
10. E. Neil Lewis, Patrick J. Treado, Robert C. Reeder, Gloria M. Story, Anthony E. Dowrey, Curtis Marcott, Ira W. Levin, Fourier Transform Step-Scan Imaging Interferometry: High Definition Chemical Imaging in the Infrared Spectral Region, *Anal. Chem.* 67, (1995) 3377.
11. Patrick J. Treado, Chemical Imaging Reveals More Than the Microscope, *Laser Focus World* 31, (1995) 75.
12. Hannah R. Morris, Clifford C Hoyt, and Patrick J. Treado, Imaging Spectrometers for Fluorescence Microscopy: Acousto-Optic and Liquid Crystal Tunable Filters, *Appl. Spectrosc.* 48, (1994) 857.
13. Patrick J. Treado, Ira W. Levin, and E. Neil Lewis, Indium Antimonide (InSb) Focal Plane Array (FPA) Detection for Near-Infrared Imaging Microscopy, *Appl. Spectrosc.* 48, (1994) 607.
14. E. Neil Lewis, Patrick J. Treado, and Ira W. Levin, Near-Infrared and Raman Spectroscopic Imaging, *Amer. Lab.* 26, (1994) 16.
15. Patrick J. Treado and Michael D. Morris, Infrared and Raman Spectroscopic Imaging, *Spectroscopic and Microscopic Imaging of the Chemical State*, M.D. Morris, Ed. (Marcell Dekker, New York, 1992) pp. 71-108.
16. Patrick J. Treado, Ira W. Levin and E. Neil Lewis, High-Fidelity Raman Imaging Spectrometry: A Rapid Method Using an Acousto-optic Tunable Filter, *Appl. Spectrosc.* 46, (1992) 1211.
17. Patrick J. Treado and Michael D. Morris, Multichannel Hadamard Transform Raman Microscopy, *Appl. Spectrosc.* 44, (1990) 1.

J. Equipment, Instrumentation, Computers, and FacilitiesJ.1 Facilities available at C.R.I.

Of particular importance to this project is the C.R.I. liquid crystal filter fabrication facility. This includes an 8 x 12 foot class-100 clean room with complete thermal and humidity control; a 12 x 24 foot class-1000 clean room with complete thermal and humidity control; all necessary equipment for fabricating liquid crystal elements of the highest optical quality on glass and quartz substrates, including a semiconductor-class wash line, photoresist and etch process lines, spin-coating equipment, spacer-deposition chambers, ovens (atmospheric and vacuum), DI water filtration units, desiccant storage vaults, along with equipment for buffing, assembly and filling of liquid crystal cells. There are several class 100 horizontal flow hoods located within the class 1000 space, for overall filter assembly in a particle-free, laminar flow environment. This facility, staffed by two technicians and a senior process engineer, produces liquid crystal cells of unsurpassed optical quality and transmission.

Test equipment at C.R.I. includes a 0.5-meter SPEX spectrometer with 300 and 1200 line/mm gratings for high-resolution spectroscopy (0.025 nm); a quarter-meter visible ISA spectrometer with an EG&G 1024-element reticon detector; a Scitec optical chopper and Stanford Research 810 lock-in amplifier; quartz-halogen, mercury, Kanthal, and Xe arc continuum sources with collimation optics; a mercury line source for wavelength scale calibration; and a variety of silicon, germanium, PbSe, and InGaAs photodiodes, and photodiode preamps with NIST-traceable calibration. General optical equipment includes a 4' x 8' air-suspended optical table, a Neslab RTD-110 controlled temperature system with heat sink mount for temperature control of optical samples to +/- 0.02 °C; He-Ne, Ar⁺⁺, and Nd:YAG lasers with spatial mode filters and beam expanding optics; 6-inch and 1-inch Labsphere integrating spheres; PC/pentium computers with high-speed data acquisition hardware and software.

Imaging equipment includes a Zeiss Axioskop microscope equipped for epi- and kohler illumination; a Dage MTI CCD-72 camera with TEC-1 cooler, single-line gate, and controller; a Matrox MVP-AT frame grabber; Optimus, MetaMorph, and ImagePro image processing software; and a Sony Trinitron RGB monitor. C.R.I. maintains a network of PC/486 and PC/pentium computers with printers, tape drives, B and C size plotters, and Internet access. MatLab and ENVI software are available for the data reduction tasks described in the Plan Of Work.

In addition, C.R.I. has a PC/pentium-based CAD center for electronic and mechanical design using AutoCAD, PowerPCB, and ViewLogic design tools; a software development lab for programming the Intel 8031 and 80196 family of embedded microcontrollers; and an electronics test and production lab equipped to handle analog, digital, and microprocessor assemblies. We have access to complete metal-working facilities for fabricating jigs, special optical fixtures, and the like.

J.2 Facilities available to Prof. Treado at the University of Pittsburgh Laboratory Facilities:

Prof. Treado has approximately 1200 ft² of modern laboratory space, equipped for analytical spectroscopy (visible/NIR, Raman and fluorescence), optical

microscopy, scanning electron microscopy (SEM), wet chemistry and sample preparation.

Computer:

Data collection is controlled by PCs (Pentiums and 486s) running commercial programs, including ChemImage, a Windows program for multispectral image visualization and analysis. The PCs are networked to a Silicon Graphics IRIS Indigo R4K workstation fileserver with mass data storage, backup and retrieval. The workstation serves as an advanced spectral image processing workstation using MATLAB and ENVI.

Major equipment in Prof. Treado's laboratory:

(2) Princeton Instruments CCD detectors interfaced to a Gateway 2000 50 MHz 80486 DX2 computer running BioScan OPTIMAS image processing software; Coherent 330 Krypton ion laser, 400 mW 752 nm, 1 W multiline red; Coherent CR3 Argon ion laser, 150 mW 514.5 nm; (2) Chromex 0.5 m spectrographs for dispersive optical spectroscopy, and spectral calibration of the LCTFs; (2) Olympus BH2 upright microscopes interfaced to Cohu 4910 b&w video cameras for sample positioning and focusing; Kinetic Systems research grade optical table, 4' x 10'; Newport research grade optical table, 5' x 10'; EG&G PAR 5110 lock-in amplifier; E-Tec scanning electron microscope; Electro-Optic Systems InSb photodiode; CRI VariSpec LCTF for fluorescence imaging and for Raman imaging; Scanalytics CellScan Numerical Deconvolution Confocal microscopy software.

Industrial materials:

Sophisticated samples suitable for Raman microscopy applications including Martian meteorites, corrosion samples (steam-generator components), polymeric composites, thin films and coatings, silicon semiconductors, combinatorial substrates, and microelectrodes, as well as pharmaceuticals, will be provided by Prof. Treado's external collaborators in the defense, pharmaceutical, semiconductor and polymer industries.

Other:

The chemistry department maintains the usual array of modern spectroscopic instrumentation available for general access. Fully equipped electronics and machine shops for instrument and prototype fabrication are available.

K. Current and Pending Support of P.I. and Senior Personnel

The P.I. has no current or pending support for development of Raman imaging filters. He has a commitment of 1.5 months to N.I.H. contract #2 R44 MH53690-02, entitled "High-efficiency Tuneable Fluorescence Emission Filter", during the first year of the Phase II period of performance. Further commitments to commercially-sponsored liquid-crystal tunable filter development contracts are approximately 25% at present, and this level is anticipated during Phase II.

L. Equivalent or Overlapping Proposals to Other Federal Agencies

There are no equivalent proposals pending for development of Raman imaging filters, nor any which overlap the present Plan of Work.

Year 1 Budget

APPENDIX D

(SEE INSTRUCTIONS ON REVERSE

BEFORE COMPLETING)

PROPOSAL BUDGET

FOR NSF USE ONLY

ORGANIZATION Cambridge Research & Instrumentation, Inc.		PROPOSAL NO. DMI-9560600		DURATION (MONTHS) Proposed: 24 Granted: 	
PRINCIPAL INVESTIGATOR/PROJECT DIRECTOR Peter J. Miller		AWARD NO.			
A. SENIOR PERSONNEL: P/PI and Other Senior Associates (List each separately with title, A.G., show number in brackets)		NSF Funded Person-mos.	Funds Requested By Proposer	Funds Granted By NSF (if Different)	
		CAL			
1. P.I.		4.6	\$ 28,000	\$	
2.					
3.					
4.					
5.					
6. () OTHERS (LIST INDIVIDUALLY ON BUDGET EXPLANATION PAGE)					
7. () TOTAL SENIOR PERSONNEL (1-5)					
B. OTHER PERSONNEL (SHOW NUMBERS IN BRACKETS)					
1. () POST DOCTORAL ASSOCIATES					
2. (2) OTHER PROFESSIONALS (TECHNICIAN, PROGRAMMER, ETC.)		2.2	7,000		
3. () GRADUATE STUDENTS					
4. () UNDERGRADUATE STUDENTS					
5. () SECRETARIAL - CLERICAL					
6. () OTHER					
TOTAL SALARIES AND WAGES (A+B)			35,000		
C. FRINGE BENEFITS (IF CHARGED AS DIRECT COSTS) $0.38 \times (A+B)$			13,300		
TOTAL SALARIES, WAGES AND FRINGE BENEFITS (A+B+C)			48,300		
D. PERMANENT EQUIPMENT (LIST ITEM AND DOLLAR AMOUNT FOR EACH ITEM EXCEEDING \$5,000.) see list					
TOTAL PERMANENT EQUIPMENT			39,600		
E. TRAVEL 1. DOMESTIC (INCL. CANADA AND U.S. POSSESSIONS)			2,000		
2. FOREIGN (Do not use for Phase I)			-		
F. PARTICIPANT SUPPORT COSTS					
1. STIPENDS \$					
2. TRAVEL					
3. SUBSISTENCE					
4. OTHER					
() TOTAL PARTICIPANT COSTS					
G. OTHER DIRECT COSTS					
1. MATERIALS AND SUPPLIES (Attach itemized list if over \$5,000) LCTF materials-see list			10,000		
2. PUBLICATION COSTS/DOCUMENTATION/DISSEMINATION			1,000		
3. CONSULTANT SERVICES (Attach confirmation letters) (Daily rate not over \$443)			14,000		
4. COMPUTER (ADPE) SERVICES			1,000		
5. SUBCONTRACTS Univ. Pittsburgh (grad student, 3.5 mos.)			9,000		
6. OTHER					
TOTAL OTHER DIRECT COSTS					
H. TOTAL DIRECT COSTS (A THROUGH G)			124,900		
I. INDIRECT COSTS (SPECIFY) Overhead = $0.46 \times (A+B+C) = 22,218$					
TOTAL INDIRECT COSTS G&A = $0.16 \times (H+overhead) = 23,539$			45,757		
J. TOTAL DIRECT AND INDIRECT COSTS (H+I)			170,657	170,657	
K. FEE (If requested; maximum equals 7% of J)			9,786	205,443	
L. TOTAL COST AND FEE (J+K)			\$180,442	\$180,559	
PI/PI D TYPED NAME & SIGNATURE Peter J. Miller <i>PMJ</i>		DATE 10/23/96	FOR NSF USE ONLY		
CO. REP. TYPED NAME & SIGNATURE Peter V. Foukal <i>Poukal</i>		DATE 10/24/96	INDIRECT COST RATE VERIFICATION		
			Date Checked	Date of Rate Sheet	Initials-DGA

Year 2 Budget

APPENDIX D

(SEE INSTRUCTIONS ON REVERSE)

BEFORE COMPLETING

PROPOSAL BUDGET

FOR NSF USE ONLY

ORGANIZATION Cambridge Research & Instrumentation		PROPOSAL NO. DMT-9560600		DURATION (MONTHS) Proposed: 24, Granted:	
PRINCIPAL INVESTIGATOR/PROJECT DIRECTOR Peter J. Miller		AWARD NO.			
A. SENIOR PERSONNEL: PVPD and Other Senior Associates (List each separately with title, A.G., show number in brackets)		NSF Funded Person-mos.	Funds Requested By Proposer	Funds Granted By NSF (if Different)	
		CAL			
1. P. T.		4.4	\$26,000	\$	
2.					
3.					
4.					
5.					
6. () OTHERS (LIST INDIVIDUALLY ON BUDGET EXPLANATION PAGE)					
7. () TOTAL SENIOR PERSONNEL (1-5)					
B. OTHER PERSONNEL (SHOW NUMBERS IN BRACKETS)					
1. () POST DOCTORAL ASSOCIATES					
2. () OTHER PROFESSIONALS (TECHNICIAN, PROGRAMMER, ETC.)		1.8	6,000		
3. () GRADUATE STUDENTS					
4. () UNDERGRADUATE STUDENTS					
5. () SECRETARIAL - CLERICAL					
6. () OTHER					
TOTAL SALARIES AND WAGES (A+B)			32,000		
C. FRINGE BENEFITS (IF CHARGED AS DIRECT COSTS) 0.38 x (A+B)			12,160		
TOTAL SALARIES, WAGES AND FRINGE BENEFITS (A+B+C)			44,160		
D. PERMANENT EQUIPMENT (LIST ITEM AND DOLLAR AMOUNT FOR EACH ITEM EXCEEDING \$5,000.)					
TOTAL PERMANENT EQUIPMENT see list			3,000		
E. TRAVEL 1. DOMESTIC (INCL. CANADA AND U.S. POSSESSIONS)			3,500		
2. FOREIGN (Do not use for Phase I)			-		
F. PARTICIPANT SUPPORT COSTS					
1. STIPENDS \$					
2. TRAVEL					
3. SUBSISTENCE					
4. OTHER					
() TOTAL PARTICIPANT COSTS			-		
G. OTHER DIRECT COSTS					
1. MATERIALS AND SUPPLIES (Attach itemized list if over \$5,000)			-		
2. PUBLICATION COSTS/DOCUMENTATION/DISSEMINATION			1,500		
3. CONSULTANT SERVICES (Attach confirmation letters) (Daily rate not over \$443)		11,200	14,000	(2,800)	
4. COMPUTER (ADPE) SERVICES		4	2,000		
5. SUBCONTRACTS Univ. Pittsburgh (grad student 3.8 mos)			9,000		
6. OTHER					
TOTAL OTHER DIRECT COSTS			27,160	24,360	
H. TOTAL DIRECT COSTS (A THROUGH G)			27,160	24,360	
I. INDIRECT COSTS (SPECIFY) overhead = 0.46 x (A+B+C) = 20,314					
G&A = 0.16 x (H+overhead) = 15,596			35,910	35,462	
TOTAL INDIRECT COSTS			35,910	35,462	
J. TOTAL DIRECT AND INDIRECT COSTS (H+I)		15,148	113,070	109,822	
K. FEE (if requested; maximum equals 7% of J)			6,488	6,488	
L. TOTAL COST AND FEE (J + K)			\$119,558	\$116,194	
PVPD TYPED NAME & SIGNATURE Peter J. Miller		DATE 10/23/96	FOR NSF USE ONLY		
CO. REP. TYPED NAME & SIGNATURE Peter V. Foukal		DATE 10/24/96	INDIRECT COST RATE VERIFICATION		
		Date Checked	Date of Rate Sheet	Initials-DGA	

Summary Budget

APPENDIX D

(SEE INSTRUCTIONS ON REVERSE)

BEFORE COMPLETING		PROPOSAL BUDGET		FOR NSF USE ONLY	
ORGANIZATION Cambridge Research & Instrumentation, Inc.		PROPOSAL NO. DMI-9560600		DURATION (MONTHS) Proposed: 24, Granted:	
PRINCIPAL INVESTIGATOR/PROJECT DIRECTOR Peter J. Miller		AWARD NO.			
A. SENIOR PERSONNEL: P/PI and Other Senior Associates (List each separately with title, A.S., show number in brackets)		NSF Funded Person-mos.	Funds Requested By Proposer	Funds Granted By NSF (If Different)	
		CAL			
1. P-I.		9	\$ 54,000	\$	
2.					
3.					
4.					
5.					
6. () OTHERS (LIST INDIVIDUALLY ON BUDGET EXPLANATION PAGE)					
7. () TOTAL SENIOR PERSONNEL (1-5)					
B. OTHER PERSONNEL (SHOW NUMBERS IN BRACKETS)					
1. () POST DOCTORAL ASSOCIATES					
2. (2) OTHER PROFESSIONALS (TECHNICIAN, PROGRAMMER, ETC.)		4	13,000		
3. () GRADUATE STUDENTS					
4. () UNDERGRADUATE STUDENTS					
5. () SECRETARIAL - CLERICAL					
6. () OTHER					
TOTAL SALARIES AND WAGES (A+B)			67,000		
C. FRINGE BENEFITS (IF CHARGED AS DIRECT COSTS)			25,460		
TOTAL SALARIES, WAGES AND FRINGE BENEFITS (A+B+C)			92,460		
D. PERMANENT EQUIPMENT (LIST ITEM AND DOLLAR AMOUNT FOR EACH ITEM EXCEEDING \$5,000.)					
see list					
TOTAL PERMANENT EQUIPMENT			42,600		
E. TRAVEL 1. DOMESTIC (INCL. CANADA AND U.S. POSSESSIONS)			5,500		
2. FOREIGN (Do not use for Phase I)			-		
F. PARTICIPANT SUPPORT COSTS					
1. STIPENDS \$ _____					
2. TRAVEL _____					
3. SUBSISTENCE _____					
4. OTHER _____					
() TOTAL PARTICIPANT COSTS					
G. OTHER DIRECT COSTS					
1. MATERIALS AND SUPPLIES (Attach Itemized list if over \$5,000) LCIF Supplies - see list			10,000		
2. PUBLICATION COSTS/DOCUMENTATION/DISSEMINATION			2,500		
3. CONSULTANT SERVICES (Attach confirmation letters) (Daily rate not over \$443)			28,000	25,200	
4. COMPUTER (ADPE) SERVICES 8			3,000		
5. SUBCONTRACTS Univ. Pittsburgh (grad student, 7 months)			18,000		
6. OTHER					
TOTAL OTHER DIRECT COSTS					
H. TOTAL DIRECT COSTS (A THROUGH G)			202,060	155,760	
I. INDIRECT COSTS (SPECIFY) Overhead $0.46 \times (A+B+C) = 42,532$					
TOTAL INDIRECT COSTS G&A $0.16 \times (H+\text{overhead}) = 39,135$ 38,687			81,667	81,215	
J. TOTAL DIRECT AND INDIRECT COSTS (H+I)			283,726	236,975	
K. FEE (If requested; maximum equals 7% of J)			16,274	16,274	
L. TOTAL COST AND FEE (J + K)			\$300,000	\$253,249	
PI/PI D TYPED NAME & SIGNATURE		DATE	FOR NSF USE ONLY		
Peter J. Miller <i>PJM</i>		10/23/96	INDIRECT COST RATE VERIFICATION		
CO. REP. TYPED NAME & SIGNATURE		DATE	Date Checked	Date of Rate Sheet	Initials-DGA
Peter V. Foukal <i>PVF</i>		10/23/96			

0.05484
0.05802216

M.1 Justification of Permanent Equipment Items

Year 1

Spectrometers (Kaiser HoloSpec f/2.2 HFG-650, HFG-850)	\$11,600
CCD (Princeton Instr. STC-133/RTE-CCD-64-H)	\$ 9,000
LiNbO ₃ substrate blanks (64 @ \$125/ea.)	\$ 8,000
Polishing of LiNbO ₃ substrates (64 @ \$125/ea.)	\$ 8,000
Holographic optical elements (3 @ \$1,000/ea)	\$ 3,000

Year 2

Holographic optical elements (3 @ \$1,000/ea)	\$ 3,000
---	----------

The spectrometers will be used to characterize the retarder components and filters used in this work. Existing equipment used for this work is the Spex 0.5M spectrometer. This is a mechanically-scanned instrument, and it is not possible to obtain wide spectral coverage by outfitting it with a CCD array detector. The time to acquire a spectrum is so long (20 minutes) that characterization of important parameters required herein, such as thermal drift and off-axis response, become impractical. In contrast, the Kaiser instruments use a transmissive holographic grating to image the entire working range onto a 25 mm CCD array detector. Reliability is improved relative to the present equipment, by removing the moving parts; this is especially important since present equipment requires unattended operation for days at a time. More important, data acquisition time is reduced by a factor of >100 due to parallel data collection at the CCD, making the Plan of Work practical.

The Kaiser grating HFG-650 covers the range 500 - 800 nm, and the NIR grating HFG-850 spans 655 - 1045 nm, with a resolution of 10 cm⁻¹ or better at a 1024-element CCD. Due to the pricing of the Kaiser components, there is only a modest premium (16%) for buying two spectrometers, compared to one spectrometer with two gratings. This is a transmissive spectrometer, with no provision for a rotating turret to switch between various gratings. For this reason, and to minimize the risk of damaging the valuable gratings in handling, the purchase of two spectrometers is proposed.

The CCD will be used in concert with the spectrometers to obtain spectral data on the retarders and assembled LCTF, not for acquisition of Raman images. Coupling is by means of a rugged, detachable adapter so one CCD can be readily used with both spectrometers. Princeton Instruments has expressed an interest in the imaging LCTF Raman technology, and has agreed to provide a model STC-133 camera with RTE/CCD-64-H readout electronics at a significantly reduced price (\$9,000 vs. \$12,980 list) in order to learn more about the application. Thermoelectric cooling of the CCD array is sufficient, as even the most demanding tests (such as the assessment of spectral leakage in completed filters) require exposures of only a few seconds.

The LiNbO₃ blanks, polished to form precision waveplates, are used to build the visible and NIR prototypes, as per Objective iii). Based on the Phase I experience, we anticipate that 64 LiNbO₃ blanks (of selected thicknesses) will yield between 40 - 50 good parts; 32 are required to complete the Plan of Work.

Holographic optical elements (HOEs) are used in the Raman imaging microscope to block Rayleigh scatter at the laser wavelength. There are existing HOE's at U/Pitt for the wavelengths up to 647 nm; however, with the development of the NIR filter, we intend to operate at new, longer wavelengths up to at least 780 nm. Each wavelength requires a dedicated HOE, and this budget item will be used to procure these, for use at U/Pitt and at beta-sites in Year 2.

M.2 Justification of travel expenses

Travel between Cambridge and U/Pitt by the P.I. or Dr. Treado is anticipated, and is budgeted as 2 round-trip visits per year during the project at \$500 per visit. Conference travel is budgeted as \$1,000 per year. In the second year the P.I. plans to visit the beta-site laboratories; one is local (M.I.T.), but others are expected to require airfare and lodging costs.

M.3 Justification of materials costs

Year 1

Materials

NIR polarizers (32 @ \$125 each)	\$ 4,000
liquid crystal material, substrates, epoxies, etc.	\$ 4,000
optical coating charges (4 lots @ \$500 each)	\$ 2,000

Year 2

(none)

All supplies will be used to construct the Phase II prototypes. Coating charges are for anti-reflection coatings in the NIR and visible, which are deposited on LiNbO₃ and on glass; a total of four coatings lots are required.

M.4 Justification of Consultant and Subcontract services

Consulting funds of \$28K are budgeted for Dr. Treado to perform his portion of the work at U/Pitt. Dr. Treado will be principally responsible for the task of meeting objective iv), the evaluation of applications targeted as having commercial potential. This is a laboratory research task, involving imaging Raman analysis of various samples relevant to the target applications. Initially, Dr. Treado will use the Phase I prototype, and this will be replaced with improved Phase II parts as they become available. He will be assisted in this work by a graduate student at the University.

Dr. Treado's rate for this work is \$442 per day, and an effort equivalent to three calendar months (62 working days) is budgeted during the 2-year Phase II period of performance. Seven months of graduate student support is included as well, through a subcontract to the Univ. of Pittsburgh for \$2.6K per month of student support; this includes their overhead, and a lesser amount is paid the student. A letter from the University is attached to this Proposal, indicating the terms of this arrangement.

References

1. J. W. Evans, "The Birefringent Filter", J. O.S.A. 39, 3, 229 (1949).
2. J.A. Faust, A. Biswas, G.H. Bearman, T. Chrien. P.J. Miller, "Development of a compact imaging spectrometer using liquid crystal tunable filter technology", O.S.A. 1996 Annual meeting, talk Th117 (1996).

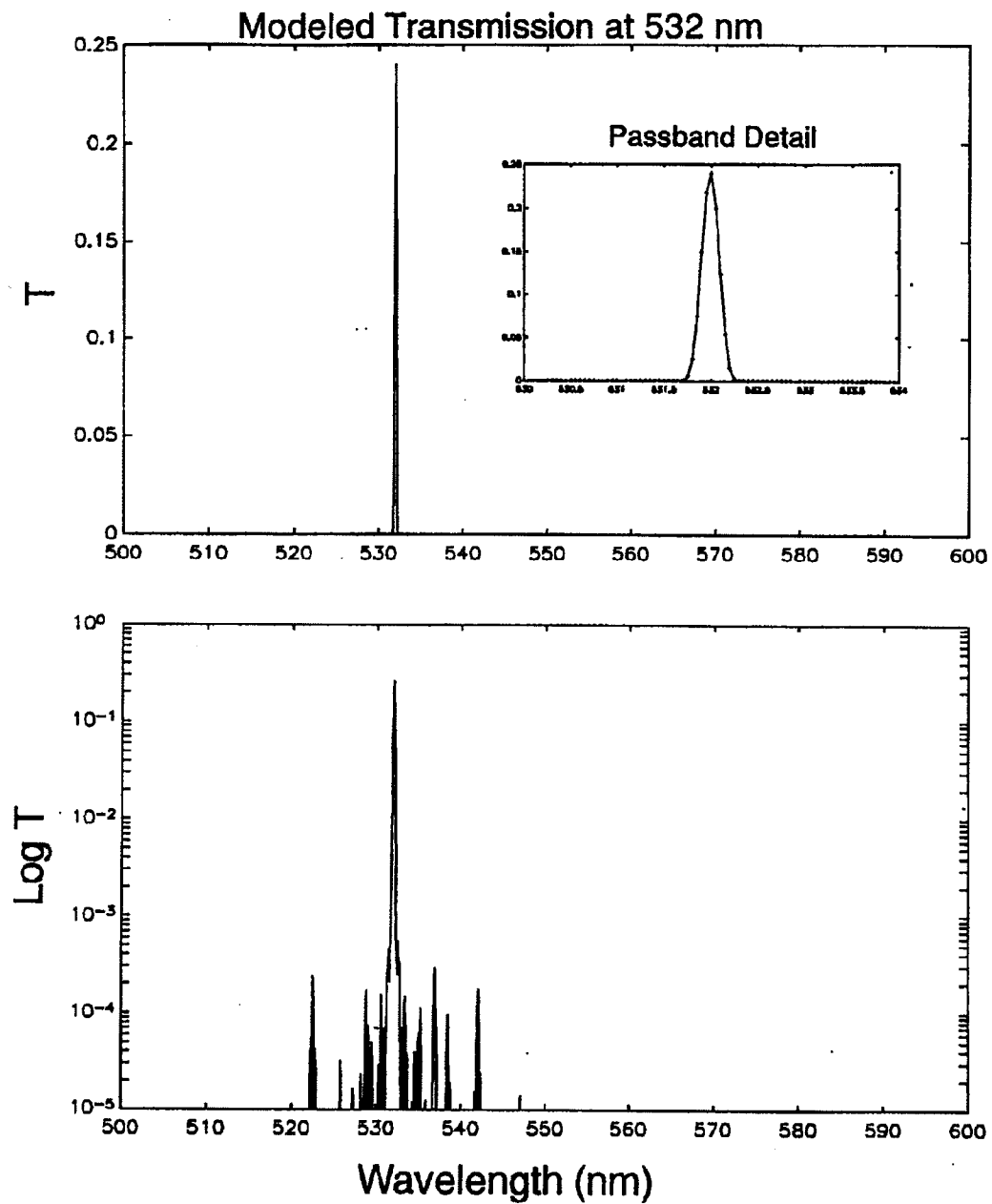


Figure 1. Model LCTF performance when tuned to 532 nm, shown on linear and logarithmic scales. Passband detail is shown in the inset.

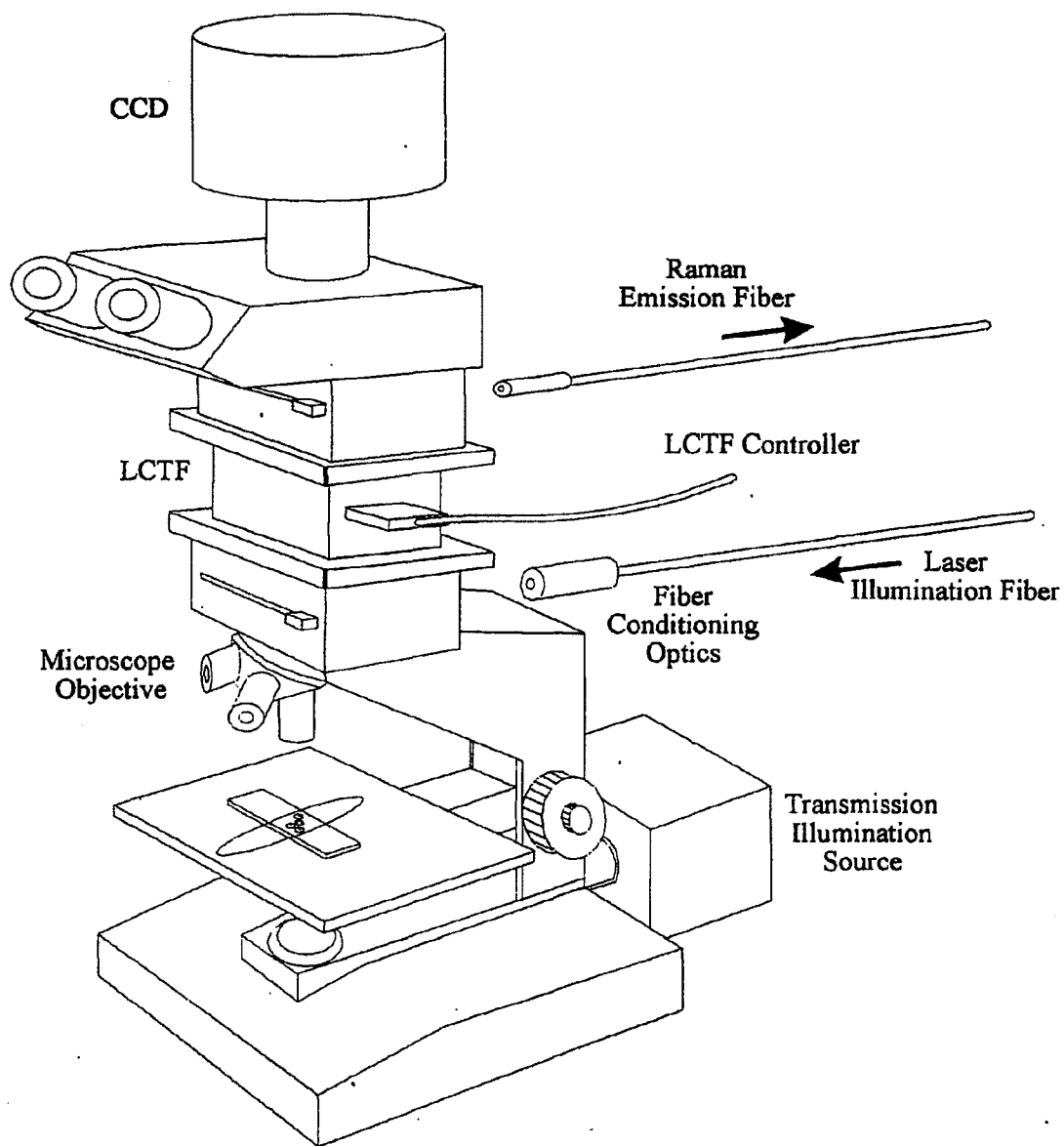


Figure 2. Diagram of the LCTF Raman filter integrated onto the optical microscope.

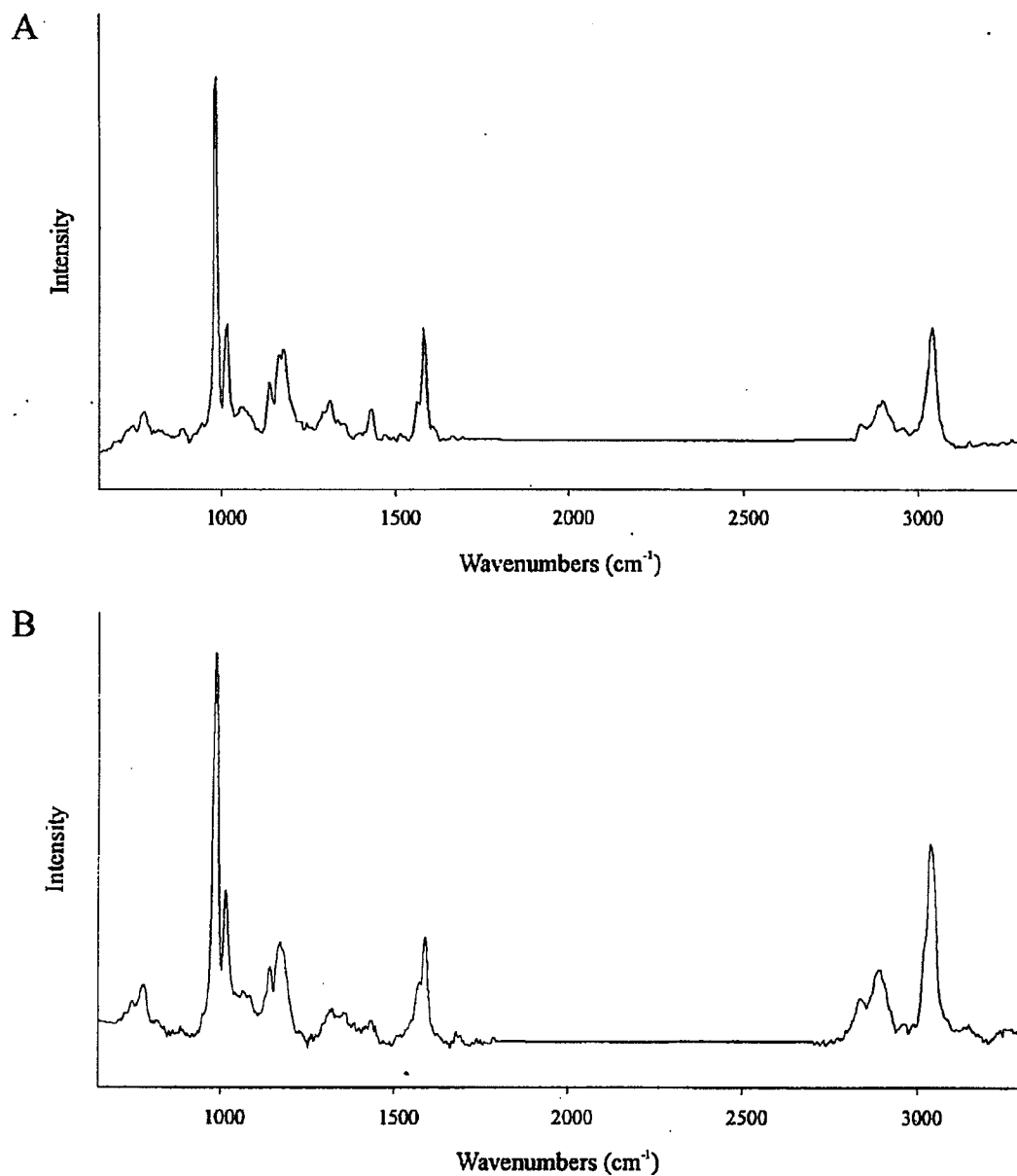


Figure 3. The top figure shows a Raman spectrum of polystyrene microsphere, obtained with the LCTF, while the lower figure shows the Raman spectrum of the same sample taken through a conventional (non-imaging) dispersive spectrometer system.

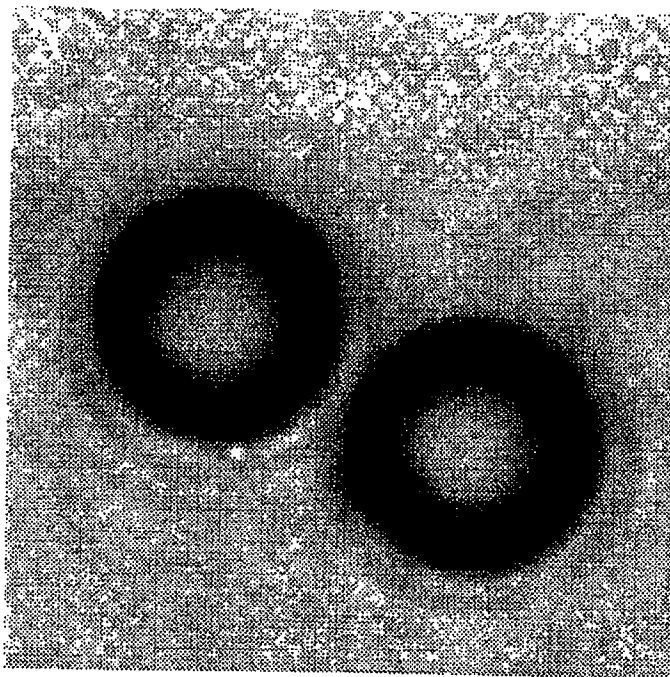


Figure 4. Diffraction-limited image of 2 μm polystyrene spheres (brightfield).

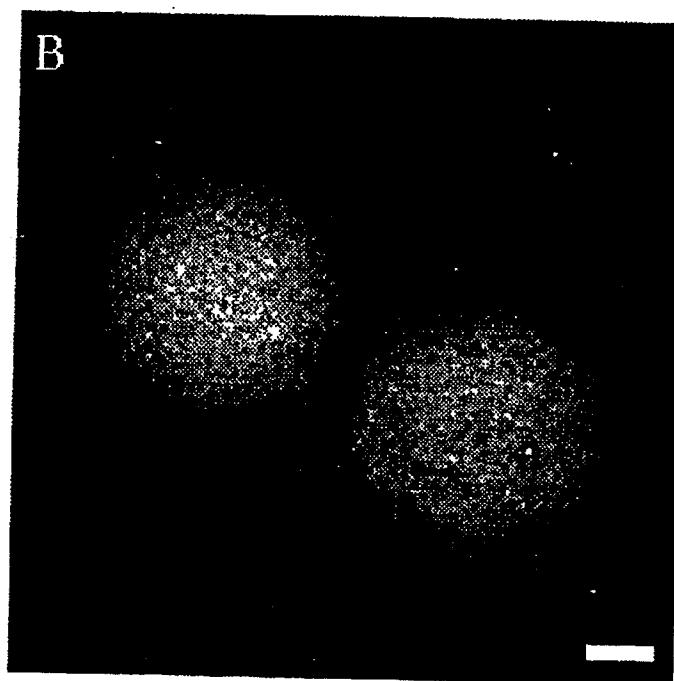


Figure 5. Raman image at 992 cm^{-1} of the same sample. Note 500 nm size bar shown for reference.

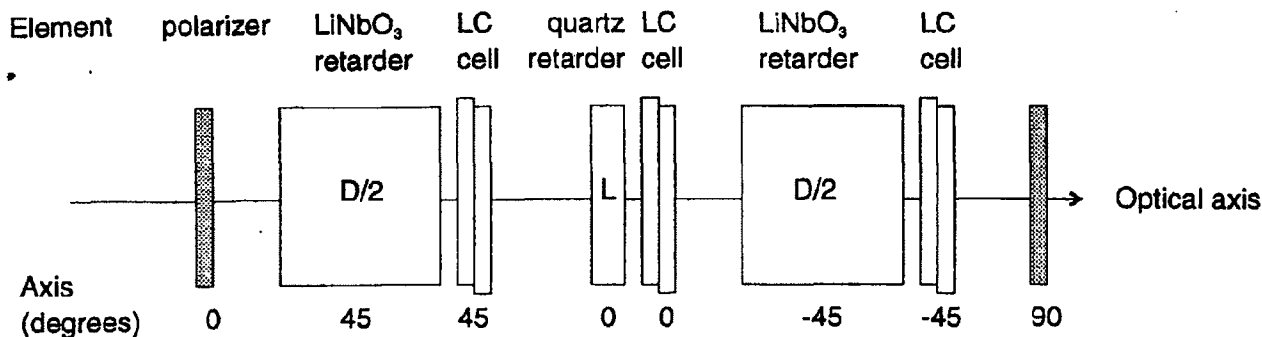


Figure 6. Diagram of an Evans split element stage. Thicknesses and spacing between elements is greatly exaggerated for clarity. Axes indicated are the transmission axis for polarizers, and the fast axis for LC cells and retarders.

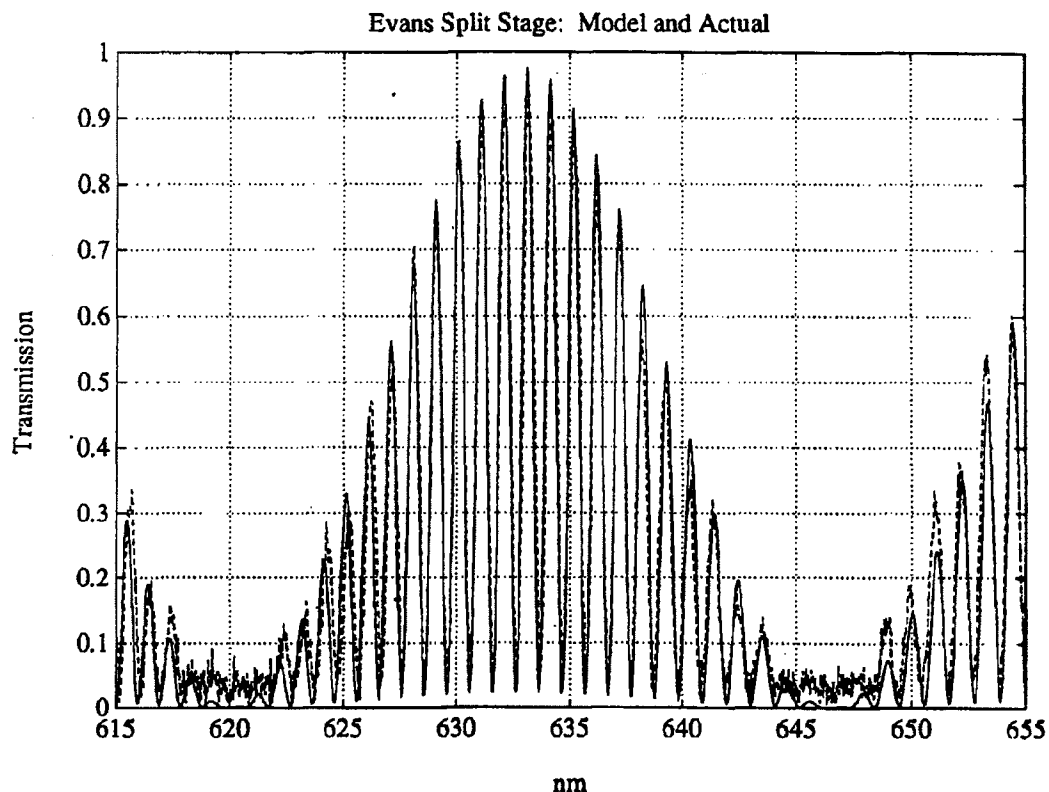


Figure 7. Transmission of a single Evans split element stage, constructed in Phase I, along with model predictions. The high-frequency structure is produced by the D/2 retarders, and the envelope is generated by the R_L quartz retarder.

APPENDIX E

CERTIFICATE OF CURRENT COST OR PRICING DATA


This is to certify that, to the best of my knowledge and belief, the cost or pricing data (as defined in section 15.801 of the Federal Acquisition Regulations), submitted either actually or by specific identification in writing, to the Grant Officer or to the Grants Officer's representative in support of DMI-9560600 * are accurate, complete, and current as of 10/17/96 .**

This certification includes the cost or pricing data supporting any advance agreements and forward pricing rate agreements between the offeror and the Government that are part of the proposal.

COMPANY NAME: Cambridge Research & Instrumentation, Inc.

REPRESENTATIVE NAME: Peter V. Foukal

REPRESENTATIVE TITLE: President

REPRESENTATIVE
SIGNATURE: 

DATE OF
EXECUTION***: 10/17/96

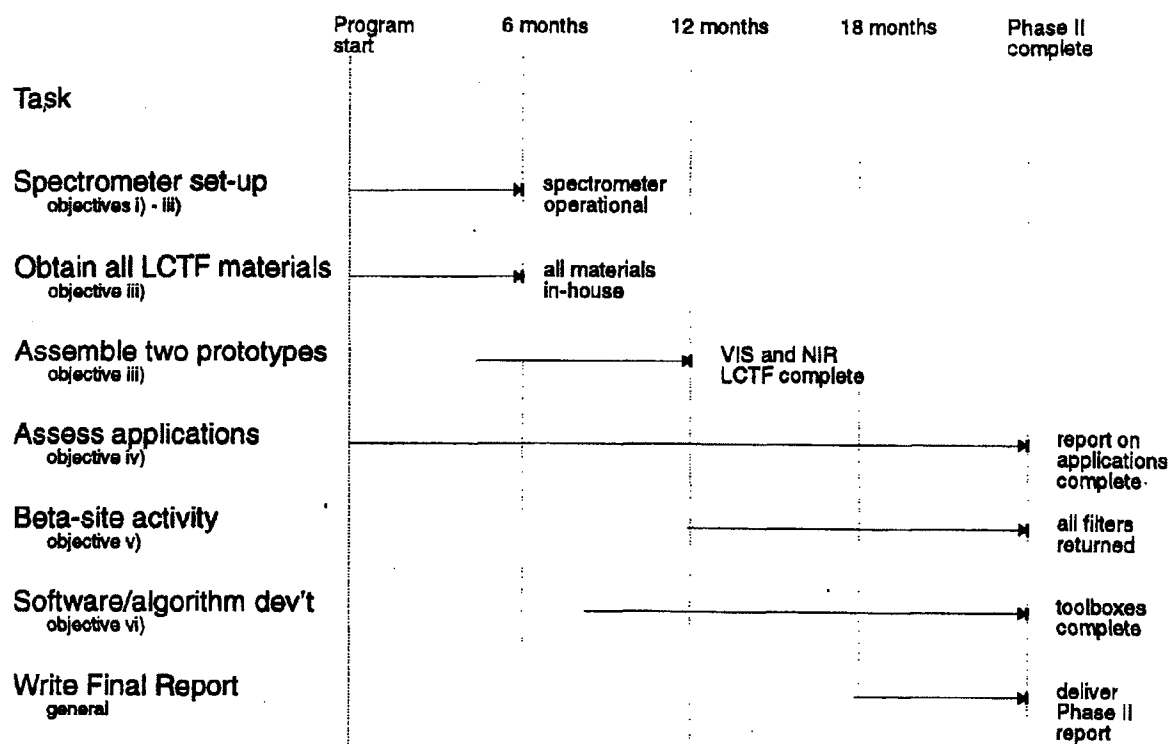
SBIR Organizations are required to submit this certificate with their proposal. If the proposal is recommended for funding, a second certificate will be requested by NSF subsequent to a pre-award budget review, but prior to award.

* Identify the SBIR Phase II Proposal Number.

** (1) Insert the date, month, and year for proposal submission when submitting with proposal, (2) or the date, month, and year when notified by NSF that the proposal has been recommend for award and price negotiations are completed.

*** Insert the date, month, and year of signing

Appendix 1. SBIR Phase II Milestone chart



Effort (months)	1-6	7-12	13-18	19-24
Key personnel	2.60	2.00	2.00	2.40
Consultants	0.25	0.25	0.25	0.25
Subcontracts	1.75	1.75	1.75	1.75

Estimated Expenditures

Key personnel	21,520	16,560	16,560	19,872
Consultants	7,000	7,000	7,000	7,000
Subcontracts	4,500	4,500	4,500	4,500
Perm. Equip.	36,600	3,000	3,000	-
Materials	10,000	-	-	-
Other	38,547	21,429	24,172	26,466

Appendix 2A: Indicators of Commercial Potential

The clearest indicators of commercial potential are: C.R.I.'s demonstrated history of successes in commercializing SBIR developments; the presence of a Phase III partner who has committed to a follow-on funding agreement to gain access to the instruments being developed; and, a commercialization plan which seeks to exploit commercially the inherent potential of the LCTF Raman technology being developed.

C.R.I.'s demonstrated success in commercializing SBIR technology

Cambridge Research and Instrumentation, Inc., (CRI, Inc.) is a small (17 permanent employees) high-tech firm founded in 1985, with strengths in electro-optics and in space physics. Projected revenues in the current year are \$3.2 M, of which about 70% is derived from commercial sales and the remainder from federal agency research contracts and grants. About 40% of the commercial sales consist of exports, primarily to Japan and W. Europe.

CRI's first (NSF SBIR-supported) product was a cryogenic absolute radiometer, for highest accuracy radiative flux measurements. The LaserRad and CryoRad-series radiometers, which sell for \$75K - 150K, are now in use at national and aerospace metrology laboratories world-wide, as primary irradiance standards. A second successful product whose development was also supported in part by NASA and NSF SBIR awards, is an electro-optic servo system, priced between \$4K - 8K, for control of laser power and removal of laser flux variations. The LPC-series stabilizers won two industrial awards in 1989, and CRI is the major world wide supplier of such systems into applications ranging from biomedical research to semi-conductor manufacturing. Cumulative sales in these two CRI products already exceed \$5M, and annual sales continue to rise.

Phase III partnership and follow-on funding

A Phase III Follow-on Funding Commitment (FOFC) has been negotiated between C.R.I. and ChemIcon in the amount of \$200,000, in return for first access to the technology being developed in Phase I and Phase II work. The FOFC is attached as an Appendix to the Proposal. ChemIcon has already introduced a line of Raman microscopes based on the Phase I prototype, and have quotations pending with several customers totaling over \$300K. They anticipate significantly larger markets as the improved Phase II devices become available, and the utility of this new approach is assessed in key industrial applications.

Commercialization plant to exploit LCTF Raman technology

The commercialization plan follows, and outlines the product, company, competitors, and marketing and production plans for the Phase III (commercial) phase of this project.

Appendix 2.B Commercialization Plan**Company**

Cambridge Research & Instrumentation, Inc., was founded by Dr. Peter Foukal in 1985 to perform solar-terrestrial physics research, and to develop scientific equipment related to the precision measurement and control of light. Among its products are the Laser Power Controller, which won the R&D 100 and Photonics Circle of Excellence awards when it was introduced in 1989, and which is widely used today in research and in semiconductor wafer marking; the LaseRad and CryoRad cryogenic absolute radiometers, which are used as the primary standard of light measurement at NIST, as well as at the National laboratories in Germany, Canada, Sweden, the Netherlands, Spain, and China; and the VariSPEC liquid crystal tunable filters. The VariSPEC line has received great commercial success, also received numerous awards, including the R&D 100, Laser Focus World CTA, and Photonics Circle of Excellence.

C.R.I. has 18 employees, is privately held, and has been profitable every year since its formation. Sales for the current fiscal year are approximately \$3.2M, of which approximately 30% are overseas exports. C.R.I. has been awarded patents for liquid crystal components related to LCTF construction, and holds exclusive license to others, including key patents on RGB color filters and a polarization microscope system developed by the Marine Biological Laboratory at Woods Hole.

SBIR Project

This SBIR project seeks to exploit narrowband tunable filters, similar to C.R.I.'s existing line of VariSPEC filters, to take images of the Raman emission of samples in microscopes. In this way, the chemical 'fingerprint' of the sample is obtained with great specificity. There is essentially no sample preparation, and the measurement is nondestructive. The information which is obtained provides a highly detailed picture, or image, of the location and quantities of different chemical species in the sample.

Such highly detailed imaging information is otherwise difficult or impossible to obtain, and provides a wealth of information on heterogeneous samples such as patterned silicon wafers, cellular tissue, thin films, and a variety of real-world items which have structures within them.

By making and optimizing the filters used in this approach, and then testing the overall imaging system in key target applications, C.R.I. seeks to identify suitable markets for this new instrument.

Commercial Applications

Applications for a Raman imaging microscope are diverse because almost every manufactured or natural material has a unique, intrinsic Raman spectral fingerprint. The Raman spectra can be harnessed to generate molecule-specific image contrast that is not derived from time consuming, potentially invasive sample staining processes. As a result almost every material analysis application can potentially benefit from Raman imaging analysis. The broad applicability of this technique is one of the attractive features of Raman imaging.

The major criteria for applicability are that the material of interest evidence molecular chemical heterogeneity on a spatial scale that can be

probed by an optical microscope (>200 nm) and that the heterogeneity be stable on the time scale of a typical Raman imaging analysis (mins.); a broad range of materials and potential applications fall within these guidelines.

Prof. Treado's research at the University of Pittsburgh has been focused in the past several years on identifying the applications that derive the most benefit from Raman image analysis. A partial list of applications follows:

- non-invasive characterization of ion implantation and thermal annealing on silicon semiconductors;
- characterization of phosphate-initiated corrosion in steam generator components;
- analysis of bio-initiated corrosion in implantable medical devices;
- thin film and coatings characterization, including analysis of molecular compositional and conformational heterogeneity in diamond films, polymer films, and ferroelectric thin films;
- polymer blend domain structure analysis;
- content uniformity characterization and polymorphism content analysis of intact pharmaceutical tablets;
- oriented polymer fiber characterization;
- adhesion characteristics of thin polymer films;
- surface crystallinity content analysis of controlled-release polymer drug delivery systems;
- non-invasive analysis of combinatorial systems employed in biosensors and in drug discovery;
- quantitative histopathology;
- the search for life on Mars with the implementation of LCTF Raman imaging technology in a Mars lander.

Patent Status

C.R.I. holds two key patents related to the construction of liquid crystal tunable filters (LCTFs), and another is pending. These protect the core technology, including the work described in the present SBIR proposal. No patents have been filed as a result of the Phase I effort, but it is anticipated that patentable work may result from the Phase II project and a periodic evaluation of the patentability of the research will be performed and acted upon where appropriate.

Innovation

Compared to existing, non-imaging systems, the Raman LCTF system adds the powerful ability to visualize the distribution (morphology and architecture) of chemical species in heterogeneous samples with molecular compositional specificity. Raman images can be collected rapidly, non-invasively, with limited or no sample preparation, at high spatial resolution (< 250 nm) and with high fidelity where the number of image pixels is limited by the number of pixels on the CCD detector. Most importantly, every image pixel has associated with it a Raman spectrum whose quality is identical to that obtained with conventional non-imaging spectrometers. These key benefits make Raman imaging practical for the analysis of real-world samples, which are chemically heterogeneous on the spatial scales of interest.

Improvements in Phase II will result in higher efficiency, and extend its usefulness into the NIR range for use with red and infra-red lasers.

Markets (anticipated after 5 years)

Based on preliminary feedback from industrial and academic researchers, the following markets are predicted for imaging Raman LCTF systems two years after the Phase II effort, when the market is mature:

Markets (Segmented by Industry)	Size/year (\$M)
Semiconductor	4
Biomedical Pathology	3
Endoscopy (in vivo)	2
Polymers	3
Pharmaceutical	3
Federal labs and academics	2
Power generation	2
Environmental	1
Coatings	1

Each system will cost between \$125K - \$200K, and the aggregate market of \$21M corresponds to approximately 100 - 125 LCTF filters/yr.

Competition

The LCTF represents the only technology that is capable of rapidly collecting high spatial/spectral resolution Raman images at high image fidelity. C.R.I. has a controlling position in the LCTF technology due to the expertise of the P.I., strong patent positions, qualified design and fabrication personnel, and extensive fabrication and testing facilities. C.R.I. has consistently demonstrated the ability to commercialize technologies developed under SBIR program support. C.R.I.'s LCTF capability in combination with Prof. Treado, a recognized leader in Raman imaging, represents a potent alliance. The concept to adapt CRI's LCTF technology specifically for Raman imaging was originally put forth by Prof. Treado, and it has been due to the close collaboration between CRI and Prof. Treado and with the support of the Phase I effort, that the technology has been developed, demonstrated and been received with such success (see the attached feature cover article describing the technology).

Principal competition will be from non-imaging methods, which is the present approach. As the advantages of the imaging methods become known to the user community, non-imaging methods will give way to C.R.I.'s technology except where imaging is of little benefit. Identifying which applications will gain from imaging methods, and which will not, is a key component of the Phase II work.

Production Plan

C.R.I. will fabricate LCTF Raman filters for sale to integrators of Raman systems such as ChemIcon, as well as to individual researchers. It does not anticipate selling complete systems, which would lie outside the areas of C.R.I.'s core strengths.

The existing C.R.I. liquid crystal production line, on which the Phase I prototype was built, has a capacity in excess of 100 narrowband filters/yr, as well as several thousand broadband RGB filters. A senior process scientist was hired recently to oversee further production improvements and expansion which will more than double this figure within the coming year. So, while there will be a need to bring vendors on-line for the LiNbO_3 , and to develop internal procedures for Q/C, handling, and characterization of the narrowband elements involved, the production of these filters will occur as part of the overall growth of the VarisPEC filter product line.

Marketing Plan

Marketing will be through two channels: first, we will work with O.E.M. firms and integrators such as ChemIcon, Kaiser, Renishaw, and Nicolet as they adopt this technology in their commercial Raman systems. C.R.I. has high visibility in this field, mainly due to Prof. Treado's work and the Phase I efforts, and we have been contacted by most of these firms already. Most of them have a purely technical interest at present, and will not become actively interested from a business standpoint until applications develop which justify their efforts to adopt and incorporate this technology. In contrast, ChemIcon has taken a very active role in marketing this technology, and is likely to garner the sales to 'visionaries' who see a compelling reason to use the LCTF Raman technique.

At the same time, C.R.I. will market the LCTF filters directly to scientific researchers, engineers, and other end-users. This is the primary market channel for the VarisPEC filters in fluorescence, remote sensing, and other applications, and we will use a similar blend of advertising, direct mail, technical articles, and trade shows to promote this product as it emerges. C.R.I. has a network of foreign representatives and agents which sell and support our other, similarly complex, opto-electronic products worldwide, and they will also sell the Raman LCTF.

Underpinning the market success, however, is the identification of technical research or applications which exploit the compelling technical advantages of LCTF Raman systems. This will drive the interest of O.E.M.s and integrators, and will lead to development of fruitful research areas, and thus, to end-user sales. For this, the key ingredient is an assessment of which applications are likely to be aided by this product, which is addressed in Phase II both through our own study of applications and through the beta-site program.



SBIR Phase III Follow-on Funding Commitment

Whereas ChemIcon Inc. of Pittsburgh, PA desires to obtain access to the LCTF Raman imaging technology being developed by Cambridge Research & Instrumentation, Inc. (CRI) of Cambridge MA, with application development support from Patrick J. Treado and the University of Pittsburgh, ChemIcon agrees to provide long-term funding to gain access to this technology, in the amount of \$200,000 against which Cambridge Research & Instrumentation will provide LCTF Raman imaging tunable filters.

This financial support is contingent upon technical progress being achieved during the Phase II effort, substantially in compliance with the Technical Objectives and Milestones contained herein as Section E and Appendix 1. In addition, this financial support is contingent on CRI's LCTF Raman imaging tunable filter technology being cost competitive with alternative Raman imaging technology, that may exist at some time during the term of this funding commitment. In addition, this financial support is contingent on the market acceptance of ChemIcon Raman microscopes that employ LCTF Raman imaging tunable filter technology.

Release of the funds will be over a period not to exceed 24 months beginning at the conclusion of the Phase II period of performance, and may begin sooner by mutual agreement, as technical progress warrants.

We certify to the best of our knowledge that this funding commitment will be used by the NSF in evaluating the commercial potential of CRI's innovation and therefore, will be a significant factor in determining whether the SBIR Phase II proposal will be funded. We further understand that willfully making a false statement or concealing a material fact in this commitment or any other communication submitted to the NSF is a criminal offense.

This commitment and support are offered and accepted by:

PATRICK J. TREADO
(name)

PRESIDENT
(title)

Pat Treado
(signature)

10/24/96
(date)

Peter Foukal
(name)

President
(title)

Peter Foukal
(signature)

10/25/96
(date)



University of Pittsburgh

Faculty of Arts and Sciences
Department of Chemistry

314 Chevron Science Center
Pittsburgh, Pennsylvania 15260
412-624-8621
Fax: 412-624-8552
E-mail: treado+@pitt.edu

October 28, 1996

Mr. Peter Miller
Cambridge Research & Instrumentation, Inc.
21 Erie Street
Cambridge, MA 02139

Dear Mr. Miller:

I have long-standing research interests in Raman chemical imaging and its application to the analysis of materials. CRI's liquid crystal tunable filter (LCTF) technology represents a revolutionary advancement in imaging spectrometer technology that is ideally suited to Raman imaging microscopy.

I am providing this letter as a consultant in support of CRI's Phase II SBIR application to the National Science Foundation entitled "High-Definition Raman Imaging Microscope." My role in this project is to assist in the development of liquid crystal tunable filters (LCTFs) and their application to Raman imaging. Through my involvement with industrial and clinical end users of Raman chemical imaging I will also contribute to the commercialization of the technology. My consultant rate is \$420/day and I will provide 60 days of effort over the term of the anticipated grant.

I look forward to CRI's continued success in the development of high quality LCTF technology for Raman imaging.

Sincerely,

A handwritten signature in cursive script that reads "Pat Treado".

Patrick J. Treado
Assistant Professor

CRI000703

SUMMARY PROPOSAL BUDGET

CUMULATIVE BUDGET

ORGANIZATION				PROPOSAL NO.		DURATION (MONTHS)	
University of Pittsburgh						Proposed	
PRINCIPAL INVESTIGATOR/PROJECT DIRECTOR				AWARD NO.		Granted	
Patrick Treado							
A. SENIOR PERSONNEL: P/VPD, Co-PI's, Faculty and Other Senior Associates (List each separately with title, A.7. show number in brackets)				NSF-Funded Person-months		Funds Requested By Proposer	Funds Granted By NSF (If Different)
				CAL	ACAD	SUMR	
1.							
2.							
3.							
4.							
5.							
6. () OTHERS (LIST INDIVIDUALLY ON BUDGET EXPLANATION PAGE)							
7. () TOTAL SENIOR PERSONNEL (1-6)							
B. OTHER PERSONNEL (SHOW NUMBERS IN BRACKETS)							
1. () POST DOCTORAL ASSOCIATES							
2. () OTHER PROFESSIONALS (TECHNICIAN, PROGRAMMER, ETC.)							
3. () GRADUATE STUDENTS (8 months)						9,782	
4. () UNDERGRADUATE STUDENTS							
5. () SECRETARIAL - CLERICAL (IF CHARGED DIRECTLY)							
6. () OTHER							
TOTAL SALARIES AND WAGES (A+B)						9,782	
C. FRINGE BENEFITS (IF CHARGED AS DIRECT COSTS) 34.7 B3						3,326	
TOTAL SALARIES, WAGES AND FRINGE BENEFITS (A+B+C)						13,108	
D. EQUIPMENT (LIST ITEM AND DOLLAR AMOUNT FOR EACH ITEM EXCEEDING \$5,000.)							
TOTAL EQUIPMENT							
E. TRAVEL 1. DOMESTIC (INCL. CANADA, MEXICO AND U.S. POSSESSIONS)							
2. FOREIGN							
F. PARTICIPANT SUPPORT COSTS							
1. STIPENDS \$							
2. TRAVEL							
3. SUBSISTENCE							
4. OTHER							
() TOTAL PARTICIPANT COSTS							
G. OTHER DIRECT COSTS							
1. MATERIALS AND SUPPLIES				132			
2. PUBLICATION COSTS/DOCUMENTATION/DISSEMINATION							
3. CONSULTANT SERVICES							
4. COMPUTER SERVICES							
5. SUBAWARDS							
6. OTHER							
TOTAL OTHER DIRECT COSTS				132			
H. TOTAL DIRECT COSTS (A THROUGH G)				13,240			
I. INDIRECT COSTS (SPECIFY RATE AND BASE)							
48% MTDC; Base 9,914							
TOTAL INDIRECT COSTS				4,760			
J. TOTAL DIRECT AND INDIRECT COSTS (H + I)				18,000			
K. RESIDUAL FUNDS (IF FOR FURTHER SUPPORT OF CURRENT PROJECT SEE GPG II.D.7.J)							
L. AMOUNT OF THIS REQUEST (J) OR (J MINUS K)				\$18,000			
M. COST-SHARING: PROPOSED LEVEL \$				AGREED LEVEL IF DIFFERENT \$			
P/VPD TYPED NAME & SIGNATURE*				DATE			
Patrick Treado				10/30/96			
ORG. REP. TYPED NAME & SIGNATURE*				DATE			
Michael M. Crouch				10/30/96			
				FOR NSF USE ONLY			
				INDIRECT COST RATE VERIFICATION			
				Date Checked			
				Date of Rate Sheet			
				Initials-ORG			

NSF Form 1030 (7/95) Supersedes All Previous Editions

*SIGNATURES REQUIRED ONLY FOR REVISED BUDGET (GPG III.B)

TOTAL P. 01

CRI000704

EXHIBIT M

TITLE

CHEMICAL IMAGING SYSTEM

FIELD OF INVENTION

The invention relates to spectroscopic imaging systems in general and Raman chemical imaging systems in particular. The invention also relates to the use of chemical imaging systems in medical diagnosis.

BACKGROUND OF THE INVENTION

Chemical imaging is a new scientific discipline, which combines the chemical analysis power of optical spectroscopy, including Raman, infrared and fluorescence techniques, with high-resolution optical imaging. It has powerful capability for materials characterization, process monitoring, quality control and disease-state determination. This invention relates to a system for obtaining spectroscopically resolved images of materials, including biological samples, using electronically tunable imaging spectrometers employing liquid crystal elements.

Raman and infrared chemical imaging provide molecular-specific image contrast without the use of stains or dyes. Raman and infrared image contrast is derived from a material's intrinsic vibrational spectroscopic signature, which is highly sensitive to the composition and structure of the material and its local chemical environment. As a result, Raman and infrared imaging can be performed with little or no sample preparation and are widely applicable for materials research, failure analysis, process monitoring and clinical diagnostics.

09064347.042299

Several approaches to Raman imaging have been demonstrated that employ means to simultaneously record spatial and Raman spectral information. Almost exclusively, modern Raman imaging methods employ multi-channel charge-coupled device (CCD) detection. CCDs are employed to record two dimensions of the three-dimensional information inherent in Raman image data sets. Raman imaging systems can be differentiated by the means they employ to collect the third dimension of information. Raman imaging systems employing dispersive monochromators coupled to CCDs have been devised that rely on two-dimensional point scanning, one-dimensional line scanning, and spatial multiplexing. In addition, Michelson interferometers have been employed in point scanning systems, while a number of tunable filter spectrometers have been described in the past several years.

Of the imaging spectrometers that have been employed for Raman imaging, including liquid crystal tunable filters (LCTFs), acousto-optic tunable filters (AOTFs) and Fabry-Perot filters, LCTFs are the most effective. In general, tunable filter methods employ wide-field laser illumination in combination with multichannel detection. The two spatial dimensions of the image are recorded directly by the CCD camera, while the multispectral information is acquired by capturing images at discrete wavelengths selected by the tunable filter. Under computer control it is possible to collect a data set with a Raman spectrum at each pixel of the image. An advantage of tunable filters is that they provide image fidelity that is limited only by the number of pixels in the camera. As a result, the use of high-definition detectors allows the efficient collection of high-definition images. Prior to the introduction of LCTFs, a key limitation of tunable filters that had handicapped Raman microscopy had been the lack of the availability of tunable filters that simultaneously provided narrow spectral bandpass, broad free spectral range

and high image quality. For example, AOTF Raman imaging systems provide high throughput and broad spectral coverage, but AOTFs have distinct limitations. AOTFs suffer from broad spectral bandpass, and imaging performance is degraded appreciably from the diffraction-limited conditions. In effect, AOTFs provide spectral resolution that is an order of magnitude worse than that of a typical Raman spectrometer, and spatial resolution that is approximately 2.5 times worse than the diffraction limit.

A better alternative to the AOTF is the LCTF. In general, LCTFs are electro-optically controllable spectral bandpass filters which can function from the visible to the near-infrared. A number of LCTF designs have been demonstrated for use in multispectral imaging. LCTFs based on the Lyot filter design have been used primarily as red-green-blue (RGB) color filters and fluorescence imaging filters. A nematic LCTF based on the design of the Lyot birefringent filter has been used in a Raman imaging system. The multistage Lyot filter is comprised of a fixed retardance birefringent element and a nematic liquid crystal wave plate placed between parallel linear polarizers. The nematic liquid crystal wave plates incorporated within the Lyot filter act as electronically controlled phase retarders. The LC wave plates can be adjusted over a continuous range of retardance levels, enabling continuous tunability of wavelength. In general, Lyot filters suffer from low peak transmittance. The two main sources of optical loss in the Lyot LCTFs are absorption in the polarizers and imperfect waveplate action arising from the use of simple $\lambda/2$ plates to construct the wide-field retarder stages. An LCTF based on a Fabry-Perot design has been demonstrated for Raman microscopy. However, Fabry-Perot filters suffer from low transmittance, low out of band rejection efficiency, limited free

spectral range and low spectral bandpass (25 cm^{-1}). In addition, Fabry-Perot filters are susceptible to thermal-induced drift in spectral bandpass unless contained in temperature-controlled housings.

John Evans described a 'split-element' design that addresses the inefficiency of the Lyot design. The 'split-element' design cuts the number of polarizers in half, plus one, reducing the absorbance of light due to the polarizers. In addition, the $\lambda/2$ waveplates are eliminated providing enhanced optical throughput. This yields an improved filter transmission ranging from 1.55 - 3.1 times that of the Lyot filter.

Unlike other tunable elements for Raman imaging, the LCTF is free of optical distortions, spectral leakage, or image shift with tuning. The first generation (Lyot) LCTFs were designed to operate with green laser excitation and operated only to 650 nm. Evans Split-Element LCTFs operate from 420-720 nm and from 650-1100 nm, as determined by the choice of polarizers. Operation in the red wavelength region has advantages, particularly for the analysis of biological systems. For example, operation in the red wavelength region provides enhanced fluorescence rejection when combined with efficient diode laser sources and takes full advantage of the enhanced red sensitivity of recent generation CCD detectors.

Compared to existing, non-imaging systems, the Raman LCTF system adds the powerful ability to visualize the distribution (morphology and architecture) of chemical species in heterogeneous samples with molecular compositional specificity. Raman images can be collected rapidly, non-invasively, with limited or no sample preparation, at high spatial resolution ($< 250 \text{ nm}$) and with high fidelity where the spatial fidelity is limited by the number of

pixels on the CCD detector. Most importantly, every image pixel has associated with it a Raman spectrum whose quality is comparable to that obtained with conventional non-imaging spectrometers.

Raman is so broadly applicable because most materials exhibit characteristic 'fingerprint' Raman vibrational spectra. Generally accepted practice in performing Raman microscopy is to use non-imaging techniques such as a scanned laser Raman microspot, which yield spectral data but limited (or inefficient) collection of spatial data. Samples exhibiting complex morphologies and well characterized spectral bands are best studied using LCTF technology because of the inherent efficiency of analyzing all spatial channels simultaneously in a massively parallel fashion. The LCTF Raman chemical imaging measurement identifies the presence and/or location of an analyte species in a sample by imaging at the characteristic analyte Raman spectral bands. In general, it is not necessary to have a complete Raman spectrum at each image pixel in order to obtain meaningful and chemically relevant image contrast. This is especially due in part to the redundancy of a typical Raman spectrum. Often only several regions of the spectrum are needed to generate analyte-specific image contrast. The Evans Split-Element LCTF represents a breakthrough technology because it provides spectral resolution comparable to a single stage dispersive monochromator while also providing diffraction-limited spatial resolution. This performance is provided without moving mechanical parts in a computer controlled device which allows automated operation.

Cancer is a major cause of death worldwide. Early definitive detection and classification of cancerous growths is often crucial to successful treatment of this disease. Currently, several biopsy techniques are used as diagnostic methods after cancerous lesions are

identified. In the case of breast cancer, lesions are typically identified with mammography or self breast exam. The most reliable method of diagnosis is examination of macroscopic-sized lesions. Macroanalysis is performed in conjunction with microscopic evaluation of paraffin-embedded biopsied tissue which is thin-sectioned to reveal microscale morphology.

The detection and diagnosis of cancer is typically accomplished through the use of optical microscopy. A tissue biopsy is obtained from a patient and that tissue is sectioned and stained. The prepared tissue is then analyzed by a trained oncologist who can differentiate between normal, malignant and benign tissue based on tissue morphology. Because of the tissue preparation required, this process is relatively slow. Moreover, the differentiation made by the oncologist is based on subtle morphological differences between normal, malignant and benign tissue based on tissue morphology. For this reason, there is a need for an imaging device that can rapidly and quantitatively diagnose malignant and benign tissue.

Alternatives to traditional surgical biopsy include fine needle aspiration cytology and needle biopsy. These non-surgical techniques are becoming more prevalent as breast cancer diagnostic techniques because they are less invasive than biopsy techniques that harvest relatively large tissue masses. Fine needle aspiration cytology has the advantage of being a rapid, minimally invasive, non-surgical technique that retrieves isolated cells that are often adequate for evaluation of disease state. However, in fine needle biopsies intact breast tissue morphology is disrupted often leaving only cellular structure for analysis which is often less revealing of disease state. In contrast, needle biopsies use a much larger gauge needle which retrieve intact tissue samples that are better suited to morphology analysis. However, needle

biopsies necessitate an outpatient surgical procedure and the resulting needle core sample must be embedded or frozen prior to analysis.

A variety of "optical biopsy" techniques have potential as non-invasive, highly sensitive approaches that will augment, or even be alternatives to current diagnostic methods for early detection of cancer, including breast cancer. Optical biopsies employ optical spectroscopy to non-invasively probe suspect tissue regions *in situ*, without extensive sample preparation. Diagnostic information is provided by the resultant spectroscopically unique signatures that allow differentiation of normal and abnormal tissues. One biodiagnostic technique is fluorescence optical biopsy. Due to the nonspecific nature of tissue autofluorescence and the need to add staining agents to augment the specificity of fluorescence approaches, this technique has limitations.

In contrast to other techniques, Raman spectroscopy holds promise as an optical biopsy technique that is anticipated to be broadly applicable for characterization of a variety of cancerous disease states. A number of researchers have shown that Raman spectroscopy has utility in differentiating normal vs. malignant tissue and differentiating normal vs benign tissue. In general, the Raman spectra of malignant and benign tissues show an increase in protein content and a decrease in lipid content versus normal breast tissue, demonstrating that cancer disease states have a molecular basis for their origin.

However, difficulties exist when trying to use Raman spectroscopy alone to differentiate benign vs. malignant tissues due to the spectral similarities of these tissue types. In addition, Raman spectroscopy of breast tissue samples requires large numbers of cell populations. If only a small portion of the cells are cancerous, as in the early stages of lesion

development, then Raman spectroscopy will be insensitive to the disease. It would be advantageous to have a technique capable of the spatial sensitivity needed for discrimination of cancerous from normal cells in early stage breast cancer diagnosis.

Chemical imaging based on optical spectroscopy, in particular Raman spectroscopy, provides the clinician with important information. Chemical imaging simultaneously provides image information on the size, shape and distribution (the image morphology) of molecular chemical species present within the sample. By utilizing molecular-specific imaging, based on chemical imaging, the trained clinician can make a determination on the disease-state of a tissue or cellular sample based on recognizable changes in morphology without the need for sample staining or modification.

SUMMARY OF THE INVENTION

A Raman chemical imaging system is provided which can be used to make a rapid, quantitative cancer diagnosis that is applicable to histopathology and *in vivo* applications. In the system, a sample is obtained from the patient through traditional biopsy procedures. A laser illumination source, coupled via directly beaming the laser into the entrance aperture of the system or via a fiber optic, illuminates an area of the sample to be diagnosed. An objective collects an image of scattered light from the illuminated area of the sample and produces a beam therefrom. An Evans Split-Element liquid crystal tunable filter selects a Raman image of the beam. A detector collects the filtered Raman images which are then processed to determine quantitatively whether the Raman images conform to normal, malignant or benign tissues and cells.

In this method, the processor compares the Raman spectra at each Raman image pixel with a library of Raman spectra stored for healthy tissue and cancerous tissue. The processor selects the closest match between the Raman image and the library of Raman spectra. The processor then produces an image of the tissue sample from said selected matches.

An objective of this invention is to provide an LCTF suitable for Raman imaging which can readily and rapidly distinguish between various materials. The LCTF, an Evans Split-Element-type filter, provides diffraction-limited spatial resolution and spectral resolution that is comparable to that provided by a dispersive Raman monochromator. The Evans Split-Element-type LCTF provides high out-of-band rejection, broad free spectral range, high peak transmittance, and highly reproducible computer-controlled tuning.

BRIEF DESCRIPTION OF THE DRAWINGS

Figure 1 is a schematic diagram of a presently preferred embodiment of the Raman chemical imaging system of the present invention.

Figure 2 is a brightfield image of a human tissue biopsy thin section.

Figure 3 shows Raman spectra of normal tissue and malignant cancer tissue.

Figures 4A-4B
Figure 4 are Raman images of the same human tissue biopsy of Figure 2 collected with the Raman chemical imaging system of the present invention using an Evans Split-Element LCTF. 4A shows a Raman image of cancerous cells within the breast tissue biopsy. 4B shows a Raman image of normal cells within the breast tissue biopsy.

DETAILED DESCRIPTION OF PREFERRED EMBODIMENTS

In Raman spectroscopy, laser light induces a scattering effect of the sample. Chemical composition and structure are determined by the light emitted by the sample. Typical data is output as intensity values at wavelengths in a predefined range.

In Raman chemical imaging, Raman spectroscopy is combined with imaging processes. Light intensity is recorded as a function of both wavelength and location. The image domain contains the full image at each individual wavelength. The spectroscopy domain contains the fully resolved spectrum at each individual pixel. As a result of Raman chemical imaging, both structural and compositional information can be determined consistently.

Figure 1 is a schematic diagram of the LCTF Raman chemical imaging system. Laser epi-illumination is provided by a laser 1, such as a Spectra Physics Millennia II Nd:YVO₄ laser, beamed directly into the microscope or imaging optic. Alternatively, the laser light is coupled via optical fiber to the imaging optic 5, such as an infinity-corrected Olympus BX60 microscope. A bandpass filter 2 such as a dielectric bandpass filter, efficiently removes SiO₂ Raman bands that arise from the laser excitation fiber optic. The laser light is directed to a bandreject optical filter 7 optimized for oblique illumination at 7° relative to normal incidence. The reflected light propagates through an imaging optic 4 and illuminates the sample 5. The Raman emission is collected with the same objective and is transmitted through the notch filter which rejects light at the laser wavelength. A second notch filter is positioned after the first filter and provides additional rejection of the laser source.

Confocal Raman point microspectroscopy is performed by employing a swing away mirror 8 placed before the LCTF to redirect the Raman emission to a fiber-optic 10. The other end of the fiber is configured in a linear geometry and is focused on the entrance slit of a spectrograph 15. The Raman spectrum is collected with a CCD detector located at the exit focal plane of the spectrometer 16.

In imaging mode, the magnified Raman image is coupled through the Evans Split-Element LCTF 11 and collected on a high dynamic range, cooled charge-coupled device (CCD) detector 14.

The LCTF Split-Element design includes a high-order fixed retarder of thickness D , having retardance R_h , constructed as two elements of thickness $D/2$, with their fast and slow axes crossed. A low-order retarder of retardance R_l is interposed with its fast axis at 45° to that of the $D/2$ elements. Each retarder has an associated liquid crystal tuning element. Such an assembly, placed between suitably oriented crossed polarizers, has a transmission of

$$T(\lambda) = \sin^2(\pi R_l / \lambda) \times \sin^2(\pi R_h / \lambda).$$

The split-element stage is equivalent in its spectral performance to two Lyot stages. By constructing the LCTF as groups of split-element stages, one collapses an N -stage Lyot filter into $N/2$ split-element Lyot stages, and reduces the number of polarizers by $N/2$. The reduction of polarizers is compensated by the increased number of liquid crystal tuning elements which enhance the overall optical throughput.

A processing unit 17, typically a Pentium computer, is used for Raman image collection and processing. The CCD detector 14 is operated with commercial software, such as ChemIcon, ChemImage.

Every material has a characteristic "fingerprint" based on molecular composition. For this reason, the ability of the Raman chemical imaging system to measure quantitative responses of analyzed materials renders it suitable for a variety of purposes. For example, Raman imaging systems can be used to detect metal corrosion, determine polymer architecture and molecular composition. In addition, the Raman chemical imaging system can also be used in pathology analysis wherein the molecular specificity of Raman imaging provides a mechanism for the diagnostic evaluation of tissue.

Because Raman spectroscopy can readily detect the characteristic "fingerprint" of discrete molecular compositions, it has the potential to make histopathology analysis more quantitative. Using traditional Raman spectroscopy, the differences between normal tissue and lesions, such as lipids and proteins, can be readily determined based on the Raman spectrum. However, traditional Raman spectroscopy is unable to distinguish between benign and malignant tissue. However, the use of a Evans Split-Element LCTF provides the ability to distinguish between normal tissue, malignant tissue and benign tissue.

The optimized LCTF Raman microscope provides high spatial and spectral resolution. The image quality of the LCTF is shown in Figure 2, a brightfield image of a human tissue biopsy sample. Figure 2 is collected with the LCTF in the optical path and fine morphological details of the tissue sample, including individual cellular components, are

observable. Malignant breast cells are visible in the left portion of the image. Normal breast cells are visible in the right portion of the image.

Figure 3 shows the spectra of normal tissue and malignant cancerous tissue. The spectra were collected by coupling the Raman scatter from discrete sample regions (normal or diseased) to the dispersive Raman spectrometer via fiber optics. Figure 3 shows that the differences between the spectra of normal tissue and benign and malignant cancerous tissue which can be distinguished using Raman spectroscopy. In particular, differences in the lipid Raman band at 1445 cm^{-1} are observable due to the decrease in the relative amount of lipid.

Figure 4 are Raman images of the same human tissue biopsy of Figure 2 collected with the LCTF. The images are collected by tuning the LCTF from 1200 to 1800 cm^{-1} and capturing images at discrete intervals. The image data set is then processed using multivariate image analysis routines that classify the image pixels which are linearly independent Raman spectra by their similarity to a library spectrum of normal or diseased material. The Raman image of Figure 4 (left) distinguishes the malignant cancer tissue of the sample. The Raman image of Figure 4 (right) distinguishes the normal cancer tissue of the sample. The Raman image in Figure 4 is unparalleled in Raman imaging and was collected in 10 minutes.

The advantage of LCTF technology over competitive approaches is the ability to simultaneously collect high spectral/spatial information. The benefit is best realized in the analysis of multicomponent heterogeneous systems, where having a high-quality Raman spectrum at each pixel of the image makes the analysis of complex matrices less subjective and based primarily on quantitative parameters. From the high-quality spectra, sample composition and quantitation has been demonstrated. In this manner, the present Raman chemical imaging

system can be used to provide a diagnosis of cancer or other pathology determinations. As a result, specific outcomes are anticipated, including: (1) real-time diagnosis of suspicious lesions sites identified through self-breast exam and/or mammography that are made accessible via needle core biopsy; (2) immediate feedback to the clinician as to the severity of the clinical situation with results being communicated to the patient upon completion of Raman biopsy; (3) potential information on prognostic indicators of disease such as growth rate through quantitative evaluation of cellular nucleic acid composition; (4) minimal patient discomfort; (5) no cosmetic defect of the breast; and (6) reduced exposure to ionizing radiation (x-rays) through overall reduction in use of mammography for lesion screening.

Although present preferred embodiments of the invention have been shown and described, it should be distinctly understood that the invention is not limited thereto but may be variously embodied within the scope of the following claims.

I claim:

1. A chemical imaging system comprising:
 - (a) a laser illumination source for illuminating an area of a sample;
 - (b) an objective for collecting a spectrum of scattered light from said illuminated area of said sample and producing a collimated beam therefrom;
 - (c) a liquid crystal tunable filter for selecting a chemical image of said collimated beam, said filter being an Evans Split-Element liquid crystal tunable filter; and
 - (d) detector for collecting said filtered chemical images.

2. The system of claim further comprising processing means for producing a chemical image of said sample.

3. A method of detecting cancerous tissue or cells in a sample comprising the steps of:

- (a) producing a Raman image of a sample of tissue or cellular material;
- (b) comparing said Raman image with a library of Raman spectra stored for healthy tissue or cellular material and cancerous tissue or cellular material;

- (c) selecting the closest match between said Raman image of said library of Raman spectra; and
 - (d) producing an image of said tissue or cellular material sample from said selected matches.
-

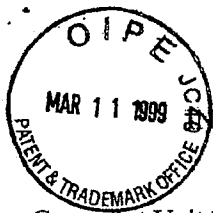
09064347-04290
862240-44549060

09/06/0347

ABSTRACT OF THE DISCLOSURE

A Raman chemical imaging system uses a laser illumination source for illuminating an area of a sample. The spectrum of scattered light from the illuminated area of the sample is collected and a collimated beam is produced therefrom. An Evans Split-Element type liquid crystal tunable filter (LCTF) selects a Raman image of the collimated beam. A detector collects the filtered Raman images which are subsequently processed to determine the constituent materials. The Evans Split-Element-type LCTF suitable for high-definition Raman chemical imaging is incorporated into an efficient Raman imaging system that provides significant performance advantages relative to any previous approach to Raman microscopy. The LCTF and associated optical path is physically compact, which accommodates integration of the LCTF within an infinity-corrected optical microscope. The LCTF simultaneously provides diffraction-limited spatial resolution and 9 cm^{-1} spectral bandpass across the full free spectral range of the imaging spectrometer. The LCTF Raman microscope successfully integrates the utility of optical imaging and the analytical capabilities of Raman spectroscopy which has practical significance in materials analysis, including the diagnosis of cancer.

EXHIBIT N



THE UNITED STATES PATENT AND TRADEMARK OFFICE

Group Art Unit 2877

Examiner K. P. Hantis

In re application of

PATRICK TREADO

Serial No. 09/064,347

Filed April 22, 1998

CHEMICAL IMAGING SYSTEM

5/24/98
DECLARATION
NO MAR 23 PM 1:36

RULE 1.132 DECLARATION OF PATRICK TREADO

I, Patrick Treado, do declare and state as follows:

1. I am the sole inventor of United States Patent Application Serial No. 09/064,347 for a Chemical Imaging System.
2. I have been active in the field of Raman imaging since 1986. Since then, I have made use of a number of approaches for fully utilizing Raman imaging. Since 1991, I have studied the use of tunable filters, including those based on liquid crystals and acousto-optics, used in connection with a Raman imaging system.
3. Persons having ordinary skill in the art of Raman imaging would not have thought to use an Evans Split Element liquid crystal tunable filter (LCTF) in place of traditional liquid crystal filters.
4. The -Evans Split Element filter was invented for color imaging and display which is very different than Raman imaging. Typically, these LCTFs are characterized by high speed, high throughput, broad spectral bandpasses, but reduced out of passband rejection efficiency, and inhomogeneous response across the filter. Requirements of color filters are very

different than the requirements of a Raman imaging spectrometer. To those practiced in the art of color imaging, Raman imaging would be far afield and a non-obvious application. Color imaging relies on high light levels to form images in real-time. Raman imaging is forced to rely on low light levels to form images relatively slowly where most of the light is background fluorescence light and only a small fraction is Raman light. In Raman imaging, high performance instrumentation is employed including high power lasers and ultrasensitive imaging detectors.

5. To those practiced in the art of Raman imaging, color imaging filter characteristics would teach away from their potential use as Raman imaging devices. One of the principal trends in Raman spectroscopy and imaging involved the use of multichannel detectors to capture spectra and images. These multichannel detectors helped to revolutionize traditional Raman spectroscopy which had relied on single element detectors in combination with scanning spectrometers. The operation of color filters teaches away from the art because they rely upon scanning of the spectral dimension in order to build up the color (i.e. spectral) information. To those practiced in the art of Raman spectroscopy, the concept of relying upon a spectral dimension scanning approach goes against recent trends. I recognized that much of the Raman spectrum is redundant and only a minimum number of spectral bands need to be scanned in order to build up sufficient information to analyze a material of interest.

6. Prior to my invention, Evans Split Element LCTFs were never previously envisioned for Raman imaging. Other researchers in the field of Raman imaging were not active in the tunable filter field. The Treado/Morris article appeared in 1989. The Sharp patent was issued in June 1996. The Raman imaging community is small and has several technical forums

for communication where those skilled in the art actively participate. If the invention was obvious it would have been reduced to practice prior to my invention.

7. Prior to my invention, the Evans Split Element filter was thought to not have sufficient spectral resolution for Raman spectroscopy applications. Today, due to my work, it is becoming widely recognized that Evans Split Element LCTFs are a superior technology for Raman imaging when incorporated into a well designed chemical imaging system. However, those practiced in Raman spectroscopy and imaging prior to 1998 would have assessed the performance of Evans Split Element technology based on traditional measures of Raman instrument performance and would likely have rejected the technology. For example, it is widely believed that a Raman spectrometer has to have resolution of at least 4 cm^{-1} in order to be an effective instrument. Applicant has demonstrated superior system performance using an LCTF that has a spectral resolution of 8 cm^{-1} .

8. Based on its wavelength operating range (visible wavelengths) the Evans Split Element filter was thought to not be applicable for Raman imaging of fluorescent samples. To those practiced in the art of Raman spectroscopy, it would be expected that Raman spectrometers could only be effective when background fluorescence (a source of interference when performing a Raman experiment) was not present. Strategies for eliminating background fluorescence have been developed and accepted as essential by the Raman spectroscopy community. These strategies teach away from the use of a Evans Split Element LCTF operating under conditions discussed in the application – with green wavelength laser sources. Namely, that Evans Split Element LCTFs employed in imaging mode can be used to investigate highly fluorescent species using visible laser illumination and detection. I have recognized that the key to imaging fluorescent samples is that the impurities that typically cause fluorescence are often

not homogeneously distributed throughout the sample and are spatially localized within the material. With the imaging capability of the Evans Split Element filter, the spatially resolved fluorescence interference can often be differentiated from the Raman information that is diagnostic of the sample material of interest.

9. To those practiced in the art of solid-state tunable filters, the Evans Split Element filter is relatively slow (msec tuning speed) as a scanning imaging spectrometer when compared to alternative technologies. The Evans Split Element filter is much slower than other tunable filters such as acousto-optic tunable filters (AOTFs) (microsec tuning speed). The use of AOTFs in Raman imaging was pioneered by me and AOTFs represented state of the art technology when I first used them. Because they were state of the art, a perception developed in the Raman imaging community that AOTFs were suitable for Raman imaging despite key limitations, including low spectral resolution and poor imaging performance. To those practiced in the art, AOTFs would have appeared to be superior to Evans Split Element technology on the basis of tuning speed. However, I recognized that tuning speed is a minor consideration in Raman imaging, because overall image acquisition time is dominated by the low light level conditions which require long signal acquisition times (1-30 secs). The subsecond tuning speeds provided by tunable filters, including Evans Split Element filters, are adequate.

10. Narrow bandpass Evans Split Element filter have an inherently low peak transmittance. For example, the filter can transmit 10% of the light presented to it on average. The low peak transmittance teaches away from its use in a low light level imaging technique like Raman imaging. The peak transmittance of the Evans Split Element filter is relatively low compared with competitive, dispersive Raman spectrometer technology such as volume holographic diffraction gratings that produce greater than 50% transmittance. However, what is

not appreciated by those practiced in the art within the Raman community is that the clear aperture of the Evans Split Element LCTF is substantially larger than the clear aperture of even the most efficient dispersive spectrometers. As a result, the total throughput of the Evans Split Element filter is comparable to or better than competitive technology.

11. Liquid crystal optics are susceptible to temperature drift. The Evans Split Element filter spectral performance is susceptible to temperature induced drift. The drift is more significant than dispersive Raman spectroscopy technology. As a result, to those practiced in the art of Raman spectroscopy, the poor temperature drift performance of the technology would teach away from the technology. A drift compensation approach based on capacitance coupled feedback has been effectively employed by the manufacturer of the Evans Split Element filter. The drift compensation approach would increase in complexity with the number of liquid crystal cells employed in the device. As a result, to those practiced in the art of Evans Split Element filter manufacturing, fabricating a multi-element Evans Split Element filter with adequate temperature compensation would have been viewed as impractical. In order to achieve broad tunability (500-750 nm) and narrow spectral bandpass 8 cm^{-1} (0.25 nm @ 500 nm) simultaneously, the Evans Split Element LCTF requires more than 20 liquid crystal elements. Each of the stages that comprises the Split Element liquid crystal filter passes several bandpasses simultaneously. Optimizing the Evans Split Element filter to pass a single passband and reject out of band light is a daunting fabricating challenge, but as it turns out, it can be accomplished on a routine basis.

12. Fabricating an ultra-narrow bandpass Evans Split Element filter would have been viewed as impractical. Evans Split Element liquid crystal filters were invented for color imaging and display applications. In those applications, spectral bandpasses of ten to a

hundred nanometers are typically employed. For Raman imaging, filters with bandpasses of less than 10 cm^{-1} are required. To those practiced in the art of Evans Split Element filter technology, it would appear impractical to fabricate such a device. Given that the technology had been envisioned for color imaging applications, to those practiced in the art of Raman spectroscopy, it would have appeared impractical that such a device could be fabricated to produce such a narrow spectral bandpass. In essence, the manufactured technology taught away from the art.

13. The inhomogeneous response of the Evans Split Element filter due to off-axis effects teaches away from the use of the device for Raman imaging in two ways. First, inhomogeneous distribution of transmittance in the Evans Split Element filter teaches away from the art. The inhomogeneous transmittance is attributed to an off-axis effect that has been well characterized and previously described (Title and Rosenberg, 1979; Deng, Ai and Wang, 1997). To those practiced in the art of Raman imaging, Raman imaging contrast is based on local intensity variations across the image field of view. Inhomogeneous transmittance would present a real challenge because the Raman intensity images would have superimposed an inhomogeneous transmittance pattern due to the Evans Split Element filter that cannot be compensated using traditional Raman image data processing schemes. I recognized that the inhomogeneous transmittance does not affect the spectral performance of the Evans Split Element filter and Raman imaging data processing of the spectral patterns is an effective approach.

14. The software used in my invention employs a data processing means that corrects for brightness differences - based on multivariate image analysis. Specifically, Raman chemical images that are displayed by my invention are based on spectral shapes and not based

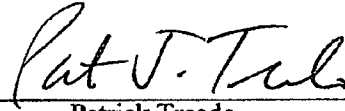
on spectral intensity. As a result, local intensity variations that arise from the inhomogeneous transmittance are compensated.

15. Second, I recognized that the inhomogeneous response of the Evans Split Element filter also manifests itself as inhomogeneous out-of-band rejection efficiency across the Evans Split Element filter. The inhomogeneous out-of-band rejection efficiency teaches away from the art. It is widely recognized that typical Raman applications are background limited. This means that the interference species present in the sample limit the ability to probe the sample. A typical interference is fluorescence background due to impurities in the sample. Another interference is the laser illumination stray light that appears in the microscope due to inefficient mirrors and optical filters. My invention employs carefully placed intermediate apertures that reduce the laser illumination stray light component.

16. However, when a fluorescence background is present, the inhomogeneous out-of-band rejection efficiency cannot be compensated with intermediate apertures. I recognized that the use of spectral patterns recognition approach that compensates for inhomogeneous transmittance also compensates for inhomogeneous out-of-band rejection efficiency. The software used in my invention employs a data processing means that corrects for out-of-band rejection differences - based on multivariate image analysis. As a result, Raman chemical images displayed by my invention that are based on spectral shapes and local intensity variations that arise from the inhomogeneous out-of-band rejection efficiency are compensated.

I declare that the foregoing is true and correct, that all statements made on information and belief are believed to true, and, further, that these statements were made with the knowledge that willful false statements and the like so made are punishable by fine,

imprisonment, or both, under Section 1001 of Title 18 of the United States Code, and that any false statements may jeopardize the validity of this Declaration and the above-identified patent.



Patrick Treado

EXHIBIT O



US006002476A

United States Patent [19]
Treado

[11] **Patent Number:** **6,002,476**
 [45] **Date of Patent:** **Dec. 14, 1999**

[54] **CHEMICAL IMAGING SYSTEM**[75] **Inventor:** Patrick Treado, Pittsburgh, Pa.[73] **Assignee:** ChemIcon Inc., Pittsburgh, Pa.[21] **Appl. No.:** 09/064,347[22] **Filed:** Apr. 22, 1998[51] **Int. Cl.⁶** G01J 3/44[52] **U.S. Cl.** 356/301[58] **Field of Search** 356/301, 310,
 356/326, 328, 330-334[56] **References Cited****U.S. PATENT DOCUMENTS**

5,194,912 3/1993 Batchelder et al. .

5,442,438 8/1995 Batchelder et al. .

5,528,393 6/1996 Sharp et al. .

5,623,342 4/1997 Baldwin et al. .

5,689,333 11/1997 Batchelder et al. .

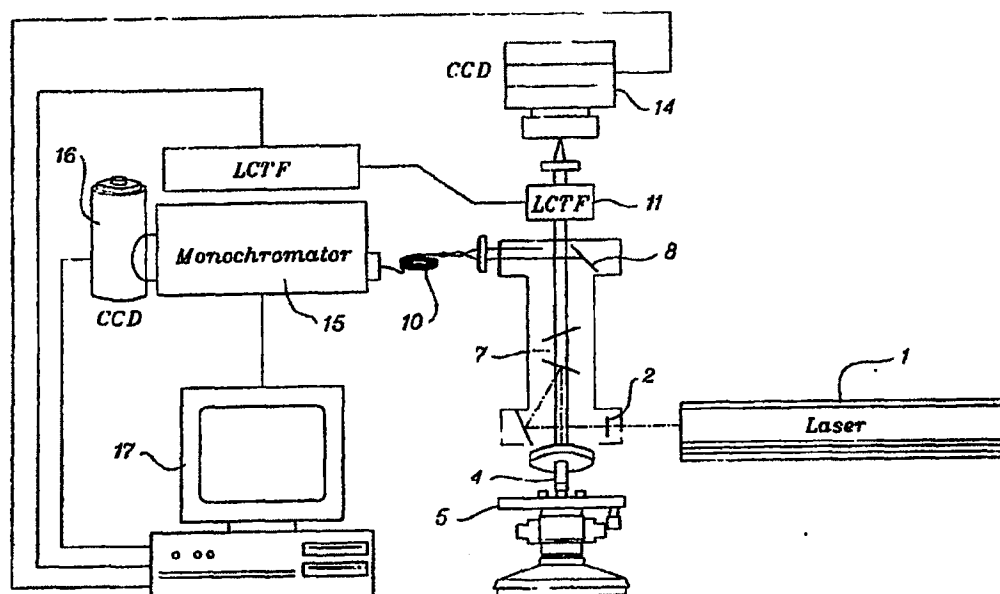
OTHER PUBLICATIONS

Treado et al "A Thousand Points of Light: The Hadamard Transform" *Analytical Chemistry* 61 (1989) Jun. 1, No. 11, pp. 722-734.

H. Morris, C. Hoyt, P. Miller and P. Treado "Liquid Crystal Tunable Filter Raman Chemical Imaging", vol. 50 *Applied Spectroscopy* No. 6, pp. 805-811 (1996).

*Primary Examiner—K. P. Hantis**Attorney, Agent, or Firm—Buchanan Ingersoll, P.C.*[57] **ABSTRACT**

A Raman chemical imaging system uses a laser illumination source for illuminating an area of a sample. The spectrum of scattered light from the illuminated area of the sample is collected and a collimated beam is produced therefrom. An Evans Split-Element type liquid crystal tunable filter (LCTF) selects a Raman image of the collimated beam. A detector collects the filtered Raman images which are subsequently processed to determine the constituent materials. The Evans Split-Element-type LCTF suitable for high-definition Raman chemical imaging is incorporated into an efficient Raman imaging system that provides significant performance advantages relative to any previous approach to Raman microscopy. The LCTF and associated optical path is physically compact, which accommodates integration of the LCTF within an infinity-corrected optical microscope. The LCTF simultaneously provides diffraction-limited spatial resolution and 9 cm^{-1} spectral bandpass across the full free spectral range of the imaging spectrometer. The LCTF Raman microscope successfully integrates the utility of optical imaging and the analytical capabilities of Raman spectroscopy which has practical significance in materials analysis, including the diagnosis of cancer.

2 Claims, 4 Drawing Sheets

CRI001156

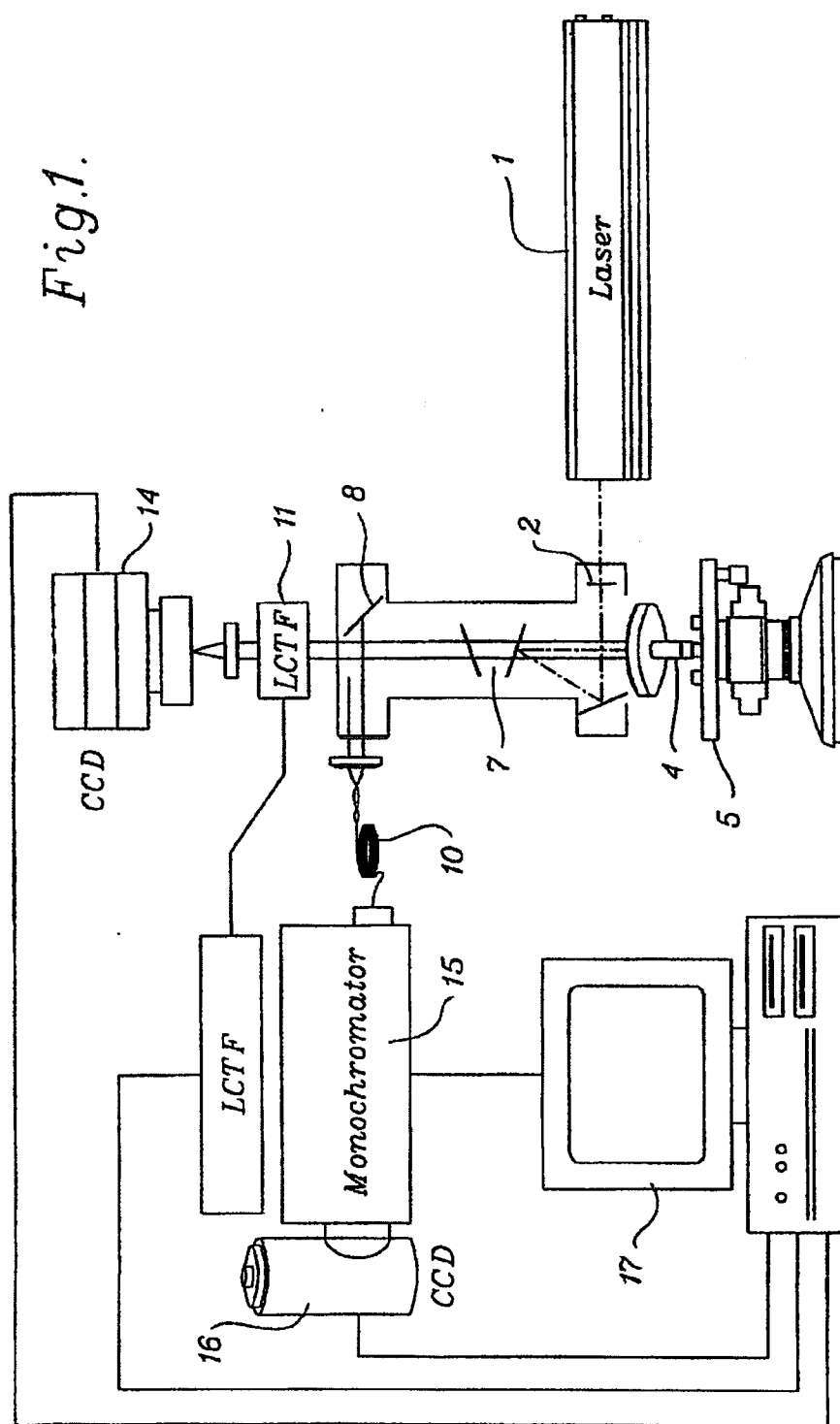
U.S. Patent

Dec. 14, 1999

Sheet 1 of 4

6,002,476

Fig. 1.



U.S. Patent

Dec. 14, 1999

Sheet 2 of 4

6,002,476

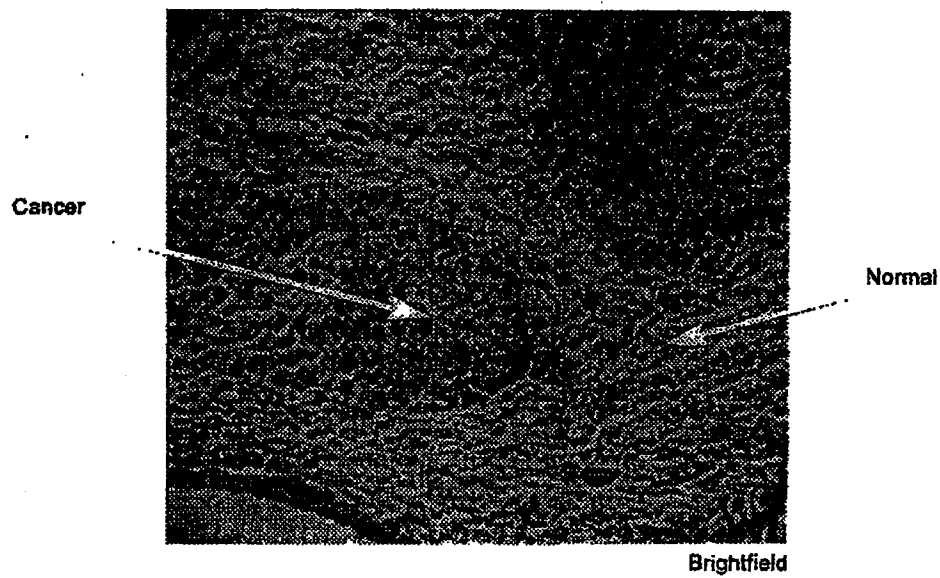


Figure 2.

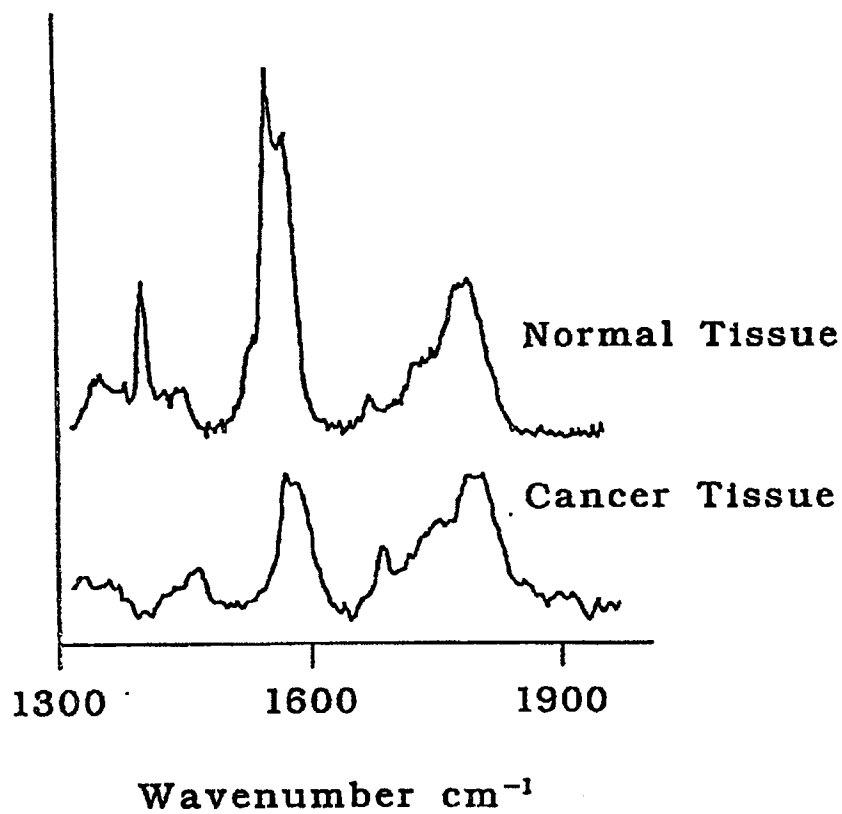
U.S. Patent

Dec. 14, 1999

Sheet 3 of 4

6,002,476

Fig. 3.



U.S. Patent

Dec. 14, 1999

Sheet 4 of 4

6,002,476

Raman image of Human Breast Cancer

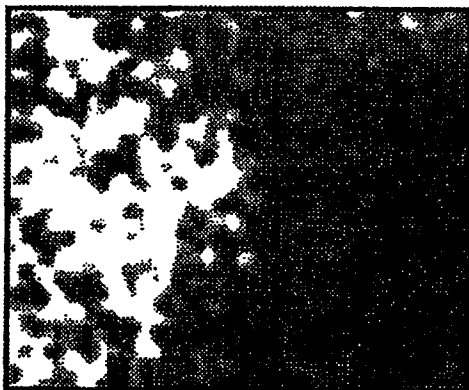


Figure 4a.

Raman image of Normal Tissue

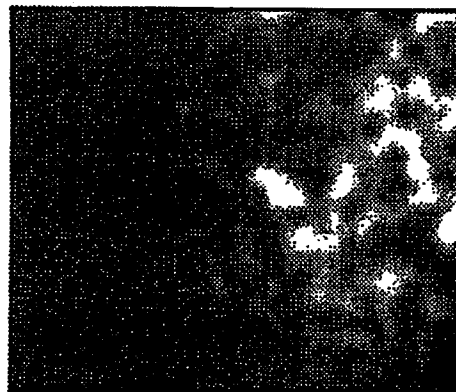


Figure 4b.

6,002,476

1

CHEMICAL IMAGING SYSTEM

FIELD OF THE INVENTION

The invention relates to spectroscopic imaging systems in general and Raman chemical imaging systems in particular. The invention also relates to the use of chemical imaging systems in medical diagnosis.

BACKGROUND OF THE INVENTION

Chemical imaging is a new scientific discipline, which combines the chemical analysis power of optical spectroscopy, including Raman, infrared and fluorescence techniques, with high-resolution optical imaging. It has powerful capability for materials characterization, process monitoring, quality control and disease-state determination. This invention relates to a system for obtaining spectroscopically resolved images of materials, including biological samples, using electronically tunable imaging spectrometers employing liquid crystal elements.

Raman and infrared chemical imaging provide molecular-specific image contrast without the use of stains or dyes. Raman and infrared image contrast is derived from a material's intrinsic vibrational spectroscopic signature, which is highly sensitive to the composition and structure of the material and its local chemical environment. As a result, Raman and infrared imaging can be performed with little or no sample preparation and are widely applicable for materials research, failure analysis, process monitoring and clinical diagnostics.

Several approaches to Raman imaging have been demonstrated that employ means to simultaneously record spatial and Raman spectral information. Almost exclusively, modern Raman imaging methods employ multi-channel charge-coupled device (CCD) detection. CCDs are employed to record two dimensions of the three-dimensional information inherent in Raman image data sets. Raman imaging systems can be differentiated by the means they employ to collect the third dimension of information. Raman imaging systems employing dispersive monochromators coupled to CCDs have been devised that rely on two-dimensional point scanning, one-dimensional line scanning, and spatial multiplexing. In addition, Michelson interferometers have been employed in point scanning systems, while a number of tunable filter spectrometers have been described in the past several years.

Of the imaging spectrometers that have been employed for Raman imaging, including liquid crystal tunable filters (LCTFs), acousto-optic tunable filters (AOTFs) and Fabry-Perot filters, LCTFs are the most effective. In general, tunable filter methods employ wide-field laser illumination in combination with multichannel detection. The two spatial dimensions of the image are recorded directly by the CCD camera, while the multispectral information is acquired by capturing images at discrete wavelengths selected by the tunable filter. Under computer control it is possible to collect a data set with a Raman spectrum at each pixel of the image. An advantage of tunable filters is that they provide image fidelity that is limited only by the number of pixels in the camera. As a result, the use of high-definition detectors allows the efficient collection of high-definition images. Prior to the introduction of LCTFs, a key limitation of tunable filters that had handicapped Raman microscopy had been the lack of the availability of tunable filters that simultaneously provided narrow spectral bandpass, broad free spectral range and high image quality. For example, AOTF Raman imaging systems provide high throughput and

2

broad spectral coverage, but AOTFs have distinct limitations. AOTFs suffer from broad spectral bandpass, and imaging performance is degraded appreciably from the diffraction-limited conditions. In effect, AOTFs provide spectral resolution that is an order of magnitude worse than that of a typical Raman spectrometer, and spatial resolution that is approximately 2.5 times worse than the diffraction limit.

A better alternative to the AOTF is the LCTF. In general, LCTFs are electro-optically controllable spectral bandpass filters which can function from the visible to the near-infrared. A number of LCTF designs have been demonstrated for use in multispectral imaging. LCTFs based on the Lyot filter design have been used primarily as red-green-blue (RGB) color filters and fluorescence imaging filters. A nematic LCTF based on the design of the Lyot birefringent filter has been used in a Raman imaging system. The multistage Lyot filter is comprised of a fixed retardance birefringent element and a nematic liquid crystal wave plate placed between parallel linear polarizers. The nematic liquid crystal wave plates incorporated within the Lyot filter act as electronically controlled phase retarders. The LC wave plates can be adjusted over a continuous range of retardance levels, enabling continuous tunability of wavelength. In general, Lyot filters suffer from low peak transmittance. The two main sources of optical loss in the Lyot LCTFs are absorption in the polarizers and imperfect waveplate action arising from the use of simple $\lambda/2$ plates to construct the wide-field retarder stages. An LCTF based on a Fabry-Perot design has been demonstrated for Raman microscopy. However, Fabry-Perot filters suffer from low transmittance, low out of band rejection efficiency, limited free spectral range and low spectral bandpass (25 cm^{-1}). In addition, Fabry-Perot filters are susceptible to thermal-induced drift in spectral bandpass unless contained in temperature-controlled housings.

John Evans described a 'split-element' design that addresses the inefficiency of the Lyot design. The 'split-element' design cuts the number of polarizers in half, plus one, reducing the absorbance of light due to the polarizers. In addition, the $\lambda/2$ waveplates are eliminated providing enhanced optical throughput. This yields an improved filter transmission ranging from 1.55–3.1 times that of the Lyot filter.

Unlike other tunable elements for Raman imaging, the LCTF is free of optical distortions, spectral leakage, or image shift with tuning. The first generation (Lyot) LCTFs were designed to operate with green laser excitation and operated only to 650 nm. Evans Split-Element LCTFs operate from 420–720 nm and from 650–1100 nm, as determined by the choice of polarizers. Operation in the red wavelength region has advantages, particularly for the analysis of biological systems. For example, operation in the red wavelength region provides enhanced fluorescence rejection when combined with efficient diode laser sources and takes full advantage of the enhanced red sensitivity of recent generation CCD detectors.

Compared to existing, non-imaging systems, the Raman LCTF system adds the powerful ability to visualize the distribution (morphology and architecture) of chemical species in heterogeneous samples with molecular compositional specificity. Raman images can be collected rapidly, non-invasively, with limited or no sample preparation, at high spatial resolution ($<250 \text{ nm}$) and with high fidelity where the spatial fidelity is limited by the number of pixels on the CCD detector. Most importantly, every image pixel has associated with it a Raman spectrum whose quality is comparable to that obtained with conventional non-imaging spectrometers.

6,002,476

3

Raman is so broadly applicable because most materials exhibit characteristic "fingerprint" Raman vibrational spectra. Generally accepted practice in performing Raman microscopy is to use non-imaging techniques such as a scanned laser Raman microspot, which yield spectral data but limited (or inefficient) collection of spatial data. Samples exhibiting complex morphologies and well characterized spectral bands are best studied using LCTF technology because of the inherent efficiency of analyzing all spatial channels simultaneously in a massively parallel fashion. The LCTF Raman chemical imaging measurement identifies the presence and/or location of an analyte species in a sample by imaging at the characteristic analyte Raman spectral bands. In general, it is not necessary to have a complete Raman spectrum at each image pixel in order to obtain meaningful and chemically relevant image contrast. This is especially due in part to the redundancy of a typical Raman spectrum. Often only several regions of the spectrum are needed to generate analyte-specific image contrast. The Evans Split-Element LCTF represents a breakthrough technology because it provides spectral resolution comparable to a single stage dispersive monochromator while also providing diffraction-limited spatial resolution. This performance is provided without moving mechanical parts in a computer controlled device which allows automated operation.

Cancer is a major cause of death worldwide. Early definitive detection and classification of cancerous growths is often crucial to successful treatment of this disease. Currently, several biopsy techniques are used as diagnostic methods after cancerous lesions are identified. In the case of breast cancer, lesions are typically identified with mammography or self breast exam. The most reliable method of diagnosis is examination of macroscopic-sized lesions. Macroanalysis is performed in conjunction with microscopic evaluation of paraffin-embedded biopsied tissue which is thin-sectioned to reveal microscale morphology.

The detection and diagnosis of cancer is typically accomplished through the use of optical microscopy. A tissue biopsy is obtained from a patient and that tissue is sectioned and stained. The prepared tissue is then analyzed by a trained oncologist who can differentiate between normal, malignant and benign tissue based on tissue morphology. Because of the tissue preparation required, this process is relatively slow. Moreover, the differentiation made by the oncologist is based on subtle morphological differences between normal, malignant and benign tissue based on tissue morphology. For this reason, there is a need for an imaging device that can rapidly and quantitatively diagnose malignant and benign tissue.

Alternatives to traditional surgical biopsy include fine needle aspiration cytology and needle biopsy. These non-surgical techniques are becoming more prevalent as breast cancer diagnostic techniques because they are less invasive than biopsy techniques that harvest relatively large tissue masses. Fine needle aspiration cytology has the advantage of being a rapid, minimally invasive, non-surgical technique that retrieves isolated cells that are often adequate for evaluation of disease state. However, in fine needle biopsies intact breast tissue morphology is disrupted often leaving only cellular structure for analysis which is often less revealing of disease state. In contrast, needle biopsies use a much larger gauge needle which retrieve intact tissue samples that are better suited to morphology analysis. However, needle biopsies necessitate an outpatient surgical procedure and the resulting needle core sample must be embedded or frozen prior to analysis.

A variety of "optical biopsy" techniques have potential as non-invasive, highly sensitive approaches that will augment,

4

or even be alternatives to current diagnostic methods for early detection of cancer, including breast cancer. Optical biopsies employ optical spectroscopy to non-invasively probe suspect tissue regions in situ, without extensive sample preparation. Diagnostic information is provided by the resultant spectroscopically unique signatures that allow differentiation of normal and abnormal tissues. One biodiagnostic technique is fluorescence optical biopsy. Due to the nonspecific nature of tissue autofluorescence and the need to add staining agents to augment the specificity of fluorescence approaches, this technique has limitations.

In contrast to other techniques, Raman spectroscopy holds promise as an optical biopsy technique that is anticipated to be broadly applicable for characterization of a variety of cancerous disease states. A number of researchers have shown that Raman spectroscopy has utility in differentiating normal vs. malignant tissue and differentiating normal vs. benign tissue. In general, the Raman spectra of malignant and benign tissues show an increase in protein content and a decrease in lipid content versus normal breast tissue, demonstrating that cancer disease states have a molecular basis for their origin.

However, difficulties exist when trying to use Raman spectroscopy alone to differentiate benign vs. malignant tissues due to the spectral similarities of these tissue types. In addition, Raman spectroscopy of breast tissue samples requires large numbers of cell populations. If only a small portion of the cells are cancerous, as in the early stages of lesion development, then Raman spectroscopy will be insensitive to the disease. It would be advantageous to have a technique capable of the spatial sensitivity needed for discrimination of cancerous from normal cells in early stage breast cancer diagnosis.

Chemical imaging based on optical spectroscopy, in particular Raman spectroscopy, provides the clinician with important information. Chemical imaging simultaneously provides image information on the size, shape and distribution (the image morphology) of molecular chemical species present within the sample. By utilizing molecular-specific imaging, based on chemical imaging, the trained clinician can make a determination on the disease-state of a tissue or cellular sample based on recognizable changes in morphology without the need for sample staining or modification.

SUMMARY OF THE INVENTION

A Raman chemical imaging system is provided which can be used to make a rapid, quantitative cancer diagnosis that is applicable to histopathology and in vivo applications. In the system, a sample is obtained from the patient through traditional biopsy procedures. A laser illumination source, coupled via directly beaming the laser into the entrance aperture of the system or via a fiber optic, illuminates an area of the sample to be diagnosed. An objective collects an image of scattered light from the illuminated area of the sample and produces a beam therefrom. An Evans Split-Element liquid crystal tunable filter selects a Raman image of the beam. A detector collects the filtered Raman images which are then processed to determine quantitatively whether the Raman images conform to normal, malignant or benign tissues and cells.

In this method, the processor compares the Raman spectra at each Raman image pixel with a library of Raman spectra stored for healthy tissue and cancerous tissue. The processor selects the closest match between the Raman image and the library of Raman spectra. The processor then produces an image of the tissue sample from said selected matches.

CRI001162

6,002,476

5

An objective of this invention is to provide an LCTF suitable for Raman imaging which can readily and rapidly distinguish between various materials. The LCTF, an Evans Split-Element-type filter, provides diffraction-limited spatial resolution and spectral resolution that is comparable to that provided by a dispersive Raman monochromator. The Evans Split-Element-type LCTF provides high out-of-band rejection, broad free spectral range, high peak transmittance, and highly reproducible computer-controlled tuning.

BRIEF DESCRIPTION OF THE DRAWINGS

FIG. 1 is a schematic diagram of a presently preferred embodiment of the Raman chemical imaging system of the present invention.

FIG. 2 is a brightfield image of a human tissue biopsy thin section.

FIG. 3 shows Raman spectra of normal tissue and malignant cancer tissue.

FIGS. 4a-4b are Raman images of the same human tissue biopsy of FIG. 2 collected with the Raman chemical imaging system of the present invention using an Evans Split-Element LCTF. 4A shows a Raman image of cancerous cells within the breast tissue biopsy. 4B shows a Raman image of normal cells within the breast tissue biopsy.

DETAILED DESCRIPTION OF PREFERRED EMBODIMENTS

In Raman spectroscopy, laser light induces a scattering effect of the sample. Chemical composition and structure are determined by the light emitted by the sample. Typical data is output as intensity values at wavelengths in a predefined range.

In Raman chemical imaging, Raman spectroscopy is combined with imaging processes. Light intensity is recorded as a function of both wavelength and location. The image domain contains the full image at each individual wavelength. The spectroscopy domain contains the fully resolved spectrum at each individual pixel. As a result of Raman chemical imaging, both structural and compositional information can be determined consistently.

FIG. 1 is a schematic diagram of the LCTF Raman chemical imaging system. Laser epi-illumination is provided by a laser 1, such as a Spectra Physics Millennia II Nd:YVO₄ laser, beamed directly into the microscope or imaging optic. Alternatively, the laser light is coupled via optical fiber to the imaging optic 5, such as an infinity-corrected Olympus BX50 microscope. A bandpass filter 2 such as a dielectric bandpass filter, efficiently removes SiO₂ Raman bands that arise from the laser excitation fiber optic. The laser light is directed to a bandreject optical filter 7 optimized for oblique illumination at 7° relative to normal incidence. The reflected light propagates through an imaging optic 4 and illuminates the sample 5. The Raman emission is collected with the same objective and is transmitted through the notch filter which rejects light at the laser wavelength. A second notch filter is positioned after the first filter and provides additional rejection of the laser source.

Confocal Raman point microspectroscopy is performed by employing a swing away mirror 8 placed before the LCTF to redirect the Raman emission to a fiber-optic 10. The other end of the fiber is configured in a linear geometry and is focused on the entrance slit of a spectrograph 15. The Raman spectrum is collected with a CCD detector located at the exit focal plane of the spectrometer 16.

In imaging mode, the magnified Raman image is coupled through the Evans Split-Element LCTF 11 and collected on a high dynamic range, cooled charge-coupled device (CCD) detector 14.

6

The LCTF Split-Element design includes a high-order fixed retarder of thickness D, having retardance R_h, constructed as two elements of thickness D/2, with their fast and slow axes crossed. A low-order retarder of retardance R_l is interposed with its fast axis at 45° to that of the D/2 elements. Each retarder has an associated liquid crystal tuning element. Such an assembly, placed between suitably oriented crossed polarizers, has a transmission of

$$T(\lambda) = \sin^2(\pi R_h/\lambda) \cos^2(\pi R_l/\lambda).$$

The split-element stage is equivalent in its spectral performance to two Lyot stages. By constructing the LCTF as groups of split-element stages, one collapses an N-stage Lyot filter into N/2 split-element Lyot stages, and reduces the number of polarizers by N/2. The reduction of polarizers is compensated by the increased number of liquid crystal tuning elements which enhance the overall optical throughput.

A processing unit 17, typically a Pentium computer, is used for Raman image collection and processing. The CCD detector 14 is operated with commercial software, such as ChemIcon, ChemImage.

Every material has a characteristic "fingerprint" based on molecular composition. For this reason, the ability of the Raman chemical imaging system to measure quantitative responses of analyzed materials renders it suitable for a variety of purposes. For example, Raman imaging systems can be used to detect metal corrosion, determine polymer architecture and molecular composition. In addition, the Raman chemical imaging system can also be used in pathology analysis wherein the molecular specificity of Raman imaging provides a mechanism for the diagnostic evaluation of tissue.

Because Raman spectroscopy can readily detect the characteristic "fingerprint" of discrete molecular compositions, it has the potential to make histopathology analysis more quantitative. Using traditional Raman spectroscopy, the differences between normal tissue and lesions, such as lipids and proteins, can be readily determined based on the Raman spectrum. However, traditional Raman spectroscopy is unable to distinguish between benign and malignant tissue. However, the use of an Evans Split-Element LCTF provides the ability to distinguish between normal tissue, malignant tissue and benign tissue.

The optimized LCTF Raman microscope provides high spatial and spectral resolution. The image quality of the LCTF is shown in FIG. 2, a brightfield image of a human tissue biopsy sample. FIG. 2 is collected with the LCTF in the optical path and fine morphological details of the tissue sample, including individual cellular components, are observable. Malignant breast cells are visible in the left portion of the image. Normal breast cells are visible in the right portion of the image.

FIG. 3 shows the spectra of normal tissue and malignant cancerous tissue. The spectra were collected by coupling the Raman scatter from discrete sample regions (normal or diseased) to the dispersive Raman spectrometer via fiber optics. FIG. 3 shows that the differences between the spectra of normal tissue and benign and malignant cancerous tissue which can be distinguished using Raman spectroscopy. In particular, differences in the lipid Raman band at 1445 cm⁻¹ are observable due to the decrease in the relative amount of lipid.

FIG. 4 are Raman images of the same human tissue biopsy of FIG. 2 collected with the LCTF. The images are collected by tuning the LCTF from 1200 to 1800 cm⁻¹ and capturing images at discrete intervals. The image data set is

6,002,476

7

then processed using multivariate image analysis routines that classify the image pixels which are linearly independent Raman spectra by their similarity to a library spectrum of normal or diseased material. The Raman image of FIG. 4 (left) distinguishes the malignant cancer tissue of the sample. The Raman image of FIG. 4 (right) distinguishes the normal cancer tissue of the sample. The Raman image in FIG. 4 is unparalleled in Raman imaging and was collected in 10 minutes.

The advantage of LCTF technology over competitive approaches is the ability to simultaneously collect high spectral/spatial information. The benefit is best realized in the analysis of multicomponent heterogeneous systems, where having a high-quality Raman spectrum at each pixel of the image makes the analysis of complex matrices less subjective and based primarily on quantitative parameters. From the high-quality spectra, sample composition and quantitation has been demonstrated. In this manner, the present Raman chemical imaging system can be used to provide a diagnosis of cancer or other pathology determinations. As a result, specific outcomes are anticipated, including: (1) real-time diagnosis of suspicious lesions sites identified through self-breast exam and/or mammography that are made accessible via needle core biopsy; (2) immediate feedback to the clinician as to the severity of the clinical situation with results being communicated to the patient upon completion of Raman biopsy; (3) potential information on prognostic indicators of disease such as growth rate through quantitative evaluation of cellular

8

nucleic acid composition; (4) minimal patient discomfort; (5) no cosmetic defect of the breast; and (6) reduced exposure to ionizing radiation (x-rays) through overall reduction in use of mammography for lesion screening.

Although present preferred embodiments of the invention have been shown and described, it should be distinctly understood that the invention is not limited thereto but may be variously embodied within the scope of the following claims.

I claim:

1. A chemical imaging system comprising:

- (a) a laser illumination source for illuminating an area of a sample;
- (b) an objective for collecting a Raman spectrum of scattered light from said illuminated area of said sample and producing a collimated beam therefrom;
- (c) a liquid crystal tunable filter for selecting a Raman chemical image of said collimated beam and producing a filtered Raman chemical image therefrom, said filter being an Evans Split-Element liquid crystal tunable filter; and
- (d) detector for collecting said filtered Raman chemical image.

2. The system of claim 1 further comprising processing means for producing a Raman chemical image of said sample.

* * * * *

EXHIBITS P-U

**BEING FILED BY HAND WITH
COPY OF
MOTION TO IMPOUND**

EXHIBIT V

10-16-00

BIIPSIF2-7/95

Approved for use through 04/11/98, OMB 0651-0037
Patent and Trademark Office; U.S. DEPARTMENT OF COMMERCE

PROVISIONAL APPLICATION COVER SHEET

A/PROV

This is a request for filing a PROVISIONAL APPLICATION under 37 CFR 1.53 (b)(2).

Docket Number		000852		Type a plus sign (+) inside this box →	
INVENTOR(S)/APPLICANT(S)					
LAST NAME	FIRST NAME	MIDDLE INITIAL	RESIDENCE (CITY AND EITHER STATE OR FOREIGN COUNTRY)		
Treado	Patrick	J.	315 S. Lexington Ave Pittsburgh, PA 15208		
TITLE OF THE INVENTION (250 characters max)					
NEAR INFRARED CHEMICAL IMAGING MICROSCOPE					
CORRESPONDENCE ADDRESS					
Buchanan Ingersoll, P.C. One Oxford Centre, 20 th Floor 301 Grant Street, Pittsburgh					
STATE	PA	ZIP CODE	15219-1410	COUNTRY	USA
ENCLOSED APPLICATION PARTS (check all that apply)					
<input checked="" type="checkbox"/>	Specification	Number of Pages	336	<input checked="" type="checkbox"/>	Small Entity Statement
<input type="checkbox"/>	Drawing(s)	Number of Sheets	0	<input type="checkbox"/>	Other (specify)
METHOD OF PAYMENT (check one)					
<input checked="" type="checkbox"/>	A check or money order is enclosed to cover the Provisional Filing fee			PROVISIONAL FILING FEE AMOUNT (\$)	\$75.00
<input checked="" type="checkbox"/>	The Commissioner is hereby authorized to charge filing fee and credit Deposit Account Number:			02-4553	

The invention was made by an agency of the United States Government or under a contract with an agency of the United States Government.

☒ No.☐ Yes, the name of the U.S. Government agency and the Government contract number are: _____

Respectfully submitted,

SIGNATURE

Date 10/13/00

TYPED or PRINTED NAME Michael L. Dever

REGISTRATION NO.
(if appropriate)

32,216

☒ Additional inventors are being named on separately numbered sheets attached hereto

PROVISIONAL APPLICATION FILING ONLY

Burden Hour Statement: This form is estimated to take 2 hours to complete. Time will vary depending upon the needs of the individual case. Any comments on the amount of time you are required to complete this form should be sent to the Office of Assistance Quality Improvement, Patent and Trademark Office, Washington, DC 20231, and to the Office of Information and Regulatory Affairs, Office of Management and Budget (Project 0651-0037), Washington, DC 20503. DO NOT SEND FEES OR COMPLETED FORMS TO THIS ADDRESS. SEND TO: Assistant Commissioner for Patents, Washington, DC 20231.

CRI001524

PROVISIONAL APPLICATION COVER SHEET
Additional Page

Docket Number		000852	Type a plus sign (+) inside this box →	+
INVENTOR(S)/APPLICANT(S)				
LAST NAME	FIRST NAME	MIDDLE INITIAL	RESIDENCE (CITY AND EITHER STATE OR FOREIGN COUNTRY)	
Nelson	Matthew	P.	3941 Dowling Ave Pittsburgh, PA 15221	
Keitzer	Scott	A.	207 Lockwood Rd Export, PA 15632	
Ribar	Juliana		1024 Harvard Street Monroeville, PA 15146	

NEAR INFRARED CHEMICAL IMAGING MICROSCOPE

This work is supported by the National Institute of Standards and Technology (NIST) under the Advanced Technology Program (ATP) award (Contract Number 70NANB8H4021)

Description of the Invention

Field of Invention

A near-infrared (NIR) spectroscopic microscope apparatus employing NIR absorption molecular spectroscopy for materials characterization is disclosed. The microscope design is novel in several key areas: (1) using NIR optimized liquid crystal (LC) imaging spectrometer technology for wavelength selection; (2) using a NIR optimized refractive microscope in conjunction with infinity-corrected objectives to form the NIR image on the detector without the use of a tube lens; (3) an integrated parfocal analog color CCD detector for real-time sample positioning and focusing; (4) a means for fusing the color image and the NIR image in software; (5) the use of the NIR microscope as a volumetric imaging instrument through the means of moving the sample through focus, collecting images in and out of focus and reconstructing a volumetric image of the sample in software, or through the means of keeping the sample fixed and changing the wavelength dependent depth of penetration in conjunction with a refractive tube lens with a well characterized chromatic effect; (6) coupling the output of the microscope to a NIR spectrometer either via direct optical coupling or via a fiber optic; (7) the Chemical Imaging Addition Method for seeding the sample with a material of known composition, structure and/or concentration and then generating the NIR image suitable for qualitative and quantitative analysis; (8) means for analyzing and visualizing the NIR chemical images using

chemical image analysis software. While this invention has been demonstrated on a microscope optic platform, the novel concepts are also applicable to other image gathering platforms, namely fiberscopes, macrolens systems and telescopes.

As the demand for high quality, low cost X-ray, γ -ray and imaging detector devices increases, there is a need to improve the quality and production yield of semiconductor materials used in these devices. One effective strategy for improving semiconductor device yield is through the use of better device characterization tools that can rapidly and nondestructively identify defects at early stages in the fabrication process. Early screening helps to elucidate the underlying causes of defects and to reduce downstream costs associated with processing defect laden materials that are ultimately scrapped. The present invention can be used to characterize tellurium inclusion defects in cadmium zinc telluride (CdZnTe) semiconductor materials based on near infrared imaging. With this approach, large area wafers can be inspected rapidly and non-destructively in two and three spatial dimensions by collecting NIR image frames at multiple regions of interest throughout the wafer using an automated NIR imaging system. The NIR image frames are subjected to image processing algorithms including background correction and image binarization. Particle analysis is performed on the binarized images to reveal tellurium inclusion statistics, sufficient to pass or fail wafers. In addition, data visualization software is used to view the tellurium inclusions in two and three spatial dimensions.

Prior Art

In exploring what prior art exists in this field, we have encountered the following:

U.S. Patent No. 5,377,003 Spectroscopic Imaging Devices Employing Imaging Quality Spectral Filters.

Patrick J. Treado, Ira W. Levin, and E. Neil Lewis, Indium Antimonide (InSb) Focal Plane Array (FPA) Detection for Near-Infrared Imaging Microscopy, Appl. Spectrosc. 48, (1994) 607.

Patrick J. Treado, Ira W. Levin and E. Neil Lewis, Near-Infrared Acousto-Optic Filtered Spectroscopic Microscopy: A Solid State Approach to Chemical Imaging, Appl. Spectrosc 46, (1992) 553.

Patrick J. Treado and Michael D. Morris, Infrared and Raman Spectroscopic Imaging, Spectroscopic and Microscopic Imaging of the Chemical State, M.D. Morris, Ed. (Marcell Dekker, New York, 1992) pp. 71-108.

John F. Turner II and Patrick J. Treado, LCTF Raman Chemical Imaging in the Near-Infrared, Proc. SPIE 3061, (1997) 1024.

Spectral Dimensions, NIR Systems Product Information,
<http://www.spectraldimensions.com/products/b-nir.html>

Advantages Over Currently Available Technology

The present invention uses NIR optimized liquid crystal (LC) imaging spectrometer technology for wavelength selection. The LC imaging spectrometer may be of the following types: Lyot liquid crystal tunable filter (LCTF); Evans Split-Element LCTF; Solc LCTF; Ferroelectric LCTF; Liquid crystal Fabry Perot (LCFP); or a hybrid filter technology comprised of a combination of the above-mentioned LC filter types or the above mentioned filter types in combination with fixed bandpass and bandreject filters comprised of dielectric, rugate, holographic, color absorption, acousto-optic or polarization types.

60239069-101300

The present invention uses a NIR optimized refractive microscope in conjunction with infinity-corrected objectives to form the NIR image on the detector without the use of a tube lens. The microscope can be optimized for NIR operation through inherent design of objective and associated anti-reflective coatings, condenser and light source. To simultaneously provide high numerical apertures the objective should be refractive. To minimize chromatic aberration, maximize throughput and reduce cost the conventional tube lens can be eliminated, while having the NIR objective form the NIR image directly onto the NIR focal plane array (FPA) detector, typically of the InGaAs type. The FPA can also be comprised of Si, SiGe, PtSi, InSb, HgCdTe, PdSi, Ge, analog vidicon types. The FPA output is digitized using a frame grabber approach.

The present invention uses an integrated parfocal analog CCD detector for real-time sample positioning and focusing. An analog video camera sensitive to visible radiation, typically a color or monochrome CCD detector, but may be comprised of a CMOS type, is positioned parfocal with the NIR FPA detector to facilitate sample positioning and focusing without requiring direct viewing of the sample through conventional eyepieces. The video camera output is digitized using a frame grabber approach.

The present invention uses a means for fusing the color image and the NIR image in software. While the NIR and visible cameras often generate images having differing contrast, the sample fields of view can be matched through a combination of optical and software manipulations. As a result, the NIR and visible images can be compared and even fused through the use of overlay techniques and correlation techniques to provide the user a near-real time view of both detector outputs on the same computer display. The comparative and integrated views of the sample can significantly enhance the understanding of sample morphology and architecture.

By comparing the visible, NIR and NIR chemical images, additional useful information can be acquired about the chemical composition, structure and concentration of species in samples.

The present invention uses the NIR microscope as a volumetric imaging instrument through the means of moving the sample through focus, collecting images in and out of focus and reconstructing a volumetric image of the sample in software. For samples having some volume (bulk materials, surfaces, interfaces, interphases), volumetric chemical imaging in the NIR has been shown to be useful for failure analysis, product development and routine quality monitoring. The potential also exists for performing quantitative analysis simultaneous with volumetric analysis. Volumetric imaging can be performed in a non-contact mode without modifying the sample through the use of numerical confocal techniques, which require that the sample be imaged at discrete focal planes. The resulting images are processed and reconstructed and visualized. An alternative to sample positioning is to employ a tube lens in the microscope which introduces chromatic aberration. As a result the sample can be interrogated as a function of sample depth by exercising the LC imaging spectrometer, collecting images at different wavelengths which penetrate to differing degrees into bulk materials. These wavelength dependent, depth dependent images can be reconstructed to form volumetric images of materials without requiring the sample to be moved.

The present invention couples the output of the microscope to a NIR spectrometer either via direct optical coupling or via a fiber optic. This allows conventional spectroscopic tools to be used to gather NIR spectra for traditional, high speed spectral analysis. The spectrometers can be of the following types: fixed filter spectrometers; grating based spectrometers; Fourier Transform spectrometers; or Acousto-Optic spectrometers



Date: January 19, 2000
Report Number: CI-R-1238

Chemical Imaging of Silicon Germanium Semiconductor Defects

REPORT No. CI-R 1238

1 INTRODUCTION

Chemical imaging is a new discipline in chemistry that combines high definition digital imaging with molecular spectroscopy (e.g., infrared, Raman, fluorescence and photoluminescence) techniques for the chemical analysis of condensed phase materials. Chemical imaging is a powerful approach that rapidly and non-invasively visualizes molecular and chemical heterogeneity by gathering high-quality digital images at multiple spectral bands. Subsequently, computer enhancement and chemometrics processes are employed to analyze the images and extract chemical information.

Chemicon Inc., headquartered in Pittsburgh, Pennsylvania, designs and manufactures innovative high-performance instruments for materials characterization and offers a broad range of instrumentation and chemical imaging services.

Chemicon's premiere chemical imaging product is the Falcon™ Raman Chemical Imaging Microscope. The Falcon™ is able to create two-dimensional molecular images that detail the molecular architecture of materials as well as the size, shape, and distribution of molecular components. The Falcon™ displays three unique features: Duet Vision Technology™, the Liquid Crystal Tunable Filter (LCTF) and the Falcon™ Dispersive Raman Spectrometer. Duet Vision Technology™ delivers real-time simultaneous imaging and spectroscopy, allowing users to quickly and easily identify regions of critical interest. The Liquid Crystal Tunable Filter (LCTF) Imaging Spectrometer provides high spectral and spatial resolution for high throughput screening of materials. The Falcon Dispersive Raman Spectrometer provides a fast and efficient view of the entire spectrum reducing the possibility of missing spectral features of interest. These three components combined allow the Falcon™ to deliver an unprecedented level of performance.

Chemicon has successfully applied chemical imaging technologies to numerous market segments with an emphasis placed on the polymer, pharmaceutical, and semiconductor industries. Chemicon is widely recognized as the technology leader in providing efficient chemical imaging materials characterization technology.

Chemicon was recently granted a National Institute of Standards and Technology (NIST) \$3 million award through the Advanced Technology Program (ATP) to develop instrumentation for automated inspection of structural defects in

832



Date: January 19, 2000
Report Number: CI-R-1238

semiconductors. Chemical Imaging for Semiconductor Metrology (CHISM) has already been demonstrated to be an important enabling technique for compound semiconductor manufacturers to assist them in high throughput screening of materials. A direct result will be an overall improvement in manufacturing processes that will improve the yields of compound semiconductors. Under the CHISM program, several powerful imaging modalities, including Raman, infrared, photoluminescence and polarized light, are being combined in a single integrated system to improve the metrology yield of semiconductors.

Chemlcon has until recently focused its ATP-related materials research efforts on CdZnTe, SiC and GaN Semiconductor materials. Eric Borguet Assistant Professor, Department of Chemistry and Surface Science Center at the University of Pittsburgh additionally provided Chemlcon Inc. with SiGe semiconductor material supplied by Virginia Semiconductor Inc. (VSI).

Chemlcon is suited to study SiGe because of its expertise in Raman and IR Chemical Imaging of solid-state materials, including semiconductors, using Chemlcon's Falcon™ instrument, its demonstrated success in imaging bulk properties and surface properties of semiconductors, and its expertise in semiconductor defect characterization.

2 METHODOLOGY

2.1 Optical Microscopy, Raman Spectroscopy and Chemical Imaging Analysis

A Falcon™ Raman Chemical Imaging System (Chemlcon Inc.) equipped with 532 nm laser excitation and a 100 W quartz tungsten halogen (QTH) broad-band source was used to collect brightfield microscopic images, LCTF transmission images, Raman Chemical Images and dispersive Raman spectra. The Falcon™ was equipped with DVT, which enables the user to acquire Raman images and spectra simultaneously to rapidly identify areas of interest. The Falcon™ provides high spectral resolution and submicron (250nm) spatial resolution. Chemlcon's software suite consisting of Acquisition Manager, ChemImage and Speclmage software packages was used to perform data analysis. Dispersive Raman spectra were acquired by coupling the Falcon™ via fiber optic to a 0.5m dispersive monochromator equipped with a TE-cooled slow-scan CCD. The spectrometer was equipped with a 150 gr/mm grating that provided 0.56 nm resolving power.

2.2 Infrared (IR) Chemical Imaging Instrumentation

IR absorption spectroscopic imaging was performed to determine the visible absorption character of the sample. An infrared (IR) chemical imaging system equipped with a broadband QTH light source was used to collect IR chemical



Date: January 19, 2000
Report Number: CI-R-1238

images of the sample in the 1000-1700 nm wavelength range. An IR liquid crystal tunable filter (LCTF) under computer control was tuned between 1000 nm and 1700 nm with a constant step size of 10 nm. IR chemical images of the sample were acquired using a room temperature InGaAs focal plane array (FPA) camera. The IR chemical imaging system was operated in both reflectance and transmittance modes.

2.3 SEM Elemental Analysis

Elemental analysis was performed using a scanning electron microscope (SEM) outfitted with secondary electron and backscatter electron detection capability, as well as an energy dispersive spectrometer with point analysis and elemental mapping capability. The backscattered operational mode of the SEM generates elemental images that directly correlate pixel intensity values to atomic weight. The secondary electron operational mode of the SEM provides high fidelity images of sample surface topography.

2.4 Cosine Correlation Analysis (CCA)

Cosine correlation analysis (CCA), a multivariate image analysis technique developed by Chemicon, was applied to the chemical image data sets. CCA assesses similarity in spectral image data while simultaneously suppressing background effects. CCA assesses chemical heterogeneity without the need for extensive training sets. CCA identifies differences in spectral shape and effectively provides chemical image based contrast that is independent of absolute intensity.

2.5 Principal Component Analyses

Principal component analysis was applied to the chemical imaging data sets to gain insight into the complex distribution of components present in the sample. PCA is a powerful multivariate chemometric technique for data analysis. It is a data reduction technique that reduces the data with many variables to a few important latent variables called principal components (PC). These PCs are orthogonal to each other, thus explaining orthogonal information in the original data. The outputs of PCA are scores and loadings, which provide insight into the data structure.

3 RESULTS

IR Chemical Imaging

Infrared (IR) reflectance chemical imaging reveals compositional information near the surface of a sample. Figures 1A is a brightfield reflectance image of a defect

60239969.101300

234



Date: January 19, 2000
Report Number: CI-R-1238

on a SiGe wafer obtained using the Falcon Ramian Chemical Imaging microscope equipped with a slow-scan Si-CCD. The image shows the surface morphology associated with the SiGe defect and the surrounding bulk alloy. Figure 1B shows a color composite reflectance IR chemical image of the same field of view (FOV) as that of figure 1A. Each pixel in the raw chemical image data set has an IR spectrum associated with it. PCA and CCA were applied to the chemical image data set. PCA score images and CCA images that were well correlated with the bulk SiGe, the defect region, and the interfacial region where assigned the blue, red, and green color channels, respectively. The composite image reveals image contrast based on compositional information extracted from its reflectance IR spectral signature.

IR transmittance chemical imaging provides bulk volume chemical information. Figure 1C shows a color composite transmittance IR chemical image that correlates with the figure 1A FOV. PCA and CCA were applied to the chemical image data set. PCA score images and CCA images that were well correlated with the bulk SiGe, the defect region, and the interfacial region where assigned to the blue, red, and green color channels, respectively. The chemical image reveals image contrast based on bulk volume compositional information extracted from its IR transmittance spectral signature.

Figure 1D shows a macro scale transmittance IR chemical image of the entire GaN wafer. This image shows that there are no visible defects on a macro scale.

Figure 1E shows representative LCTF generated IR spectra that correlate with the bulk alloy (blue), interphase (green) and defect (red) regions, respectively. The transmittance edge at approximately 1180 nm correlates well with the band gap energy for SiGe having a 90:10 (Si:Ge) stoichiometric ratio.¹

Raman Chemical Imaging

The development of high power laser sources, multichannel detectors for low light level applications, and high performance tunable filters has made chemical imaging a practical technique. The thickness of the sample probed is on the order of the optical penetration depth of the sample. It is believed that the probe depth of the Raman chemical images acquired in this work is on the order of several hundred nanometers. The images shown here are based predominately on surface chemical composition.

Raman chemical images were collected on the defect region between 539.8 nm and 549.2 nm (272 cm^{-1} and 589 cm^{-1}) at 0.2 nm increments with an integration time of 10 seconds per frame. The sample surface was irradiated by 1.5 W of 532 nm laser power (at head).

Figure 2B is a Raman composite chemical image of the SiGe defect and surrounding bulk alloy. Image contrast is based on variations in Raman response over the sample surface. Each pixel of the Raman chemical image has



Date: January 19, 2000
Report Number: CI-R-1238

a corresponding Raman spectrum. PCA and CCA were applied to the chemical image data set. The color composite image was generated by assigning images correlating with the bulk SiGe, defect and interphase region Raman signatures to the blue, red and green channels, respectively. Figure 3B shows LCTF generated Raman spectra associated with the bulk alloy, defect, and interphase regions of the SiGe wafer. Peak positions and shifts reveal information about the semiconductor composition and lattice order. The peak centered near 300 cm^{-1} is characteristic of the bulk Si-Ge alloy. The fundamental optical phonon band of Si (approximately 500 cm^{-1}) is most intense in the defect region, suggesting that the chemical composition of the defect is Si.² The shift in the fundamental optical phonon band for Si can be correlated with strain in the crystal lattice.

For comparison, figure 3 shows dispersive Raman spectra of the bulk alloy and defect regions, respectively. A Raman band centered near 300 cm^{-1} , visible in the bulk spectrum, is characteristic of Si-Ge alloy composition. Conversely, a spectrum taken in the defect region displays a reduced peak intensity at 300 cm^{-1} and an increase in the intensity of the Si 500 cm^{-1} fundamental optical phonon band relative to the bulk spectrum, indicating the defect region is germanium-deficient. These findings agree with the data acquired from the Raman chemical imaging results.

Scanning Electron Microscopy

Scanning electron microscopy (SEM) was performed on the SiGe defect region and surrounding bulk alloy to confirm the compositional assignment made from the Raman chemical imaging results. Figures 4A and 4B are SEM images of the SiGe defect region operated in backscattered and secondary electron emission modes, respectively. The backscattered image reveals contrast based on differences in atomic masses. The darker region (lower atomic mass) corresponds to the Si defect while the lighter regions (higher average atomic mass) corresponds to the Si-Ge alloy. The secondary electron image shows a higher fidelity image of the defect region.

Figures 5A and 5B are energy dispersive spectra associated with the defect region (color coded green in figure 4B) and the bulk alloy (color coded red in figure 4B), respectively. It is evident from these spectra that the defect consists of predominately Si while the bulk alloy is composed of Si and Ge.

Figure 6 is a color composite x-ray fluorescent map of the SiGe defect and surrounding bulk alloy. The blue regions depict areas that have both Si and Ge character. The green regions depict areas rich in Si and deficient in Ge.

60239969.101300

136



Date: January 19, 2000
Report Number: CI-R-1238

4 CONCLUSIONS

Chemicon has successfully applied a host of chemical imaging techniques to assess a Si-rich defect in a Si-Ge semiconductor wafer. IR reflectance chemical imaging revealed surface compositional information specific to the defect, surrounding bulk alloy and interphase regions based on the sample's inherent IR spectral signatures. IR transmittance chemical imaging provided information related to the bulk volume at the same region of interest. The IR transmittance edge associated with the SiGe material correlated well with the band gap energy for the SiGe alloy composition. Raman chemical imaging and dispersive Raman spectroscopy revealed that the defect was composed primarily of Si. In addition, shifts in the Raman spectra provided information related to defect-induced strain in the semiconductor lattice. Finally, SEM analysis confirmed the elemental composition of the defect and surrounding bulk alloy.

The Raman and IR results shown here were collected on two separate imaging instruments. However, both instruments are constructed from Chemicon's base FALCON chemical imaging system platform. It is practical to incorporate both capabilities (Raman and IR) onto a single instrument.

5 REFERENCES

- (1) Seeger, K., "Semiconductor Physics", Springer-Verlag, New York (1996) pp 337-338.
- (2) Yu, Peter Y. and Cardona, Michael, "Fundamentals of Semiconductors Physics and Materials Properties 2nd Edition," Springer-Verlag, New York (1999) pp. 375-379.

60239959.101300

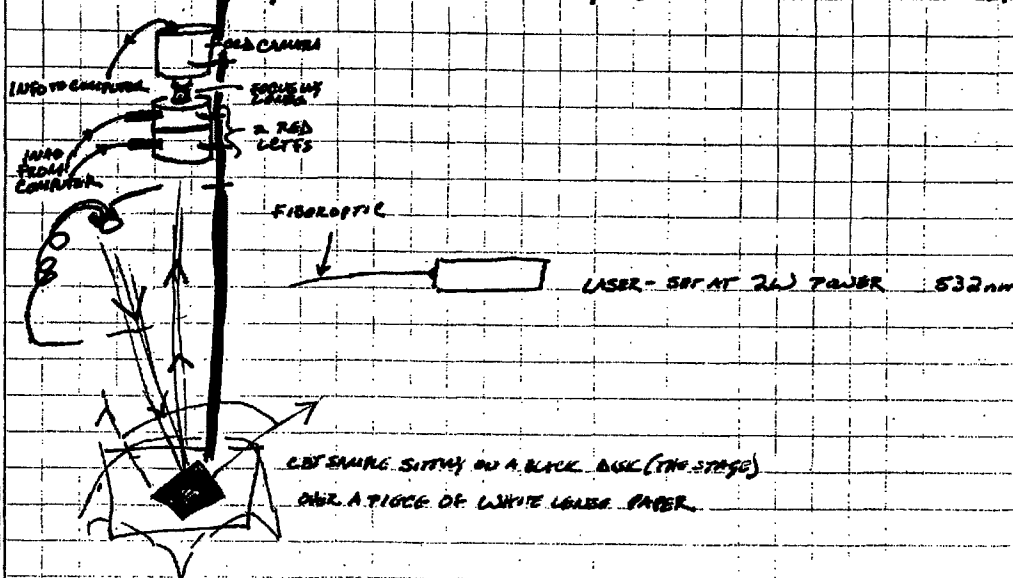
34 PROJECT *Chiron - Mac - System*

Note

MACRO IMAGING SCHEMATIC

GREEN

5-10-99



PRELIMINARY OBSERVATIONS

- 25 s. ACQUISITION TIME WAS ADDED TO ~~FOUR~~ FLOPPIES
- AT 885 885 nm THE DEFECTS IN THE SAMPLE BECOME APPARENT.



860nm 25% (SOME DEFECTS BECOME VISIBLE)
865 - NOT AS STRONG



870 nm x 865 - VERY STRONG EVIDENT.

★ ETCHED CUT BROKE 5-12-99

65

Continued on Page

Read and Understood By

Johanna M. Rito
Signed

5/12/99
Date

[Signature]
Signed

[Signature]
Date

EXHIBITS W-X

**BEING FILED BY HAND WITH
COPY OF
MOTION TO IMPOUND**

EXHIBIT Y

NEAR INFRARED CHEMICAL IMAGING MICROSCOPE

This application claims the benefit of U.S. Provisional Application No. 60/239,969, entitled "Near Infrared Chemical Imaging Microscope" filed October 13, 2000.

This work is supported by the National Institute of Standards and Technology (NIST) under the Advanced Technology Program (ATP) award (Contract Number 70NANB8H4021)

Field of Invention

The present invention is related to near-infrared (NIR) microscopes for spectroscopic and image analysis, and, in particular, to microscopes useful for both NIR spectroscopy, NIR chemical imaging and NIR volumetric chemical imaging.

Background of the Invention

NIR spectroscopy is a mature, non-contact, non-destructive analytical characterization tool that has been widely applied to a broad range of materials. The NIR region of the electromagnetic spectrum encompasses radiation with wavelengths of 0.78 to 2.5 μm (12,800 to 4,000 cm^{-1}). NIR spectra result from the overtone and combination bands of fundamental mid-infrared (MIR) bands. Among the many desirable characteristics, NIR is used to rapidly obtain both qualitative and quantitative information about the molecular makeup of a material. Digital imaging, on the other hand, provides a means to obtain optical (i.e., spatial – morphological, topographical, etc.) information about a material. By combining the spatial information obtained from digital imagery and the spectral information obtained from NIR spectroscopy, the chemical makeup of complex material matrices can be mapped out in both two and three spatial dimensions. NIR chemical imaging combines NIR spectroscopy and digital imaging for the

molecular-specific analysis of materials. A NIR chemical imaging microscope apparatus employing NIR absorption molecular spectroscopy for materials characterization is disclosed.

State-of-the-Art Instrumentation

NIR microscopes are used to obtain NIR absorption, transmittance or reflectance spectra (e.g., NIR microspectra) from samples ranging in size between 1 and 1000 μm . These instruments are typically equipped with a digital camera to visually locate a region of interest on a sample upon which a NIR light beam from a Fourier transform (FT) spectrometer is focused. Reflective optics are used to direct the transmitted or reflected light from the sample to a NIR detector. The output is a NIR absorption spectrum collected in transmittance or reflectance mode.

NIR chemical imaging can be considered an extension of NIR microspectroscopy. Much of the imaging performed since the development of the first NIR microprobes has involved spatial scanning of samples beneath NIR microscopes in order to construct NIR "maps" of surfaces. In point by point scanning with NIR microscopes, the NIR light beam is focused onto the surface of a sample or apertured to illuminate a small region of a sample and a spectrum from each spatial position is collected. Images are obtained by rastering the sample through the focused or apertured NIR light beam and the spectra recorded are then reconstructed to form an image. Although point scanning produces images based on NIR contrast, long experimental times are common since the duration of the experiment is proportional to the number of image pixels. As a direct result, point scan images are captured at low image definition, which relates directly to the limited utility of the technique as an imaging tool for the routine assessment of material morphology. The spatial resolution of the image is limited by the size of the NIR

illumination spot on the sample (no less than 1 μm) and the rastering mechanism, which requires the use of moving mechanical parts that are challenging to operate reproducibly.

NIR imaging cameras have been used in photography for decades. Until recently, however, it has not been easily accessible to those not versed in traditional photographic processes. By using optical filters (e.g., cold filters) that block the visible wavelengths (0.4-0.78 μm), charge-coupled devices (CCDs) used in digital cameras and camcorders can be used to sense NIR light out to around 1100 nm. Other regions of the NIR spectrum can be viewed using devices such as indium gallium arsenide (InGaAs – 0.9 μm to 1.7 μm) and indium antimonide (InSb – 1.0 μm to 5.0 μm) focal plane array (FPA) detectors. These integrated wavelength NIR imaging approaches allow one to study relative light intensities of objects over broad ranges of the NIR spectrum, but useful chemical information is unattainable without the use of some type of discrete wavelength filtering device.

The use of dielectric interference filters in combination with NIR FPAs is one method in which chemical information can be obtained from a sample. To form NIR chemical images, a NIR light beam is defocused to illuminate a wide field of view and the reflected or transmitted light from the illuminated area is imaged onto a two-dimensional NIR detector. A selection of discrete dielectric interference filters provided in a filter wheel, or a linearly variable or circularly variable format can be positioned in front of a broadband NIR light source, or in front of the NIR FPA itself in order to collect NIR wavelength resolved images. Typically, the use of several fixed bandpass filters is required to access the entire NIR spectrum. The spatial resolution of the NIR image approaches that of the optical microscope, while spectral resolution of several nanometers has been demonstrated. Key limitations of the dielectric filter approach include the need for a multitude of discrete filters to provide appreciable free spectral range, or

the reliance on moving mechanical parts in employing continuously tunable dielectric interference filters as a requirement to form wavelength resolved images. While moving mechanical assemblies can be engineered they add cost and complexity to NIR chemical imaging systems. Alternatives to moving mechanical assemblies are generally more cost effective and provide performance advantages.

Acousto-optic tunable filters (AOTFs) have been employed as no-moving-parts imaging spectrometers for NIR imaging. The AOTF is a solid-state device that is capable of functioning from the UV to the mid-IR depending on the choice of the filter's crystal material. Operation of the AOTF is based on the interaction of light with a traveling acoustic sound wave in an anisotropic crystal medium. The incident light is diffracted with a narrow spectral bandpass when an rf signal is applied to the device. By changing the applied rf frequency under computer control the spectral passband can be tuned rapidly with the benefit of non-moving parts.

For use in NIR chemical imaging, AOTFs have distinct limitations. AOTFs have imaging performance that is degraded appreciably from diffraction-limited conditions due to dispersion effects and image shifting effects. Furthermore, AOTFs suffer from temperature instability and exhibit nonlinear properties that complicate their use as imaging spectrometers.

An aim of NIR chemical imaging technology development has been to develop a NIR imaging technique that combines diffraction-limited spatial resolution with high spectral resolution. NIR chemical imaging techniques have only recently achieved a degree of technological maturity that allow the collection of high resolution (spectral and spatial) data with the advent of the liquid crystal (LC) imaging spectrometers. In general, LC devices provide diffraction-limited spatial resolution. The spectral resolution of the LC imaging spectrometer is comparable to that provided by dispersive monochromator and Fourier transform

interferometers. In addition, LC technology provides high out of band rejection, broad free spectral range, moderate transmittance, high overall etendue and highly reproducible random access computer controlled tuning.

Under normal NIR imaging operation, LC imaging spectrometers allow NIR chemical images of samples to be recorded at discrete wavelengths (energies). A spectrum is generated corresponding to thousands of spatial locations at the sample surface by tuning the LC imaging spectrometer over a range of wavelengths and collecting NIR images systematically. Contrast is generated in the images based on the relative amounts of NIR absorption, transmittance or reflectance that is generated by the different species located throughout the sample. Since a high quality NIR spectrum is generated for each pixel location, a wide variety of chemometric analysis tools, both univariate and multivariate, can be applied to the NIR image data to extract pertinent information. Correlative multivariate routines are particularly powerful when applied to chemical images collected from samples intentionally seeded with a known standard material. This approach of incorporating calibration standards within an image field of view can be extended to quantitative chemical image analysis. In addition, digital image analysis procedures can also be applied to high image quality NIR chemical images to perform routine particle analysis in both two (2D) and three (3D) spatial dimensions. Volumetric 3D NIR chemical image analysis can be performed very effectively using numerical deconvolution computational strategies.

Summary of the Invention

To address the need for a device that can provide video imaging, NIR spectroscopy and high resolution (spatial and spectral) NIR chemical imaging in two and three spatial dimensions, a

novel NIR chemical imaging microscope has been developed that is NIR chemical imaging capable.

The microscope design uses NIR optimized liquid crystal (LC) imaging spectrometer technology for wavelength selection. The NIR optimized refractive microscope is used in conjunction with infinity-corrected objectives to form the NIR image on the detector with or without the use of a tube lens. An integrated parfocal analog color CCD detector provides real-time sample positioning and focusing. The color image and the NIR image are fused in software. In one configuration, the NIR microscope may be used as a volumetric imaging instrument through the means of moving the sample through focus, collecting images at varying focal depths and reconstructing a volumetric image of the sample in software, or through the means of keeping the sample fixed and changing the wavelength dependent depth of penetration in conjunction with a refractive tube lens with a well characterized chromatic effect. The output of the microscope can be coupled to a NIR spectrometer either via direct optical coupling or via a fiber optic. A Chemical Imaging Addition Method seeds the sample with a material of known composition, structure and/or concentration and then generates the NIR image suitable for qualitative and quantitative analysis. The microscope generates NIR chemical image data that is analyzed and visualized using chemical image analysis software in a systematic and comprehensive manner. While this invention has been demonstrated on a microscope optic platform, the novel concepts are also applicable to other image gathering platforms, namely fiberscopes, macrolens systems and telescopes.

Brief Description of the Drawings

Figure 1 shows a schematic diagram of the near-infrared (NIR) chemical imaging microscope

Figure 2 shows a diagram of the chemical imaging data analysis cycle performed in software.

Figure 3 is a digital brightfield image of a CdZnTe semiconductor material decorated with tellurium inclusions.

Figure 4 an NIR microscopic transmittance image of a CdZnTe semiconductor material decorated with tellurium inclusions.

Figure 5A illustrates a raw NIR image frame of a CdZnTe wafer sample.

Figure 5B illustrates an NIR image frame of the sample of Figure 5A in which the threshold value for the image was set too low.

Figure 5C illustrates an NIR image frame of the sample of Figure 5A in which the threshold value for the image was set too high.

Figure 5D illustrates an NIR image frame of the sample of Figure 5A in which the threshold value for the image was set to an intermediate level.

Figure 6A is the original raw image of four adjacent regions of interest on a CdZnTe wafer.

Figure 6B is the background-corrected image corresponding to the four adjacent regions of interest of the CdZnTe wafer of Figure 6A.

Figure 6C is the binarized image corresponding to the four adjacent regions of interest of the CdZnTe wafer of Figure 6A.

Figure 7 is a three-dimensional view of tellurium inclusions in a CdZnTe wafer.

Detailed Description of the Invention

The NIR chemical imaging microscope combines in a single platform a NIR optimized refractive optical microscope base, which is equipped with NIR optimized infinity-corrected microscope objectives, an automated XYZ translational microscope stage and quartz tungsten halogen (QTH) lamps to secure and illuminate samples for NIR spectroscopy and imaging, an analog color charge-coupled device (CCD) detector for ordinary optical image collection and digital image collection, a NIR LC imaging spectrometer for NIR chemical image wavelength selection and a room temperature or optionally cooled NIR FPA for NIR image capture.

Figure 1 is a schematic diagram of the NIR chemical imaging microscope. NIR illumination is directed to the sample in a reflected light configuration using a QTH source or other broadband white light source, including metal halide or Xe arc lamps 1 or a transmitted light configuration using QTH or suitable NIR source 2 of an NIR optimized refractive optical microscope platform 3. The reflected or transmitted NIR light is collected from the sample positioned on the automated XYZ translational microscope stage 4 through an infinity-corrected NIR optimized microscope objective 5.

Ordinary optical imagery of the sample can be obtained using a mirror or beamsplitter or prism arrangement inserted into turret 6 and collecting an image with an analog or digital color or monochrome charge-coupled device (CCD) or CMOS detector 7. In NIR chemical imaging mode, the magnified NIR image is coupled through a NIR LC imaging spectrometer 8 and collected on a room temperature or cooled NIR focal plane array (FPA) detector 9. The FPA is typically comprised of indium gallium arsenide (InGaAs), but may be comprised of other NIR sensitive materials, including platinum silicide (PtSi), indium antimonide (InSb) or mercury cadmium telluride (HgCdTe). Using a beamsplitting element inserted into turret 6, NIR and

ordinary optical imagery can be collected with an analog monochrome or color CCD detector 7 and NIR FPA 9 simultaneously.

A central processing unit 10, typically a Pentium computer, is used for NIR chemical image collection and processing. The analog color CCD 7, NIR FPA 9, automated XYZ translational microscope stage 4 controlled via a controller 12 and NIR LC imaging spectrometer 8 (through LC imaging spectrometer controller 11) are operated with commercial software, such as Acquisition Manager (ChemIcon Inc.) in conjunction with ChemImage (ChemIcon Inc.).

By introducing a polarization sensitive beam splitting element in the optical path prior to the NIR LC imaging spectrometer 8 (not shown in schematic diagram), a portion of the NIR light from the sample may be coupled to a remote NIR spectrometer (also not shown in schematic diagram).

Preferably, NIR optimized liquid crystal (LC) imaging spectrometer technology is used for wavelength selection. The LC imaging spectrometer may be of the following types: Lyot liquid crystal tunable filter (LCTF); Evans Split-Element LCTF; Solc LCTF; Ferroelectric LCTF; Liquid crystal Fabry Perot (LCFP); or a hybrid filter technology comprised of a combination of the above-mentioned LC filter types or the above mentioned filter types in combination with fixed bandpass and bandreject filters comprised of dielectric, rugate, holographic, color absorption, acousto-optic or polarization types.

One novel component of this invention, is that a NIR optimized refractive microscope is used in conjunction with infinity-corrected objectives to form the NIR image on the detector without the use of a tube lens. The microscope can be optimized for NIR operation through inherent design of objective and associated anti-reflective coatings, condenser and light source. To simultaneously provide high numerical apertures the objective should be refractive. To

minimize chromatic aberration, maximize throughput and reduce cost the conventional tube lens can be eliminated, while having the NIR objective form the NIR image directly onto the NIR focal plane array (FPA) detector, typically of the InGaAs type. The FPA can also be comprised of Si, SiGe, PtSi, InSb, HgCdTe, PdSi, Ge, analog vidicon types. The FPA output is digitized using an analog or digital frame grabber approach.

An integrated parfocal analog CCD detector provides real-time sample positioning and focusing. An analog video camera sensitive to visible radiation, typically a color or monochrome CCD detector, but may be comprised of a CMOS type, is positioned parfocal with the NIR FPA detector to facilitate sample positioning and focusing without requiring direct viewing of the sample through conventional eyepieces. The video camera output is typically digitized using a frame grabber approach.

The color image and the NIR image are fused using software. While the NIR and visible cameras often generate images having differing contrast, the sample fields of view can be matched through a combination of optical and software manipulations. As a result, the NIR and visible images can be compared and even fused through the use of overlay techniques and correlation techniques to provide the user a near-real time view of both detector outputs on the same computer display. The comparative and integrated views of the sample can significantly enhance the understanding of sample morphology and architecture. By comparing the visible, NIR and NIR chemical images, additional useful information can be acquired about the chemical composition, structure and concentration of species in samples.

The NIR microscope can be used as a volumetric imaging instrument through the means of moving the sample through focus in the Z, axial dimension, collecting images in and out of focus and reconstructing a volumetric image of the sample in software. For samples having

some volume (bulk materials, surfaces, interfaces, interphases), volumetric chemical imaging in the NIR has been shown to be useful for failure analysis, product development and routine quality monitoring. The potential also exists for performing quantitative analysis simultaneous with volumetric analysis. Volumetric imaging can be performed in a non-contact mode without modifying the sample through the use of numerical confocal techniques, which require that the sample be imaged at discrete focal planes. The resulting images are processed and reconstructed and visualized. Computational optical sectioning reconstruction techniques based on a variety of strategies have been demonstrated, including nearest neighbors and iterative deconvolution.

An alternative to sample positioning combined with computation reconstruction is to employ a tube lens in the image formation path of the microscope which introduces chromatic aberration. As a result the sample can be interrogated as a function of sample depth by exercising the LC imaging spectrometer, collecting images at different wavelengths which penetrate to differing degrees into bulk materials. These wavelength dependent, depth dependent images can be reconstructed to form volumetric images of materials without requiring the sample to be moved, again through application of computational optical sectioning reconstruction algorithms.

The output of the microscope can be coupled to a NIR spectrometer either via direct optical coupling or via a fiber optic cable. This allows conventional spectroscopic tools to be used to gather NIR spectra for traditional, high speed spectral analysis. The spectrometers can be of the following types: fixed filter spectrometers; grating based spectrometers; Fourier Transform spectrometers; or Acousto-Optic spectrometers

A novel method that is readily employed by the disclosed microscope invention is a method described as the Chemical Imaging Addition Method which involves seeding the sample

097691-104201
102097-169266

with a material of known composition, structure and/or concentration and then generating the NIR image suitable for qualitative and quantitative analysis. The Chemical Imaging Addition Method is a novel extension of a standard analytical chemical analysis technique, the Standard Addition Method. A common practice in quantitative chemical analysis is to construct a *standard calibration curve* which is a plot of analytical response for a particular technique as a function of known analyte concentration. By measuring the analytical response from an unknown sample, an estimate of the analyte concentration can then be extrapolated from the calibration curve. In the Standard Addition Method, known quantities of the analyte are added to the samples and the increase in analytical response is measured. When the analytical response is linearly related to concentration, the concentration of the unknown analyte can be found by plotting the analytical response from a series of standards and extrapolating the unknown concentration from the curve. In this graph, however, the x-axis is the concentration of added analyte after being mixed with the sample. The x-intercept of the curve is the concentration of the unknown following dilution. The primary advantage of the standard addition method is that the matrix remains constant for all samples.

While the Standard Addition Method is used specifically for quantitative analysis, the Chemical Imaging Addition Method can be used for qualitative and quantitative analysis. The Chemical Imaging Addition Method relies upon spatially isolating analyte standards in order to calibrate the Chemical Imaging analysis. In chemical imaging, thousands of linearly independent, spatially-resolved spectra are collected in parallel of analytes found within complex host matrices. These spectra can then be processed to generate unique contrast intrinsic to analyte species without the use of stains, dyes, or contrast agents. Various spectroscopic methods including near-infrared (NIR) absorption spectroscopy can be used to probe molecular

composition and structure without being destructive to the sample. Similarly, in NIR chemical imaging the contrast that is generated reveals the spatial distribution of properties revealed in the underlying NIR spectra.

The Chemical Imaging Addition Method can involve several data processing steps, typically including, but not limited to:

1. Ratiometric correction in which the sample NIR image is divided by the background NIR image to produce a result having a floating point data type.
2. The divided image is normalized by dividing each intensity value at every pixel in the image by the vector norm for its corresponding pixel spectrum. Where the vector norm is the square root of the sum of the squares of pixel intensity values for each pixel spectrum. Normalization is applied for qualitative analysis of NIR chemical images. For quantitative analysis, normalization is not employed, but relies instead on the use of partial least squares regression (PLSR) techniques.
3. Correlation analysis, including Euclidian Distance and Cosine correlation analysis (CCA) are established multivariate image analysis techniques that assess similarity in spectral image data while simultaneously suppressing background effects. More specifically, CCA assesses chemical heterogeneity without the need for training sets, identifies differences in spectral shape and efficiently provides chemical image based contrast that is independent of absolute intensity. The CCA algorithm treats each pixel spectrum as a projected vector in n-dimensional space, where n is the number of wavelengths sampled in the image. An orthonormal basis set of vectors is chosen as the set of reference vectors and the cosine of the angles between each pixel spectrum vector and the reference vectors are calculated. The intensity values displayed in the resulting CCA images are these cosine values, where a cosine

value of 1 indicates the pixel spectrum and reference spectrum are identical, and a cosine value of 0 indicates the pixel spectrum and the reference spectrum are orthogonal (no correlation). The dimensions of the resulting CCA image is the same as the original image because the orthonormal basis set provides n reference vectors, resulting in n CCA images.

4. Principal component analysis (PCA) is a data space dimensionality reduction technique. A least squares fit is drawn through the maximum variance in the n -dimensional dataset. The vector resulting from this least squares fit is termed the first principal component (PC) or the first loading. After subtracting the variance explained from the first PC, the operation is repeated and the second principal component is calculated. This process is repeated until some percentage of the total variance in the data space is explained (normally 95% or greater). PC Score images can then be visualized to reveal orthogonal information including sample information, as well as instrument response, including noise. Reconstruction of spectral dimension data can then be performed guided by cluster analysis, including without PCs that describe material or instrument parameters that one desires to amplify or suppress, depending on the needs of the sensing application.

Effective materials characterization with the disclosed NIR chemical imaging microscope invention typically requires application of a multitude of software procedures to the NIR chemical image. A schematic of the chemical image analysis cycle is shown in Figure 2. A fairly comprehensive description of the variety of steps used to process chemical images is described below.

Until recently, seamless integration of spectral analysis, chemometric analysis and digital image analysis has not been commercially available. Individual communities have independently developed advanced software applicable to their specific requirements. For

example, digital imaging software packages that treat single-frame gray-scale images and spectral processing programs that apply chemometric techniques have both reached a relatively mature state. One limitation to the development of chemical imaging, however, has been the lack of integrated software that combines enough of the features of each of these individual disciplines to have practical utility.

Historically, practitioners of chemical imaging were forced to develop their own software routines to perform each of the key steps of the data analysis. Typically, routines were prototyped using packages that supported scripting capability, such as Matlab, IDL, Grams or LabView. These packages, while flexible, are limited by steep learning curves, computational inefficiencies, and the need for individual practitioners to develop their own graphical user interface (GUI). Today, commercially available software does exist that provides efficient data processing and the ease of use of a simple GUI.

Software that meets these goals must address the entirety of the chemical imaging process. The chemical imaging analysis cycle illustrates the steps needed to successfully extract information from chemical images and to tap the full potential provided by chemical imaging systems. The cycle begins with the selection of sample measurement strategies and continues through to the presentation of a measurement solution. The first step is the collection of images. The related software must accommodate the full complement of chemical image acquisition configurations, including support of various spectroscopic techniques, the associated spectrometers and imaging detectors, and the sampling flexibility required by differing sample sizes and collection times. Ideally, even relatively disparate instrument designs can have one intuitive GUI to facilitate ease of use and ease of adoption.

FOR FILING

The second step in the analysis cycle is data preprocessing. In general, preprocessing steps attempt to minimize contributions from chemical imaging instrument response that are not related to variations in the chemical composition of the imaged sample. Some of the functionalities needed include: correction for detector response, including variations in detector quantum efficiency, bad detector pixels and cosmic events; variation in source illumination intensity across the sample; and gross differentiation between spectral lineshapes based on baseline fitting and subtraction. Examples of tools available for preprocessing include ratiometric correction of detector pixel response; spectral operations such as Fourier filters and other spectral filters, normalization, mean centering, baseline correction, and smoothing; spatial operations such as cosmic filtering, low-pass filters, high-pass filters, and a number of other spatial filters.

Once instrument response has been suppressed, qualitative processing can be employed. Qualitative chemical image analysis attempts to address a simple question, "What is present and how is it distributed?". Many chemometric tools fall under this category. A partial list includes: correlation techniques such as cosine correlation and Euclidean distance correlation; classification techniques such as principal components analysis, cluster analysis, discriminant analysis, and multi-way analysis; and spectral deconvolution techniques such as SIMPLISMA, linear spectral unmixing and multivariate curve resolution.

Quantitative analysis deals with the development of concentration map images. Just as in quantitative spectral analysis, a number of multivariate chemometric techniques can be used to build the calibration models. In applying quantitative chemical imaging, all of the challenges experienced in non-imaging spectral analysis are present in quantitative chemical imaging, such as the selection of the calibration set and the verification of the model. However, in chemical

imaging additional challenges exist, such as variations in sample thickness and the variability of multiple detector elements, to name a few. Depending on the quality of the models developed, the results can range from semi-quantitative concentration maps to rigorous quantitative measurements.

Results obtained from preprocessing, qualitative analysis and quantitative analysis must be visualized. Software tools must provide scaling, automapping, pseudo-color image representation, surface maps, volumetric representation, and multiple modes of presentation such as single image frame views, montage views, and animation of multidimensional chemical images, as well as a variety of digital image analysis algorithms for look up table (LUT) manipulation and contrast enhancement.

Once digital chemical images have been generated, traditional digital image analysis can be applied. For example, Spatial Analysis and Chemical Image Measurement involve binarization of the high bit depth (typically 32 bits/pixel) chemical image using threshold and segmentation strategies. Once binary images have been generated, analysis tools can examine a number of image domain features such as size, location, alignment, shape factors, domain count, domain density, and classification of domains based on any of the selected features. Results of these calculations can be used to develop key quantitative image parameters that can be used to characterize materials.

The final category of tools, Automated Image Processing, involves the automation of key steps or of the entire chemical image analysis process. For example, the detection of well defined features in an image can be completely automated and the results of these automated analyses can be tabulated based on any number of criteria (particle size, shape, chemical

composition, etc). Automated chemical imaging platforms have been developed that can run for hours in an unsupervised fashion.

This invention incorporates a comprehensive analysis approach that allows user's to carefully plan experiments and optimize instrument parameters and should allow the maximum amount of information to be extracted from chemical images so that the user can make intelligent decisions.

EXAMPLE

Overview

As the demand for high quality, low cost X-ray, γ -ray and imaging detector devices increases, there is a need to improve the quality and production yield of semiconductor materials used in these devices. One effective strategy for improving semiconductor device yield is through the use of better device characterization tools that can rapidly and nondestructively identify defects at early stages in the fabrication process. Early screening helps to elucidate the underlying causes of defects and to reduce downstream costs associated with processing defect laden materials that are ultimately scrapped. The present invention can be used to characterize tellurium inclusion defects in cadmium zinc telluride (CdZnTe) semiconductor materials based on near infrared imaging. With this approach, large area wafers can be inspected rapidly and non-destructively in two and three spatial dimensions by collecting NIR image frames at multiple regions of interest throughout the wafer using an automated NIR imaging system. The NIR image frames are subjected to image processing algorithms including background correction and image binarization. Particle analysis is performed on the binarized images to reveal tellurium inclusion statistics, sufficient to pass or fail wafers. In addition, data visualization software is used to view the tellurium inclusions in two and three spatial dimensions.

Background

The present invention has been used to automatically inspect tellurium inclusions in CdZnTe. Compound semiconductors are challenging to fabricate. There are several steps along the manufacturing process in which defects can arise. The chemical nature associated with semiconductor defects often plays a vital role in device performance. Device fabrication and device processing defects can be difficult and time consuming to measure during manufacturing. Unfortunately, defective devices are often left undiagnosed until latter stages in the manufacturing process because of the inadequacy of the metrology tools being used. This results in low production yields and high costs which can be an impediment to growth in the semiconductor device market potential.

There is a general need in the semiconductor industry for metrology technologies that can nondestructively assess semiconductor material defects and ultimately increase manufacturing yields. A potential solution is to develop a high throughput screening system capable of fusing multiple chemical imaging modalities into a single instrument. Chemical imaging combines digital imaging and molecular spectroscopy for the chemical analysis of materials. A modality of based on near-infrared (NIR) chemical imaging can be used to inspect tellurium inclusions in CdZnTe compound semiconductor materials.

CdZnTe is a leading material for use in room temperature X-ray detectors, γ -ray radiation detectors and imaging devices. Applications for these devices include nuclear diagnostics, digital radiography, high-resolution astrophysical X-ray and γ -ray imaging, industrial web gauging and nuclear nonproliferation. These devices are often decorated with microscopic and macroscopic defects limiting the yield of large-size, high-quality materials. Defects commonly found in these materials include cracks, grain boundaries, twin boundaries, pipes, precipitates

and inclusions. CdZnTe wafers are often graded based on the size and number of Te inclusion defects present.

The definition used by Rudolph and Muhlberg for tellurium inclusions (i.e., tellurium-rich domains in the 1 – 50 μm size range that originate as a result of morphological instabilities at the growth interface as tellurium-rich melt droplets are captured from the boundary layer ahead of the interface) has been adopted and is used herein. There have been numerous studies on the composition and distribution of tellurium inclusions in CdZnTe material. It has been demonstrated that the presence of tellurium inclusions can impair the electronic properties of CdZnTe materials – consequently degrading the end-product device performance.

The current procedure used by low volume semiconductor manufacturers for characterizing tellurium inclusions in CdZnTe is labor intensive, susceptible to human error and provides little information on inclusions in the 1-5 μm size scale. Inclusions are viewed and counted manually by a human operator using an IR microscope platform. When an inclusion is identified that is suspected to exceed a specified size limit, a Polaroid film photograph is taken. An overlay of a stage micrometer is laid over the photograph to determine the size. This analysis is relatively time consuming, often taking several minutes to characterize a region of interest from a large wafer.

The present invention can be used for automated characterization of microscale tellurium inclusions in CdZnTe based on volumetric NIR chemical imaging. The system takes advantage of the fact that CdZnTe is transparent to infrared wavelengths ($> 850\text{ nm}$). When viewing CdZnTe with an infrared focal plane array (IR-FPA) through a NIR LC imaging spectrometer, tellurium inclusions appear as dark, absorbing domains. The invention images wafers in two and three spatial dimensions capturing raw infrared images at each region of interest. Images are

automatically background equilibrated, binarized and processed. The processed data provides particle statistical information such as inclusion counts, sizes, density, area and shape. The system provides a rapid method for characterizing tellurium inclusions as small as 0.5 μm while virtually eliminating the subjectivity associated with manual inspection.

Sample Description

Tellurium-rich CdZnTe samples were produced by a commercial supplier (eV Products) for analysis. Samples containing high tellurium inclusion densities were purposely acquired to effectively demonstrate the capabilities of the automated tellurium inclusions mapping system. The CdZnTe materials were grown by the Horizontal Bridgman (HB) method and contained a nominal zinc cation loading concentration of 4% and an average etch pit density of $4 \times 10^4/\text{cm}^2$. The materials displayed a face A $\langle 111 \rangle$ orientation and were polished on both sides. Sample thicknesses ranged from approximately 1 mm to 15 mm. No further sample preparation was necessary for the automated tellurium inclusion mapping analysis.

Data Collection

Volumetric maps of the tellurium inclusions in the CdZnTe samples were obtained by first placing the sample on the XYZ-translational stage of the automated mapping system. NIR image frames were then captured through the LC imaging spectrometer at a wavelength that maximized the Te precipitate contrast relative to the surrounding CdZnTe matrix in the X-Y direction at multiple regions of interest across the samples. Depth profiling was achieved by translating the sample focus under the microscope at user-defined increments. This process was then repeated in an iterative fashion until the entire wafer was characterized.

Data Processing

Once imaging data was collected, ChemImage was used to process the data. For each wafer, the software generates a background-corrected grayscale image, a binarized image using the threshold value selected for each frame of the image, a montage view of the binarized image and particle statistics. The particle statistics table includes information such as particle counts, particle sizes, particles densities, and a number of geometrical parameters such as particle area and particle aspect ratios.

NIR Imaging

Figures 3 and 4, respectively, show a digital macro brightfield image and a raw NIR microscopic transmittance image of a CdZnTe semiconductor material with numerous tellurium inclusions. The left half of the wafer has been polished. The tellurium inclusions appear as dark spots in the microscopic NIR image. The raw NIR microscopic image was acquired using the automated near-infrared tellurium inclusion volumetric mapping system.

Background Correction and Image Binarization

The automated particle analysis begins by applying a background correction preprocessing routine to the raw image frames. One of the biggest problems with the raw images collected is the gradually varying background across each image frame. As a result, a particle in one area of a frame may have a higher intensity value than the background of another area of that frame.

Figures 5A - 5D illustrate the difficulty associated with selecting a threshold value for an image with a widely varying background. In Figures 5A - 5D, regions 1 and 2 have mean intensity values of approximately 2600 and 1950, respectively. The whole of region 1 is primarily a particle whereas region 2 is primarily background with a small particle in the center.

Figure 5A shows a raw NIR image frame collected from a single region of interest in a CdZnTe wafer. At wavelengths longer than approximately 850 nm, CdZnTe is transparent while tellurium inclusions remain opaque. A NIR image of the sample is light where there are no precipitates and dark where there are precipitates. In Figure 5B, the threshold value is set low enough (value = 1520) that the particle in region 2 is correctly identified, but most of the remaining particles are not found. In Figure 5C, the threshold value is set high enough (value = 2470) so that all particles are detected. Unfortunately, a large area of the frame is incorrectly identified as one very large particle. Figure 5D displays the case in which the threshold is set to an intermediate value (value = 1960). Many of the particles are correctly identified, but the particle in region 2 is identified as being larger than it actually is.

To address this issue, a background correction step is used to force the background to be essentially constant across a given image frame. The procedure applies a moving window across the image frame and smoothes the resulting background before subtracting it from the frame. Other operations such as low pass filtering and selective removal of bad camera pixels are also applied.

The second step in the automated particle analysis is the selection of the threshold value resulting in the binarized image which best reflects the number and size of particles actually present in the sample being imaged. A human operator would typically approach this problem by trying multiple threshold values and comparing the resulting binarized images to the actual image to see which binarized image best matches their perception of the particles in the actual image. The algorithm employed by the NIR chemical imaging microscope system takes essentially the same approach. A series of threshold values are used to generate binarized images. Each binarized image is submitted to a routine that finds the particles present in the

image. A set of particle morphology rules was developed to determine the point at which the threshold value identifies the particles consistent with results obtained by a trained human operator. This threshold value is then further refined with using derivative operations.

Figures 6A - 6C show montage views of raw, background-corrected, and binarized NIR image frames, respectively, corresponding to four adjacent regions of interest from a CdZnTe wafer. A visual inspection of these images suggests that the particle analysis adequately identifies the particles in an automated fashion.

Volumetric Reconstruction and Visualization

It is of particular interest to the semiconductor manufacturing industry to view defects, including tellurium inclusions in this example, in a three dimensional volumetric view. Individual binarized image frames generated at discrete axial planes of focus have been reconstructed into a volumetric view allowing users to view tellurium inclusions in three-dimensional space.

Figure 7 shows a 3D volumetric view of tellurium inclusions in CdZnTe generated from 50 individual image slices. Figure 7 is constructed using a nearest neighbors computational approach for volume reconstruction. Improved results can be obtained using more sophisticated strategies that deconvolve the entire image volume using iterative deconvolution approaches. The starting time of the sensor used to gather the volumetric data was less than 1 sec. The total acquisition time for the data generated in this figure was well under a minute. Note how the inclusions tend to form in planes described as veils. These veils are believed to be subgrain boundaries within the CdZnTe material. Grain boundaries provide low energy nucleation sites for the inclusions to form during the growth process.

Table 1 provides tabulated statistical information on the volumetric data shown in Figure

7.

Table 1. Particle Statistics

Slice Number and Depth (μm)

Parameters	0 (0)	10 (89.77)	20 (189.52)	30 (289.26)	40 (389.01)	50 (488.75)
# of Inclusions	25	30	27	24	25	36
Mean Diameter (μm)	12.12	11.38	12.75	15.70	12.89	13.73
Density (Inclusions/ cm^2)	4368	5241	4717	4193	4368	6289
Area (μm^2)	97.48	73.78	91.67	119.25	96.29	98.15
Perimeter (μm)	40.40	37.32	43.27	50.72	41.93	43.98
Shape Factor	0.60	0.60	0.58	0.53	0.60	0.55
Maximum Chord Length	12.12	11.38	12.75	15.70	12.89	13.73
Feret 1 Diameter	9.17	9.56	11.33	12.64	10.48	10.16
Feret 2 Diameter	10.26	9.01	10.10	12.18	10.37	11.60
Aspect Ratio	1.02	1.19	1.16	1.08	1.02	0.95

Defects such as tellurium inclusions affect the electrical properties in CdZnTe semiconductor materials, degrading end-product device performance. Having the ability to rapidly and non-invasively identify and quantify tellurium inclusion defects at critical stages in the fabrication process provides semiconductor manufacturers with information that will enable

them to optimize the manufacturing process and reduce production costs. The Automated NIR Volumetric Mapping System described here is capable of providing such information. The system provides qualitative and quantitative information about tellurium inclusions present in CdZnTe wafers in two and three spatial dimensions. This system boasts improved spatial resolution ($\sim 0.5 \mu\text{m}$) compared to systems currently used by many semiconductor manufacturers and it virtually eliminates the subjectivity associated with human counting and sizing measurements. Whole wafers are capable of being characterized in minutes.

While in the above example, the present invention has been demonstrated in connection with the characterization of semiconductors, it is to be expressly understood that the present invention can also be used in the characterization of other materials including, but not limited to, food and agricultural products, paper products, pharmaceutical materials, polymers, thin films and in medical uses.

Although present preferred embodiments of the invention have been shown and described, it should be distinctly understood that the invention is not limited thereto but may be variously embodied within the scope of the following claims.

We Claim:

1. A near infrared radiation chemical imaging system comprising:
 - a) an illumination source for illuminating an area of a sample using light in the near infrared radiation wavelength;
 - b) a device for collecting a spectrum of near infrared wavelength radiation light transmitted, reflected, emitted or scattered from said illuminated area of said sample and producing a collimated beam therefrom;
 - c) a near infrared imaging spectrometer for selecting a near infrared radiation image of said collimated beam; and
 - d) a detector for collecting said filtered near infrared images
2. The system of claim 1 wherein said illumination source is one of a quartz tungsten halogen lamp, a tunable laser, a metal halide lamp, and a xenon arc lamp.
3. The system of claim 1 wherein said device for collecting is one of a refractive type infinity-corrected near infrared optimized microscope objective, a refractive fixed tube length microscope objective, and a reflecting microscope objective.
4. The system of claim 1 wherein said near infrared imaging spectrometer is selected from the group consisting of Lyot liquid crystal tunable filters; Evans Split-Element liquid crystal tunable filters; Solc liquid crystal tunable filters; Ferroelectric liquid crystal tunable filters; Liquid crystal Fabry Perot filters; a hybrid filter formed from a combination of liquid crystal tunable filters; and a combination of a liquid crystal tunable filter and a fixed bandpass and bandreject filters.

5. The system of claim 1 wherein said detector is a near infrared radiation focal plane array detector.
6. The system of claim 5 wherein said detector is selected from the group consisting of indium gallium arsenide, platinum silicide, indium antimonide, palladium silicide, indium germanide, and mercury cadmium telluride.
7. The system of claim 1 further comprising a visible wavelength imagery system.
8. The system of claim 7 wherein said visible imagery system comprises:
 - a) an illumination source for illuminating an area of said sample using light in the visible optical wavelengths; and
 - b) a device for detecting said visible wavelength light from said illuminated area of said sample.
9. The system of claim 8 wherein said device for detecting said visible wavelength light comprises an analog and digital detector based on at least one of a silicon charge-coupled device detector and a silicon CMOS detectors.
10. The system of claim 8 further comprising a processor for producing a near infrared radiation chemical image of said sample.
11. The system of claim 8 further comprising an algorithm for combining the near infrared and visible image data.
12. A chemical imaging system comprising a near infrared imaging detection system and a visible imagery system.

13. The chemical imaging system of claim 12 wherein said near infrared imaging detection system comprises:

- a) an illumination source for illuminating an area of a sample using light in the near infrared radiation wavelength;
- b) a device for collecting a spectrum of near infrared wavelength radiation light transmitted, reflected, emitted or scattered from said illuminated area of said sample and producing a collimated beam therefrom;
- c) a near infrared imaging spectrometer for selecting a near infrared radiation image of said collimated beam; and
- d) detector for collecting said filtered near infrared images.
- e) an algorithm for processing the near infrared and visible image data.

14. The chemical imaging system of claim 12 wherein said visible imagery system comprises:

- a) an illumination source for illuminating an area of said sample using light in the visible wavelength; and
- b) a device for detecting said visible wavelength light from said illuminated area of said sample.

15. A chemical imaging system comprising:

- a) an illumination source for illuminating an area of a sample using light in the near infrared radiation wavelength and light in the visible wavelength;

- b) a device for collecting a spectrum of near infrared wavelength radiation light transmitted, reflected, emitted or scattered from said illuminated area of said sample and producing a collimated beam therefrom;
- c) a near infrared imaging spectrometer for selecting a near infrared radiation image of said collimated beam;
- d) detector for collecting said filtered near infrared images; and
- e) a device for detecting said visible wavelength light from said illuminated area of said sample.
16. A chemical imaging method comprising the steps of:
- a) illuminating an area of a sample using light in the near infrared radiation wavelength and light in the visible wavelength;
- b) collecting a spectrum of near infrared wavelength radiation light transmitted, reflected, emitted or scattered from said illuminated area of said sample and producing a collimated beam therefrom;
- c) filtering said collimated beam to produce a near infrared radiation image of said collimated beam while simultaneously detecting said optical wavelength light from said illuminated area of said sample;
- d) collecting said filtered near infrared images; and
- e) processing said collected near infrared images to produce a chemical image of said sample.

17. A method for producing a volumetric image of a sample comprising the steps of:
- moving said sample through an objective;
 - collecting images of said sample through said objective in a plurality of focus depths; and
 - processing said collected images to reconstruct an image of said sample.
18. A method for producing a volumetric image of a sample comprising the steps of:
- incorporating a refractive image formation optic exhibiting a chromatic response in the optical path of the microscope before the near infrared detector;
 - collecting images of said sample at a plurality of near infrared wavelengths through said objective at a fixed focus condition; and
 - processing said collected images to reconstruct a depth resolved image of said sample.
19. A method for chemically analyzing a sample comprising the steps of:
- seeding said sample with a plurality of analytes having at least one of a known composition, structure and concentration;
 - collecting a plurality of spatially-resolved spectra for said plurality of analytes;
 - producing a plurality of chemical images of said sample containing said plurality of analytes; and

- d) processing said plurality of chemical images to generate a chemical image of said sample.

20. The method of claim 19 wherein said processing step comprises at least one of:

- a) correcting the image by dividing a near infrared image of said sample by a near infrared image of a background of said image to produce a resulting ratioed image ;
- b) normalizing the divided image by dividing each intensity value at every pixel in the image by the vector norm for its corresponding pixel spectrum, said vector norm being the square root of the sum of the squares of pixel intensity values for each pixel spectrum;
- c) processing said image using a cosine correlation analysis method wherein each pixel spectrum is treated as a projected vector in n-dimensional space, wherein n is the number of wavelengths sampled in the image; and
- d) processing said image using a principal component analysis method wherein a least squares fit is drawn through the maximum variance in the n-dimensional dataset.

Abstract of the Disclosure

A chemical imaging system is provided which uses a near infrared radiation microscope. The system includes an illumination source which illuminates an area of a sample using light in the near infrared radiation wavelength and light in the visible wavelength. A multitude of spatially resolved spectra of transmitted, reflected, emitted or scattered near infrared wavelength radiation light from the illuminated area of the sample is collected and a collimated beam is produced therefrom. A near infrared imaging spectrometer is provided for selecting a near infrared radiation image of the collimated beam. The filtered images are collected by a detector for further processing. The visible wavelength light from the illuminated area of the sample is simultaneously detected providing for the simultaneous visible and near infrared chemical imaging analysis of the sample. Two efficient means for performing three dimensional near infrared chemical imaging microscopy are provided.

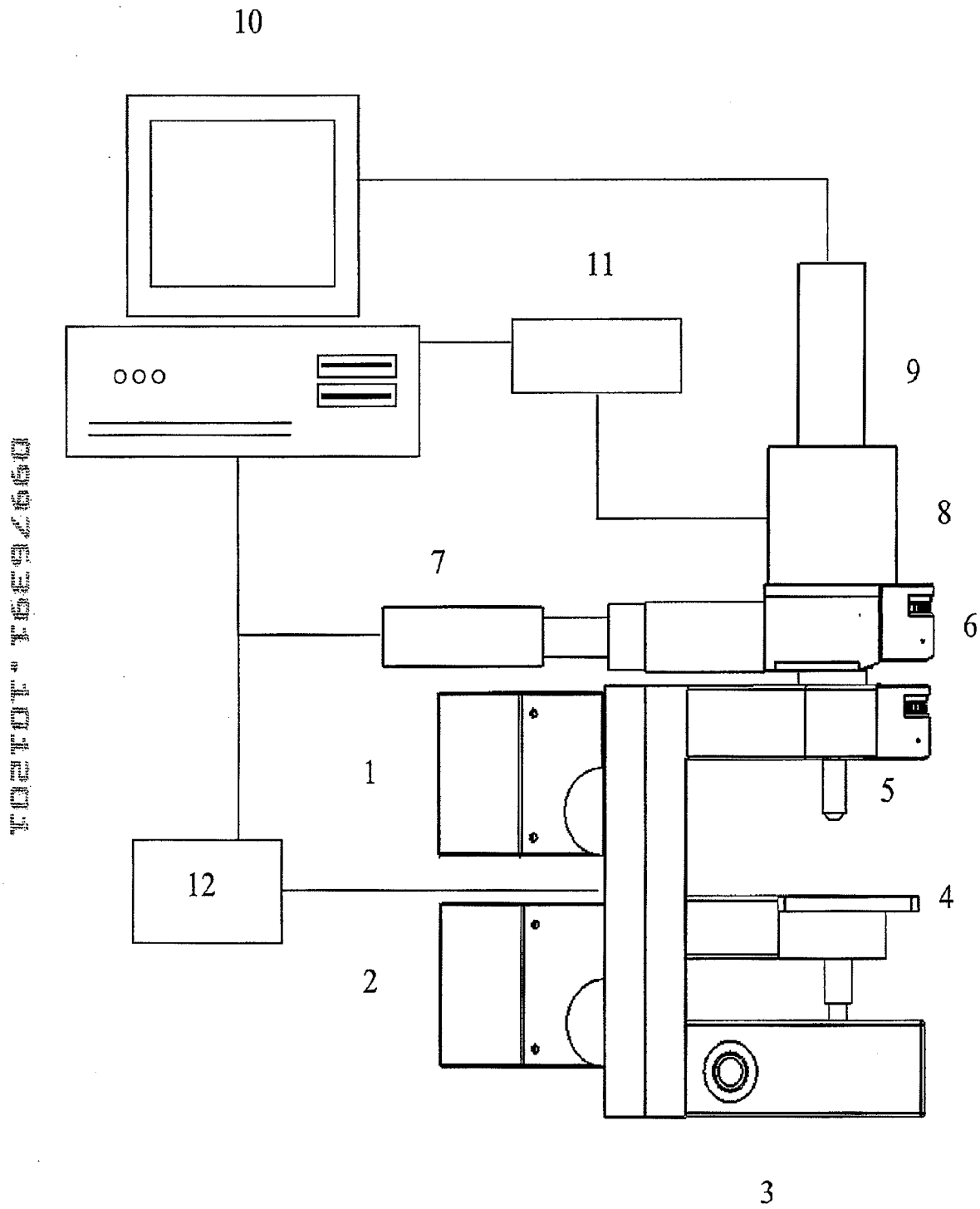


Figure 1

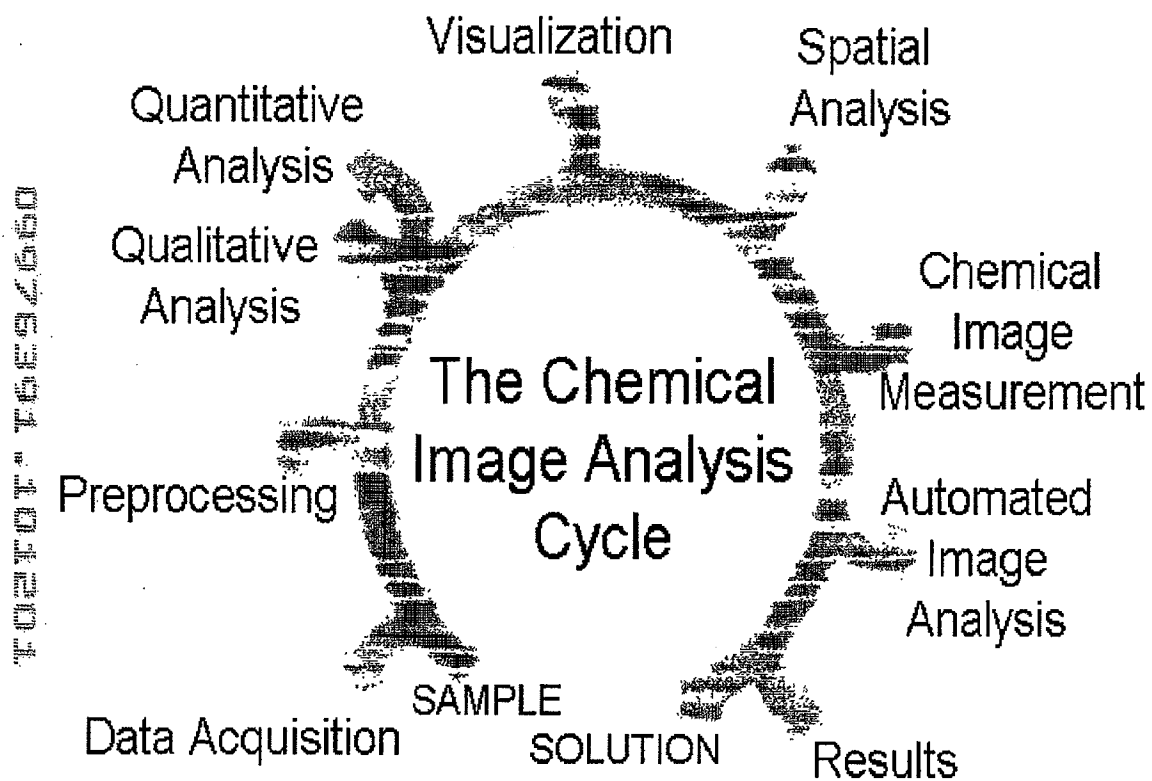


Figure 2

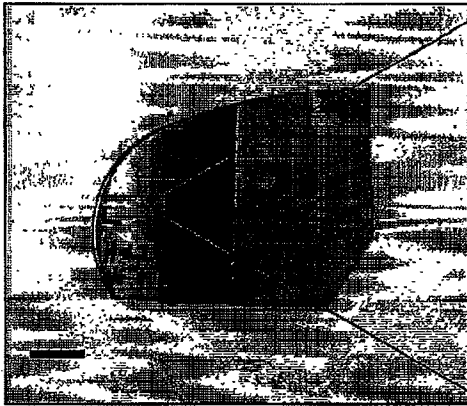


Figure 3

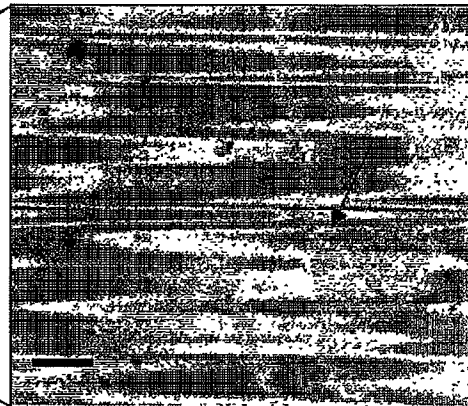


Figure 4

Figure 5A

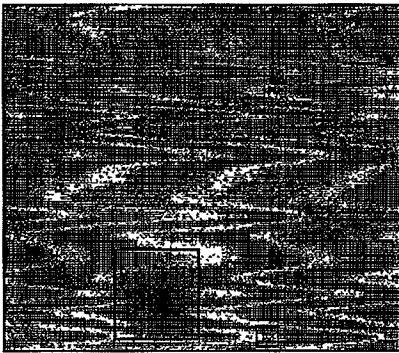


Figure 5B

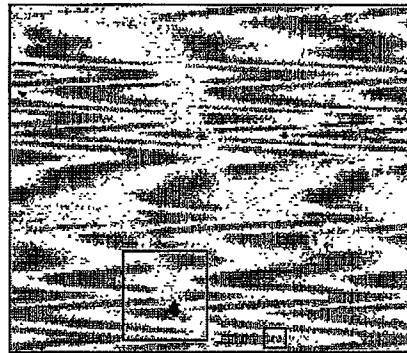


Figure 5C

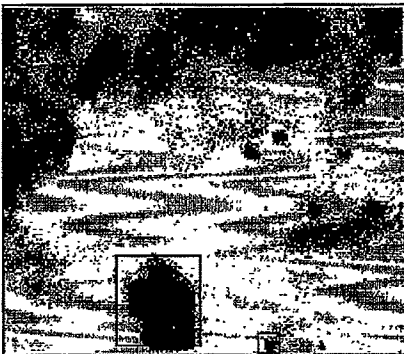
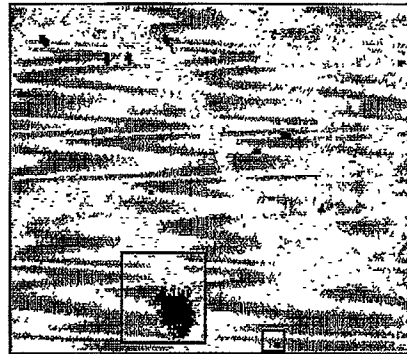


Figure 5D



09070301 101201

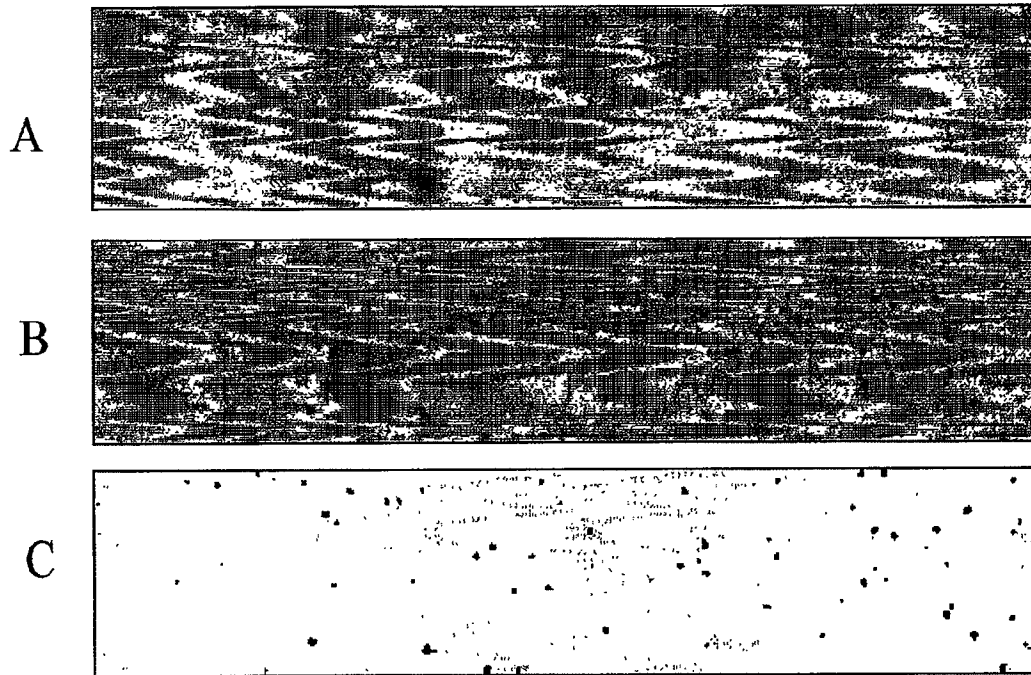


Figure 6

059263914301

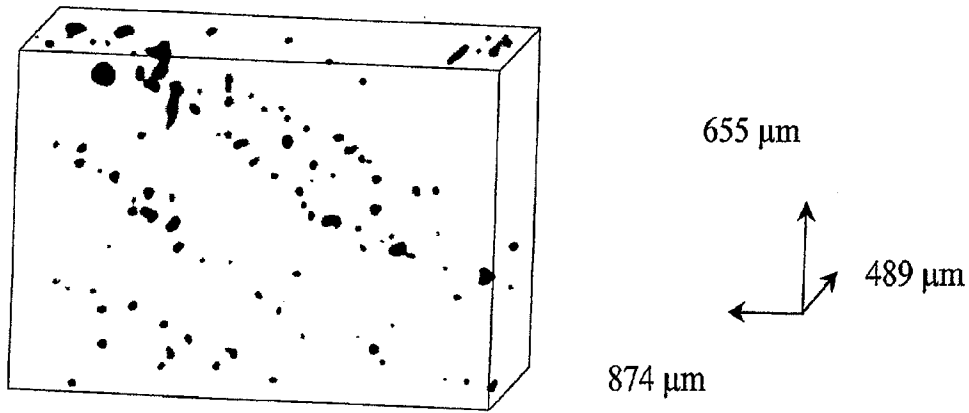


Figure 7

EXHIBIT Z

OPR/ASSIGNMENTS 2/4/04 3:47 PAGE 2/6 RightFAX



UNITED STATES DEPARTMENT OF COMMERCE
Patent and Trademark Office
ASSISTANT SECRETARY AND COMMISSIONER
OF PATENTS AND TRADEMARKS
Washington, D.C. 20231



700063882A

FEBRUARY 04, 2004

PTAS

BUCHANAN INGERSOLL, P.C.
DUANE A. STEWART III
301 GRANT STREET
20TH FLOOR
PITTSBURGH, PA 15219

UNITED STATES PATENT AND TRADEMARK OFFICE
NOTICE OF RECORDATION OF ASSIGNMENT DOCUMENT

THE ENCLOSED DOCUMENT HAS BEEN RECORDED BY THE ASSIGNMENT DIVISION OF THE U.S. PATENT AND TRADEMARK OFFICE. A COMPLETE MICROFILM COPY IS AVAILABLE AT THE ASSIGNMENT SEARCH ROOM ON THE REEL AND FRAME NUMBER REFERENCED BELOW.

PLEASE REVIEW ALL INFORMATION CONTAINED ON THIS NOTICE. THE INFORMATION CONTAINED ON THIS RECORDATION NOTICE REFLECTS THE DATA PRESENT IN THE PATENT AND TRADEMARK ASSIGNMENT SYSTEM. IF YOU SHOULD FIND ANY ERRORS OR HAVE QUESTIONS CONCERNING THIS NOTICE, YOU MAY CONTACT THE EMPLOYEE WHOSE NAME APPEARS ON THIS NOTICE AT 703-308-9723. PLEASE SEND REQUEST FOR CORRECTION TO: U.S. PATENT AND TRADEMARK OFFICE, ASSIGNMENT DIVISION, BOX ASSIGNMENTS, CG-4, 1213 JEFFERSON DAVIS HWY, SUITE 320, WASHINGTON, D.C. 20231.

RECORDATION DATE: 02/03/2004

REEL/FRAME: 014302/0906
NUMBER OF PAGES: 5

BRIEF: ASSIGNMENT OF ASSIGNOR'S INTEREST (SEE DOCUMENT FOR DETAILS).

ASSIGNOR:

KEITZER, SCOTT

DOC DATE: 01/26/2004

ASSIGNOR:

TREADO, PATRICK J.

DOC DATE: 01/14/2004

ASSIGNOR:

NELSON, MATTHEW

DOC DATE: 01/12/2004

ASSIGNEE:

CHEMIMAGE CORPORATION
7301 PENN AVENUE
PITTSBURGH, PENNSYLVANIA 15208

SERIAL NUMBER: 09976391
PATENT NUMBER:

FILING DATE: 10/12/2001
ISSUE DATE:

CRI002027

OPR/ASSIGNMENTS 2/4/04 3:47 PAGE 3/6 RightFAX

014302/0906 PAGE 2


SAUNDRA BALLENGER, EXAMINER
ASSIGNMENT DIVISION
OFFICE OF PUBLIC RECORDS

CR1002028

OPR/ASSIGNMENTS 2/4/04 3:47 PAGE 4/6 RightFAX
 FEB 03 '04 11:30 FR BUCHANAN JUDGE
 02/03/2004
 700063882
 TD 917033865995 P.06/10

FORM PTO-1619A (Rev. 05/2003) OMB 0591-0020		U.S. Department of Commerce Patent and Trademark Office PATENT	
RECORDATION FORM COVER SHEET PATENTS ONLY			
TO: The Commissioner of Patents and Trademarks. Please record the attached original document(s) or copy(ies).			
Submission Type <input checked="" type="checkbox"/> New <input type="checkbox"/> Reissuance (Non-Continuation) Document ID: _____ <input type="checkbox"/> Correction of PTO Error Serial # _____ Frame # _____ <input type="checkbox"/> Corrective Document Serial # _____ Frame # _____		Conveyance Type <input checked="" type="checkbox"/> Assignment <input type="checkbox"/> Security Agreement <input type="checkbox"/> License <input type="checkbox"/> Change of Name <input type="checkbox"/> Merger <input type="checkbox"/> Other _____ (For Use Only by U.S. Government Agencies) <input type="checkbox"/> Departmental File <input type="checkbox"/> Secret File	
Conveying Party(ies) <input checked="" type="checkbox"/> Mark if additional names of conveying parties attached			
Name (line 1) <u>Patrick J. Treudo</u>		Expiration Date Month Day Year <u>01 14 04</u>	
Name (line 2) _____			
Second Party			
Name (line 1) <u>Matthew Nelson</u>		Expiration Date Month Day Year <u>01 12 04</u>	
Name (line 2) _____			
Receiving Party <input type="checkbox"/> Mark if additional names of receiving parties attached			
Name (line 1) <u>ChemImage Corporation</u>		<input type="checkbox"/> If document to be recorded is an assignment and the recording party is not disclosed in the United States, an appointment of a domestic representative is attached. (Designation must be a separate document from Assignment.)	
Name (line 2) _____			
Address (line 1) <u>7301 Penn Avenue</u>			
Address (line 2) _____			
Address (line 3) <u>Pittsburgh</u> <u>Pennsylvania</u> <u>15208</u>			
City State Zip			
Domestic Representative Name and Address Enter for the first Receiving Party only.			
Name _____			
Address (line 1) _____			
Address (line 2) _____			
Address (line 3) _____			
Address (line 4) _____			
FOR OFFICE USE ONLY			
<small>Patent law requires reporting to this collection of documents to be submitted to the Patent and Trademark Office, including the fee for recording the document and protecting the data needed to complete the record. Send comments regarding this form to the U.S. Patent and Trademark Office, Chief Information Officer, Washington, D.C. 20231 and to the Office of Information and Regulatory Affairs, Office of Management and Budget, Paperwork Reduction Project (0591-0020), Washington, D.C. 20503. This form is part of the Collection Budget Package 0591-0020, Patent and Trademark Assignment Form. DO NOT SEND REQUESTS TO RECORD ASSIGNMENT DOCUMENTS TO THE AGENCIES.</small>			
<small>Mail documents to be recorded with required cover sheet(s) information to: Commissioner of Patents and Trademarks, Box Assignments, Washington, D.C. 20231</small>			

OPR/ASSIGNMENTS 2/4/04 3:47 PAGE 5/6 RightFAX
 FEB 03 '04 11:30 FR BUCHANAN INGERSOLL TO 91783385995 P.07/10

FORM PTO-1619B <small>Patent Office</small>		Page 2		<small>U.S. Department of Commerce Patent and Trademark Office</small> PATENT	
Correspondent Name and Address					
Area Code and Telephone Number 412-562-1622				Name Duane A. Stewart III	
Address (line 1) Buchanan Ingersoll, P.C.					
Address (line 2) 301 Grant Street, 20th Floor					
Address (line 3) Pittsburgh, PA 15219					
Address (line 4)					
Pages Enter the total number of pages of the attached conveyance document including any attachments. # 2					
Application Number(s) or Patent Number(s)					
<small>Enter either the Patent Application Number or the Patent Number (DO NOT ENTER BOTH numbers for the same property).</small>					
Patent Application Number(s)			Patent Number(s)		
09/976,391					
<small>If this document is being filed together with a new Patent Application, enter the date the patent application was signed by the first named consulting inventor.</small>					
Patent Cooperation Treaty (PCT)					
Enter PCT application number only if a U.S. Application Number has not been assigned.					
PCT		PCT		PCT	
Number of Properties					
Enter the total number of properties involved. # 1					
Fee Amount					
Fee Amount for Properties Listed (37 CFR 1.41): \$ 40.00					
Method of Payment: Enclosed <input type="checkbox"/> Deposit Account <input checked="" type="checkbox"/>					
<small>Enter for payment by deposit account or if additional fees can be charged to the account.</small>					
Deposit Account Number: # 02-4553					
Authorization to charge additional fees: Yes <input checked="" type="checkbox"/> No <input type="checkbox"/>					
Statement and Signature					
To the best of my knowledge and belief, the foregoing information is true and correct and any attached copy is a true copy of the original document. Charges to deposit account are authorized, as indicated herein.					
Duane A. Stewart III				February 3, 2004	
Name of Person Signing		Signature		Date	

CRI002030

OPR/ASSIGNMENTS 2/4/04 3:47 PAGE 6/6 RightFAX
 FEB 03 '04 11:30 FR BUCHANAN INDESOIL TO 917833855935 P.08/10

FORM PTO-1619C <small>October 2003 Edition Patent Office</small>	RECORDATION FORM COVER SHEET CONTINUATION PATENTS ONLY	U.S. Department of Commerce Patent and Trademark Office PATENT																																				
Conveying Party(ies) <input type="checkbox"/> Mark if additional copies of conveying parties attached Enter additional Conveying Parties																																						
Name (line 1) <u>Scott Keltner</u>	Execution Date Month Day Year <u>01 26 04</u>																																					
Name (line 2) _____																																						
Name (line 3) _____	Execution Date Month Day Year _____																																					
Name (line 4) _____																																						
Name (line 5) _____	Execution Date Month Day Year _____																																					
Name (line 6) _____																																						
Receiving Party(ies) <input type="checkbox"/> Mark if additional copies of receiving parties attached Enter additional Receiving Party(ies)																																						
Name (line 1) _____	<input type="checkbox"/> If document to be recorded is an assignment and the receiving party is not domiciled in the United States, an appointment of a domestic representative is attached. (Designation must be a separate document from Assignment.)																																					
Name (line 2) _____																																						
Address (line 1) _____	<input type="checkbox"/> If document to be recorded is an assignment and the receiving party is not domiciled in the United States, an appointment of a domestic representative is attached. (Designation must be a separate document from Assignment.)																																					
Address (line 2) _____																																						
Address (line 3) _____	City _____ State/County _____ Zip Code _____																																					
Name (line 4) _____	<input type="checkbox"/> If document to be recorded is an assignment and the receiving party is not domiciled in the United States, an appointment of a domestic representative is attached. (Designation must be a separate document from Assignment.)																																					
Name (line 5) _____																																						
Address (line 4) _____	<input type="checkbox"/> If document to be recorded is an assignment and the receiving party is not domiciled in the United States, an appointment of a domestic representative is attached. (Designation must be a separate document from Assignment.)																																					
Address (line 5) _____																																						
Address (line 6) _____	City _____ State/County _____ Zip Code _____																																					
Application Number(s) or Patent Number(s) <input type="checkbox"/> Mark if additional numbers attached Enter either the Patent Application Number or the Patent Number (DO NOT ENTER BOTH numbers for the same property).																																						
<table border="1" style="width: 100%; border-collapse: collapse;"> <thead> <tr> <th colspan="3" style="text-align: left;">Patent Application Number(s)</th> <th colspan="3" style="text-align: left;">Patent Number(s)</th> </tr> </thead> <tbody> <tr><td> </td><td> </td><td> </td><td> </td><td> </td><td> </td></tr> <tr><td> </td><td> </td><td> </td><td> </td><td> </td><td> </td></tr> <tr><td> </td><td> </td><td> </td><td> </td><td> </td><td> </td></tr> <tr><td> </td><td> </td><td> </td><td> </td><td> </td><td> </td></tr> <tr><td> </td><td> </td><td> </td><td> </td><td> </td><td> </td></tr> </tbody> </table>			Patent Application Number(s)			Patent Number(s)																																
Patent Application Number(s)			Patent Number(s)																																			

Atty. Ref. No. 011311

ASSIGNMENT

WHEREAS, We, Patrick J. Treado, Matthew Nelson and Scott Keitzer, residing at Allegheny County, Pittsburgh, Pennsylvania; Allegheny County, Pittsburgh, Pennsylvania; and Westmoreland County, Export, Pennsylvania respectively, have invented certain new and useful apparatus, inventions, discoveries and/or improvements disclosed in a U.S. patent application entitled "Near Infrared Chemical Imaging Microscope" for which an application for United States Letters Patent was filed in the United States Patent and Trademark Office on October 12, 2001 bearing Serial No. 09/976,391;

AND WHEREAS, ChemImage Corporation, having a place of business at 7301 Penn Avenue, Pittsburgh, Pennsylvania 15208 (hereinafter the "Assignee"), is desirous of acquiring the entire right, title and interest in and to said application and the apparatus, inventions, discoveries, and improvements therein disclosed;

NOW THEREFORE, in consideration of One Dollar (\$1.00) and other good and valuable consideration paid to us by said Assignee, receipt whereof we hereby acknowledge, we do hereby assign, sell, transfer, and set over unto said Assignee the entire right, title, and interest in and to said application and the apparatus, inventions, discoveries and improvements therein disclosed for the United States and all foreign countries and any Letters Patent which may issue therefor in the United States and all foreign countries and all divisions, reissues, continuations, renewals, and/or extensions thereof, including all priority rights under the International Convention associated therewith for each country and the United States, said Assignee to have and to hold the interests herein assigned to the full ends of the terms of said Letters Patent and any and all divisions, reissues, continuations, renewals, and/or extensions thereof, respectively, as fully and entirely as the same would have been held and enjoyed by us had this Assignment not been made.

The Commissioner of Patents and Trademarks is requested to issue such Letters Patent in accordance herewith. We covenant that we are the lawful owners of the said application, apparatus, inventions, discoveries and improvements, that the same are unencumbered, that no license has been granted to make, use, or vend the said apparatus, inventions, discoveries or improvements or any of them, and that we have the full right to make this Assignment.

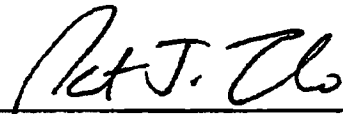
And for said consideration, we agree jointly and individually that we will communicate to said Assignee or the representatives thereof any facts known to us respecting said apparatus, inventions, discoveries and improvements, and will, upon request, but without expense to us, testify in any legal proceedings, sign all lawful papers, execute all divisional, reissue, continuation, renewal, and/or extension applications, make all rightful oaths, and generally do all other and further lawful acts, deemed necessary or expedient by said Assignee or by counsel for said Assignee, to assist or enable said Assignee to obtain and enforce full benefits from the rights and interests herein assigned, and, in the event of any application or Letters Patent assigned herein becoming involved in Interference, to cooperate to the best of the ability of the undersigned in the matters of preparing and executing the preliminary statement and giving and producing evidence in support thereof. This Assignment shall be binding upon our heirs,

Atty. Ref. No. 011311

executors, administrators, and/or assigns, and shall inure to the benefit of the heirs, executors, administrators, successors, and/or assigns, as the case may be, of said Assignee.


And for said consideration, the undersigned hereby agrees to execute, at the request of said Assignee, all documents in connection with any application for foreign letters patent therefor.

Executed: 1/14/04



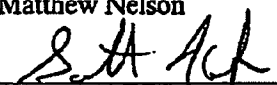
Patrick J. Treado

Executed: 1-12-04



Matthew Nelson

Executed: 1/26/04



Scott Keitzer

EXHIBIT AA

(10) **Patent No.:** **US 6,734,962 B2**
(45) **Date of Patent:** **May 11, 2004**

5,911,017 A	6/1999	Wach et al.	385/12
5,943,122 A	8/1999	Holmes	356/73
6,002,476 A	12/1999	Treado et al.	356/301
6,088,100 A	7/2000	Brenan et al.	356/346
6,483,641 B1	11/2002	MacAulay	359/385
6,571,117 B1	5/2003	Marbach	600/473

(57) **ABSTRACT**

16 Claims, 6 Drawing Sheets

US 6,734,962 B2

Page 2

OTHER PUBLICATIONS

Treado et al. "A Thousand Points of Light: The Hadamard Transform" *Analytical Chemistry* 61 (1989) Jun. 1, No. 11, pp 723-734.

P. Treado et al., "High-Fidelity Raman Imaging Spectrometry: A Rapid Method Using an Acousto-Optic Tunable Filter". vol. 46 *Applied Spectroscopy*, No. 8, pp. 1211-(1992).

H. Morris, C. Hoyt, P. Miller and P. Treado, "Liquid Crystal Tunable Filter Raman Chemical Imaging", vol. 50 *Applied Spectroscopy*, No. 6, pp. 805-811 (1996).

Patrick J. Treado, Ira W. Levin and E. Neil Lewis, Near-Infrared Acousto-Optic Filtered Spectroscopic Microscopy: A

Solid-State Approach to Chemical Imaging, *Applied Spectroscopy* 46, (1992) 553-559.

Patrick J. Treado and Michael D. Morris, *Infrared and Raman Spectroscopic Imaging* (Marcell Decker, New York, 1992) pp. 71-108.

John F. Turner H and Patrick J. Treado, LCTF Raman Chemical Imaging in the Near-Infrared, *Proc. SPIE* 3061, (1997) 280-283.

Spectral Dimensions. NIR Systems Product Information, <http://www.spectraldimensions.com/products/b-nir.html>.

* cited by examiner

U.S. Patent

May 11, 2004

Sheet 1 of 6

US 6,734,962 B2

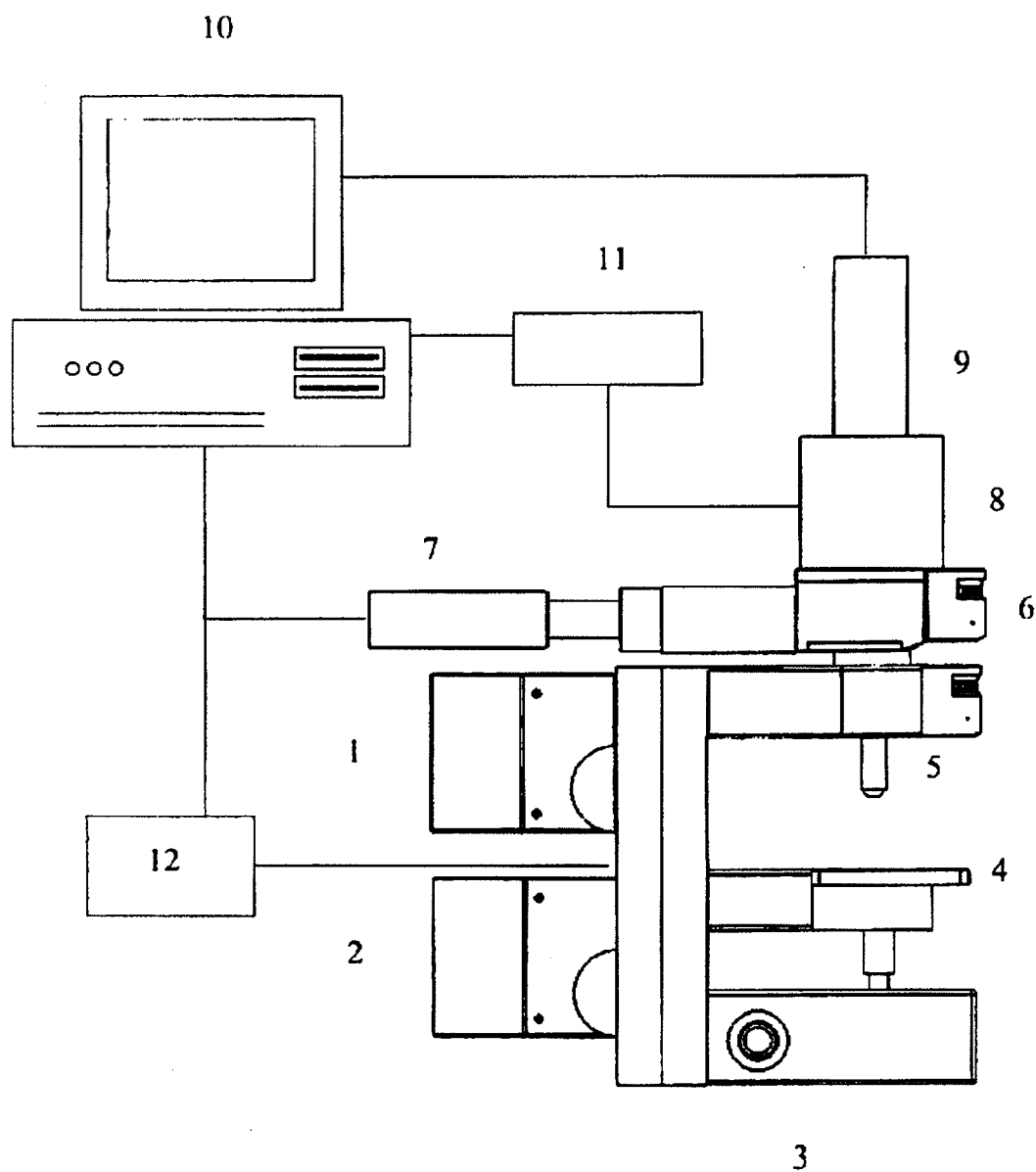


Figure 1

U.S. Patent

May 11, 2004

Sheet 2 of 6

US 6,734,962 B2

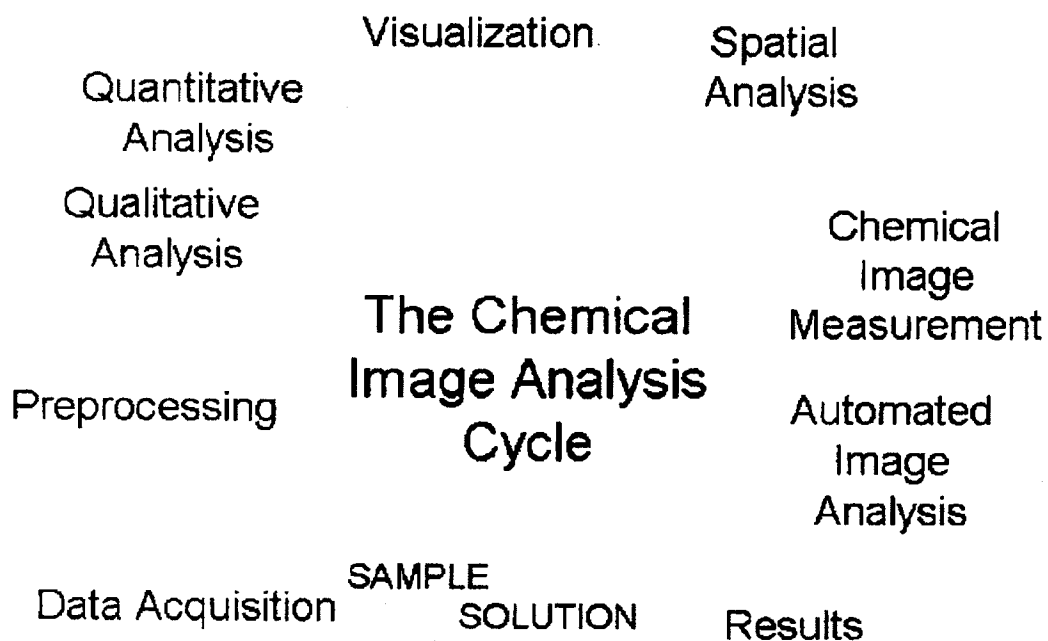


Figure 2

U.S. Patent

May 11, 2004

Sheet 3 of 6

US 6,734,962 B2

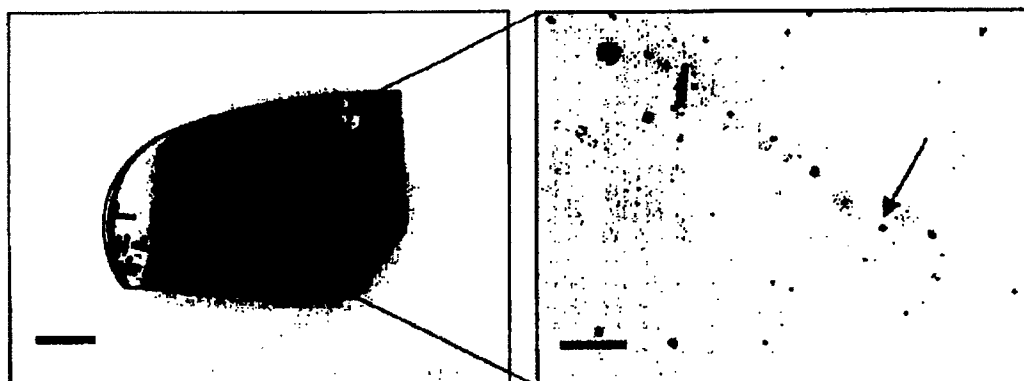


Figure 3

Figure 4

U.S. Patent

May 11, 2004

Sheet 4 of 6

US 6,734,962 B2

Figure 5A



Figure 5B

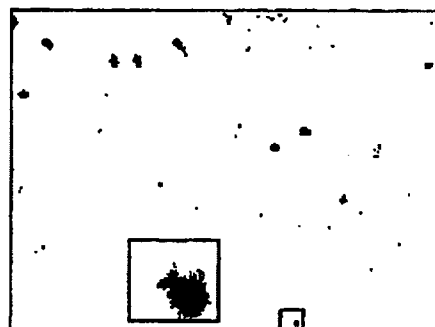
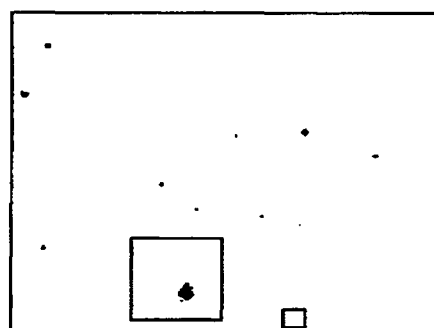


Figure 5C

Figure 5D

U.S. Patent

May 11, 2004

Sheet 5 of 6

US 6,734,962 B2

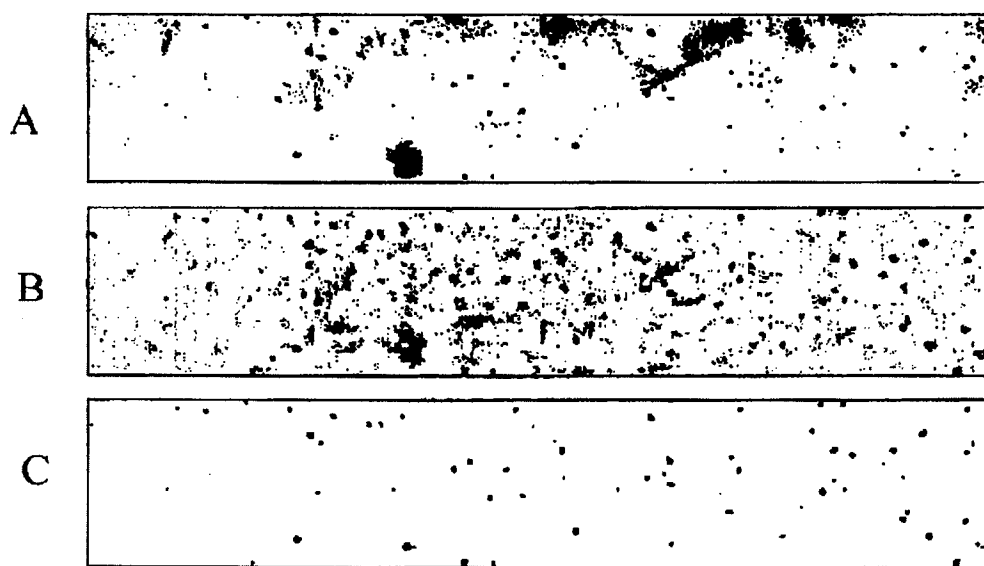


Figure 6

U.S. Patent

May 11, 2004

Sheet 6 of 6

US 6,734,962 B2

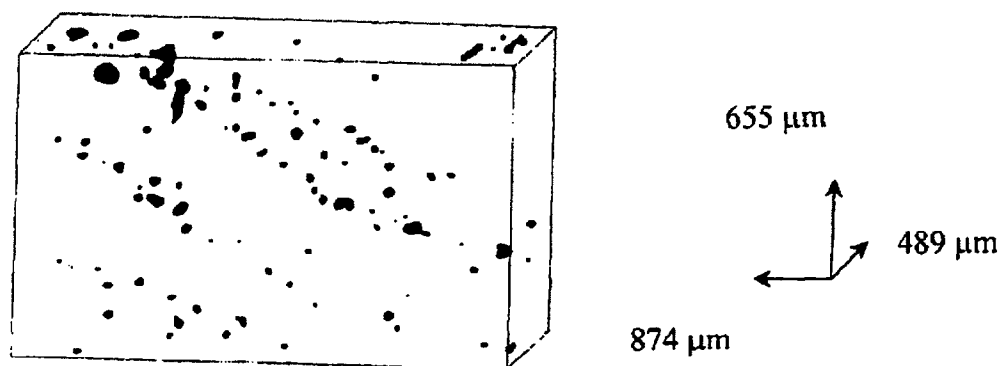


Figure 7

US 6,734,962 B2

1

NEAR INFRARED CHEMICAL IMAGING MICROSCOPE

This application claims the benefit of U.S. Provisional Application No. 60/239,969, entitled "Near Infrared Chemical Imaging Microscope" filed Oct. 13, 2000.

This work is supported by the National Institute of Standards and Technology (NIST) under the Advanced Technology Program (ATP) award (Contract Number 70NANB8H4021)

FIELD OF INVENTION

The present invention is related to near-infrared (NIR) microscopes for spectroscopic and image analysis, and, in particular, to microscopes useful for both NIR spectroscopy, NIR chemical imaging and NIR volumetric chemical imaging.

BACKGROUND OF THE INVENTION

NIR spectroscopy is a mature, non-contact, non-destructive analytical characterization tool that has been widely applied to a broad range of materials. The NIR region of the electromagnetic spectrum encompasses radiation with wavelengths of 0.78 to 2.5 μm (12,800 to 4,000 cm^{-1}). NIR spectra result from the overtone and combination bands of fundamental mid-infrared (MIR) bands. Among the many desirable characteristics, NIR is used to rapidly obtain both qualitative and quantitative information about the molecular makeup of a material. Digital imaging, on the other hand, provides a means to obtain optical (i.e., spatial—morphological, topographical, etc.) information about a material. By combining the spatial information obtained from digital imagery and the spectral information obtained from NIR spectroscopy, the chemical makeup of complex material matrices can be mapped out in both two and three spatial dimensions. NIR chemical imaging combines NIR spectroscopy and digital imaging for the molecular-specific analysis of materials. A NIR chemical imaging microscope apparatus employing NIR absorption molecular spectroscopy for materials characterization is disclosed.

State-of-the-Art Instrumentation

NIR microscopes are used to obtain NIR absorption, transmittance or reflectance spectra (e.g., NIR microspectra) from samples ranging in size between 1 and 1000 μm . These instruments are typically equipped with a digital camera to visually locate a region of interest on a sample upon which a NIR light beam from a Fourier transform (FT) spectrometer is focused. Reflective optics are used to direct the transmitted or reflected light from the sample to a NIR detector. The output is a NIR absorption spectrum collected in transmittance or reflectance mode.

NIR chemical imaging can be considered an extension of NIR microspectroscopy. Much of the imaging performed since the development of the first NIR microprobes has involved spatial scanning of samples beneath NIR microscopes in order to construct NIR "maps" of surfaces. In point by point scanning with NIR microscopes, the NIR light beam is focused onto the surface of a sample or apertured to illuminate a small region of a sample and a spectrum from each spatial position is collected. Images are obtained by rastering the sample through the focused or apertured NIR light beam and the spectra recorded are then reconstructed to form an image. Although point scanning produces images based on NIR contrast, long experimental times are common since the duration of the experiment is proportional to the number of image pixels. As a direct result, point scan images

2

are captured at low image definition, which relates directly to the limited utility of the technique as an imaging tool for the routine assessment of material morphology. The spatial resolution of the image is limited by the size of the NIR illumination spot on the sample (no less than 1 μm) and the rastering mechanism, which requires the use of moving mechanical parts that are challenging to operate reproducibly.

NIR imaging cameras have been used in photography for decades. Until recently, however, it has not been easily accessible to those not versed in traditional photographic processes. By using optical filters (e.g., cold filters) that block the visible wavelengths (0.4–0.78 μm), charge-coupled devices (CCDs) used in digital cameras and camcorders can be used to sense NIR light out to around 1100 nm. Other regions of the NIR spectrum can be viewed using devices such as indium gallium arsenide (InGaAs—0.9 μm to 1.7 μm) and indium antimonide (InSb—1.0 μm to 5.0 μm) focal plane array (FPA) detectors. These integrated wavelength NIR imaging approaches allow one to study relative light intensities of objects over broad ranges of the NIR spectrum, but useful chemical information is unattainable without the use of some type of discrete wavelength filtering device.

The use of dielectric interference filters in combination with NIR FPAs is one method in which chemical information can be obtained from a sample. To form NIR chemical images, a NIR light beam is defocused to illuminate a wide field of view and the reflected or transmitted light from the illuminated area is imaged onto a two-dimensional NIR detector. A selection of discrete dielectric interference filters provided in a filter wheel, or a linearly variable or circularly variable format can be positioned in front of a broadband NIR light source, or in front of the NIR FPA itself in order to collect NIR wavelength resolved images. Typically, the use of several fixed bandpass filters is required to access the entire NIR spectrum. The spatial resolution of the NIR image approaches that of the optical microscope, while spectral resolution of several nanometers has been demonstrated. Key limitations of the dielectric filter approach include the need for a multitude of discrete filters to provide appreciable free spectral range, or the reliance on moving mechanical parts in employing continuously tunable dielectric interference filters as a requirement to form wavelength resolved images. While moving mechanical assemblies can be engineered they add cost and complexity to NIR chemical imaging systems. Alternatives to moving mechanical assemblies are generally more cost effective and provide performance advantages.

Acousto-optic tunable filters (AOTFs) have been employed as no-moving-parts imaging spectrometers for NIR imaging. The AOTF is a solid-state device that is capable of functioning from the UV to the mid-IR depending on the choice of the filter's crystal material. Operation of the AOTF is based on the interaction of light with a traveling acoustic sound wave in an anisotropic crystal medium. The incident light is diffracted with a narrow spectral bandpass when an rf signal is applied to the device. By changing the applied rf frequency under computer control the spectral passband can be tuned rapidly with the benefit of non-moving parts.

For use in NIR chemical imaging, AOTFs have distinct limitations. AOTFs have imaging performance that is degraded appreciably from diffraction-limited conditions due to dispersion effects and image shifting effects. Furthermore, AOTFs suffer from temperature instability and exhibit nonlinear properties that complicate their use as imaging spectrometers.

US 6,734,962 B2

3

An aim of NIR chemical imaging technology development has been to develop a NIR imaging technique that combines diffraction-limited spatial resolution with high spectral resolution. NIR chemical imaging techniques have only recently achieved a degree of technological maturity that allow the collection of high resolution (spectral and spatial) data with the advent of the liquid crystal (LC) imaging spectrometers. In general, LC devices provide diffraction-limited spatial resolution. The spectral resolution of the LC imaging spectrometer is comparable to that provided by dispersive monochromator and Fourier transform interferometers. In addition, LC technology provides high out of band rejection, broad free spectral range, moderate transmittance, high overall etendue and highly reproducible random access computer controlled tuning.

Under normal NIR imaging operation, LC imaging spectrometers allow NIR chemical images of samples to be recorded at discrete wavelengths (energies). A spectrum is generated corresponding to thousands of spatial locations at the sample surface by tuning the LC imaging spectrometer over a range of wavelengths and collecting NIR images systematically. Contrast is generated in the images based on the relative amounts of NIR absorption, transmittance or reflectance that is generated by the different species located throughout the sample. Since a high quality NIR spectrum is generated for each pixel location, a wide variety of chemometric analysis tools, both univariate and multivariate, can be applied to the NIR image data to extract pertinent information. Correlative multivariate routines are particularly powerful when applied to chemical images collected from samples intentionally seeded with a known standard material. This approach of incorporating calibration standards within an image field of view can be extended to quantitative chemical image analysis. In addition, digital image analysis procedures can also be applied to high image quality NIR chemical images to perform routine particle analysis in both two (2D) and three (3D) spatial dimensions. Volumetric 3D NIR chemical image analysis can be performed very effectively using numerical deconvolution computational strategies.

SUMMARY OF THE INVENTION

To address the need for a device that can provide video imaging, NIR spectroscopy and high resolution (spatial and spectral) NIR chemical imaging in two and three spatial dimensions, a novel NIR chemical imaging microscope has been developed that is NIR chemical imaging capable.

The microscope design uses NIR optimized liquid crystal (LC) imaging spectrometer technology for wavelength selection. The NIR optimized refractive microscope is used in conjunction with infinity-corrected objectives to form the NIR image on the detector with or without the use of a tube lens. An integrated parfocal analog color CCD detector provides real-time sample positioning and focusing. The color image and the NIR image are fused in software. In one configuration, the NIR microscope may be used as a volumetric imaging instrument through the means of moving the sample through focus, collecting images at varying focal depths and reconstructing a volumetric image of the sample in software, or through the means of keeping the sample fixed and changing the wavelength dependent depth of penetration in conjunction with a refractive tube lens with a well characterized chromatic effect. The output of the microscope can be coupled to a NIR spectrometer either via direct optical coupling or via a fiber optic. A Chemical Imaging Addition Method seeds the sample with a material of known composition, structure and/or concentration and then gen-

4

erates the NIR image suitable for qualitative and quantitative analysis. The microscope generates NIR chemical image data that is analyzed and visualized using chemical image analysis software in a systematic and comprehensive manner. While this invention has been demonstrated on a microscope optic platform, the novel concepts are also applicable to other image gathering platforms, namely fiberscopes, macrolens systems and telescopes.

BRIEF DESCRIPTION OF THE DRAWINGS

FIG. 1 shows a schematic diagram of the near-infrared (NIR) chemical imaging microscope

FIG. 2 shows a diagram of the chemical imaging data analysis cycle performed in software.

FIG. 3 is a digital brightfield image of a CdZnTe semiconductor material decorated with tellurium inclusions.

FIG. 4 is an NIR microscopic transmittance image of a CdZnTe semiconductor material decorated with tellurium inclusions.

FIG. 5A illustrates a raw NIR image frame of a CdZnTe wafer sample.

FIG. 5B illustrates an NIR image frame of the sample of FIG. 5A in which the threshold value for the image was set too low.

FIG. 5C illustrates an NIR image frame of the sample of FIG. 5A in which the threshold value for the image was set too high.

FIG. 5D illustrates an NIR image frame of the sample of FIG. 5A in which the threshold value for the image was set to an intermediate level.

FIG. 6A is the original raw image of four adjacent regions of interest on a CdZnTe wafer.

FIG. 6B is the background-corrected image corresponding to the four adjacent regions of interest of the CdZnTe wafer of FIG. 6A.

FIG. 6C is the binarized image corresponding to the four adjacent regions of interest of the CdZnTe wafer of FIG. 6A.

FIG. 7 is a three-dimensional view of tellurium inclusions in a CdZnTe wafer.

DETAILED DESCRIPTION OF THE INVENTION

The NIR chemical imaging microscope combines in a single platform a NIR optimized refractive optical microscope base, which is equipped with NIR optimized infinity-corrected microscope objectives, an automated XYZ translational microscope stage and quartz tungsten halogen (QTH) lamps to secure and illuminate samples for NIR spectroscopy and imaging, an analog color charge-coupled device (CCD) detector for ordinary optical image collection and digital image collection, a NIR LC imaging spectrometer for NIR chemical image wavelength selection and a room temperature or optionally cooled NIR FPA for NIR image capture.

FIG. 1 is a schematic diagram of the NIR chemical imaging microscope. NIR illumination is directed to the sample in a reflected light configuration using a QTH source or other broadband white light source, including metal halide or Xe arc lamps 1 or a transmitted light configuration using QTH or suitable NIR source 2 of an NIR optimized refractive optical microscope platform 3. The reflected or transmitted NIR light is collected from the sample positioned on the automated XYZ translational microscope stage 4 through an infinity-corrected NIR optimized microscope objective 5.

US 6,734,962 B2

5

Ordinary optical imagery of the sample can be obtained using a mirror or beamsplitter or prism arrangement inserted into turret 6 and collecting an image with an analog or digital color or monochrome charge-coupled device (CCD) or CMOS detector 7. In NIR chemical imaging mode, the magnified NIR image is coupled through a NIR LC imaging spectrometer 8 and collected on a room temperature or cooled NIR focal plane array (FPA) detector 9. The FPA is typically comprised of indium gallium arsenide (InGaAs), but may be comprised of other NIR sensitive materials, including platinum silicide (PtSi), indium antimonide (InSb) or mercury cadmium telluride (HgCdTe). Using a beam-splitting element inserted into turret 6, NIR and ordinary optical imagery can be collected with an analog monochrome or color CCD detector 7 and NIR FPA 9 simultaneously.

A central processing unit 10, typically a Pentium computer, is used for NIR chemical image collection and processing. The analog color CCD 7, NIR FPA 9, automated XYZ translational microscope stage 4 controlled via a controller 12 and NIR LC imaging spectrometer 8 (through LC imaging spectrometer controller 11) are operated with commercial software, such as Acquisition Manager (Chemleon Inc.) in conjunction with ChemImage (Chemleon Inc.).

By introducing a polarization sensitive beam splitting element in the optical path prior to the NIR LC imaging spectrometer 8 (not shown in schematic diagram), a portion of the NIR light from the sample may be coupled to a remote NIR spectrometer (also not shown in schematic diagram).

Preferably, NIR optimized liquid crystal (LC) imaging spectrometer technology is used for wavelength selection. The LC imaging spectrometer may be of the following types: Lyot liquid crystal tunable filter (LCTF); Evans Split-Element LCTF; Sole LCTF; Ferroelectric LCTF; Liquid crystal Fabry Perot (LCFP); or a hybrid filter technology comprised of a combination of the above-mentioned LC filter types or the above mentioned filter types in combination with fixed bandpass and bandreject filters comprised of dielectric, rugate, holographic, color absorption, acousto-optic or polarization types.

One novel component of this invention, is that a NIR optimized refractive microscope is used in conjunction with infinity-corrected objectives to form the NIR image on the detector without the use of a tube lens. The microscope can be optimized for NIR operation through inherent design of objective and associated anti-reflective coatings, condenser and light source. To simultaneously provide high numerical apertures the objective should be refractive. To minimize chromatic aberration, maximize throughput and reduce cost the conventional tube lens can be eliminated, while having the NIR objective form the NIR image directly onto the NIR focal plane array (FPA) detector, typically of the InGaAs type. The FPA can also be comprised of Si, SiGe, PtSi, InSb, HgCdTe, PdSi, Ge, analog vidicon types. The FPA output is digitized using an analog or digital frame grabber approach.

An integrated parfocal analog CCD detector provides real-time sample positioning and focusing. An analog video camera sensitive to visible radiation, typically a color or monochrome CCD detector, but may be comprised of a CMOS type, is positioned parfocal with the NIR FPA detector to facilitate sample positioning and focusing without requiring direct viewing of the sample through conventional eyepieces. The video camera output is typically digitized using a frame grabber approach.

The color image and the NIR image are fused using software. While the NIR and visible cameras often generate

6

images having differing contrast, the sample fields of view can be matched through a combination of optical and software manipulations. As a result, the NIR and visible images can be compared and even fused through the use of overlay techniques and correlation techniques to provide the user a near-real time view of both detector outputs on the same computer display. The comparative and integrated views of the sample can significantly enhance the understanding of sample morphology and architecture. By comparing the visible, NIR and NIR chemical images, additional useful information can be acquired about the chemical composition, structure and concentration of species in samples.

The NIR microscope can be used as a volumetric imaging instrument through the means of moving the sample through focus in the Z, axial dimension, collecting images in and out of focus and reconstructing a volumetric image of the sample in software. For samples having some volume (bulk materials, surfaces, interfaces, interphases), volumetric chemical imaging in the NIR has been shown to be useful for failure analysis, product development and routine quality monitoring. The potential also exists for performing quantitative analysis simultaneous with volumetric analysis. Volumetric imaging can be performed in a non-contact mode without modifying the sample through the use of numerical confocal techniques, which require that the sample be imaged at discrete focal planes. The resulting images are processed and reconstructed and visualized. Computational optical sectioning reconstruction techniques based on a variety of strategies have been demonstrated, including nearest neighbors and iterative deconvolution.

An alternative to sample positioning combined with computation reconstruction is to employ a tube lens in the image formation path of the microscope which introduces chromatic aberration. As a result the sample can be interrogated as a function of sample depth by exercising the LC imaging spectrometer, collecting images at different wavelengths which penetrate to differing degrees into bulk materials. These wavelength dependent, depth dependent images can be reconstructed to form volumetric images of materials without requiring the sample to be moved, again through application of computational optical sectioning reconstruction algorithms.

The output of the microscope can be coupled to a NIR spectrometer either via direct optical coupling or via a fiber optic cable. This allows conventional spectroscopic tools to be used to gather NIR spectra for traditional, high speed spectral analysis. The spectrometers can be of the following types: fixed filter spectrometers; grating based spectrometers; Fourier Transform spectrometers; or Acousto-Optic spectrometers.

A novel method that is readily employed by the disclosed microscope invention is a method described as the Chemical Imaging Addition Method which involves seeding the sample with a material of known composition, structure and/or concentration and then generating the NIR image suitable for qualitative and quantitative analysis. The Chemical Imaging Addition Method is a novel extension of a standard analytical chemical analysis technique, the Standard Addition Method. A common practice in quantitative chemical analysis is to construct a standard calibration curve which is a plot of analytical response for a particular technique as a function of known analyte concentration. By measuring the analytical response from an unknown sample, an estimate of the analyte concentration can then be extrapolated from the calibration curve. In the Standard Addition Method, known quantities of the analyte are added to the

CRI001546

US 6,734,962 B2

7

samples and the increase in analytical response is measured. When the analytical response is linearly related to concentration, the concentration of the unknown analyte can be found by plotting the analytical response from a series of standards and extrapolating the unknown concentration from the curve. In this graph, however, the x-axis is the concentration of added analyte after being mixed with the sample. The x-intercept of the curve is the concentration of the unknown following dilution. The primary advantage of the standard addition method is that the matrix remains constant for all samples.

While the Standard Addition Method is used specifically for quantitative analysis, the Chemical Imaging Addition Method can be used for qualitative and quantitative analysis. The Chemical Imaging Addition Method relies upon spatially isolating analyte standards in order to calibrate the Chemical Imaging analysis. In chemical imaging, thousands of linearly independent, spatially-resolved spectra are collected in parallel of analytes found within complex host matrices. These spectra can then be processed to generate unique contrast intrinsic to analyte species without the use of stains, dyes, or contrast agents. Various spectroscopic methods including near-infrared (NIR) absorption spectroscopy can be used to probe molecular composition and structure without being destructive to the sample. Similarly, in NIR chemical imaging the contrast that is generated reveals the spatial distribution of properties revealed in the underlying NIR spectra.

The Chemical Imaging Addition Method can involve several data processing steps, typically including, but not limited to:

1. Ratiometric correction in which the sample NIR image is divided by the background NIR image to produce a result having a floating point data type.
2. The divided image is normalized by dividing each intensity value at every pixel in the image by the vector norm for its corresponding pixel spectrum. Where the vector norm is the square root of the sum of the squares of pixel intensity values for each pixel spectrum. Normalization is applied for qualitative analysis of NIR chemical images. For quantitative analysis, normalization is not employed, but relies instead on the use of partial least squares regression (PLSR) techniques.
3. Correlation analysis, including Euclidian Distance and Cosine correlation analysis (CCA) are established multivariate image analysis techniques that assess similarity in spectral image data while simultaneously suppressing background effects. More specifically, CCA assesses chemical heterogeneity without the need for training sets, identifies differences in spectral shape and efficiently provides chemical image based contrast that is independent of absolute intensity. The CCA algorithm treats each pixel spectrum as a projected vector in n-dimensional space, where n is the number of wavelengths sampled in the image. An orthonormal basis set of vectors is chosen as the set of reference vectors and the cosine of the angles between each pixel spectrum vector and the reference vectors are calculated. The intensity values displayed in the resulting CCA images are these cosine values, where a cosine value of 1 indicates the pixel spectrum and reference spectrum are identical, and a cosine value of 0 indicates the pixel spectrum and the reference spectrum are orthogonal (no correlation). The dimensions of the resulting CCA image is the same as the original image because the orthonormal basis set provides n reference vectors, resulting in n CCA images.

8

4. Principal component analysis (PCA) is a data space dimensionality reduction technique. A least squares fit is drawn through the maximum variance in the n-dimensional dataset. The vector resulting from this least squares fit is termed the first principal component (PC) or the first loading. After subtracting the variance explained from the first PC, the operation is repeated and the second principal component is calculated. This process is repeated until some percentage of the total variance in the data space is explained (normally 95% or greater). PC Score images can then be visualized to reveal orthogonal information including sample information, as well as instrument response, including noise. Reconstruction of spectral dimension data can then be performed guided by cluster analysis, including without PCs that describe material or instrument parameters that one desires to amplify or suppress, depending on the needs of the sensing application.

Effective materials characterization with the disclosed NIR chemical imaging microscope invention typically requires application of a multitude of software procedures to the NIR chemical image. A schematic of the chemical image analysis cycle is shown in FIG. 2. A fairly comprehensive description of the variety of steps used to process chemical images is described below.

Until recently, seamless integration of spectral analysis, chemometric analysis and digital image analysis has not been commercially available. Individual communities have independently developed advanced software applicable to their specific requirements. For example, digital imaging software packages that treat single-frame gray-scale images and spectral processing programs that apply chemometric techniques have both reached a relatively mature state. One limitation to the development of chemical imaging, however, has been the lack of integrated software that combines enough of the features of each of these individual disciplines to have practical utility.

Historically, practitioners of chemical imaging were forced to develop their own software routines to perform each of the key steps of the data analysis. Typically, routines were prototyped using packages that supported scripting capability, such as Matlab, IDL, Grams or LabView. These packages, while flexible, are limited by steep learning curves, computational inefficiencies, and the need for individual practitioners to develop their own graphical user interface (GUI). Today, commercially available software does exist that provides efficient data processing and the ease of use of a simple GUI.

Software that meets these goals must address the entirety of the chemical imaging process. The chemical imaging analysis cycle illustrates the steps needed to successfully extract information from chemical images and to tap the full potential provided by chemical imaging systems. The cycle begins with the selection of sample measurement strategies and continues through to the presentation of a measurement solution. The first step is the collection of images. The related software must accommodate the full complement of chemical image acquisition configurations, including support of various spectroscopic techniques, the associated spectrometers and imaging detectors, and the sampling flexibility required by differing sample sizes and collection times. Ideally, even relatively disparate instrument designs can have one intuitive GUI to facilitate ease of use and ease of adoption.

The second step in the analysis cycle is data preprocessing. In general, preprocessing steps attempt to minimize contributions from chemical imaging instrument response

US 6,734,962 B2

9

that are not related to variations in the chemical composition of the imaged sample. Some of the functionalities needed include: correction for detector response, including variations in detector quantum efficiency, bad detector pixels and cosmic events; variation in source illumination intensity across the sample; and gross differentiation between spectral lineshapes based on baseline fitting and subtraction. Examples of tools available for preprocessing include ratio-metric correction of detector pixel response; spectral operations such as Fourier filters and other spectral filters, normalization, mean centering, baseline correction, and smoothing; spatial operations such as cosmic filtering, low-pass filters, high-pass filters, and a number of other spatial filters.

Once instrument response has been suppressed, qualitative processing can be employed. Qualitative chemical image analysis attempts to address a simple question, "What is present and how is it distributed?". Many chemometric tools fall under this category. A partial list includes: correlation techniques such as cosine correlation and Euclidean distance correlation; classification techniques such as principal components analysis, cluster analysis, discriminant analysis, and multi-way analysis; and spectral deconvolution techniques such as SIMPLISMA, linear spectral unmixing and multivariate curve resolution.

Quantitative analysis deals with the development of concentration map images. Just as in quantitative spectral analysis, a number of multivariate chemometric techniques can be used to build the calibration models. In applying quantitative chemical imaging, all of the challenges experienced in non-imaging spectral analysis are present in quantitative chemical imaging, such as the selection of the calibration set and the verification of the model. However, in chemical imaging additional challenges exist, such as variations in sample thickness and the variability of multiple detector elements, to name a few. Depending on the quality of the models developed, the results can range from semi-quantitative concentration maps to rigorous quantitative measurements.

Results obtained from preprocessing, qualitative analysis and quantitative analysis must be visualized. Software tools must provide scaling, automapping, pseudo-color image representation, surface maps, volumetric representation, and multiple modes of presentation such as single image frame views, montage views, and animation of multidimensional chemical images, as well as a variety of digital image analysis algorithms for look up table (LUT) manipulation and contrast enhancement.

Once digital chemical images have been generated, traditional digital image analysis can be applied. For example, Spatial Analysis and Chemical Image Measurement involve binarization of the high bit depth (typically 32 bits/pixel) chemical image using threshold and segmentation strategies. Once binary images have been generated, analysis tools can examine a number of image domain features such as size, location, alignment, shape factors, domain count, domain density, and classification of domains based on any of the selected features. Results of these calculations can be used to develop key quantitative image parameters that can be used to characterize materials.

The final category of tools, Automated Image Processing, involves the automation of key steps or of the entire chemical image analysis process. For example, the detection of well defined features in an image can be completely automated and the results of these automated analyses can be tabulated based on any number of criteria (particle size, shape, chemical composition, etc). Automated chemical

10

imaging platforms have been developed that can run for hours in an unsupervised fashion.

This invention incorporates a comprehensive analysis approach that allows user's to carefully plan experiments and optimize instrument parameters and should allow the maximum amount of information to be extracted from chemical images so that the user can make intelligent decisions.

EXAMPLE

Overview

As the demand for high quality, low cost X-ray, γ -ray and imaging detector devices increases, there is a need to improve the quality and production yield of semiconductor materials used in these devices. One effective strategy for improving semiconductor device yield is through the use of better device characterization tools that can rapidly and nondestructively identify defects at early stages in the fabrication process. Early screening helps to elucidate the underlying causes of defects and to reduce downstream costs associated with processing defect laden materials that are ultimately scrapped. The present invention can be used to characterize tellurium inclusion defects in cadmium zinc telluride (CdZnTe) semiconductor materials based on near infrared imaging. With this approach, large area wafers can be inspected rapidly and non-destructively in two and three spatial dimensions by collecting NIR image frames at multiple regions of interest throughout the wafer using an automated NIR imaging system. The NIR image frames are subjected to image processing algorithms including background correction and image binarization. Particle analysis is performed on the binarized images to reveal tellurium inclusion statistics, sufficient to pass or fail wafers. In addition, data visualization software is used to view the tellurium inclusions in two and three spatial dimensions.

Background

The present invention has been used to automatically inspect tellurium inclusions in CdZnTe. Compound semiconductors are challenging to fabricate. There are several steps along the manufacturing process in which defects can arise. The chemical nature associated with semiconductor defects often plays a vital role in device performance. Device fabrication and device processing defects can be difficult and time consuming to measure during manufacturing. Unfortunately, defective devices are often left undiagnosed until latter stages in the manufacturing process because of the inadequacy of the metrology tools being used. This results in low production yields and high costs which can be an impediment to growth in the semiconductor device market potential.

There is a general need in the semiconductor industry for metrology technologies that can nondestructively assess semiconductor material defects and ultimately increase manufacturing yields. A potential solution is to develop a high throughput screening system capable of fusing multiple chemical imaging modalities into a single instrument. Chemical imaging combines digital imaging and molecular spectroscopy for the chemical analysis of materials. A modality of based on near-infrared (NIR) chemical imaging can be used to inspect tellurium inclusions in CdZnTe compound semiconductor materials.

CdZnTe is a leading material for use in room temperature X-ray detectors, γ -ray radiation detectors and imaging devices. Applications for these devices include nuclear diagnostics, digital radiography, high-resolution astrophysical X-ray and γ -ray imaging, industrial web gauging and nuclear nonproliferation. These devices are often decorated with microscopic and macroscopic defects limiting the yield

US 6,734,962 B2

11

of large-size, high-quality materials. Defects commonly found in these materials include cracks, grain boundaries, twin boundaries, pipes, precipitates and inclusions. CdZnTe wafers are often graded based on the size and number of Te inclusion defects present.

The definition used by Rudolph and Muhlberg for tellurium inclusions (i.e., tellurium-rich domains in the 1–50 μm size range that originate as a result of morphological instabilities at the growth interface as tellurium-rich melt droplets are captured from the boundary layer ahead of the interface) has been adopted and is used herein. There have been numerous studies on the composition and distribution of tellurium inclusions in CdZnTe material. It has been demonstrated that the presence of tellurium inclusions can impair the electronic properties of CdZnTe materials—consequently degrading the end-product device performance.

The current procedure used by low volume semiconductor manufacturers for characterizing tellurium inclusions in CdZnTe is labor intensive, susceptible to human error and provides little information on inclusions in the 1–5 μm size scale. Inclusions are viewed and counted manually by a human operator using an IR microscope platform. When an inclusion is identified that is suspected to exceed a specified size limit, a Polaroid film photograph is taken. An overlay of a stage micrometer is laid over the photograph to determine the size. This analysis is relatively time consuming, often taking several minutes to characterize a region of interest from a large wafer.

The present invention can be used for automated characterization of microscale tellurium inclusions in CdZnTe based on volumetric NIR chemical imaging. The system takes advantage of the fact that CdZnTe is transparent to infrared wavelengths ($>850\text{ nm}$). When viewing CdZnTe with an infrared focal plane array (IR-FPA) through a NIR LC imaging spectrometer, tellurium inclusions appear as dark, absorbing domains. The invention images wafers in two and three spatial dimensions capturing raw infrared images at each region of interest. Images are automatically background equilibrated, binarized and processed. The processed data provides particle statistical information such as inclusion counts, sizes, density, area and shape. The system provides a rapid method for characterizing tellurium inclusions as small as 0.5 μm while virtually eliminating the subjectivity associated with manual inspection.

Sample Description

Tellurium-rich CdZnTe samples were produced by a commercial supplier (eV Products) for analysis. Samples containing high tellurium inclusion densities were purposely acquired to effectively demonstrate the capabilities of the automated tellurium inclusions mapping system. The CdZnTe materials were grown by the Horizontal Bridgman (HB) method and contained a nominal zinc cation loading concentration of 4% and an average etch pit density of $4 \times 10^4/\text{cm}^2$. The materials displayed a face A $\langle 111 \rangle$ orientation and were polished on both sides. Sample thicknesses ranged from approximately 1 mm to 15 mm. No further sample preparation was necessary for the automated tellurium inclusion mapping analysis.

Data Collection

Volumetric maps of the tellurium inclusions in the CdZnTe samples were obtained by first placing the sample on the XYZ-translational stage of the automated mapping system. NIR image frames were then captured through the LC imaging spectrometer at a wavelength that maximized the Te precipitate contrast relative to the surrounding CdZnTe matrix in the X-Y direction at multiple regions of

12

interest across the samples. Depth profiling was achieved by translating the sample focus under the microscope at user-defined increments. This process was then repeated in an iterative fashion until the entire wafer was characterized.

Data Processing

Once imaging data was collected, ChemImage was used to process the data. For each wafer, the software generates a background-corrected grayscale image, a binarized image using the threshold value selected for each frame of the image, a montage view of the binarized image and particle statistics. The particle statistics table includes information such as particle counts, particle sizes, particles densities, and a number of geometrical parameters such as particle area and particle aspect ratios.

NIR Imaging

FIGS. 3 and 4, respectively, show a digital macro bright-field image and a raw NIR microscopic transmittance image of a CdZnTe semiconductor material with numerous tellurium inclusions. The left half of the wafer has been polished. The tellurium inclusions appear as dark spots in the microscopic NIR image. The raw NIR microscopic image was acquired using the automated near-infrared tellurium inclusion volumetric mapping system.

Background Correction and Image Binarization

The automated particle analysis begins by applying a background correction preprocessing routine to the raw image frames. One of the biggest problems with the raw images collected is the gradually varying background across each image frame. As a result, a particle in one area of a frame may have a higher intensity value than the background of another area of that frame.

FIGS. 5A–5D illustrate the difficulty associated with selecting a threshold value for an image with a widely varying background. In FIGS. 5A–5D, regions 1 and 2 have mean intensity values of approximately 2600 and 1950, respectively. The whole of region 1 is primarily a particle whereas region 2 is primarily background with a small particle in the center. FIG. 5A shows a raw NIR image frame collected from a single region of interest in a CdZnTe wafer.

At wavelengths longer than approximately 850 nm, CdZnTe is transparent while tellurium inclusions remain opaque. A NIR image of the sample is light where there are no precipitates and dark where there are precipitates. In FIG. 5B, the threshold value is set low enough (value=1520) that the particle in region 2 is correctly identified, but most of the remaining particles are not found. In FIG. 5C, the threshold value is set high enough (value=2470) so that all particles are detected. Unfortunately, a large area of the frame is incorrectly identified as one very large particle. FIG. 5D displays the case in which the threshold is set to an intermediate value (value=1960). Many of the particles are correctly identified, but the particle in region 2 is identified as being larger than it actually is.

To address this issue, a background correction step is used to force the background to be essentially constant across a given image frame. The procedure applies a moving window across the image frame and smoothes the resulting background before subtracting it from the frame. Other operations such as low pass filtering and selective removal of bad camera pixels are also applied.

The second step in the automated particle analysis is the selection of the threshold value resulting in the binarized image which best reflects the number and size of particles actually present in the sample being imaged. A human operator would typically approach this problem by trying multiple threshold values and comparing the resulting binarized images to the actual image to see which binarized

US 6,734,962 B2

13

image best matches their perception of the particles in the actual image. The algorithm employed by the NIR chemical imaging microscope system takes essentially the same approach. A series of threshold values are used to generate binarized images. Each binarized image is submitted to a routine that finds the particles present in the image. A set of particle morphology rules was developed to determine the point at which the threshold value identifies the particles consistent with results obtained by a trained human operator. This threshold value is then further refined with using derivative operations.

FIGS. 6A-6C show montage views of raw, background-corrected, and binarized NIR image frames, respectively, corresponding to four adjacent regions of interest from a CdZnTe wafer. A visual inspection of these images suggests that the particle analysis adequately identifies the particles in an automated fashion.

Volumetric Reconstruction and Visualization

It is of particular interest to the semiconductor manufacturing industry to view defects, including tellurium inclusions in this example, in a three dimensional volumetric view. Individual binarized image frames generated at discrete axial planes of focus have been reconstructed into a volumetric view allowing users to view tellurium inclusions in three-dimensional space.

FIG. 7 shows a 3D volumetric view of tellurium inclusions in CdZnTe generated from 50 individual image slices. FIG. 7 is constructed using a nearest neighbors computational approach for volume reconstruction. Improved results can be obtained using more sophisticated strategies that deconvolve the entire image volume using iterative deconvolution approaches. The starting time of the sensor used to gather the volumetric data was less than 1 sec. The total acquisition time for the data generated in this figure was well under a minute. Note how the inclusions tend to form in planes described as veils. These veils are believed to be subgrain boundaries within the CdZnTe material. Grain boundaries provide low energy nucleation sites for the inclusions to form during the growth process.

Table 1 provides tabulated statistical information on the volumetric data shown in FIG. 7.

TABLE 1

Parameters	Particle Statistics					
	Slice Number and Depth (μm)					
	0 (0)	10 (89.77)	20 (189.52)	30 (289.26)	40 (389.01)	50 (488.75)
# of Inclusions	25	30	27	24	25	36
Mean Diameter (μm)	12.12	11.38	12.75	15.70	12.89	13.73
Density (Inclusions/ cm^2)	4368	5241	4717	4193	4368	6289
Area (μm^2)	97.48	73.78	91.67	119.25	96.29	98.15
Perimeter (μm)	40.40	37.32	43.27	50.72	41.93	43.98
Shape Factor	0.60	0.60	0.58	0.53	0.60	0.55
Maximum Chord Length	12.12	11.38	12.75	15.70	12.89	13.73
Feret 1 Diameter	9.17	9.56	11.33	12.64	10.48	10.16
Feret 2 Diameter	10.26	9.01	10.10	12.18	10.37	11.60
Aspect Ratio	1.02	1.19	1.16	1.08	1.02	0.95

Defects such as tellurium inclusions affect the electrical properties in CdZnTe semiconductor materials, degrading end-product device performance. Having the ability to rapidly and non-invasively identify and quantify tellurium inclusion defects at critical stages in the fabrication process provides semiconductor manufacturers with information that will enable them to optimize the manufacturing process and reduce production costs. The Automated NIR Volumetric Mapping System described here is capable of providing such information. The system provides qualitative and quan-

14

titative information about tellurium inclusions present in CdZnTe wafers in two and three spatial dimensions. This system boasts improved spatial resolution ($\sim 0.5 \mu\text{m}$) compared to systems currently used by many semiconductor manufacturers and it virtually eliminates the subjectivity associated with human counting and sizing measurements. Whole wafers are capable of being characterized in minutes.

While in the above example, the present invention has been demonstrated in connection with the characterization of semiconductors, it is to be expressly understood that the present invention can also be used in the characterization of other materials including, but not limited to, food and agricultural products, paper products, pharmaceutical materials, polymers, thin films and in medical uses.

Although present preferred embodiments of the invention have been shown and described, it should be distinctly understood that the invention is not limited thereto but may be variously embodied within the scope of the following claims.

We claim:

1. A near infrared radiation chemical imaging system comprising:

- a) an illumination source for illuminating an area of a sample using light in the near infrared radiation wavelength;
- b) a device for collecting a spectrum of near infrared wavelength radiation light transmitted, reflected, emitted or scattered from said illuminated area of said sample and producing a collimated beam therefrom;
- c) a near infrared imaging spectrometer for selecting a near infrared radiation image of said collimated beam; and
- d) a detector for collecting said filtered near infrared images.

2. The system of claim 1 wherein said illumination source is one of a quartz tungsten halogen lamp, a tunable laser, a metal halide lamp, and a xenon arc lamp.

3. The system of claim 1 wherein said device for collecting is one of a refractive type infinity-corrected near infrared optimized microscope objective, a refractive fixed tube length microscope objective, and a reflecting microscope objective.

4. The system of claim 1 wherein said near infrared imaging spectrometer is selected from the group consisting of Lyot liquid crystal tunable filters; Evans Split-Element liquid crystal tunable filters; Solc liquid crystal tunable filters; Ferroelectric liquid crystal tunable filters; Liquid crystal Fabry Perot filters; a hybrid filter formed from a combination of liquid crystal tunable filters; and a combination of a liquid crystal tunable filter and a fixed bandpass and bandreject filters.

US 6,734,962 B2

15

5. The system of claim 1 wherein said detector is a near infrared radiation focal plane array detector.

6. The system of claim 5 wherein said detector is selected from the group consisting of indium gallium arsenide, platinum silicide, indium antimonide, palladium silicide, indium germanide, and mercury cadmium telluride.

7. The system of claim 1 further comprising a visible wavelength imagery system.

8. The system of claim 7 wherein said visible imagery system comprises:

a) an illumination source for illuminating an area of said sample using light in the visible optical wavelengths; and

b) a device for detecting said visible wavelength light from said illuminated area of said sample.

9. The system of claim 8 wherein said device for detecting said visible wavelength light comprises an analog and digital detector based on at least one of a silicon charge-coupled device detector and a silicon CMOS detectors.

10. The system of claim 8 further comprising a processor for producing a near infrared radiation chemical image of said sample.

11. The system of claim 8 further comprising an algorithm for combining the near infrared and visible image data.

12. A chemical imaging system comprising:

a) an illumination source for illuminating an area of a sample using light in the near infrared radiation wavelength and light in the visible wavelength;

b) a device for collecting a spectrum of near infrared wavelength radiation light transmitted, reflected, emitted or scattered from said illuminated area of said sample and producing a collimated beam therefrom;

c) a near infrared imaging spectrometer for selecting a near infrared radiation image of said collimated beam;

d) detector for collecting said filtered near infrared images; and

e) a device for detecting said visible wavelength light from said illuminated area of said sample.

13. A chemical imaging method comprising the steps of:

a) illuminating an area of a sample using light in the near infrared radiation wavelength and light in the visible wavelength;

b) collecting a spectrum of near infrared wavelength radiation light transmitted, reflected, emitted or scattered from said illuminated area of said sample and producing a collimated beam therefrom;

c) filtering said collimated beam to produce a near infrared radiation image of said collimated beam while

16

simultaneously detecting said optical wavelength light from said illuminated area of said sample;

d) collecting said filtered near infrared images; and

e) processing said collected near infrared images to produce a chemical image of said sample.

14. A method for producing a volumetric image of a sample comprising the steps of:

a) incorporating a refractive image formation optic exhibiting a chromatic response in the optical path of the microscope before the near infrared detector;

b) collecting images of said sample at a plurality of near infrared wavelengths through said objective at a fixed focus condition; and

c) processing said collected images to reconstruct a depth resolved image of said sample.

15. A method for chemically analyzing a sample comprising the steps of:

a) seeding said sample with a plurality of analytes having at least one of a known composition, structure and concentration;

b) collecting a plurality of spatially-resolved spectra for said plurality of analytes;

c) producing a plurality of chemical images of said sample containing said plurality of analytes; and

d) processing said plurality of chemical images to generate a chemical image of said sample.

16. The method of claim 15 wherein said processing step comprises at least one of:

a) correcting the image by dividing a near infrared image of said sample by a near infrared image of a background of said image to produce a resulting ratioed image;

b) normalizing the divided image by dividing each intensity value at every pixel in the image by the vector norm for its corresponding pixel spectrum, said vector norm being the square root of the sum of the squares of pixel intensity values for each pixel spectrum;

c) processing said image using a cosine correlation analysis method wherein each pixel spectrum is treated as a projected vector in n-dimensional space, wherein n is the number of wavelengths sampled in the image; and

d) processing said image using a principal component analysis method wherein a least squares fit is drawn through the maximum variance in the n-dimensional dataset.

* * * * *

EXHIBIT BB

FROM MORGAN LEWIS PHILADELPHIA NEC-9-3

(THU) 1. 20' 05 10:10/ST. 10:00/NO. 4862192958 P 2

Morgan, Lewis & Bockius LLP
1701 Market Street
Philadelphia, PA 19103-2921
Tel: 215.963.5000
Fax: 215.963.5001
www.morganlewis.com

Morgan Lewis
COUNSELORS AT LAW

Daniel H. Golub
215.963.5055
dgolub@morganlewis.com

January 20, 2005

VIA FACSIMILE (212)972-5487

Martin B. Pavane, Esquire
Cohen Pontani Lieberman & Pavane
551 Fifth Avenue
New York, NY 10176

Re: U.S. Patent No. 6,734,962

Dear Mr. Pavane:

We have your letter dated December 29, 2004, which asserts that "the '962 patent is infirm at least because Peter Miller should have been named as a co-inventor."

We have reviewed the SBIR proposal included with your letter, and strongly disagree that it constitutes evidence that Peter Miller was a co-inventor of the '962 patent. While the SBIR proposal suggests that Peter Miller and Dr. Treado collaborated on certain technology, much of the subject matter described in the SBIR proposal was invented by Dr. Treado before any such collaboration took place. The fact that Peter Miller and Dr. Treado may have collaborated on ideas previously invented by Dr. Treado does not in any way diminish Dr. Treado's position as the sole inventor of the technology that he (and Chemicon) brought to the SBIR proposal.

As you know, a party challenging inventorship in connection with an issued patent bears the burden of proof by clear and convincing evidence. The SBIR proposal provided with your December 29, 2004 letter does not come close to meeting this exacting standard. The fact that Peter Miller is listed as an investigator on the SBIR proposal does not, as you suggest, represent evidence that he is an inventor of technology described therein. Typically, a person asserting that he should be named as patent inventor provides written documentation such as lab notebook entries, evidencing that party's conception and reduction to practice of the technology at issue.

Philadelphia Washington New York Los Angeles San Francisco Miami Pittsburgh Princeton
Chicago Palo Alto Dallas Harrisburg Irvine Boston London Paris Brussels Frankfurt Tokyo

BEST AVAILABLE COPY

CRI003044

FROM MORGAN LEWIS PHILADELPHIA NEC-9-3

(THU) 1.20.05 10:10/ST. 10:00/NO. 4862192958 P 3

Morgan Lewis
COUNSELORS AT LAW

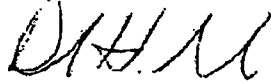
Martin B. Pavane, Esquire
January 20, 2005
Page 2

To the extent that you have evidence such as laboratory notebook entries that you believe are relevant to the claims of the '962 patent, we ask that you provide us copies of these materials so that we can consider them. However, based on our understanding of the facts, and the materials that you have provided to date, we can only conclude that Peter Miller's claim of co-inventorship of the '962 patent is utterly without merit.

In view of the above, ChemImage will certainly not be advised to execute the covenant not to sue that CRI has proposed in connection with this matter.

Should you have any questions about this letter, or wish to discuss this matter further, please feel free to contact me.

Very truly yours,



Daniel H. Golub

BEST AVAILABLE COPY

CRI003045

EXHIBIT CC

PATENT
ATTORNEY DOCKET NO. 056751-5008 RE

IN THE UNITED STATES PATENT AND TRADEMARK OFFICE

In re Application of:)
U.S. Patent No. 6,734,962)
Issue Date: May 11, 2004)
Filing Date: October 12, 2001)
Reissue Application No.: (Not Assigned))
For: NEAR INFRARED CHEMICAL IMAGING)
MICROSCOPE)

Mail Stop Reissue
Commissioner for Patents
P.O. Box 1450
Alexandria, VA 22313-1450

Sir:

REISSUE DECLARATION BY THE INVENTORS

We hereby declare that:

1. Each inventor's residence, mailing address and citizenship are stated below next to his name.
2. We believe that the inventors named below are the original and first inventor(s) of the subject matter which is described and claimed in United States Patent No. 6,734,962 (the "962 patent"), issued on May 11, 2004 and for which a reissue patent is sought on the invention entitled: NEAR INFRARED CHEMICAL IMAGING MICROSCOPE the specification of which is attached hereto.
3. We have reviewed and understand the contents of the above identified specification, including the claims, as amended by any amendment made during the prosecution of the application and any amendment submitted concurrently herewith.
4. We acknowledge the duty to disclose information which is material to patentability as defined in 37 C.F.R. §1.56.
5. We verily believe the original patent to be wholly or partly inoperative or invalid by reason of the patentee claiming more or less than the patentee had the right to claim in the patent.

CRI002954

Attorney Docket No. 56751-5008 RE
Reissue Application of U.S. Patent No. 6,734,962
Page 2

6. At least one error upon which this reissue application is based is described as follows:
- (a) As issued, claims 1 and 12 of the '962 patent are directed to a near infrared radiation chemical imaging system that includes "a device for collecting a spectrum of near infrared wavelength radiation light transmitted, reflected, emitted or scattered from said illuminated area of said sample and producing a collimated beam therefrom". Similarly, claim 13 is directed to a chemical imaging method that includes "collecting a spectrum of near infrared wavelength radiation light transmitted, reflected, emitted or scattered from said illuminated area of said sample and producing a collimated beam therefrom."
 - (b) Further, claims 1 and 12 of the issued '962 patent refer to a near infrared imaging spectrometer, without further description of the type of filter included in the spectrometer. Similarly, claim 13 includes a filtering step, without reference to the type of filter used to perform the step.
 - (c) Two articles were submitted to the Patent and Trademark Office for consideration during the prosecution of the '962 patent: Patrick J. Treado, Ira W. Levin, and E. Neil Lewis, "Indium Antimonide (InSb) Focal Plan Array (FPA) Detection for Near-Infrared Imaging Microscopy", Applied Spectroscopy 48, 607 (1994) ("Acousto-Optic Tunable Filter Reference"); and H. Morris, C. Hoyt, P. Filler and P. Treado, "Liquid Crystal Tunable Filter Raman Chemical Imaging", Vol. 50, Applied Spectroscopy, No. 6, pp. 805-811 (1996) ("Raman Spectroscopy Reference"). The Acousto-Optic Tunable Filter Reference and the Raman Spectroscopy Reference are referred to collectively herein as Prior Art.
 - (d) The Acousto-Optic Tunable Filter Reference discloses near infrared spectroscopy using a refractive optical microscope and an acousto-optic tunable filter to display spectroscopic images of biological and polymeric systems. The Raman Spectroscopy Reference discloses use of a liquid crystal tunable filter suitable for high definition Raman chemical imaging. Raman chemical imaging involves Raman scattering and measures the energy differences between the incident light and the light that is scattered upon striking a sample, i.e., inelastic scattering. The resulting Raman scattered light is referred to as inelastically scattered light.
 - (e) As a result of the inclusion of the term "scattered", and failure to specify that the type of filter used is a "liquid crystal tunable filter" in claims 1, 12 and 13, it appears that we may have claimed more than we were entitled to claim in claims 1, 12 and 13 of the '962 patent in view of the Prior Art.
 - (f) We failed to appreciate this error during the prosecution of the patent application. However, the oversight was not a result of any deceptive intent. In fact, this Prior

Attorney Docket No. 56751-5008 RE
Reissue Application of U.S. Patent No. 6,734,962
Page 3

Art was submitted by the applicants during the prosecution of the '962 patent, was considered by the examiner, and is listed on the face of the '962 patent.

- (g) Claims 1, 12 and 13 of the present reissue application have been amended such that they claim subject matter that does not read on the Prior Art, as follows:
- (1) Element (b) of claims 1 and 12, and step (b) of claim 13, include the term "scattered". Claims 1, 12 and 13 have been amended to delete this term.
- (2) Element (c) of claims 1 and 12 fails to specify the type of filter included in the spectrometer. Similarly, claim 13 fails to indicate the type of filter that performs the filtering step (c). Claims 1 and 12 and claim 13 have been amended to specify, respectively, that the "spectrometer comprises a liquid crystal tunable filter" and the "filtering is performed using a liquid crystal tunable filter."
- (h) In addition, the reissue claims seek to remove the following apparent typographical errors which were discovered during the preparation of the present reissue application. The amendments to the following claims have thus been made in order to bring the claims into compliance with 35 U.S.C. § 112, second paragraph:
- (1) Element (d) of claim 1 recites "a detector for collecting said filtered near infrared images", referring back to element (c) which recites "a near infrared imaging spectrometer for selecting a near infrared radiation image" (emphasis added). Thus, element (c) of claim 1 has been amended to include the plural term "images" and element (d) of claim 1 has been amended to include the term "said selected near infrared images" rather than "said filtered near infrared images", thereby providing proper antecedent basis in this claim.
- (2) Element (d) of claim 12 recites "a detector for collecting said filtered near infrared images", referring back to element (c) which recites "a near infrared imaging spectrometer for selecting a near infrared radiation image" (emphasis added). Thus, element (c) of claim 12 has been amended to include the plural term "images" and element (d) of claim 12 has been amended to include the term "said selected near infrared images" rather than "said filtered near infrared images", thereby providing proper antecedent basis in this claim.
- (3) Step (d) of claim 13 recites "collecting said filtered near infrared images", referring back to element (c) which recites "filtering said collimated beam to produce a near infrared radiation image". Thus, step (c) of claim 13 has been amended to include the plural term "images", thereby providing proper antecedent basis for this claim.

Attorney Docket No. 56751-5008 RE
Reissue Application of U.S. Patent No. 6,734,962
Page 4

(i) Accordingly, reissue claims 1, 12, and 13 seek to amend claims 1, 12 and 13 as follows:

1. (Amended) A near infrared radiation chemical imaging system comprising:

a) an illumination source for illuminating an area of a sample using light in the near infrared radiation wavelength;

b) a device for collecting a spectrum of near infrared wavelength radiation light transmitted, reflected[,] or emitted [or scattered] from said illuminated area of said sample and producing a collimated beam therefrom;

c) a near infrared imaging spectrometer for selecting [a] near infrared radiation images of said collimated beam, wherein the spectrometer comprises a liquid crystal tunable filter; and

d) a detector for collecting said selected [filtered] near infrared images.

12. (Amended) A chemical imaging system comprising:

a) an illumination source for illuminating an area of a sample using light in the near infrared radiation wavelength and light in the visible wavelength;

b) a device for collecting a spectrum of near infrared wavelength radiation light transmitted, reflected[,] or emitted [or scattered] from said illuminated area of said sample and producing a collimated beam therefrom;

c) a near infrared imaging spectrometer for selecting [a] near infrared radiation images of said collimated beam, wherein the spectrometer comprises a liquid crystal tunable filter;

d) detector for collecting said selected [filtered] near infrared images; and

e) a device for detecting said visible wavelength light from said illuminated area of said sample.

13. (Amended) A chemical imaging method comprising the steps of:

Attorney Docket No. 56751-5008 RE
Reissue Application of U.S. Patent No. 6,734,962
Page 5

- a) illuminating an area of a sample using light in the near infrared radiation wavelength and light in the visible wavelength;
 - b) collecting a spectrum of near infrared wavelength radiation light transmitted, reflected[,] or emitted [or scattered] from said illuminated area of said sample and producing a collimated beam therefrom;
 - c) filtering said collimated beam to produce [a] near infrared radiation images of said collimated beam while simultaneously detecting said optical wavelength light from said illuminated area of said sample, wherein the filtering is performed using a liquid crystal tunable filter;
 - d) collecting said filtered near infrared images; and
 - e) processing said collected near infrared images to produce a chemical image of said sample.
7. All errors corrected in this reissue application, up to the time of the filing of this reissue application, arose without any deceptive intention on the part of the applicants.
8. We hereby appoint the following practitioner(s) to prosecute this application and to transact all business in the Patent and Trademark Office connected therewith.

Daniel H. Golub
Reg. No. 33,701
Alison B. Weisberg
Reg. No. 45,206
Sharon B. McCullen
Reg. No. 54,303
Morgan, Lewis & Bockius LLP
1701 Market Street
Philadelphia, PA 19103
(215)963-5055 (Phone)
(215)963-5001 (Fax)

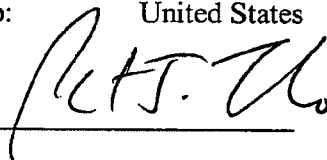
Attorney Docket No. 56751-5008 RE
Reissue Application of U.S. Patent No. 6,734,962
Page 6

We hereby declare that all statements made herein of my own knowledge are true and that all statements made on information and belief are believed to be true; and further that these statements were made with the knowledge that willful false statements and the like so made are punishable by fine or imprisonment, or both, under Section 1001 of Title 18 of the United States Code and that such willful false statements may jeopardize the validity of the application, any patent issuing thereon, or any patent to which this declaration is directed.

Inventors:

Name Printed: Patrick J. Treado
Post Office Address: 315 S. Lexington Ave.
Pittsburgh, Pennsylvania 15208


Citizenship: United States

Signed: 

Date: 3/21/05

Name Printed: Matthew Nelson
Post Office Address: 3941 Dowling Avenue
Pittsburgh, Pennsylvania 15221

Citizenship: United States

Signed: 

Date: 3/21/05

Name Printed: Scott Keitzer
Post Office Address: 207 Lockwood Road
Export, Pennsylvania 15632

Citizenship: United States

Signed: 

Date: 3/22/05

BEST AVAILABLE COPY

EXHIBIT DD



UNITED STATES PATENT AND TRADEMARK OFFICE

UNITED STATES DEPARTMENT OF COMMERCE
 United States Patent and Trademark Office
 Address: COMMISSIONER FOR PATENTS
 P.O. Box 1450
 Alexandria, Virginia 22313-1450
 www.uspto.gov

APPLICATION NO.	FILING DATE	FIRST NAMED INVENTOR	ATTORNEY DOCKET NO.	CONFIRMATION NO.
10/773,077	02/05/2004	Patrick J. Treado	030687	6027

41396 7590 08/22/2005

DUANE MORRIS LLP
 P. O. BOX 1003
 305 NORTH FRONT STREET, 5TH FLOOR
 HARRISBURG, PA 17108-1003

EXAMINER

LAUCHMAN, LAYLA G

ART UNIT

PAPER NUMBER

2877

DATE MAILED: 08/22/2005

Please find below and/or attached an Office communication concerning this application or proceeding.


Notice of Abandonment	Application No.	Applicant(s)	
	10/773,077	TREADO ET AL.	
	Examiner	Art Unit	
	L. G. Lauchman	2877	

-- The MAILING DATE of this communication appears on the cover sheet with the correspondence address--

This application is abandoned in view of:

1. ☒ Applicant's failure to timely file a proper reply to the Office letter mailed on 03 January 2005.
 - (a) ☐ A reply was received on _____ (with a Certificate of Mailing or Transmission dated _____), which is after the expiration of the period for reply (including a total extension of time of _____ month(s)) which expired on _____.
 - (b) ☐ A proposed reply was received on _____, but it does not constitute a proper reply under 37 CFR 1.113 (a) to the final rejection.
(A proper reply under 37 CFR 1.113 to a final rejection consists only of: (1) a timely filed amendment which places the application in condition for allowance; (2) a timely filed Notice of Appeal (with appeal fee); or (3) a timely filed Request for Continued Examination (RCE) in compliance with 37 CFR 1.114).
 - (c) ☐ A reply was received on _____ but it does not constitute a proper reply, or a bona fide attempt at a proper reply, to the non-final rejection. See 37 CFR 1.85(a) and 1.111. (See explanation in box 7 below).
 - (d) ☐ No reply has been received.
2. ☐ Applicant's failure to timely pay the required issue fee and publication fee, if applicable, within the statutory period of three months from the mailing date of the Notice of Allowance (PTOL-85).
 - (a) ☐ The issue fee and publication fee, if applicable, was received on _____ (with a Certificate of Mailing or Transmission dated _____), which is after the expiration of the statutory period for payment of the issue fee (and publication fee) set in the Notice of Allowance (PTOL-85).
 - (b) ☐ The submitted fee of \$_____ is insufficient. A balance of \$_____ is due.
The issue fee required by 37 CFR 1.18 is \$_____. The publication fee, if required by 37 CFR 1.18(d), is \$_____.
 - (c) ☐ The issue fee and publication fee, if applicable, has not been received.
3. ☐ Applicant's failure to timely file corrected drawings as required by, and within the three-month period set in, the Notice of Allowability (PTO-37).
 - (a) ☐ Proposed corrected drawings were received on _____ (with a Certificate of Mailing or Transmission dated _____), which is after the expiration of the period for reply.
 - (b) ☐ No corrected drawings have been received.
4. ☐ The letter of express abandonment which is signed by the attorney or agent of record, the assignee of the entire interest, or all of the applicants.
5. ☐ The letter of express abandonment which is signed by an attorney or agent (acting in a representative capacity under 37 CFR 1.34(a)) upon the filing of a continuing application.
6. ☐ The decision by the Board of Patent Appeals and Interference rendered on _____ and because the period for seeking court review of the decision has expired and there are no allowed claims.
7. ☒ The reason(s) below:

Confirmed with Mr. Golub on 8/19/2005


L. G. Lauchman
Primary Examiner
Art Unit: 2877
8/19/05

Petitions to revive under 37 CFR 1.137(a) or (b), or requests to withdraw the holding of abandonment under 37 CFR 1.181, should be promptly filed to minimize any negative effects on patent term.

EXHIBIT EE

(Rel.102-3/05 Pub.605)

FORM 11-3.1

11-27

PTO/SB/64 (09-04)

Approved for use through 07/31/2006. OMB 0651-0031

U.S. Patent and Trademark Office; U.S. DEPARTMENT OF COMMERCE

Under the Paperwork Reduction Act of 1995, no persons are required to respond to a collection of information unless it displays a valid OMB control number.

**PETITION FOR REVIVAL OF AN APPLICATION FOR PATENT
ABANDONED UNINTENTIONALLY UNDER 37 CFR 1.137(b)**

Docket Number (Optional)

First named inventor: Treado et al.Application No.: 10/773,077Art Unit: 2877Filed: Feb 5, 2004

Examiner:

Title: Near Infrared Chemical
Imaging MicroscopeLauchman, Layla GAttention: Office of Petitions
Mail Stop Petition
Commissioner for Patents
P.O. Box 1450
Alexandria, VA 22313-1450
FAX (703) 872-9306NOTE: If information or assistance is needed in completing this form, please contact Petitions
Information at (703) 305-9282.The above-identified application became abandoned for failure to file a timely and proper reply to a notice or
action by the United States Patent and Trademark Office. The date of abandonment is the day after the expiration
date of the period set for reply in the office notice or action plus an extensions of time actually obtained.**APPLICANT HEREBY PETITIONS FOR REVIVAL OF THIS APPLICATION**

NOTE: A grantable petition requires the following items:

- (1) Petition fee;
- (2) Reply and/or issue fee;
- (3) Terminal disclaimer with disclaimer fee - required for all utility and plant applications
filed before June 8, 1995; and for all design applications; and
- (4) Statement that the entire delay was unintentional.

1. Petition fee

☒ Small entity-fee \$ 750.00 (37 CFR 1.17(m)). Applicant claims small entity status. See 37 CFR 1.27.☐ Other than small entity - fee \$ _____ (37 CFR 1.17(m))

2. Reply and/or fee

A. The reply and/or fee to the above-noted Office action in
the form of Amendment (identify type of reply):☐ has been filed previously on _____
☒ is enclosed herewith.

B. The issue fee and publication fee (if applicable) of \$ _____

☐ has been paid previously on _____
☐ is enclosed herewith.

[Page 1 of 2]

This collection of information is required by 37 CFR 1.137(b). The information is required to obtain or retain a benefit by the public which is to file (and by the
USPTO to process) an application. Confidentiality is governed by 35 U.S.C. 122 and 37 CFR 1.11 and 1.14. This collection is estimated to take 1.0 hour to
complete, including gathering, preparing, and submitting the completed application form to the USPTO. Time will vary depending upon the individual case. Any
comments on the amount of time you require to complete this form and/or suggestions for reducing this burden, should be sent to the Chief Information Officer,
U.S. Patent and Trademark Office, U.S. Department of Commerce, P.O. Box 1450, Alexandria, VA 22313-1450. DO NOT SEND FEES OR COMPLETED
FORMS TO THIS ADDRESS. SEND TO: Mail Stop Petition, Commissioner for Patents, P.O. Box 1450, Alexandria, VA 22313-1450.

If you need assistance in completing the form, call 1-800-PTO-9199 and select option 2.

(Petition for Revival of an Application for Patent Abandoned Unintentionally under 37 C.F.R. § 1.137(b)
(PTO/SB/64) [11-3.1]-page 1 of 2)

10/07/2005 HLE333 00000040 10773077

01 FC:2453

750.00 DP

CRI002851

PTO/SB/64 (09-04)

Approved for use through 07/31/2008. OMB 0851-0031

U.S. Patent and Trademark Office, U.S. DEPARTMENT OF COMMERCE

Under the Paperwork Reduction Act of 1995, no persons are required to respond to a collection of information unless it displays a valid OMB control number.

3. Terminal disclaimer with disclaimer fee

- ☒ Since this utility/plant application was filed on or after June 8, 1995, no terminal disclaimer is required.
- ☐ A terminal disclaimer (and disclaimer fee (37 CFR 1.20(d)) of \$ _____ for a small entity or \$ _____ for other than a small entity) disclaiming the required period of time is enclosed herewith (see PTO/SB/63).

4. STATEMENT: The entire delay in filing the required reply from the due date for the required reply until the filing of a grantable petition under 37 CFR 1.137(b) was unintentional. [NOTE: The United States Patent and Trademark Office may require additional information if there is a question as to whether either the abandonment or the delay in filing a petition under 37 CFR 1.137(b) was unintentional (MPEP 711.03(c), subsections (III)(C) and (D)).]

WARNING: Information on this form may become public. Credit card information should not be included on this form. Provide credit card information and authorization on PTO-2038.

[Signature]
Signature

10-5-05
Date

Daniel H. Golub
Typed or printed name

33,701
Registration Number, if applicable

1701 Market Street
Address

215-963-5055
Telephone Number

Philadelphia, PA 19103
Address

Enclosures: ☒ Fee Payment

☒ Reply

☐ Terminal Disclaimer Form

☐ Additional sheets containing statements establishing unintentional delay

☒ Other: Information Disclosure Statement and
Application Data Sheet

EXPRESS MAIL CERTIFICATE (37 C.F.R. § 1.10)

Express Mail Label No. EV554289743US

Date of Deposit October 5, 2005

I hereby certify that this paper, and the papers and/or fees referred to herein as transmitted, submitted or enclosed, are being deposited with the U.S. Postal Service "Express Mail Post Office to Addressee" service under 37 C.F.R. § 1.10 on the date indicated above and is addressed to the Commissioner of Patents and Trademarks, Washington, D.C. 20231.

Name Daniel H. Golub

Signature *[Signature]*

(Petition for Revival of an Application for Patent Abandoned Unavoidably under 37 C.F.R. § 1.137(a)
(PTO/SB/64) [11-3.1]—page 2 of 2)

EXHIBIT FF



UNITED STATES PATENT AND TRADEMARK OFFICE

COMMISSIONER FOR PATENTS
UNITED STATES PATENT AND TRADEMARK OFFICE
P.O. BOX 1450
ALEXANDRIA, VA 22313-1450
www.uspto.gov

DANIEL H. GOLUB
1701 MARKET STREET
PHILADELPHIA, PA 19103

COPY MAILED

JAN 13 2006

OFFICE OF PETITIONS

In re Application of :
Treado et al. :
Application No. 10/773,077 :
Filed: February 5, 2004 :
Title of Invention: :
NEAR INFRARED CHEMICAL :
IMAGING MICROSCOPE :

This is a decision in response to the petition under 37 CFR 1.137(b), filed October 5, 2005, to revive the above-identified application.

This Petition is hereby granted.

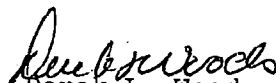
The above-identified application became abandoned for failure to timely and properly reply to the non-final Office action, mailed January 3, 2005. The Office action set a three (3) month period for reply, and provided for extensions of time under 37 CFR 1.136(a). No reply having been received, the application became abandoned on April 4, 2005. A Notice of Abandonment was mailed on August 22, 2005.

With the instant petition, Petitioner has satisfied the requirements of a grantable petition under 37 CFR 1.137(b). A response to the January 3, 2005 Office action is filed with the instant petition. Accordingly, the petition is granted.

The Revocation of Prior Powers of Attorney and New Power of Attorney has been entered and made of record.

This application is being forwarded to Technology Center Art Unit 2877 for processing of the response, filed October 5, 2005, in due course.

Telephone inquiries concerning this matter should be directed to the undersigned at (571) 272-3232.


Derek L. Woods
Attorney
Office of Petitions

CRI002900

EXHIBIT GG

Search results as of: 05-10-2006::14:38:16 E.T.

Parent Continuity Data

Description	Parent Number	Parent Filing or 371 (c) Date	Parent Status	Patent Number
This application is a Continuation of	09/976,391	10-12-2001	Patented	6,734,962
Which Claims Priority from Provisional Application	60/239,969	10-13-2000	Expired	-

Child Continuity Data

11/091,126 filed on 03-28-2005 which is Pending claims the benefit of 10/773,077
11/256,889 filed on 10-24-2005 which is Patented claims the benefit of 10/773,077
11/257,139 filed on 10-24-2005 which is Pending claims the benefit of 10/773,077
11/257,219 filed on 10-24-2005 which is Pending claims the benefit of 10/773,077
11/257,222 filed on 10-24-2005 which is Pending claims the benefit of 10/773,077
11/366,129 filed on 03-02-2006 which is Pending claims the benefit of 10/773,077
11/366,762 filed on 03-02-2006 which is Pending claims the benefit of 10/773,077
11/366,887 filed on 03-02-2006 which is Pending claims the benefit of 10/773,077

Close Window

EXHIBIT HH

PATENT

IN THE UNITED STATES PATENT AND TRADEMARK OFFICE

In Re		Group Art	
Appln. of:	Matthew P. NELSON et al.	Unit:	Not Yet Assigned
Serial No.:	Not Yet Assigned	Conf. No.:	Not Yet Assigned
Filed:	Herewith	Examiner:	Not Yet Assigned
For:	Spectroscopic Methods for Component Particle Analysis	Atty Docket No.:	E2079-00073

PRELIMINARY AMENDMENT

This Preliminary Amendment is filed together with the application for the sole purpose of reducing the filing fee.

Please amend the application as follows.

Amendments to the Claims are reflected in the listing of claims which begins on page 2 of this Amendment.

Remarks begin on page 5 of this Amendment.

Amendments to the Claims

Please amend the claims to read as follows:

1. (Original) A method of quantifying a geometric property of a particle of a substance in a sample, the method comprising irradiating the sample, generating a first infrared image of the sample at a wavelength characteristic of the substance, and quantifying the geometric property using an image processing technique.
2. (Original) The method of claim 1, wherein the first infrared image is a near infrared image.
3. (Original) The method of claim 1, wherein the first image is an image of a microscopic field.
4. (Original) The method of claim 1, comprising simultaneously quantifying the geometric property of multiple particles of the substance in the sample.
5. (Original) The method of claim 1, wherein the geometric property is characteristic of the size of the particle.
6. (Original) The method of claim 1, comprising generating an infrared image of the sample at multiple infrared wavelengths characteristic of the substance.
7. (Original) The method of claim 1, further comprising comparing the first image and a second image of the sample at a wavelength characteristic of a compound other than the substance.
8. (Original) The method of claim 7, wherein the second image is a near infrared image.
9. (Original) The method of claim 7, wherein the first and second images are combined in an aligned manner.
10. (Original) The method of claim 7, comprising determining the geometric properties of the particle of the substance and of a particle of the compound in the sample.
- 11-12. (Canceled)

13. (Original) The method of claim 1, wherein the image is a two-dimensional image.
14. (Original) The method of claim 13, wherein the geometric property is selected from the group consisting of the area, the perimeter, a Feret diameter, the maximum chord length, a shape factor, and an aspect ratio of the particle.
15. (Original) The method of claim 1, wherein the image is a three-dimensional image.
16. (Original) The method of claim 15, wherein the geometric property is selected from the group consisting of the volume, the surface area, a Feret diameter, the maximum chord length, a shape factor, and an aspect ratio of the particle.
17. (Original) The method of claim 1, wherein the particle is irradiated with substantially monochromatic light.
- 18-20. (Canceled)
21. (Original) The method of claim 1, wherein the particle is immobilized prior to generating the image.
- 22-33. (Canceled)
34. (Original) The method of claim 1, wherein the first image is generated using a near infrared radiation chemical imaging system comprising:
- a) an illumination source for illuminating an area of the sample using light in the near infrared radiation wavelength;
 - b) a device for collecting a spectrum of near infrared wavelength radiation light transmitted, reflected, emitted, or elastically scattered from the illuminated area in a focal plane and producing a collimated beam therefrom;
 - c) a near infrared imaging spectrometer for selecting a near infrared radiation image of the collimated beam; and
 - d) a detector for collecting the filtered near infrared image.
- 35-36. (Canceled)

37. (Original) A method of quantifying a geometric property of a particle of a substance in a sample including multiple particles, the method comprising irradiating the sample, identifying the particle of the substance by assessing infrared radiation at a wavelength characteristic of the substance, generating an optical image of particles in the field, and quantifying the geometric property of the particle of the substance using an image processing technique.

38-44. (Canceled)

45. (Original) A method of assessing particles of a first substance and a second substance in a sample, the method comprising irradiating the sample, generating a first infrared image of the sample at a wavelength characteristic of the first substance, and comparing the first image with a second image of the sample at a wavelength characteristic of the second substance.

46-50. (Canceled)

51. (Original) A method of assessing a geometric property of a particle of a substance in a sample, the method comprising irradiating the sample, generating a first image of infrared radiation transmitted, reflected, or elastically scattered by the sample at a wavelength characteristic of the substance, and assessing the geometric property from the image.

Remarks

Claims 1-10, 13-17, 21, 34, 37, 45, and 51 are pending in the application following entry of this Amendment. Claims 11, 12, 18-20, 22-33, 35, 35, 38-44, and 46-50 have been canceled solely for the purpose of reducing the filing fee. Claims 1, 34, 37, 45, and 51 are the only independent claims pending.

No new matter is added by the amendments and additions made herein.

Summary

The Applicant respectfully contends that each of claims 1-10, 13-17, 21, 34, 37, 45, and 51 is in condition for allowance. The Examiner is requested to issue a Notice of Allowance at the earliest possible time.

Respectfully submitted,

Matthew P. NELSON et al.

28 March 2005

(Date)

By: 

Gary D. Colby, Ph.D., J.D.

Registration No. 40,981

Customer No. 08933

DUANE MORRIS LLP

One Liberty Place

Philadelphia, PA 19103-7396

Telephone: 215-979-1000

Direct Dial: 215-979-1849

Facsimile: 215-979-1020

E-Mail: GDColby@DuaneMorris.com